POSTCRANIAL MORPHOLOGY OF *REPENOMAMUS* (EUTRICONODONTA, MAMMALIA): IMPLICATIONS FOR THE HIGHER-LEVEL PHYLOGENY OF MAMMALS

by

YAOMING HU

A dissertation submitted to the Graduate Faculty in Biology in partial fulfillment of the requirements for the degree of Doctor of Philosophy, The City University of New York

2006

UMI Number: 3213248

ProQuest Information and Learning Company
300 North Zeeb Road
P.O. Box 1346
Ann Arbor, MI 48106-1346

This manuscript has been read and accepted for the
Graduate Faculty in Biology in satisfaction of the
dissertation requirement for the degree of Doctor of Philosophy.

04/06/2006 [**required signature**] Jin Meng
Date Chair of Examining Committee: Dr. Jin Meng

04/21/2006 [**required signature**] Richard L. Chappell
Date Executive Officer: Dr. Richard L. Chappell

[typed name] Jin Meng

[typed name] Michael J. Novacek

[typed name] John H. Wahlert
Supervisory Committee

THE CITY UNIVERSITY OF NEW YORK

ABSTRACT

Postcranial morphology of *Repenomamus* (Eutriconodonta, Mammalia): Implications for the higher-level phylogeny of mammals

by

Yaoming Hu

Advisors: Drs. Jin Meng, Michael J. Novacek, and John H. Wahlert

Repenomamus **are eutriconodont mammals living in the Early Cretaceous. The genus has two species, *R. robustus* and *R. giganticus*, both from Yixian Formation, western Liaoning, China. The postcranium of *Repenomamus* is described in detail. The atlas has the neural arch and intercentrum unfused. The axis and postaxial cervical vertebrae have short ribs. There are twenty thoracic vertebrae. The scapula has a huge spine and well developed supra- and infraspinous fossa. The coracoid is reduced as the coracoid process. The humerus is stout, with an ulnar and radial condyle and an incipient trochlea. The ulna and radius are compressed transversely. The olecranon is large. The femoral head is oriented proximally and dorsomedially. The tibia is shorter than the femur. The upper ankle joint is tricontact. The astragalus has an incipient head and no distinct neck. The calcaneus has a medioventral directed tuber and a broad peroneal process. The astragalus partially overlaps the calcaneus. The metatarsal V does not contact the calcaneus. Anatomical comparison of *Repenomamus* with other Mesozoic mammals**

is conducted in the format of character analysis. 176 postcranial characters are analyzed across major clades of mammals and selected nonmammalian cynodonts. The phylogeny of Mesozoic mammals is generated with the data matrix of 57 taxa and 435 characters (176 postcranial, 151 cranial and 108 dental). The result is consistent with previous analyses regarding the monophyly of Mammalia, paraphyly of non-therian mammals and polyphyly of triconodonts. The analysis also reveals several relationships among groups of mammals, e.g. the close relationship between monotremes and multituberculates, the monophyly of eutriconodonts, the monophyly of symmetrodonts, and close relationships of "Gondwanan tribosphenic mammals" with northern continental tribosphenic mammals. Estimated body masses are 12-14 kg for *R. giganticus* and 4-6 kg for *R. robustus,* which make the genus among the largest of Mesozoic mammals. The stomach content indicates carnivory, suggesting *Repenomamus* competed with small carnivorous dinosaurs. *Repenomamus* has a mammalian type of larynx, which minimizes the interruption of respiration during mastication. This is an important adaptation in the evolution of the mammalian endothermy and lactation.

ACKNOWLEDGMENTS

I thank Chuankui Li, Jin Meng, and Yuanqing Wang for suggesting this study as my PhD project, and for their longtime support and encouragement for my work on Mesozoic mammals. I am particularly grateful to Jin Meng for mentoring me throughout the whole period of my PhD study. I am indebted to members of my PhD supervisory committee, Jin Meng, Michael J. Novacek and John H. Wahlert, for their great help and invaluable advice. Thanks are due to Eric Delson, Jin Meng (chair), Michael J. Novacek, Mark A. Norell, John H. Wahlert, and Xiaobo Yu, who served in my examining committee and spent time to read and correct various drafts of my doctoral proposal and dissertation.

The fossil material used in this study was collected by members of the "Jehol Biota Project" from the Institute of Vertebrate Paleontology and Paleoanthropology, the Chinese Academy of Sciences, Beijing, China. I thank Meemann Chang, Chuankui Li, Zhonghe Zhou, and Yuanqing Wang for coordinating the research. I am greatly indebted to Xiaolin Wang, Zhonghe Zhou, Xing Xu, Fucheng Zhang, Yuanqing Wang, Yuan Wang, Fan Jin, Jiangyong Zhang, Lianhai Hou, who participated in the project and provided suggestion on the research subject. Thanks are also due to Shuhua Xie, Haijun Wang, Shijie Li, and Amy Davidson, who skillfully prepared all the specimens. Jin Meng generously allowed me to use the photography and imaging facilities in his laboratory. My acknowledgements are extended to the staffs of the Institute of Vertebrate Paleontology and Paleoanthropology, the Chinese Academy of Sciences, Beijing, China, the American Museum of Natural History in New York, and the City University of New York for their logistic and technical supports.

My study was supported by fellowships from the American Museum of Natural History, New York, through the City University of New York. My research was also supported by funding from the Ministry of Science and Technology, People's Republic of China, the National Natural Science Foundation of China, and the Chinese Academy of Sciences.

During the course of this study, I have benefited from collaborations and communications with many colleagues. I am grateful to David J. Archibald, Richard L. Cifelli, Richard C. Fox, Zofia Kielan-Jaworowska, Zhexi Luo, Thomas Martin, Agustín G. Martinelli, Eric J. Sargis, Denise Sigogneau-Russell, Frederick S. Szalay, and John R. Wible for suggestions and/or providing literatures.

Finally, I want to thank my wife, Yanjie Sun, for her great support during these years.

TABLE OF CONTENTS

LIST OF TABLES

LIST OF ILLUSTRATIONS

1. INTRODUCTION

Triconodonts are Mesozoic mammals that have cheek teeth with three principal cusps mesiodistally aligned (Jenkins and Crompton, 1979). Among Mesozoic mammals, triconodonts have the longest geological range (McKenna and Bell, 1997; Kielan-Jaworowska *et al*., 2004). They first appeared in the Late Triassic and persisted into the Late Cretaceous. Since 1838 when the first triconodont genus, *Phascolotherium*, was named, more than forty genera of triconodonts have been found from all continents except Antarctic and Australia (Owen, 1838, 1859, 1871; Marsh, 1887; Simpson, 1925; 1928a, 1928b, 1929; Parrington, 1941; Crompton, 1964; Jenkins and Crompton, 1979; McKenna and Bell, 1997; Luo *et al*., 2002; Kielan-Jaworowska *et al*., 2004; Meng *et al*., 2005). Our current knowledge about these extinct animals can be briefly summarized as below.

Sinoconodon Patterson and Olson, 1961 is a Liassic triconodont, known from China and represented by well-preserved skulls, dentaries, and some postcranial elements (Patterson and Olson, 1961; Young, 1982; Zhang and Cui, 1983; Crompton and Sun 1985; Crompton and Luo, 1993; Zhang *et al*., 1998). *Sinoconodon* has been interpreted as one of the most primitive mammalian stem groups (Crompton and Sun, 1985; Crompton and Luo, 1993; Luo 1994; Luo *et al*., 1995; Zhang *et al*., 1998; Kielan-Jaworowska *et al*., 2004). As in other mammals, *Sinoconodon* has developed a promontorium, the ventral emergence of the petrosal, and a secondary craniomandibular joint that is comprised of the squamosal glenoid and dentary condyle. Differing from other mammals, *Sinoconodon* retains successive replacement of check teeth and lacks precise one-to-one match

between corresponding upper and lower teeth (Crompton and Luo, 1993; Luo, 1994; Zhang *et al*., 1998; Luo *et al*., 2002). Mills (1971) erected the family Sinoconodontidae based on the genus, which was adopted in the classification of McKenna and Bell (1997). Another genus placed in Sinoconodontidae is *Lufengoconodon* Young, 1982 based on a skull, a jaw and some forelimb elements from the same locality where *Sinoconodon* came from (Young, 1982; Zhang, 1984). *Lufengoconodon* differs from *Sinoconodon* in having cheek teeth that have a more distinct cingulum. However, new material of *Sinoconodon* indicates that the differences between two genera are less than previously believed, and the taxonomic status of *Lufengoconodon* is now in question (Zhang *et al.*, 1998).

Morganucodon Kühne, 1949 is among the best-known genera of Mesozoic mammals. Fossil material of *Morganucodon* includes complete skulls and numerous isolated teeth, jaw fragments, cranial and postcranial elements. They are found from the Late Triassic of Europe and Early Jurassic of Europe, Asia and North America (Clemens, 1980; Crompton, 1971, 1974; Crompton and Luo, 1993; Crompton and Luo, 1993; Jenkins and Parrington, 1976; Jenkins *et al*., 1983; Kermack *et al*., 1973, 1981; Kühne, 1949, 1958; Luo and Crompton, 1994; Luo *et al.*, 1995; Mills, 1971; Parrington, 1941, 1947, 1971, 1978; Rigney, 1963; Wible and Hopson, 1993; Young, 1978). Differing from *Sinoconodon*, *Morganucodon* has a dentition with diphyodont anterior post-canine teeth and single generation of molariforms (Parrington, 1978; Luo *et al*., 2002). Its molariforms have precise one-to-one occlusion in which the cusp a of the lowers occludes between cusps A and B of the uppers (Crompton and Jenkins, 1968). The cutting edges of cheek teeth are not present upon eruption, but developed as the result of wear (Jenkins and Crompton, 1979). *Morganucodon*, similar to *Sinoconodon*, has

postdentary bones attached to the postdentary trough on the medial side of the dentary (Kermack, 1963; Kermack *et al*., 1973). The quadrate of *Morganucodon* is suspended in the recess between squamosal and petrosal (Kermack *et al*., 1981; Meng *et al*., 2003), rather than solely suspended by the squamosal as in *Sinoconodon* (Crompton and Sun, 1985). No evidence shows the successive replacement of dentition in *Morganucodon*, which probably has a determinate growth pattern (Crompton and Luo, 1993; Gow, 1985; Luo, 1994; Luo *et al*., 2001a, 2001b, 2002). Several students regard *Morganucodon* as a junior synonym for *Eozostrodon* Parrington, 1941, but *Morganucodon* is still employed as a valid taxon by others (Clemens, 1979; Kermack *et al.*, 1973, 1981; Kielan-Jaworowska and Dashzeveg, 1998; Luo *et al*., 2002; Kielan-Jaworowska *et al*., 2004; but see Crompton and Jenkins, 1979 and McKenna and Bell, 1997).

Kühne (1958) erected the family Morganucodontidae based on *Morganucodon*. There are several other morganucodontids found during the past decades. *Erytherotherium* Crompton, 1964 is from the Lower Jurassic of South Africa. The genotype and only species, *E. parringtoni*, is based on a skull, dentition and partial postcranial skeleton of an immature individual (Crompton, 1964; Jenkins and Parrington, 1976). Its molariforms are virtually quite similar to those of *Morganucodon*, but cusp a of the lowers occludes in front of cusp B of the uppers.

Brachyzostrodon Sigogneau-Russell, 1983 is from the Upper Triassic of continental Europe. It has two species, *B. coupatezi* and *B. maior* (Sigogneau-Russell, 1983; Hahn *et al.*, 1991). *Hallautherium* Clemens, 1980 and *Helvetiodon* Clemens, 1980 are also from the Upper Triassic of continental Europe (Clemens, 1980). *Holwellconodon* Lucas and Hunt, 1990 is based on finds from the Upper Triassic of England (Lucas and Hunt, 1990).

Indotherium Yadagiri, 1984 and *Paikasigudodon* (Prasad and Manhas, 1997) Prasad and Manhas, 2002 from the Lower Jurassic of India, were originally assigned to Symmetrodonta (Yadagiri, 1984; Prasad and Manhas, 1997, 2002). The name *Indotherium* is "preoccupied by *Indotherium* Kretzoi, 1942, a synonym of *Aprotodon*, a rhinoceros, but a new name has not yet been proposed" (McKenna and Bell, 1997). *Paikasigudodon* Prasad and Manhas, 2002 is used to replace *Kotatherium* Prasad and Manhas, 1997. *Wareolestes* Freeman, 1979, represented by isolated teeth from the Middle Jurassic of England, is the youngest record of morganucodontids. A femur referred to a morganucodontid mammal is reported from the Middle Jurassic of Russia, but no dental remains are associated with it (Gambaryan and Averianov, 2001).

Megazostrodon Crompton and Jenkins, 1968 is from the Lower Jurassic of South Africa. The type and only species, *M. rudnerae*, is based on an individual specimen with dentition, partially crushed skull, lower jaws and most of the postcranial skeleton (Crompton and Jenkins, 1968; Jenkins and Parrington, 1976). The upper molariforms of *Megazostrodon* have stronger cingulum than those of *Morganucodon* and *Erythrotherium* and cusp a of lower molariforms occluded in front of cusp B of the uppers (Crompton and Jenkins, 1968). There is evidence indicating replacement of molariforms in *Megazostrodon* (Gow, 1986). *Indozostrodon* Datta and Das, 2001, most similar to *Megazostrodon*, is based on isolated teeth from the same locality as *Paikasigudon* and *Indotherium* (Datta and Das, 2001).

Dinnetherium Jenkins, Crompton and Downs, 1983, from the Lower Jurassic of North America, is known from lower jaws and dentition (Jenkins *et al.*, 1983). Its dentary, as those of most other Early Jurassic triconodonts, retains a postdentary trough (Jenkins

et al., 1983). The occlusion pattern of *Dinnetherium* is similar to that of *Morganucodon*, but its molariforms differ from those of *Morganucodon* as its cusp b and c of lower teeth are symmetrically positioned on either side of cusp a, whereas in *Morganucodon* cusp b is lower than c and closer to cusp a than does cusp c (Jenkins *et al*., 1983; Crompton and Lou, 1993). Jenkins *et al*. (1983) did not assign *Dinnetherium* to a particular family of triconodonts but suggested that it has the basic traits of the amphilestid dentition (Jenkins *et al*., 1988; Rougier *et al*., 2001). Gow (1986) erected a family, Megazostrodontidae that includes *Megazostrodon* and *Dinnetherium*. McKenna and Bell (1997) adopted the family name but excluded *Dinnetherium* from it. Other students, however, prefer to assign *Megazostrodon* to Morganucodontidae (Jenkins and Crompton, 1979; Luo *et al*., 2002). The status of *Dinnetherium* is also unstable. It was either placed in Amphilestidae (Stucky and McKenna, 1993), regarded as a sister taxon of late triconodonts (Hopson, 1994), related to *Morganucodon* (Rougier *et al*., 1996a), or considered as a member of Morganucodontidae (Luo *et al*., 2002).

Fossil evidence indicates that morganucodontids, including *Megazostrodon*, are small animals with the size of rats or shrews. They were probably nocturnal insectivores. They have a flexible body design with vertebral regions well differentiated, and were capable of moving on uneven substrates agilely with sprawling limbs (Jenkins and Parrington, 1976; Jenkins and Crompton, 1979).

One problematic taxon with triconodont teeth is *Hadrocodium* Luo, Crompton, and Sun, 2001a (Luo, *et al*., 2001a). The genotype and only species, *H. wui*, is based on a tiny skull and associated lower jaws from the Early Jurassic of Yunnan, China. This specimen was previously regarded as a juvenile morganucodontid (Crompton and Luo, 1993). Luo

et al. (2001a) considered that *Hadrocodium* "has enlarged cranial cavity, but no postdentary trough on the mandible, indicating the separation of the middle ear bones from mandible". Nevertheless, the morphological details of the only specimen, i.e. the tiny size of the skull, the large braincase, the large postcanine diastema, and the anterior position of the lower dentition, still indicate that it is possibly a juvenile morganucodontid (Wang Y.-q. *et al*., 2001; Meng *et al*., 2003; Wang *et al*., in press). Luo *et al*. (2001a) announced that *Hadrocodium* is the earliest taxon with ear ossicles detached from the lower jaws, but they did not provide a detailed description of structures on the internal side of mandible, which is crucial to evaluate their argument. Further examination shows that a trough-like structure does exist on the internal surface of the mandible (Wang *et al*., in press). It is unclear whether the structure represents the postdentary trough or other groove-like structure not associated with postdentary bones. *Hadrocodium* does not belong to any particular order or family, but it is closer to later triconodonts and other mammals than to early triconodonts, according to Luo *et al*. (2001a).

Except the little known genus *Wareolestes,* all early triconodonts disappeared in the Middle Jurassic, when later triconodonts made their first appearance. These later forms, often called eutriconodonts (Kermack *et al*., 1973), differ from early ones (possibly with the exception of *Hadrocodium*) in that their ear ossicles are definitely detached from the lower jaws and that the lower jaws have no angular process. Their lower cheek teeth are more laterally compressed than those of early groups. The first established genus of eutriconodonts is *Phascolotherium* Owen, 1838. The type and only species, *P. bucklandi* (Broderip, 1828), came from the Middle Jurassic of Stonefield, Oxfordshire, England.

Amphilestes Owen, 1859 has one species, *A. broderipii* (Owen, 1845), and was from the same locality as *P. bucklandi*. These two genera belong to the family Amphilestidae Osborn, 1888. Two other amphilestids, *Comodom* Kretzoi and Kretzoi, 2000 (*Phascolodon* Simpson, 1925; *Phascolotheridium*, Cifelli and Dykes, 2001) and *Aplocondon* Simpson, 1925 came from the Upper Jurassic of North America. Both genera are known from fragmentary material from the Morrison Formation of Wyoming. By far, amphilestids are known only from lower jaws and lower dentitions. They are characterized in having symmetrical and moralized premolariforms. Cusp b and c of molariforms are subequal and much lower than cusp a, which is high and symmetrical. Although no upper dentition is known for amphilestids, cusp a of lower teeth probably occludes in front of cusp B of upper teeth, as seeing in *Megazostrodon*. In a recentl phylogenetic analyses, the monophyly of amphilestids is questioned (Rougier *et al*., 2001)

Liaotherium Zhou, Cheng, and Wang, 1991 was originally referred to ?Amphilestidae (Zhou *et al.*, 1991). The only species is based on a well-preserved dentary with the last molariform from the Middle Jurassic of northeastern China. It can be told that, although damaged, the tooth has three cusps arranged in a line. Averianov (2002) argued that the taxon "should be considered as Mammalia *incertae sedis*, because [its] attribution to Amphilestidae or 'Symmetrodonta' is equally possible". His evidence is that *Gobiotheriodon*, a symmetrodont from Mongolia, has the last molar with three main cusps nearly linearly arranged. His argument is weak because cusp b and c of the last molariform in *Gobiotheriodon* are, although to a small degree, still lingual to cusp a, which is essentially different from triconodont molariforms with three main cusps anteroposteriorly arranged.

Triconodontidae Marsh, 1887 is another major triconodont family contemporary with amphilestids. Triconodontids differ from amphilestids in having lower molariforms with cusp b and c subequal to or slightly smaller than cusp a. Premolariforms of triconodontids are asymmetrical. In triconodontids, cusp a of lower molariforms occludes between cusp A and B of upper teeth. Among triconodontids, *Priacodon* Marsh, 1887 has four species from the Upper Jurassic of North America, known from complete dentition, most of lower jaw, basicranium, and a few postcranial elements (Marsh, 1887, 1880; Simpson, 1925, 1929; Rasmussen and Callison, 1981; Rougier *et al*., 1996a; Englemann and Callison, 1998). *Trioracodon* Simpson, 1928 is another genus known from the Upper Jurassic of North America. It is also known from Purbeck Limestone Group, Durlston Bay, Dorset, England, which is either Upper Jurassic or Lower Cretaceous (Simpson, 1928; Ensom and Kielan-Jaworowska, 1998). *Trioracodon* has remains of teeth, dentaries, and partial cranial elements (Owen, 1871; Marsh, 1880; Simpson, 1928; Kermack, 1963). In both *Priacodon* and *Trioracodon*, cusp a of the lower molariforms is slightly higher than b and c; *Priacodon* has three premolariforms, while *Trioracodon* has four. Also from the Purbeck Limestone Group is the well-known *Triconodon* Owen, 1859. *Triconodon* has four molariforms with three mains cusps subequal. Only one species has been recognized and its abundant specimens reveal morphology of dentition, upper and lower jaws, basicranium, and braincase (Owen, 1859, 1871; Simpson, 1928).

Several triconodontids came from the Lower Cretaceous of North America. *Astroconodon* Patterson, 1951 has two species from the Lower Cretaceous Antlers Formation or equivalent strata in western North America (Patterson, 1951; Slaughter, 1969; Cifelli and Madsen, 1998; Turnbull and Cifelli, 1998). *Arundelconodon* Cifelli,

Lipka, Schaff, and Rowe, 1999 is from the Lower Cretaceous Arundel Clay, Potomac Group, Maryland. Its genotype and only species, *A. hottoni,* is based on a right lower jaw with two premolariforms and three molariforms. *Corviconodon* Cifelli, Wible and Jenkins, 1998 has two species, *C. montanensis* from the Lower Cretaceous Cloverly Formation, Montana and Wyoming, and *C. utahensis* from the Lower Cretaceous Cedar Mountain Formation, Utah. Both have jaw fragments and isolated teeth preserved. *Jugulator* Cifelli and Madsen, 1998 has one species from the same locality as *C. utahensis*. *Jugulator* had a ferocious dagger of a lower incisor, indicating possible carnivorous lifestyle. The only species, *J. amplissimus*, known from jaw fragments and isolated teeth, is the largest triconodontid. *Alticonodon* Fox, 1969, including the genotype *A. lindoei* and one unnamed species, come from the Late Cretaceous Milk River Formation, Alberta, Canada (Fox, 1969). Cifelli *et al.* (1998) recognized two features shared by North American Cretaceous triconodontids: "a tall cusp d that forms part of the shearing surface and that does not overhang the distal root on the lower molars; and adjoining teeth are tightly interlocked via a tongue and groove mechanism that extends well down the molar roots". These characters possibly indicate close relationships among the North American forms.

Two triconodonts *Dyskritodon* Sigogneau-Russell, 1995 and *Ichthyoconodon* Sigogneau-Russell, 1995 came from the Lower Cretaceous of Morocco (Sigogneau-Russell, 1995). They have laterally compressed molariforms and possibly have an aquatic lifestyle. Their affinities are enigmatic, although McKenna and Bell (1997) placed them in Triconodontidae. One tooth (VPL/JU/KM/13) from the Lower/Middle Jurassic of India bears similarity to *Dyskritodon* and is named as a different species of the genus, *D.*

indicus (Prasad and Manhas, 2002). Given the significant age gap between the Indian and Morocco specimens, the taxonomic allocation of the Indian species remains an open question.

Another enigmatic triconodont is from South America. *Austrotriconodon* Bonaparte, 1986 is divided into two species from the Upper Cretaceous Los Alamitos Formation of Patagonia, Argentina (Bonaparte, 1986, 1992). It was initially referred to Triconodontidae (Bonaparte, 1986) but later was transferred to its own family, Austrotricondontidae (Bonaparte, 1992). The lower molariforms of *Austrotriconodon* are actually more similar to premolariforms than to molariforms of other triconodonts. The upper molariforms are indeed similar to those of triconodontids, with a mesial excavation for an interlocking mechanism (Cifelli *et al.,* 1998).

Gobiconodontidae and Repenomamidae are the only Early Cretaceous triconodonts. Gobiconodontidae Chow and Rich, 1984 are widely distributed in Asia, North America and Europe (Trofimov, 1978; Jenkins and Schaff, 1988; Kielan-Jaworowska and Dashzeveg, 1998; Godefroit and Gou, 1999; Rougier *et al*., 2001; Cuenca-Bescos and Canudo, 2003; Li *et al*., 2003; Meng *et al*., 2005). *Gobiconodon* Trofimov, 1978 is similar to amphilestids in lower molariform structure, but has a reduced canine and enlarged anterior lower incisor. At least some lower molariforms are replaced during the ontogeny of *Gobiconodon*. Main cusps of upper molariforms have incipient triangular arrangement. Six species have been reported, including *G. borissiaki* Trofimov, 1978 from Khoobur of Mongolia, *G. ostromi* Jenkins and Schaff, 1988 from Cloverly Formation, Montana, USA, *G. hoburensis* (Trofimov, 1978) Kielan-Jaworowska and Dashzeveg, 1998 from Khoboor of Mongolia and Guchin Us County,

Siberia, Russia, *G. hopsoni* Rougier, Novacek, McKenna *et al*., 2001 and *G. sp.* from Oshih of Mongolia, and *G. zofiae* Li, Wang, Hu, and Meng, 2003 from the lowest part of Yixian Formation, west Liaoning, China. With specimens of dentitions, jaws, skull, and many postcranial elements, *Gobiconodon* is one of the best-known eutriconodonts. The largest species, *G. ostromi*, is probably an ambulatory carnivore/scavenger. It is a robustly built animal, and "as a predator had a greater advantage in its size than in its speed" (Jenkins and Schaff, 1988). One other large gobiconodontid, *Meemannodon lujiatunensis* Meng, Hu, Wang, and Li, 2005 is recently found from the Lower Cretaceous Yixian Formation, west Liaoning, China (Meng *et al*., 2005). *Hangjinia* Godefroit and Guo, 1999 has one species from Ejinharo Formation, Ordos Basin, Inner Mongolia, China. It is perhaps a derived gobiconodontid with reduced premolariform region in dentition, but the fact that the type specimen is a mandible from a juvenile individual may have obscured the tooth count (Rougier *et al*., 2001). *Klamelia* Chow and Rich, 1984 from the Middle/Upper Jurassic Shishugou Formation, northwestern China was originally assigned to the family Gobiconodontidae (then subfamily Gobiconodontinae Chow and Rich, 1984 in the family Amphilestidae) based on foreshorting of the dentary and reduction of the antemolar region. Further examinations indicated that, with reduced cusp b and anteriorly displaced cusp a, *Klamelia* is distinctive from gobiconodontids, and is better to be excluded from the family (Jenkins and Schaff, 1988; Rougier *et al*., 2001). In addition, Tang *et al*., (2001) reported remains of gobiconodontid teeth and skull fragments from the Lower Cretaceous of Mazongshan area, Gansu, China. Gobiconodontid material is also found recently in Spain (Cuenca-Bescos and Canudo, 2003).

Repenomamidae Li, Wang, Wang, and Li, 2000, consisting of one genus and two species, *Repenomamus robustus* Li, Wang, Wang, and Li, 2000 and *R. giganticus* Hu, Meng, Wang, and Li, 2005, are from the Early Cretaceous Yixian Formation, Liaoning, China (Li *et al*., 2000; Wang *et al*., 2001; Hu *et al*., 2005b), the same locality yielding *Gobiconodon zofiae* and *Meemannodon lujiatunensis*. *Repenomamus* is most similar to *Gobiconodon* but lacks an enlarged anterior incisor. The materials of *R. robustus* include nearly complete skeletons preserved in exceptional condition (Li *et al.*, 2000; Wang Y.-q. *et al*., 2001; Meng *et al*., 2003; Hu *et al*., 2005b). *R. giganticus* is so far the largest Mesozoic mammal with substantial remains (Hu *et al*., 2005b). The family status of Repenomamidae was challenged by Luo *et al.* (2003) and Kielan-Jaworowska *et al*. (2004); the later authors treated Repenomamidae as a junior synonym of Gobiconodontidae. In Kielan-Jaworowska *et al*. (2004: p 241), the diagnostic features for Gobiconodontidae include "i1, the only lower incisor, is procumbent and enlarged", "anterior molariform teeth replaced ontogenetically in a sequential fashion", and "upper molariforms wide transversely, with well-developed labial and lingual cingula and characterized by increasing triangulation of principal cusps from M1 to M5". None of these features is present in *Repenomamus*, which weakens the argument for placing the genus in Gobiconodontidae.

Some triconodonts were not assigned to any particular family. *Tendagurodon* Heinrich, 1998 is based on one lower tooth from the Upper Jurassic of Tendagura in Tanzania. The tooth has a high cusp a, small cusp b, and tiny cusp d but no cusp f. Kielan-Jaworowska *et al*. (2004) assigned the genus to Amphilestidae, but they were not certain about the monophyly of the family.

Jeholodens Ji, Luo and Ji, 1999 has one species, *J. jenkinsi*, with one skeleton from the third member of Yixian Formation, Liaoning, China. It was originally interpreted as the sister taxon of Triconodontidae, although not put in any particular triconodont family (Ji *et al*., 1999). Because the only reported specimen is squashed, not so well preserved as originally claimed, some key features interpreted by original authors are questioned by others (Rougier *et al*., 2001).

"Hakusanodon" appears in the cladogram of Rougier *et al*., 2001, but the taxon has not been described. It seems closely related to *Comodom* (*Phascolodon*). Matsuoka (2000) described an unnamed triconodont lower jaw from the Lower Cretaceous Kuwajima Formation of Japan.

Up to now, eight families and forty genera of early mammals with triconodont dentition have been documented, most of which have been regarded as members of Triconodonta. According to Simpson (1929), the taxonomic name "Triconodonta" was first used by Osborn (1888) as a hypothetical group ancestral to then known triconodonts and other mammals. Since then, the word "triconodont" became a vernacular morphological term and, by extension, as a name for any mammal with triconodont molars. Zittel (1893) first used Triconodonta as a suborder name. Osborn (1907) elevated the group to the ordinal rank. Simpson (1925, 1928, and 1929) revised the order and included one family Triconodontidae Marsh, 1887, with two subfamilies Triconodontinae Marsh, 1897 and Amphilestinae Osborn, 1888. Simpson (1945) elevated triconodontids and amphilestids into their own families. Kermack *et al*. (1973) placed Amphilestidae and Triconodontidae into a suborder Eutriconodonta and erected another suborder, Morganucodonta, to include the Rhaeto-Liassic triconodonts. Jenkins and Crompton

(1979), following Kermack *et al*., included all triconodonts into the order Triconodonta. In the last two decades, phylogenetic analysis of Mesozoic mammals revealed that triconodont mammals never form a monophyletic group (Rowe, 1988; Wible *et al*., 1995; Rougier *et al*., 1996a, b; Hu *et al*., 1997; Ji *et al*., 1999; Wang *et al*., 2001; Luo *et al*., 2001a; Kielan-Jaworowska *et al*., 2004). In most recent classifications of mammals, early triconodonts, i.e. sinoconodontids, morganucodontids, megazostrodontids, *Dinnetherium*, and *Hadrocodium*, have been excluded from Triconodonta (McKenna and Bell, 1997; Ji *et al*., 1999; Luo *et al*., 2002). Such redefined order Triconodonta is equal to Kermack *et al*.'s Eutriconodonta. Still, the monophyly of Triconodonta is not warranted. In a recent phylogenetic analysis of eutriconodont mammals, some amphilestids are clustered closer to spalacotheriid symmetrodonts than to other eutriconodonts (Rougier, *et al*., 2001). Kielan-Jaworowska *et al*. (2004) defined Eutriconodonta as a clade of mammals including the common ancestor of Triconodontidae and any taxa more close to the family than to morganucodontids, spalacotheriids, tinodontids, and multituberculates. Under such a formal definition, the monophyly of the taxon is insured, but its content is inevitably tied to the referred phylogeny.

The non-monophyletic nature of triconodonts did not affect the central role they play in the study of mammalian evolution, which has been realized since the first triconodont mammals was found (Owen, 1871; Jenkins and Crompton, 1979). Phylogenetic studies indicate that other major mammalian groups, i.e. docodonts, multituberculates, monotremes, and therians, probably all evolved from mammals with triconodont tooth pattern (Rowe, 1988; Wible *et al*., 1995; Rougier *et al*., 1996a, b; Hu *et al*., 1997; Ji *et al*., 1999; Wang Y.-q. *et al*., 2001; Luo *et al*., 2001a, 2002; Kielan-

Jaworowska *et al*., 2004). Any increase in the knowledge of triconodonts will help us in understanding the evolution of early mammals. Unfortunately, fossil records of triconodonts are still very scarce, given their long time range (See Kielan-Jaworowska *et al*., 2004 for an updated review). Our knowledge of most triconodonts is limited to dentitions. Only a few triconodonts are known from skulls; and even fewer triconodonts are known from skeletons. Lack of information in the skeletal morphology of triconodonts especially that of eutriconodonts, hampers efforts in searching the relationships of major mammalian groups. In recent phylogenetic studies, the relationships of multituberculates, monotremes, and eutriconodonts remain unstable (Hu *et al*., 1997; Ji *et al*., 1999 and 2001; Luo *et al*., 2001a, 2002; Wang Y. -q. *et al*., 2001). Missing information in triconodonts, as well as in other taxa, is an important factor making resultant phylogeny vulnerable. Considering the central role that triconodonts play in the mammalian phylogenetic study, the finding of nearly complete skeletons of *Repenomamus* in the Lower Cretaceous is significant progress in the study of triconodonts.

The postcranium is also the least known part of skeletal systems of Mesozoic mammals. Prior to the discovery of *Repenomamus*, only three eutriconodonts have postcranial elements found together with craniodental remains. *Jeholodens* has a skeleton preserved, but the specimen is squashed and split into two halves. Many structures, i.e., the shape of bones and articular surfaces, are distorted. The original authors (Ji *et al*., 1999) were only able to publish the reconstruction of the specimen. Further observation of the specimen indicated that much of information is missing or misinterpreted (Rougier *et al*., 2001). *Gobiconodon ostromi* has some postcranial elements preserved, but much of

the skeleton, including most of cervical vertebrae, most of post-thoracic part of the vertebral column, most of the scapula, sternum, manus and pes, are unknown. *Priacodon* has only part of the forelimb preserved. Early Jurassic triconodonts, i.e. morganucodontids and sinoconodontids, also have incomplete postcranial remains preserved. Jenkins and Parrington (1976) reconstructed the skeleton of morganucodontids, but the morphologies of the vertebral column, sternal apparatus, hand, and foot are largely unknown. Our knowledge on the postcrania of other Mesozoic mammals is also very limited. Only several groups have postcranial remains associated with craniodental fossils. *Haldanodon*, a late Jurassic docodont from Guimarota, Portugal, has a specimen with a few limb bones associated with the skull (Martin and Nowotny, 2000) and some isolated elements (Martin, 2005). *Fruitafossor windscheffeli,* a digging mammal of uncertain affinity recently found from the Upper Jurassic Morrison Formation, Colorado, USA, has a partial skeleton preserved (Luo and Wible, 2005). *Henkelotherium*, an eupantothere from the same locality as *Haldanodon*, has a skeleton with majority of postcranial elements preserved (Krebs, 1991). *Zhangheotherium*, a symmetrodont from Yixian Formation, Liaoning, China, has two skeletons reported, which are preserved in squashed condition and insufficiently exposed (Hu *et al*., 1997, 1998; Luo and Ji, 2005). Another symmetrodont, *Maotherium* Rougier, Ji and Novacek, 2003 from the same formation preserved a skeleton with only the dorsal side exposed (Rougier *et al*., 2003). Recently, Li and Luo (2006) reported a third symmetrodont, *Akidolestes cifellii*, from the Yixian Formation. It is known from one specimen preserved in a squashed condition. *Vincelestes*, a therian from the Lower Cretaceous La Amarga Formation of Argentina preserved many postcranial elements and allows reconstructing the skeleton (Rougier,

1993). Some Cretaceous multituberculates have postcranial elements preserved and allow reconstruction of the postcranial skeleton of multituberculates collectively (Kielan-Jaworowska and Gambaryan, 1994 and references therein; Kielan-Jaworowska *et al*., 2002; Hu and Wang, 2002). *Eomaia*, a purported eutherian (Ji *et al*., 2002), and *Sinodelphys*, a purported metatherian (Luo *et al*., 2003), both from Yixian Formation have squashed skeletons preserved, with only impressions preserved for most skeletal elements. Some eutherians and metatherians from the Cretaceous of Mongolia preserved postcranial skeletons (Kielan-Jaworowska, 1977, 1978; Szalay and Trofimov, 1996; Novacek *et al*., 1997; Horovitz, 2000, 2003). Some of these taxa has postcranial skeletons well preserved.

The significance of nearly complete skeletons of *Repenomamus* is obvious. With most elements accurately described, *Repenomamus* can serve as the morphotype for eutriconodonts, and, to some extent, for Mesozoic mammals. Such a morphotype will be an important source in studies of comparative anatomy and phylogenetic reconstructions among major mammalian groups, and for functional morphology and paleobiology studies.

2. MATERIALS AND METHODS

In the present study, the postcranial morphology of *Repenomamus* will be documented in detail; the anatomical comparison will be conducted in the format of character analysis across major clades of mammals and selected nonmammalian cynodonts; the phylogeny of Mesozoic mammals is generated with the data matrix of 57 taxa and 435 osteological characters. Well-preserved material and associated remains of other animals also allow us to estimate the body mass, diet, and habit of *Repenomamus*. Finally, one specimen of *R. robustus* preserved remains of the hyoid and larynx elements, which allows us to explore the respiratory physiology of the animal.

2.1 GEOLOGICAL BACKGROUND AND MATERIALS

This study is based on *Repenomamus* material in the collection of the Institute of Vertebrate Paleontology and Paleoanthropology (IVPP), Chinese Academy of Sciences in Beijing, China. All materials are collected during the last five years from the lowest part of the Yixian Formation in Lujiatun locality, Shangyuan, Beipiao City, Liaoning Province, China (Figure 2-1; Li *et al*., 2000; Wang Y. -q. *et al*., 2001; Zhou *et al*., 2003). The Yixian Formation consists mostly of deposits of weakly laminated to finely bedded siliciclastic sediments, including sandstones and shales intercalated with extrusive basalts and tuffs and crosscut by occasional dykes and sills. They represent low-energy freshwater lacustrine environments. The lowest part of the formation (Lujiatun bed of Zhou *et al*., 2003; Figure 2-2), cropping out in Lujiatun and neighboring areas, is composed of conglomerate, tuffaceous sandstone and tuff, which represent the early stages of the

Figure 2-1. Map of the fossil locality.

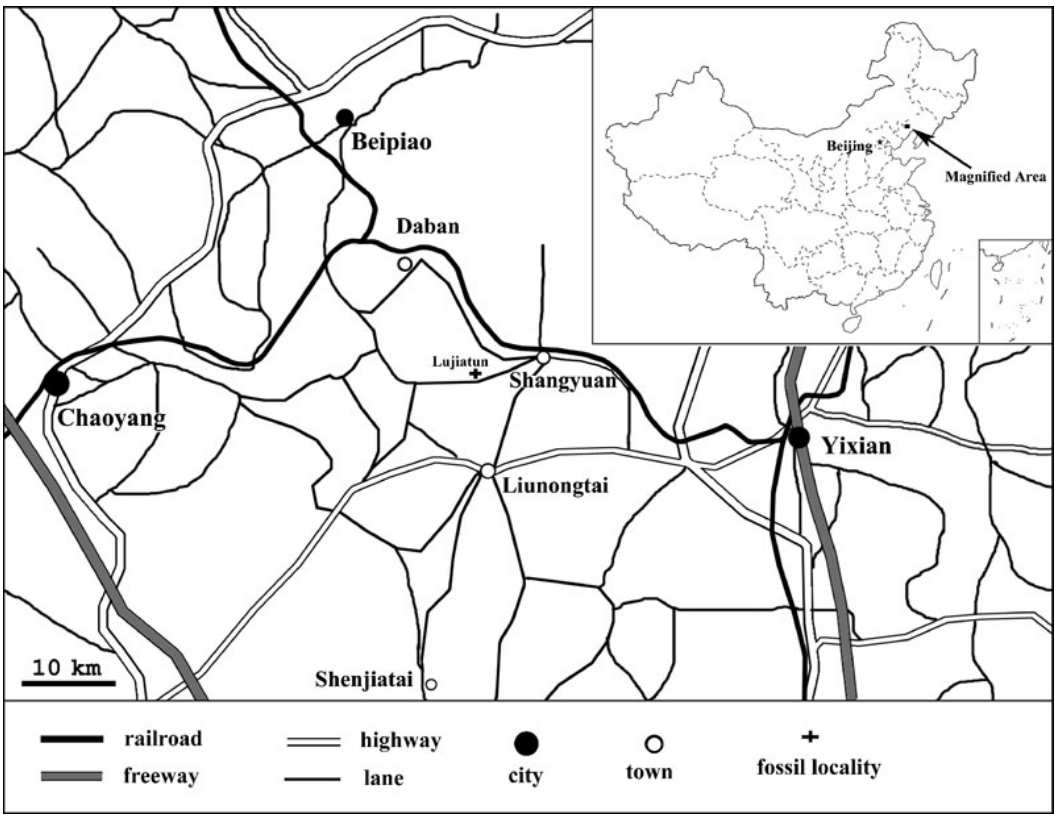

Figure 2-1

freshwater lake cycle and alluvial/fluvial faces (Wang S. -s. *et al*., 2001; Xu *et al*., 2002; Zhou *et al*., 2003). The radiometric analyses suggest that the age of this part of Yixian Formation is between 128 and 139 Myr, referral to Hauterivian stage in the geological timescale (Wang S. -s. *et al*., 2001; Zhou *et al*., 2003). Fossil materials from this part are recovered from the red or gray sandstone. Many vertebrate specimens are preserved three-dimensionally and in articulation. Some of them are even preserved in sleeping position (Xu and Norell, 2004). The fossil-bearing deposit in this locality lacks bedding structure, which suggests that the deposition and preservation of fossil materials in this locality are probably “resulted from a single, catastrophic, mass mortality event” (Zhou *et*

Figure 2-2. Stratigraphic log of Yixian and Jiufutang Formation in western Liaoning, China (modified from Wang and Zhou, 2003: figure 12). Mammals from the Jehol Fauna are indicated.

1, basalt and andesite with volcanic breccia; 2, conglomerate with volcanic breccia; 3, sandstone and conglomerate; 4, tuffaceous sandstone and tuff; 5, shale and tuff.

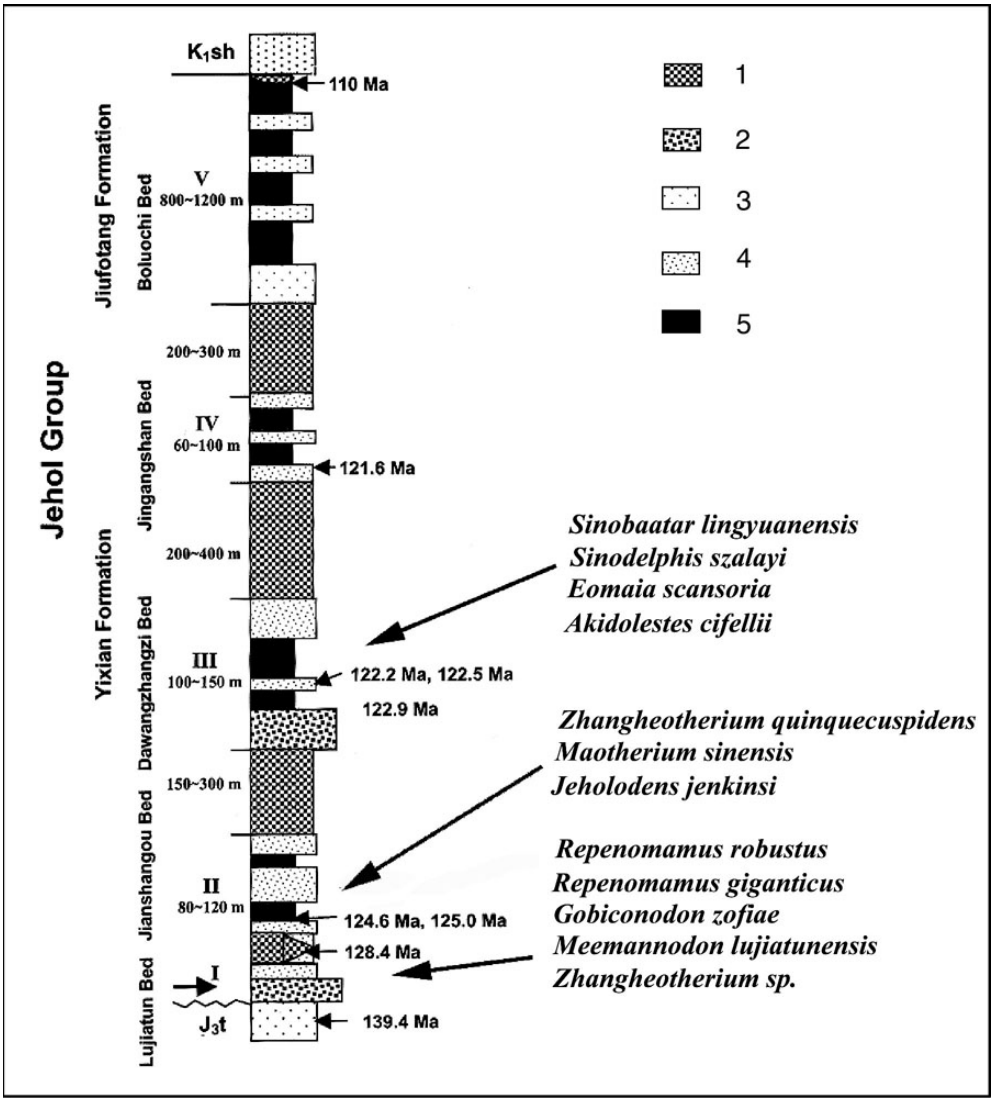

Figure 2-2

al., 2003). So far, the vertebrate fossils found from the locality include frogs (Anura indet.), squamates (Squamata indet.), dinosaurs (*Psittacosaurus sp*., *Liaoceratops yanzigouensis*, *Jeholosaurus shangyuanensis*, *Sinovenator changii*, *Incisivosaurus gauthieri, Dilong paradoxus, and Mei long,*), and mammals (*Repenomamus robustus, R. giganticus, Gobiconodon zofiae, Meemannodon lujiatunensis,* and *Zhangheotherium sp.*) (Zhou *et al*., 2003; Li *et al*., 2003; Xu *et al.*, 2004; Xu and Norell, 2004; Hu *et al*., 2005b; Meng *et al*., 2005).

Figure 2-3. Anterior half of the skeleton of *Repenomamus robustus*, IVPP V 12728, in dorsal view. The skull is removed.

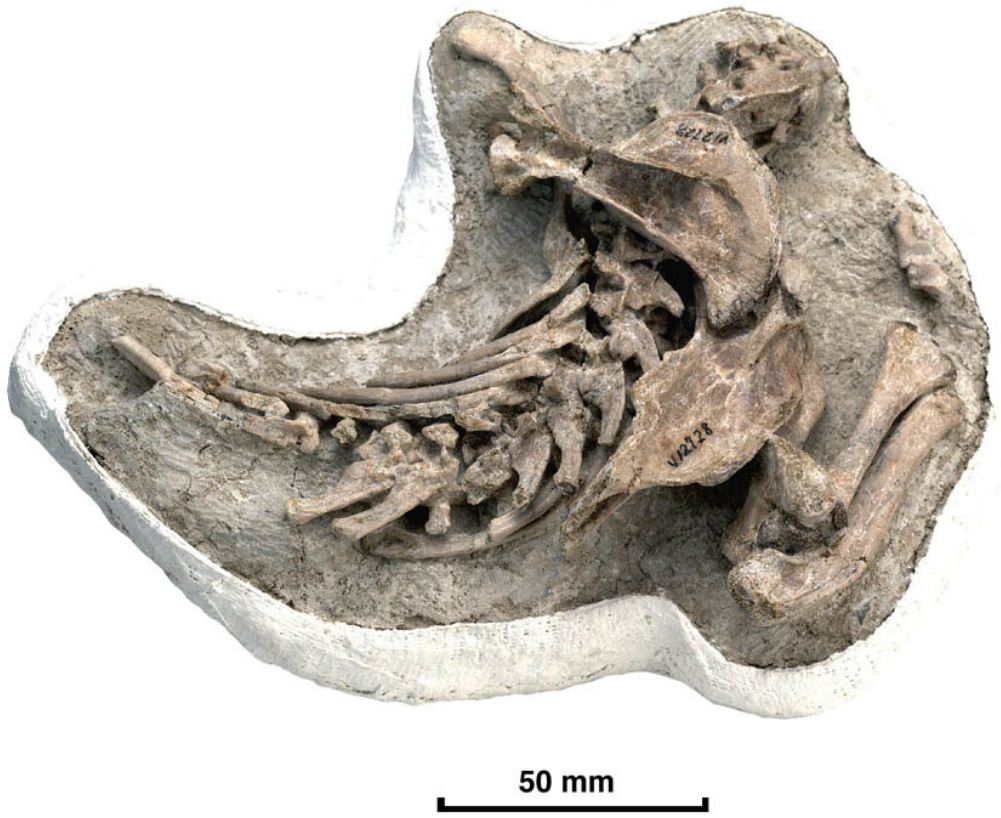

Figure 2-3

Figure 2-4. *Repenomamus robustus*, IVPP V 13605, ventral view of the postcranial skeleton. The scale bar is 50 mm.

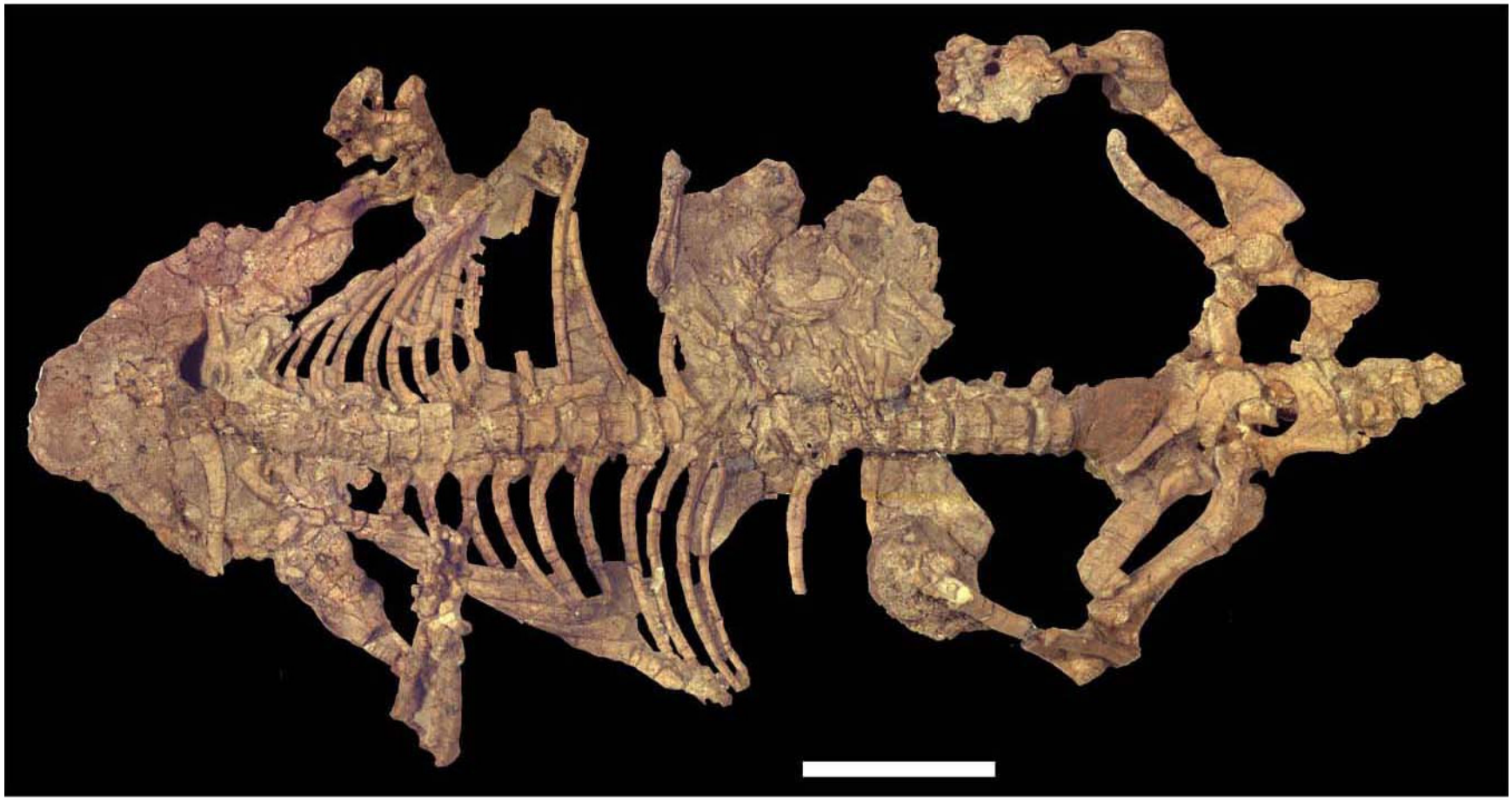

Figure 2-4

The postcranial materials of *Repenomamus* from the locality include four specimens of *R. robustus* (IVPP V12549 [holotype of *R. robustus*], partial postcranial skeleton associated with a complete skull with articulated lower jaws]; IVPP V12728, another partial postcranial skeleton associated with complete skull and articulated lower jaws [figure 2-3]; IVPP V 13605, a nearly complete postcranial skeleton associated with a

---

Figure 2-5. *Repenomamus giganticus,* IVPP V 14155, lateral view of the skeleton. C1, C10 and C 16, first, tenth and sixteenth caudal vertebrae; L6, sixth lumbar vertebra; Lr1, first lumbar rib; R1 an R2, first and second thoracic ribs; S1 and S3, first and third sacral vertebrae; T10 and T20, tenth and twentieth thoracic vertebrae.

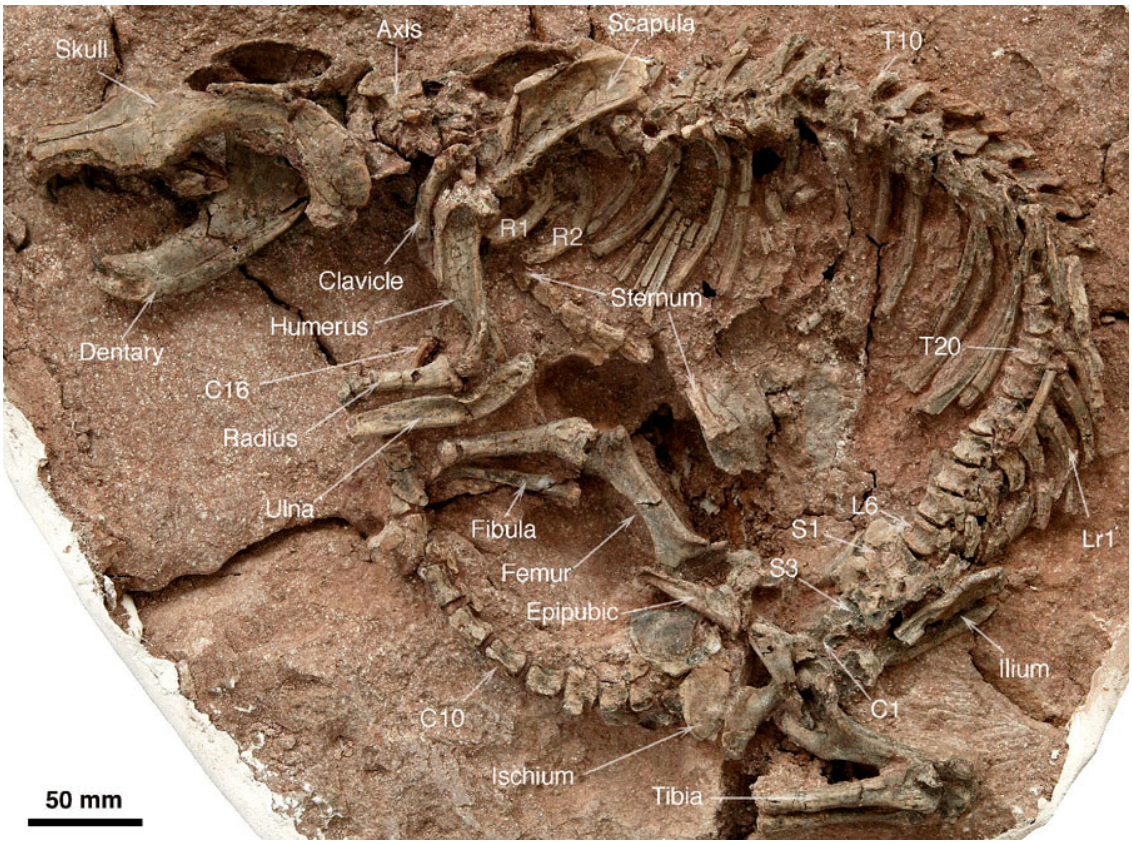

Figure 2-5

partial skull and left lower jaw [figure2-4]; and IVPP V 13606, partially preserved atlas and axis associated with the complete skull) and one specimen of *R. giganticus* (IVPP V 14155, holotype, figure 2-5). Other *Repenomamus* materials from the locality include IVPP V12613, 12732, 13066, three complete skulls with articulated lower jaws; IVPP V12585, a partial skull with articulated lower jaws; IVPP V13067, a complete skull; IVPP V13065, a partial skull; and IVPP V13068, a partial lower jaw.

2.2 METHODS

2.2.1 DETAILED DOCUMENTATION OF MORPHOLOGY

All of specimens have been prepared in the laboratory of IVPP and AMNH, using mechanic methods. Anatomical features are studied, drawn and photographed using a Nikon microscope equipped with camera Lucida attachments and RT Spot digital camera. Photographs are taken from original specimens, using 35-mm film camera to ensure the quality of images. Measurements are taken with the help of digital caliper.

From these specimens, morphologies of most aspects of postcranial skeleton, except some sacral vertebrae and some elements in manus and pes, are documented in photos and text. Description will include observable information of all preserved elements in details, aided with marked images in high resolution. Most elements in the postcranium can be observed three dimensionally. For instance, all tarsal elements are in articulation but are separated in preparation; thus, each element can be removed individually for observation in all surfaces.

2.2.2 CHARACTER ANALYSIS

Comparison among different taxa is the core of comparative biology. Character analysis, identifying characters and their states among related taxa, is a convenient way to conduct comparative study. A character comprises “two or more different attributes

(character states) found in two or more specimens that, despite their differences, can be considered alternate forms of the same thing (the character) (Platnick, 1979). The character state is heritable and group-defined (Schuh, 2000). In morphological level, a character hypothesizes the sameness and transformation of the corresponding anatomical parts of individuals among different taxa. Phylogenetic analysis also begins with character analysis. With the advances of methodological principles and applications of computer software, phylogenetic analysis has been widely accepted and used in systematic biology. However, the methodical issue of character analysis, the first step of every phylogenetic analysis, is yet to be investigated.

Character analysis, also called primary homology assessment, "has been considered subjective, contentious, under-investigated, imprecise, unquantifiable, intuitive, as a black-box, and at the same time as ultimately the most influential phase of any cladistic analysis" (Hawkins, 2000). This is exactly the situation we are confronted in the study on postcranial characters of Mesozoic mammals. Several studies on the phylogenies of Mesozoic mammals have included postcranial characters as part of data matrices (Rowe, 1988; Rougier, 1993; Hu *et al*., 1997; Ji *et al*., 1999, 2002; Luo *et al*., 2001a and b, 2002, 2003; Kielan-Jaworowska et al., 200; Luo and Wible, 2005; Li and Luo, 2006), but none of them presented detailed analysis of characters. Characters and states were just simply listed in the texts or appendices, with little explanation for the character definition and state demarcation being available. One of my goals in this study is to evaluate postcranial characters that have been used in the previous studies and to provide a set of clearly defined and well-explained character data for phylogenetic analysis and future reference.

A character hypothesizes a transformation between attributes (character states). One problem in character analysis is related to the absence/presence coding. Absence itself is a fuzzy coding, it may mean that there is no homologue to presence or simply that no homologue (that may exist) is specified (Nelson, 1994). For example, Character 119 of Kielan-Jaworowska *et al.* (2004) describes that in adult the proatlas neural arch is either (0) present or (1) absent. Here "absent" means that no homologous structure of the proatlas exists in taxa with this coding.

There is some dispute on the employment of presence/absence character in phylogenetic analysis. The main reason is that the absence coding violates the similarity criterion of Patterson (1982) and those who employ this approach to present characters deny the central role of comparative biology (Hawkins, 2000). Giving that a structure can degenerate in development, there is no reason to reject that a structure can disappear in evolution. One example is the limbless condition of snakes; most people agree that snakes evolved from legged animals. In other word, a structure in the ancestor can go absent in descendants; there is no reason to forbid using presence/absence characters in phylogenetic analysis. Of course, we should be cautious with paleontological data. In some case, absence means that no structure is directly observed while supplementary evidence implies the absence of the structure. In the above example, the proatlas of tritylodontids articulates with a pair of small facets on the neural arches of atlas; while in other taxa no proatlas are yet found and atlas arches are smooth without facets for proatlas. One alternate of above character is that proatlas is either (0) present and articulates with the atlas or (1) absent with no articular facet existing on atlas arches.

Some characters with presence/absence coding contain unspecified condition as

absence. Character 121 of Luo *et al*. (2002) describes that in adults atlas rib is either (0) present, or (1) absent. Here the "absent" most likely means that the same anlage, which develops into the atlas rib in some taxa, is fused with the pedicle of atlas and became part of transverse process in those without a separated rib. Therefore, a homologue for "presence" indeed exists, and it needs to be specified. An alternative for this character could be: Atlas rib is (0) articulated but not synotose with the pedicle or (1) fused with pedicle and becomes a part of transverse process.

One group of systematists, pattern cladists, does favor presence/absence coding. They regard presence of a character (observed similarities among taxa) as taxonomic homology, which is the only character information can be used for grouping (Patterson, 1982; Nelson and Platnick, 1991; Scotland, 2000; Williams and Sieber, 2000). They argued that characters as used in conventional cladistics practices involve unjustified assumptions on transformation of character states in addition to observed similarities, which is unnecessary for taxonomy (Nelson and Platnick, 1991; Brower, 2001). They developed a method, three-taxon statement analysis, to detect hierarchical relationships among taxa (Nelson and Platnick, 1991). The big ambition of pattern cladistics is to get rid of a prior assumption of evolution in systematics (Brower, 2000). But without an evolution assumption, i.e., descent with modification, a cladogram is simply a parsimonious grouping scheme based on shared similarities (Kluge, 2001). A theoretical framework is yet to be established before we can convert such a grouping scheme into a phylogenetic tree; and the latter is our ultimate goal to perform phylogenetic analysis. In addition, the approach of the three-taxon statement may use both plesiomorphic and apomorphic states to distinguish groups but excludes reversed states as apomorphies

(Farris *et al*., 2001). In this research, I will follow conventional approach and regard characters as homologues on sameness and transformation while keeping open eyes regarding their hypothetical nature.

In each of the previous studies (Rowe, 1988; Hu *et al*., 1997; Ji *et al*., 1999, 2002; Luo *et al*., 2001a and b, 2002, 2003; Kielan-Jaworowska et al. 2004; Luo and Wible, 2005), about 1/3 of postcranial characters employed are presence/absence characters. For example, Luo *et al*. (2002) listed 63 postcranial characters, 22 of them are presence/absence characters and need to be reexamined. Some other characters are also potentially problematic. For example, character 158 of Luo *et al.* combined two features, the shape of dorsal ischiatic margin and the development of ischiatic tuberosity into one character. Wilkinson (1995) called such coding approach as "composite coding". Most systematists avoid composite coding as it assumes a prior the interdependence of two potential characters (Hawkins, 2000).

In addition to reevaluate previous studies, this study on *Repenomamus* is expected to bring new information for character analysis. First, given the superb material of *Repenomamus*, it is expected to identify characters that are unavailable in other triconodont taxa. Particularly promising for the acquisition of new characters are the following anatomical regions: cervical vertebra, sternal apparatus, shoulder girdle, pelvic girdle, and ankle. Second, because of the articulated and complete material, some previously uncertain characters will become explicit, and new characters will be added to the list. A new data set will be generated that incorporates the new information. For completeness and for facilitating phylogenetic reconstruction, the data set will also comprise craniodental characters, which come from a joint project on the craniodental

morphology of *Repenomamus* by Drs. Jin Meng (AMNH), Yuanqing Wang, Chuankui Li (IVPP), and myself.

2.2.3. PHYLOGENETIC RECONSTRUCTIONS

The data set is constructed in Mesquite: a modular system for evolutionary analysis, version 1.06 (Maddison and Maddison, 2005a; http://mesquiteproject.org). The program is a free and open multi-platform software package for analysis in evolutionary biology, which is recently developed as the successor to MacClade by Maddison and Maddison. Its advantage in data set construction is that it allows adding notes, including images, for each data cell and therefore provides explicitness that is largely unavailable in most current data matrices built by other programs. With the new data set amassed, I will investigate phylogenetic relationships of major mammalian groups selected.

The data set will be further converted into the data matrix for phylogenetic analysis with MacClade 4.08 for OS X (Maddison and Maddison, 2005b). The computer program PAUP* 4.0b10 (Swofford, 2002) is employed to search the most parsimonious trees. Because of the new data from *Repenomamus*, triconodonts will be better represented, so that the phylogenetic resolution of mammalian groups will probably be better elucidated.

2.2.4 BODY MASS ESTIMATION

The excellent preservation of the *Repenomamus* remains allows me to estimate its body mass. Studies on extant mammals reveals that there are exponential relationships between body mass and dimensions of various skeletal elements (Alexander et al., 1979; Damuth and MacFadden, 1990; Silva and Downing, 1995). These relationships, expressed as empirical regression equations, are bases to estimate body masses of fossil

mammals, assuming that fossil and extant mammals have similar body mass-skeletal dimension relationships (Gingerich, 1990; Damuth and MacFadden, 1990). Here we employed two equations, one from Alexander *et al.* (1979) and the other from Van Valkenburgh (1990), to estimate the body mass of *Repenomamus.*

Alexander *et al.* (1979) explored the allometry of limb bones of terrestrial mammals and generated the standard allometric power equation $L = a (M)^b$, where L stands for either limb bone length or diameter (in mm) and M is for body mass (in kg). I use four dependent variables, femoral length and diameter and humeral length and diameter, to estimate the body mass of *Repenomamus.* The specific equations are:

Log (body mass) = (Log femoral length – Log 63)/0.36

Log (body mass) = (Log humeral length – Log 51)/0.36

Log (body mass) = (Log femoral diameter – Log5.2)/0.36

Log (body mass) = (Log humeral diameter – Log4.9)/0.38

The equation used by Van Valkenburgh (1990), Log (M) = a Log (L) + b, is derived exclusively from data of extant carnivores, where M is the body mass and L is the dependent variable such as skull length. We use two variables, the skull length and the head-body length, to estimate the body mass of *Repenomamus.* The specific equations are:

Log (body mass) = 3.13 x Log (skull length) - 5.59

Log (body mass) = 2.88 x Log (head-body length) - 7.24

The body mess of *Repenomamus* will be estimated with the above equations. The results are evaluated with reference to data from extant mammals with similar sizes.

2.3 TERMINOLOGY AND ABBREVIATIONS

In this study, the taxon Mammalia is defined as the latest common ancestor of *Sinoconodon*, *Morganucodon*, extant mammals, and all its descendants (Kielan-Jaworowska et al., 2004). Although the content of such a formalistic taxon is tied to the referred phylogeny, the extension of Mammalia remains relatively constant in most recent studies (Kielan-Jaworowska et al., 2004 and references therein). The term “mammal” is used as a traditional vernacular name, indicating any animal that belongs to Mammalia. The taxonomic name Theria is not used in this study, and the term "therian" is used as a vernacular name to refer to any mammal with reversed triangular cheek teeth. For example, extant marsupials and placentals are referred to as extant therians. The taxonomic name Triconodonta is abandoned. The term “triconodont” is used as a vernacular name, indicating any Mesozoic mammal with the triconodont teeth. I also use the name “eutriconodont” as a vernacular name to indicate those referred to Eutriconodonta of Kermack *et al*.

As Kielan-Jaworowska and Gambaryan (1994) indicated, the osteological terminology of major textbooks in vertebrate paleontology is different from that of *Nomina Anatomical Verterinaria*. The terminology of the latter is not followed either in several recent studies on the postcranial skeletons of Mesozoic mammals, i.e. Jenkins and Parrington (1976), Krause and Jenkins (1983), and Kielan-Jaworowska and Gambaryan (1994). The terminologies used in these studies are mainly descriptive, illustrating the shapes and sizes of the bones and structures on the bones. For facilitating comparison, I follow these studies (Jenkins and Parrington, 1976; Krause and Jenkins; 1983; Kielan-Jaworowska and Gambaryan, 1994) in description. However, the terminology for the pes

mainly follows that of Szalay (1994). Additional terms are from Evans (1993), Bernor *et al.* (1997) and, Muizon (1998) and indicated at first mentions.

Institutional abbreviations: AMNH—American Museum of Natural History, New York, USA; IVPP—Institute of Vertebrate Paleontology and Paleoanthropology, Chinese Academy of Sciences, Beijing, China.

3. DESCRIPTION

3.1 POSTCRANIAL AXIAL SKELETON

3.1.1 ATLAS-AXIS COMPLEX

Material

Most of the atlas-axis complex is preserved in IVPP V 12549, but the transverse processes in both vertebrae, the intercentrum of the atlas and the ribs of axis are missing. IVPP V 12728 preserves most of the left arch of the atlas and the whole axis except the right transverse process and ribs. IVPP V 13605 is a well-preserved skeleton of *Repenomamus robustus*, but the atlas-axial complex is totally missing. IVPP V 13606 has both arches of the atlas except the left transverse process and the anterior part of the axis preserved. The centrum of the atlas is preserved in all three specimens, and is fused with the centrum of the axis. IVPP V 14155 preserved both atlas and axis, but the ventral sides of the elements are not exposed.

Morphology

ATLAS (Figure 3-1, 3-2 and 3-3) **--**The atlas consists of four elements: the left and right halves of the neural arch, the intercentrum and the centrum. Two halves of the arch (figure 3-1: 1; figure 3-2: 1; figure 3-3: 1) are fused to each other in V 12549 and V 14155, but not so complete in V 13606 (figure 3-1: 2), which is from a younger and smaller individual than the former. The intercentrum is not preserved in specimens in which the ventral side of the bone is exposed, but the rough facets on the ventral extremity of the arch (Figure 3-1: 4; figure 3-3: 5) indicate the existence of the element. The articular facet on the ventral side of the dens (see below) also suggests the presence

of the element. The intercentrum is wide and short, judged by the space between ventral extremities of the arches. The centrum of the atlas is fused with that of the axis, forming the anterior half of the axial body.

The pedicles of the neural arch (figure 3-1: 7; figure 3-3: 8) bear two smooth articular facets on their medial side, a larger cranial facet (Figure 3-1: 3; figure 3-2: 2; figure 3-3: 2) and a smaller caudal facet (figure 3-1: 5; figure 3-3: 6). The cranial facet articulated with the occipital condyle in life. The lateral edge of the facet is elevated and forms a bony wing extending well beyond the anterior edge of the neural arch. The facet is concave and moderately deep. It faces more medially than anteriorly, and also slightly ventrally with the dorsal portion of the lateral edge elevated higher than the ventral portion. The lateral vertebral foramen (corresponding to intervertebral foramen between posterior vertebrae) is not complete. A notch (Figure3-1: 6; figure 3-3: 4) between dorsal edge of the cranial articular facet and the anterior edge of the neural arch represents part of the foramen, which was probably enclosed by ligaments in life, as seen in some specimens of *Didelphis*.

Figure 3-1. Atlas and axis of *Repenomamus robustus*, IVPP V 13606. The anterior (A), posterior (B), dorsal (C), ventral (D), and lateral (E) views of atlas, missing the intercentrum; and ventral (F), lateral (G), anterodorsal (H), and dorsal (I) views of axis.

1, neural arch; 2, suture between left and right halves of neural arch; 3, cranial articular facet; 4, facet for intercentrum; 5, caudal articular facet; 6, notch representing lateral vertebral foramen; 7, pedicle of neural arch; 8,

lamina of neural arch; 9, transverse process; 10, alar notch; 11, centrum of atlas; 12 dens; 13, trace of suture between atlantal and axial centra; 14, centrum of axis; 15, nutrient foramen on dorsal surface of atlantal centrum; 16, facet on dens for atlantal intercentrum; 17, facet for neural arch of atlas; 18, pedicle of axis, 19, dorsal root of axial transverse process; 20, anterior vertebral notch; 21, lamina of axial neural arch; 22, axial spinous process.

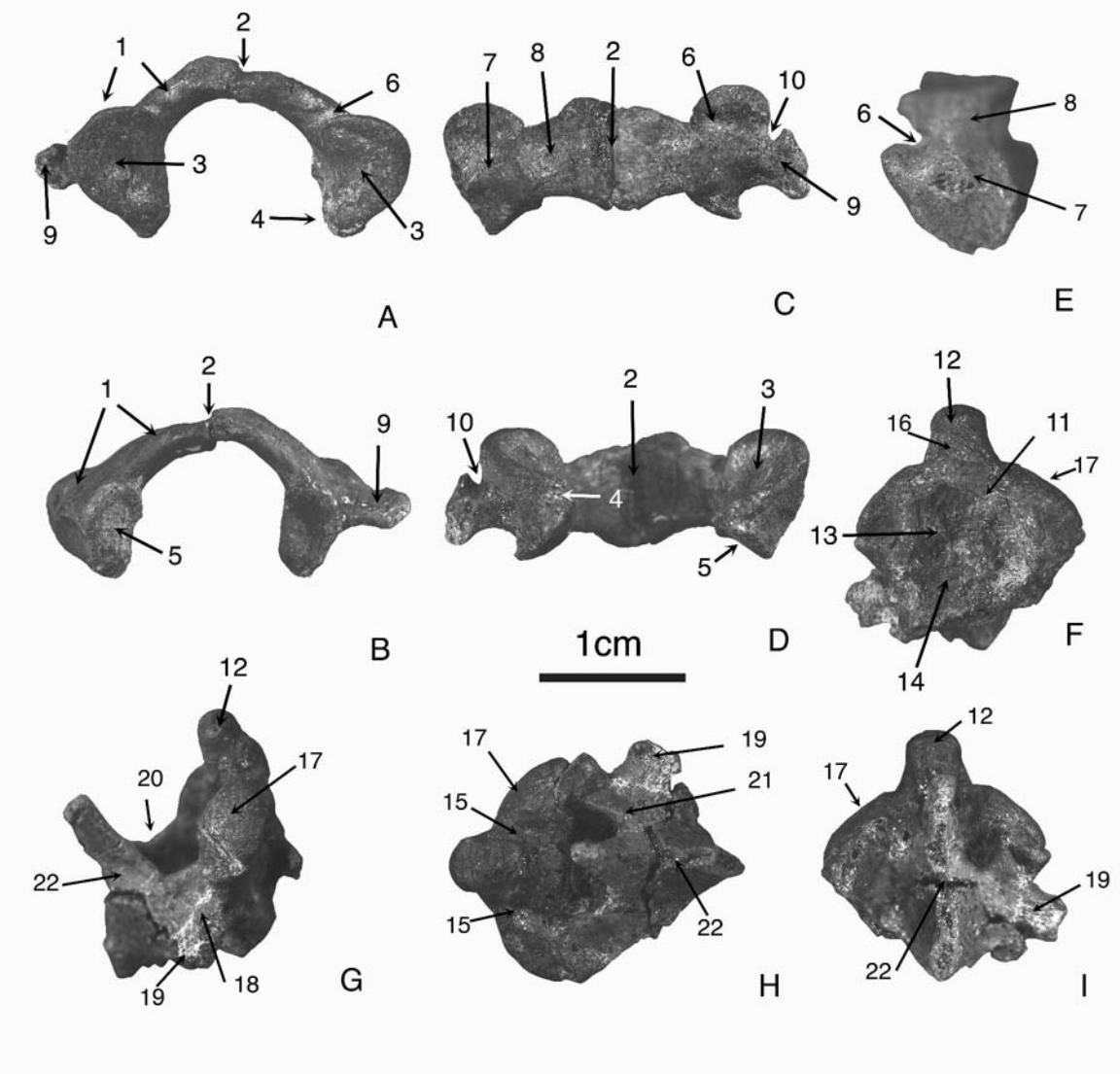

Figure 3-1

The caudal facet (figure 3-1: 5; figure 3-3: 6) articulated with the centrum of the atlas in life. It is smaller and less concave than the cranial facet. Its lateral edge extends beyond the posterior edge of the neural arch, to a lesser degree than that of the cranial facet. It faces posteromedially, in an angle of about 45˚ with the sagittal plane. There are some small pits on the medial side of the neural arch (figure: 3-3: 7), just above the articular facets. These pits are probably for the attachment of the transverse atlantal ligament, which helped the atlas to hold the dens of axis in life.

The edges of the lamina (figure 3-1: 8; figure 3-2: 3; figure 3-3: 1) of the neural arch (the portion of the arch above the pedicle) are smooth, there is no trace of pre- and postzygapophysis as seen in more posterior vertebrae; and no facet for the proatlas is visible either on the arch. It is assumed that the proatlas, often seen in nonmammalian cynodonts (Jenkins, 1971), is absent in *Repenomamus*. The left and right laminae are fused together in adults but still have suture between them in sub-adult individuals (figure 3-1: 2). The lamina is constricted at its base and becomes wider dorsally. The maximal anteroposterior length of the lamina is at the midline where the left and right laminae are fused and form small anterior and posterior tubercles. The anterior edge is roughly straight while the posterior edge is gently curved, forming the anterior notch of the second intervertebral foramen. There is no spinous process above the neural arch.

Figure 3-2. Atlas and axis of *Repenomamus robustus*, IVPP V 12549, in dorsal (A), ventral (B), lateral (C), posterior (D), and anterior (E) views. 1, neural arch; 2, cranial articular facet; 3, lamina of neural arch; 4, centrum of atlas; 6, centrum of axis; 6, dens; 7, facet for neural arch of atlas; 8,

ventral crest; 9, posterior extremity of ventral crest; 10, posterior view of the axial ventral body; 11, axial spinous process; 12, vertebral foramen; 13, lateral depression on ventral surface of axial body; 14, ventral root of transverse process of axis; 15, nutrient foramen on dorsal surface of atlantal centrum; 16, pedicle of axis.

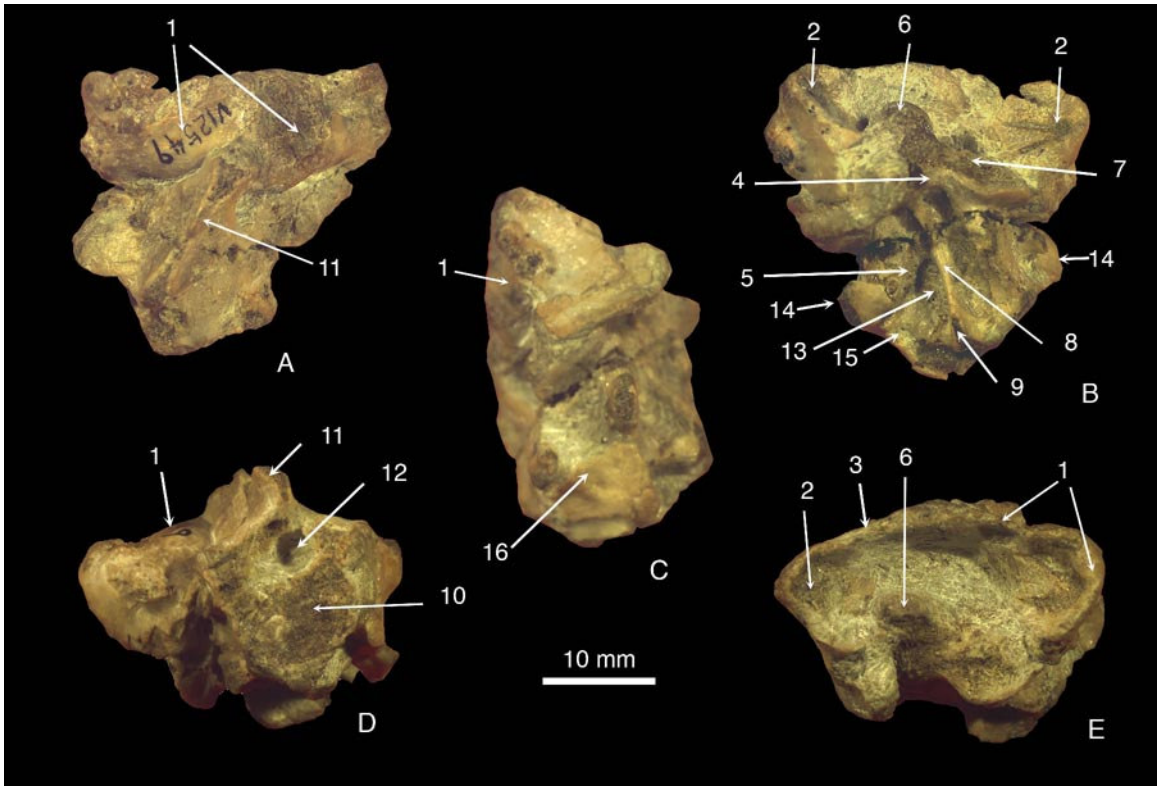

Figure 3-2

The transverse process of the atlas extends laterally from the middle of the pedicle (figure 3-1: 9; figure 3-3: 3). The process is dorsoventrally compressed and anteroposteriorly expanded, with the anterior edge slightly higher than the posterior one. However, the process, as a whole, does not expand beyond the levels of the anterior and posterior edges of the neural arch and does not have a wing-like shape as seen in many later mammals. The lateral extremity of the process is partially broken in all specimens

where this part is known. It is unlikely that a separate atlantal rib is present because there is no distinct articular facet at the extremity of the transverse process. The process is constricted near its base. A pit on the dorsal side of the process near the base of the process indicates the presence of a vascular foramen, but it is unlikely that there is a transverse foramen penetrating the process because the pit is very small and there is no corresponding anterior foramen present.

Figure 3-3. Atlas fragment of *Repenomamus robustus*, IVPP V 12728, in lateral (A), anterior (B) and medial (C) views.
1, lamina of neural arch; 2, cranial articular facet; 3, transverse process; 4, notch representing lateral vertebral foramen; 5, facet for intercentrum; 6, caudal articular facet; 7, pits for ligaments.

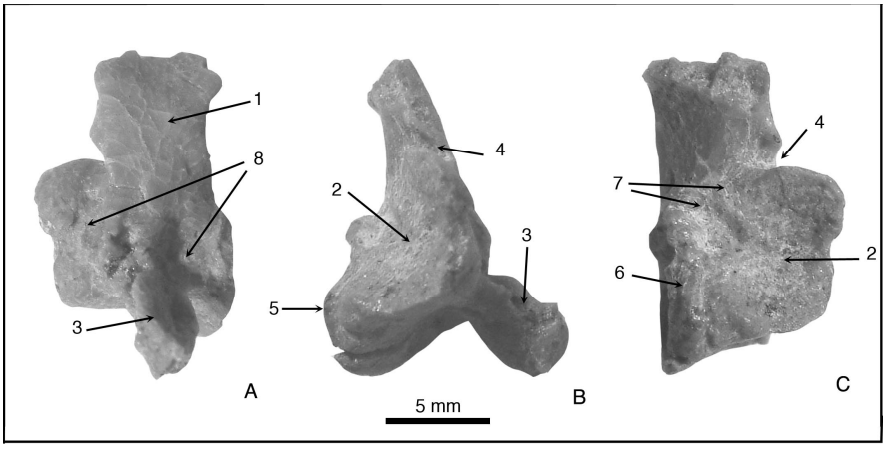

Figure 3-3

A distinct notch is present between the transverse process and the lateral edge of the anterior articular facet; this is the alar notch (figure 3-1:6; figure 3-3: 4; Evans, 1993: p 169), which connects with the notch of the lateral vertebral foramen through a groove on the lateral surface of the neural arch. The notches and the groove probably

accommodated a vertebral artery and the first cervical nerve in life, as seen in extant mammals (Evans, 1993: p624).

AXIS--The body of the axis consists of a centrum of the atlas and axis (figure 3-1: 11, 14; figure 3-2: 4, 5; figure 3-4: 2, 3). Two elements are fused, but the trace of the suture on the ventral surface of the axial body is visible (figure 3-1: 13; figure 3-4: 4). The body is dorsoventrally compressed and laterally expanded. In ventral view, there is a prominent ventral crest (figure 3-2: 8; figure 3-4: 6; midventral keel in Kühne, 1956) along the entire length of the body. The crest is not distinct in sub-adult individual (figure 3-1: F). The posterior extremity of the crest forms a distinct tubercle projecting posteroventrally (figure 3-2: 9; figure 3-4: 7). Along each side of the crest is a deep lateral depression (figure 3-2: 13; figure 3-4: 8). The depression is probably for the attachment of the longus colli muscle, an important flexor of the neck and head (Evans, 1939: p74; Muizon, 1998: p48). In V 12728, a transverse crest is developed in the middle of both depressions and crosses the ventral crest (figure 3-4: 4). This transverse crest is corresponding to the boundary between the centrum of the atlas and axis, and represents the trace of the suture between two structures, but no distinct suture is discernible, unlike in some marsupials (Muizon, 1998: p48). There is no trace indicating the presence of a distinct axial intercentrum between two centra, the element probably was degenerated or incorporated into the axial body during development. The transverse crest is only weakly developed in V 12549 (figure 3-2B) and V 13606 (figure 3-1: 13). The lateroventral edge of the axial body is thick, extending posterolaterally. Backward from the level of the transverse crest, the thickened edge is apart from the body and connects with the latter through a thin bony sheet (figure 3-4: 10). The thick edge forms the ventral root of the transverse process

(figure 3-2: 14; figure 3-4: 9). Its posterior extremity is rough, projecting posterolaterally, and contacting the axial rib in life. The edge and the bony sheet are probably partially correspondent to the inferior lamella of extant mammals, as often seen in postaxial cervical vertebrae, especially the sixth cervical vertebra, of extant mammals (Flower, 1870: p22; see character analysis for further discussion). In V 13606, the lateral edge is short and apart from the body just posterior to the level of the transverse crest; and the bony sheet is also small. In the middle of the dorsal surface of the axial body a transverse suture, corresponding to the transverse crest on the ventral surface, indicates the boundary of the atlantal and axial centra, and suggests the incomplete synosteosis of two elements in this young individual. A pair of foramina is present on the dorsal surface of the atlas centrum (figure 3-1: 15; figure 3-4: 11). Each foramen has a sulcus extending anteriorly to the junction between the anterior articular facet and the dens. A pair of similar foramina is also present on the dorsal surface of the axial centrum. They are probably just nutrient foramina, as in other mammals (Kielan-Jaworowska, 1989: p78) and nonmammalian cynodonts (Jenkins, 1971: p14). The vertebral foramen of the axis is roughly semi-circular.

Figure 3-4. Axis of *Repenomamus robustus*, IVPP V 12728, in ventral (A), lateral (B) and dorsal (C) views. The scale bar is 10 mm.

1, dens; 2, centrum of atlas; 3, central of axis; 4, crest and trace of suture between atlantal and axial centra; 5, ventral extension of articular facet for intercentrum of atlas; 6, ventral crest; 7, posterior extremity of ventral crest; 8, lateral depression; 9, ventral root of transverse process of axis; 10, bony

sheet connecting the ventral root of transverse process and vertebral body; 11, nutrient foramen on the dorsal surface of atlantal centrum; 12, facet for transverse atlantal ligament; 13, facet for neural arch of atlas; 14, pedicle of axis; 15, dorsal root of axial transverse process; 16, anterior vertebral notch of axis; 17, posterior vertebral notch of axis; 18, lamina of axial neural arch; 19, postzygapophysis of axis; 20, axial spinous process; 21, fragment of left axial rib.

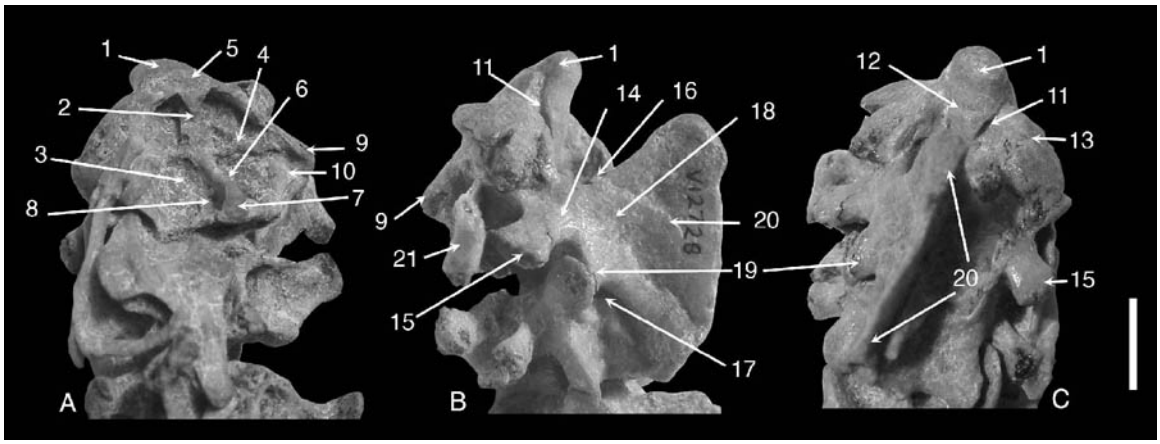

Figure 3-4

The dens of the axis is stout, pointing anterodorsally (figure 3-1: 12; figure 3-2: 6; figure 3-4: 1). It is roughly trapeziform in dorsal and ventral views and wedge-shaped in lateral view. The tip of the dens points anterodorsally. Its articular facet for the intercentrum of the atlas is gently convex and faces anteroventrally (figure 3-1: 16; figure3-4: 5). The dorsal surface of the dens next to the tip is flattened and rough, indicating the attachment of the apical ligament of the dens in life, as in recent mammals (Evans, 1993: p228). Posteriorly, there is a shallow saddle-shaped facet on the dorsal surface of the dens, which was probably for the crossing of transverse atlantal ligament in life (figure 3-4: 12). The facet is less developed in V 13606 than in V 12549 and V 12728,

probably due to its younger age than the latter. The similar facet was seen on the dens of morganucodontids (Jenkins and Parrington, 1976: p392).

Posterolateral to the dens is a broad convex articular facet on the anterior surface of the axis body (figure 3-1: 17; figure 3-2: 7; figure 3-4: 13). The facet is for articulation with the neural arch of the atlas. It is larger than its counterpart, the caudal facet on the neural arch of the atlas. The outline of the facet is roughly long oval, with an oblique long axis (having an angle of about 45˚ with the direction of vertebral column). The ventral, posterior and dorsal edges of the facet exceed beyond the range of the axial body. Anteromedially, the facet is confluent with the articular surface on the dens. Posterolaterally, the facet extends beyond the suture between atlantal and axial centra and covers the anterior base of axial neural arch laterally.

The pedicle of the axial neural arch is much shorter than the body (figure 3-1: 18; figure 3-2 16; figure 3-4: 14). It rises dorsally from the lateral edge of the axial centrum. In the middle of the lateral side of the pedicle there is a stout projection, directing lateroposteriorly and slightly ventrally. This is the dorsal root of the axial transverse process, which supported the axial rib in life (figure 3-1: 19; figure 3-4: 15). The anterior vertebral notch (figure 3-1: 20; figure 3-4: 16) is shallow than the posterior one (figure 3-4: 17). The lamina of the neural arch is thinner than the pedicle (figure 3-1: 20; figure 3-4: 18). There is no prezygapophysis. The postzygapophysis is stout, protruding posterolaterally form the posterior edge of the lamina (figure 3-4: 19). The facet of the postzygapophysis faces laterally, and slightly ventrally. The distance between left and right postzygapophyseal facets is about the width of the axial centrum.

The large axial spinous process forms a rough triangle in lateral view (figure 3-1:

22; figure 3-2: 11; figure 3-4: 20). The anteroventral edge arises from the confluence of the anterior edges of the left and right laminae of the neural arch. It is straight in lateral view, and has a gently flat surface in anterior aspect. It has an angle about 50˚ with the axis of the vertebral column. The anterodorsal corner of the spinous process is thickened, extending anteriorly to the level of the base of the dens. The posteroventral edge of the process is also straight, forming an angle of about 40 ˚ with the axis of the vertebral column. The posterodorsal corner of the process extends far beyond the posterior edge of the axial body; it even overhangs most of the third cervical vertebra in the articulated specimen of V 12728 (figure 3-4: B, C). The dorsal edge of the process is thin and straight. The lateral surface of the process is concave. In lateral view, the whole process looks like a thin bony fan supported by two thickened edges.

The axial rib is not well preserved in any specimen. In V 12728 part of the left rib is preserved between the roots of the transverse process (figure 3-4: 21). It is a bony sheet with a thickened edge on one side, and the other side of the sheet is broken. There is probably another thickened edge on the other side. The two thickened edges converge distally, and diverge proximally with the bony sheet between them. The proximal ends of the edges articulate with the roots of the transverse process and enclose a large transverse foramen between them. This reconstruction of the axial rib accords with the direction of two roots of the transverse process. A similar two-edged rib is present in more posterior cervical vertebrae (see below). Since the dorsal root of the transverse process extends to the level of the posterior edge of the axial body, it is estimated that the axial rib projects posteriorly well beyond the posterior edge of the axial body.

3.1.2 POSTAXIAL CERVICAL SERIES

Materials

V12728 preserves articulated postaxial cervicals except tips of their spinous processes. The ribs of the sixth cervical and the right rib of the seventh cervical are also preserved. Several posterior postaxial cervicals are also preserved in V 13605, but none of them preserves detailed morphology. V 14155 has all postaxial cervical vertebrae preserved, but only partially exposed.

Morphology

THE POST-AXIAL CERVICAL VERTEBRAE (C3-C7) (figure 3-5)--*Repenomamus* has five post-axial cervical vertebrae (C3-C7; figure 3-5: 2-6), which are generally similar and show morphological gradient. The vertebral body is broader than long (figure 3-5: 7). The ventral surface of the body has a strong relief, and a very strong ventral crest is developed along the midline (figure 3-5: 8). There is a deep depression (figure 3-5: 9) on each side of the crest, probably for the attachment of the longus colli muscle, as in some marsupials (Muizon, 1998: p49). The posterior tubercle (figure 3-5: 10; the posterior extremity of the ventral crest) is best developed on the third cervical vertebra, which is yet smaller than that on the axis. The tubercle becomes smaller posteriorly. The sixth and seventh cervical vertebrae don't have a posterior tubercle; the latter has a small anterior tubercle (figure 3-5: 11) at its anterior extremity of the ventral crest, which is absent in more anterior cervicals. The inferior lamella is well developed on the postaxial cervicals, protruding lateroventrally from the cervical body (figure 3-5: 12). On C3-C6, the lamella arises along the whole length of the body. It is constricted in the middle part, and further widened and thickened at the edge, with a tip pointing anteriorly and slightly ventrally.

The posterior end of the thickened edge bears a rough facet (figure 3-5: 13), facing posterodorsally. The inferior lamella is the ventral root of the transverse process, and articulated with the cervical rib in life. From C3 to C6, the lamella and the edge are gradually enlarged. On C7 the inferior lamella arises from the anterior half of the body and is less developed than those of more anterior cervicals. In posterior view, the body of seventh cervical roughly forms a laterally wide oval; with pedicles arise dorsally from the lateral edges. The posterior surface of the body is flat.

Figure 3-5. Postaxial cervical vertebrae of *Repenomamus robustus*, IVPP V 12728, in laterodorsal (A), dorsal (B), ventral (C), and lateroventral (D) views. Axis (C2) is also preserved in articulation. The scale bar is 20 mm. 1, axis (C2); 2, third cervical vertebra (C3); 3, fourth cervical vertebra (C4); 4, fifth cervical vertebra (C5); 5, sixth cervical vertebra (C6); 6, seventh cervical vertebra (C7); 7, vertebral body of C5; 8, ventral crest of cervical vertebra C4; 9lateral depression on the ventral surface of vertebral body of C4; 10, posterior tubercle on ventral surface of vertebral body of C3; 11, anterior tubercle on ventral surface of vertebral body of C7; 12, inferior lamella of cervical vertebrae; 13, facet on the inferior lamella for the cervical rib; 14, pedicles of cervical vertebrae; 15, cranial vertebral notch of C6; 16, caudal vertebral notch of C6; 17, dorsal root of right transverse process of C3; 18, lamina of neural arch of C4-C6; 19, prezygapophysis of C5; 20, postzygapophysis of C5; 21, spinous processes of C3-C7; 22, right rib of C6.

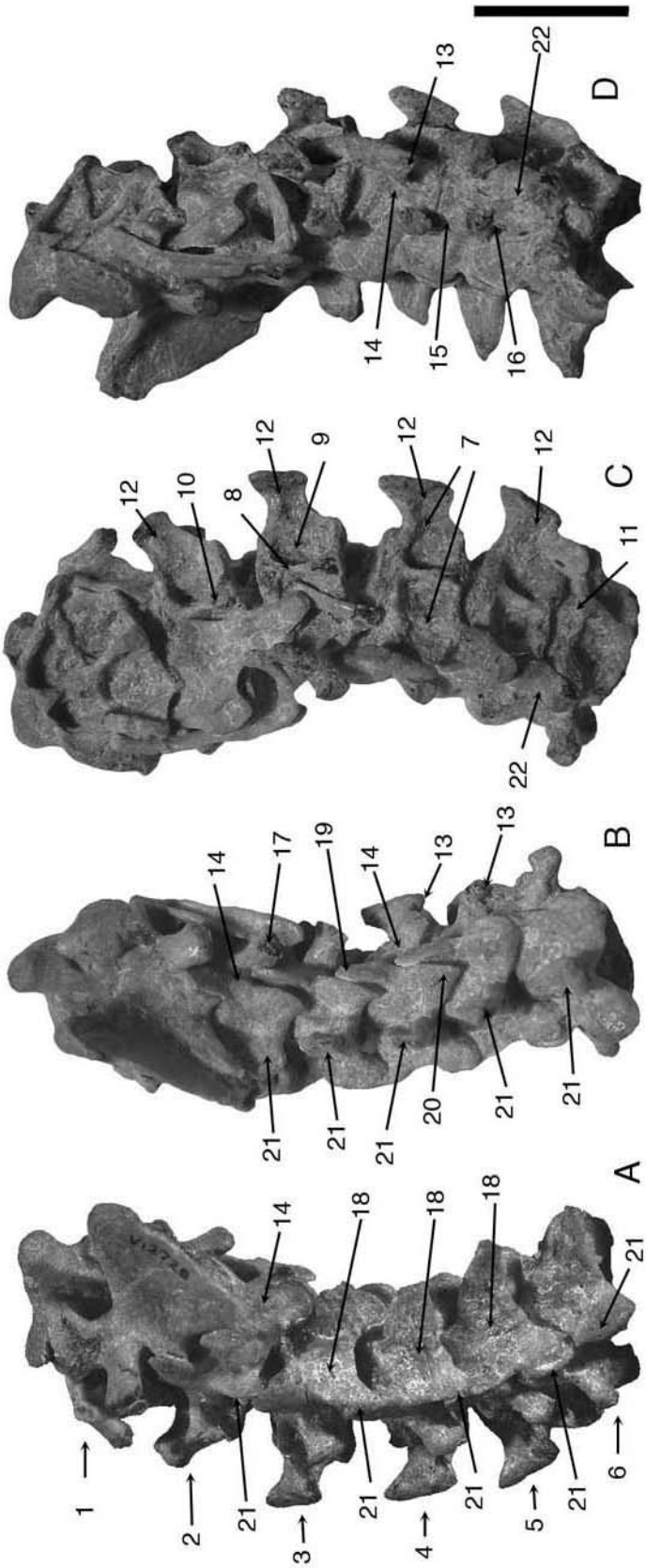

Figure 3-5

The caudal costal fovea on the posterolateral corner of the body of C7 (for the head of first thoracic rib) is indistinct. The bodies of the more anterior cervicals, not exposed in posterior (or anterior) view, probably have the same shape. In V 12728 the vertebral foramen of C7 is exposed posteriorly. It is semi-circular in shape, and smaller than that of the axis.

The pedicles are shorter than the body on postaxial cervicals (figure 3-5: 14). They are indented with cranial and caudal vertebral notch, of which the former is more deeply incised (figure 3-5: 15, 16). The dorsal root of the transverse process forms a stout projection on the lateral side of the pedicle (figure 3-5: 17). On C3 - C6, the root protrudes lateroventrally and slightly posteriorly, with a facet on the tip for the cervical rib. The root on C7 is larger than that on more anterior cervicals, and projects laterally, with the facet for cervical rib faceing lateroventrally.

The lamina is anteroposteriorly expanded on C3-C7 and nearly as long as the body; and in C7 a small portion of the lamina overhangs the posterior edge of the vertebral body (figure 3-5: 18). The prezygapophysis (figure 3-5: 19) protrudes from the lamina anterolaterally while the postzygapophysis (figure 3-5: 20) posterolaterally, to a similar degree. The articular facet on the prezygapophysis of C3 faces medially, while that on the postzygapophysis faces ventrolaterally. On other cervicals (C4-C7) the facet of the prezygapophysis faces dorsomedially, and that of the postzygapophysis faces ventrolateriorly. The facets become more horizontally oriented in more posterior vertebrae. The lateroventral surface of the prezygapophysis is convex, which becomes more prominent posteriorly, but there is no distinct mamillary process developed on any cervical vertebra, neither the accessory process.

The spinous process is well developed on all postaxial cervicals and arises from the entire length of the neural arch (figure 3-5: 21). The process of C3 is lower but thicker than those of more posterior cervicals, and dorsally covered by the spinous process of the axis. Its posterior side forms a convex surface, while its anterior edge is hidden below the spinous process of the axis in the articulated specimen (V12728). The anterior edge of the spinous process on C4-C7 is sharp, convex with an indentation at the base. The posterior side of the process forms a vertical surface with a vertical median notch at the base, which could accommodate the anterior edge of the next posterior process. In lateral view the process tapers dorsally with a more or less vertical posterior edge and oblique anterior one. The anterior edge becomes more oblique on posterior cervicals.

CERVICAL RIBS (figures 3-5, 3-6)--In V 12728, the ribs of the sixth cervical vertebra (figure 3-5:22) and the right rib of the seventh cervical vertebra (figure 3-6: 1) are well preserved. The rib of C6 comprises of two short, laterally compressed edges, which are connected distally and diverge proximally. The proximal ends of the edges articulate with two roots of the transverse process, respectively, and enclose a large transverse foramen. The rib extends posteriorly beyond the posterior rim of the vertebral body. Ribs of C3-C5 are not preserved. Since the roots of the transverse process on these vertebrae are quite similar to those on C6, it is likely that the ribs are also developed on these vertebrae, with the morphology similar to those of C6. The rib of C7 is more similar to thoracic ribs than to those of C6. It is elongate and curved, with its proximal end being anteroposteriorly compressed and dorsoventrally expanded. Two facets on its proximal extremity articulate with two roots of the transverse process, respectively. The distal end of the rib is pointed. In the middle of the rib there is a distinct node on the anterior surface. Since the inferior

lamella of C7 is more anteriorly positioned than the dorsal root, the rib must have pointed ventrolaterally and slightly anteriorly in life.

3.1.3 THORACIC SERIES

Materials

The skeleton of V 13605 preserves all thoracic vertebrae, most of which bear ribs through a double-headed articulation. V 12728 preserves T1-T8, which are in articulation with the cervicals; five middle thoracics are disarticulated and only partially preserved. V 12549 preserves fourteen thoracics in articulation and two isolated anterior thoracics. Most articulated elements have ribs associated with them. Judged by their similarity to the articulating vertebrae of V 13605 and V 12728, the articulating thoracics are probably T8-T20; and anterior vertebrae are probably T2-T3. V 14155 preserves all thoracic vertebrae in articulation, but only partially exposed.

V 12549 preserves many of its thoracic ribs, and as preserved, some middle and posterior ribs are articulated with their corresponding vertebrae. In V 12728 ribs of several anterior thoracics are preserved *in situ*. Most thoracic ribs in V 13605 are also preserved *in situ*. In V 14155 about a dozen of thoracic ribs are preserved in situ and some rib fragments are preserved near the vertebral column.

Morphology

Repenomamus has 26 dorsal vertebrae (thoracics + lumbars). The transition from thoracic region to lumbar region is gradual in vertebra morphology. The major difference between the two regions is in their ribs. The thoracic ribs are long and usually round in cross section for most of their lengths, while the lumbar ribs are short and dorsoventrally flat, anteroposteriorly expanded and tapering distally. The thoracic rib moveably

articulates with vertebrae through either dual articulations, the tuberculum with the transverse process on the pedicle and the head with the bodies, or singular articulation with the transverse process. The lumbar rib has the two articulations merging together and partially fused with the transverse process. Judged by the rib morphology, *Repenomamus* has 20 thoracic vertebrae, more than most other mammals do (Flower, 1870).

Figure 3-6. Anterior part of thoracic series, right rib of seventh cervical vertebra and sternal elements of *Repenomamus robustus*, IVPP V 12728, in dorsolateral (A), lateral (B), ventral (C), and dorsal (D) views.
1, right seventh cervical rib; 2, first thoracic vertebra (T1); 3, second thoracic vertebra (T2); 4, third thoracic vertebra (T3); 5, fourth thoracic vertebra (T4); 6, fifth thoracic vertebra (T5); 7, sixth thoracic vertebra (T6); 8, seventh thoracic vertebra (T7); 9, eighth thoracic vertebra (T8); 10, ventral crest of T1; 11, anterior tubercle of T1; 12, cranial costal fovea of T1; 13, the pedicle of T1; 14, intervertebral foramen between T1 and T2; 15, transverse process of T1; 16, dorsal projection on transverse process of T1; 17, lamina of T1; 18, prezygapophysis of T1; 19, postzygapophysis of T1, 20, spinous process of T1; 21, dorsal projection on transverse process of T3; 22, prezygapophysis of T2; 23, postzygapophysis of T2, 24, postzygapophysis of T3; 25, spinous process of T2; 26, spinous process of T3; 27, prezygapophysis of middle thoracics; 28, postzygapophysis of middle thoracics; 29, anterior tubercle of T4; 30, transverse process of T5; 31,

dorsal projection of transverse process of T5; 32, spinous process of T7; 33, sternal elements, 34, first thoracic rib; 35, second thoracic rib; 36, third thoracic rib; 37, fourth thoracic rib; 38, fifth thoracic rib; 39, facet on the rib for costal cartilage; 40, capitulum of R1; 41, tuberculum of R1; 42, median fissure between left and right pieces of second sternal segment; 43, facet for R2; 44, facet for R3.

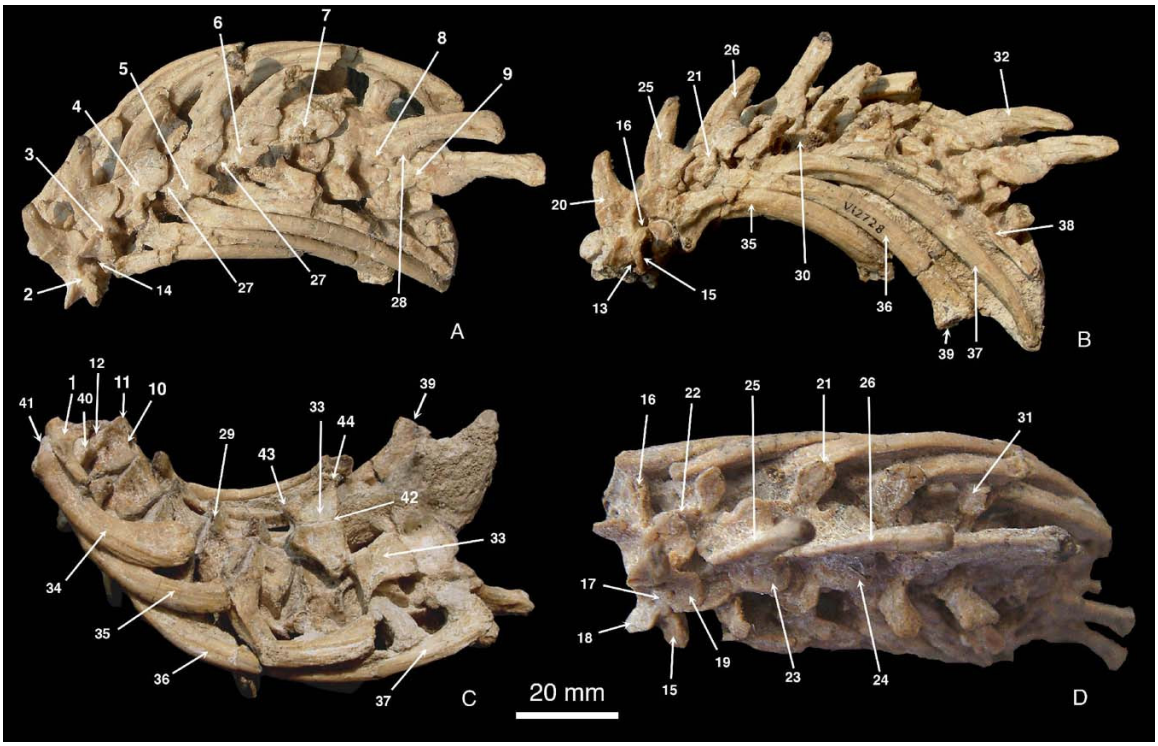

Figure 3-6

From the first thoracic vertebra backwards the morphologies of the thoracic vertebrae change gradually in the shape of the vertebral body, and the location, orientation and size of processes. Here the description of the thoracic series is divided into several sections, which does not necessarily mean that the morphologies of successive sections change discontinuously in every aspect.

FIRST THORACIC VERTEBRA (T1) (figure 3-6)--There is no obvious discontinuity in morphology between bodies of the C7 and T1. The body of T1 is as wide as that of C7 but slightly longer and stouter. It is also less compressed dorsoventrally than the latter. The ventral crest is more prominent than that of C7, and with a larger anterior tubercle. The crest reduces posteriorly. The depressions on the sides the ventral crest are less developed than those of C7 (figure 3-6: 10, 11). There are several small nutrition foramina in the center of the depressions. In ventral view, the vertebral body is wider than long. The anterior surface of the vertebral body is slightly concave and roughly oval with a height smaller than the width. A flat cranial costal fovea for the head of the first thoracic rib appears on the ventrolateral edge of the anterior surface of the body (figure 3-6: 12). The vertebral foramen is oval in shape, wider than high, and slightly smaller than that of cervical vertebrae.

The pedicle arises laterally on the anterior half of the vertebral body (figure 3-6: 13). It is strongly incised on the posterior edge, which forms three-fourths margin of the intervertebral foramen between the first two thoracic vertebrae (figure 3-6: 14). There is no accessory process (anapophysis) on the posterior edge of the pedicle. The anterior edge of the pedicle is slightly indented and forms the posterior margin of the intervertebral foramen between C7 and T1. The transverse process is stout, projecting laterally from the whole height of the pedicle (figure 3-6: 15). The process is oval in cross-section, dorsoventrally higher than anteroposterior long. It is expanded laterally, with the articular facet for the tuberculum of the first thoracic rib facing lateroventrally. Posterodorsally on the transverse process above the articular facet is a small knoblike eminence projecting laterally (figure 3-6: 16). Evans (1993: p 175) defined the small

knoblike eminence dorsal on the transverse process of the thoracic vertebrae in the dog as the mamillary process or metapophysis. The mamillary process in the dog is anterodorsal to the articular facets for the rib, which is further fused to the prezygapophysis in more posterior vertebrae. The same process in *Repenomamus* is posterodorsal to the articular facet. The homolog between the two structures is uncertain, and the eminence in *Repenomamus* is called the dorsal projection of the transverse process to avoid an unnecessary assumption of homology. Underneath the transverse process is a sulcus, which is closed laterally by the rib to form the transverse foramen.

The laminae of T1 are slightly longer than its vertebral body (figure 3-6: 17). They are broad plates and merge at the median line to form the base of spinous process. The prezygapophysis is at the junction between the pedicle and lamina. It projects anterolaterally (figure 3-6: 18). The articular facet on the prezygapophysis faces dorsomedially; the angle between the facet and the sagittal plane is about 45°. The postzygapophysis extends laterally from the junction of the lamina and spinous process (figure 3-6: 19). The width at the postzygapophysis is less than that at the prezygapophysis. The articular facet of the postzygapophysis faces lateroventrally, with an angle to the sagittal plane similar to that of the prezygapophysis.

The spinous process arises from the whole length of the laminae (figure 3-6: 20). It is thin at the base and laterally expanded toward the apex and terminates as a rough tuberosity. The process is about one and half times high as that of C7. It inclines posteriorly and tapers posterodorsally, with both anterior and posterior edges curved. The anterior edge inclines from the vertical direction with an angle of about 45°, and the posterior edge inclines about 10°. The base of the posterior edge is bifurcated and two

margins, continuing laterally with the postzygapophysis, delimit a vertical median sulcus to accommodate the anterior edge of the spinous process of the next vertebra.

THE SECOND AND THIRD THORACIC VERTEBRAE (T2-T3) (figure 3-6) --T2 and T3 are similar to T1 in the vertebral body morphology and pedicle location (figure 3-6: 3, 4). Their transverse processes are similar to that on T1 in the orientation; but the dorsal projections of their transverse processes are larger and become laterodorsally and posteriorly directed projections, separated from the facets for ribs by a sulcus. On T3, the projection (figure 3-6: 21) is further larger than that on T2 and its base reaches the level of the zygapophyses. The vertebral foramen, exposed on both T2 and T3 of V 12549, is small and oval in shape with width larger than depth.

The zygapophyses on T2 (figure 3-6: 22) and T3 extend laterally from the neural arches to a lesser degree than those of T1. The prezygapophysis of T2 faces dorsomedially to match the postzygapophysis of T1, but its postzygapophysis and both zygapophyses of T3 are nearly horizontally oriented (figure 3-6: 23, 24).

The spinous processes of T2 and T3 taper posterodorsally as that of T1 (figure 3-6: 25, 26). The process is more posterior inclined and longer on T2 than on T1, and further more posterior oriented and longer on T3. On both T2 and T3 the posterior aspect of the spinous process bears a cleft at the base, which is wider than the sulcus on the posterior aspect of the spinous process of T1.

THE MIDDLE THORACIC REGION (T4-T13) (figures 3-6, 3-7)--The most distinct characteristic of these thoracics is that the zygapophyses are recessed within the laminae (figure 3-6: 27, 28). The articular facets on the zygapophyses are nearly horizontally oriented.

A typical vertebra of this region has the vertebral body constricted in the middle and gently flat on the ventral side, except T4, which, similar to T1-T3, has a ventral crest, an anterior tubercle (figure 3-6: 29) and lateral depressions on the ventral side of its body. Both the anterolateral and posterolateral corners of the vertebral body bear distinct concave facets, representing cranial and caudal costal fovea, respectively. The vertebral foramen is exposed on T8-T11 of V 12549 and T8 of V 12728. The foramen in this region is similar to those on T2 and T3 in the size and shape.

As in T1-T3, the pedicle arises anteriorly from the vertebra body, with a strong indentation posteriorly and a shallow indentation anteriorly (figure 3-7: 2). The transverse process and its dorsal projection are similar to those on T2 and T3 on the location and orientation, but the base of the dorsal projection extends posterodorsally on to the lamina and between zygapophyses (figure 3-6: 30, 31). The dorsal projection is also larger than that on T3 but does not further increase in size from T4 backwards. The projection is dorsoventrally compressed with the apex slightly expanding anteroposteriorly.

Figure 3-7. Thoracic vertebrae and ribs of *Repenomamus giganticus*, IVPP V 14155, in lateral or lateroventral view. Scale bar is 50 mm. T3, T5, T8, T10, T17, and T20, thoracic vertebrae; R2, R3, R5, R11, R12, and R17, thoracic ribs; 1, vertebral body of T4; 2, pedicle of T5; 3, spinous process of T7; 4, platform on the top of spinous process of T 11-T20; 5, caudal cost fovea of T18; 6, cranial costal fovea of T19; 7, pedicle of T14; 8, facet on rib for costal cartilage.

Figure 3-7

The laminae of successive vertebrae imbricate with one another. The spinous process arises from the merging of the laminae posterior to the prezygapophyses, which form the anterior portions of the laminae (figure 3-6: 32; figure 3-7: 3). The spinous process is triangular in cross section due to the bifurcation of its posterior edge. The process, as those of T1-T3, inclines posteriorly, but does not incline further posteriorly from T4. The process is also higher on T4 than on T3, and does not increase height from T4 backwards. The anteroposterior dimension of the process does not change much toward the apex as the anterior and posterior edges of the process are nearly straight and parallel to each other. The anterior edge of the process is blunt in V 12728 and V 14155, but quite sharp in V 13605. The bifurcation of the posterior edge extends along the entirety of the process and its two margins delimit a sulcus for accommodating the anterior edge of the next vertebra. On T4 the apex of the spinous process forms a tubercle, as seen in T1-T3; but from T4 backwards the tubercle gradually transforms into a flat platform, which is better developed on T11 backwards (figure 3-7: 4). On T11 to T13 the posterior part of the spinous process gradually expands laterally above the base towards the apex.

THE POSTERIOR THORACIC REGION (T14- T20) (figures 3-7 and 3-8)--The most distinct characteristic of this region is that the zygapophyses form stout processes from the laminae and the main portion of the articular facets on the zygapophyses are nearly vertically oriented (figure 3-8: 6, 7). T14 (figure 3-7: T14; figure 3-8: 1) is transitional in this aspect as its prezygapophyses (figure 3-8: 4) are still largely recessed within the laminae, and face dorsally to match the horizontally oriented postzygapophysis of T13, while its postzygapophyses (figure 3-8: 5) are similar to those of other vertebrae in this

region. A small portion of the zygapophyseal articular facet extends inwards onto the surface of the lamina, which gives the whole articular facet a concave (on the prezygapophyses) or convex (on the postzygapophyses) appearance.

The vertebral body in this region is constricted in the middle to various degrees (figure 3-8: 8, 9). The ventral surface of the vertebral body is flat on T14-16 but concave on T17-20. A ventral crest is present on ventral surface of T18-T20 (figure 3-8: 10). The cranial and caudal costal foveae (figure 3-7: 5, 6) are smaller than those on middle thoracic region and gradually diminish backwards. The T20 does not have the caudal costal fovea. The vertebral body increases height compared to those of more anterior thoracics, which gives the body a less compressed contour in cross section. The vertebral

---

Figure 3-8. Posterior thoracic vertebrae and ribs and first lumbar vertebra of *Repenomamus robustus*, IVPP V 12549, in laterodorsal (A) and ventral (B) views.

1, fourteenth thoracic vertebra (T14); 2, twentieth thoracic vertebra; 3, first lumbar vertebra; 4, prezygapophysis of T14; 5, postzygapophysis of T14; 6, postzygapophysis of T18; 7, prezygapophysis of T19; 8, vertebral body of fifteenth thoracic vertebra; 9, vertebral body of seventeenth thoracic vertebra; 10, ventral crest on body of T20; 11, transverse process of T19; 12, dorsal projection of transverse process of T19; 13, mamillary process on T17, 14, lamina of T17; 15, spinous process of T18; 16, anterodorsal ridge on R18; 17, posterodorsal ridge

on R16; 18, ventral ridge on R14, 19, prezygapophysis of L1; 20, postzygapophysis of L1.

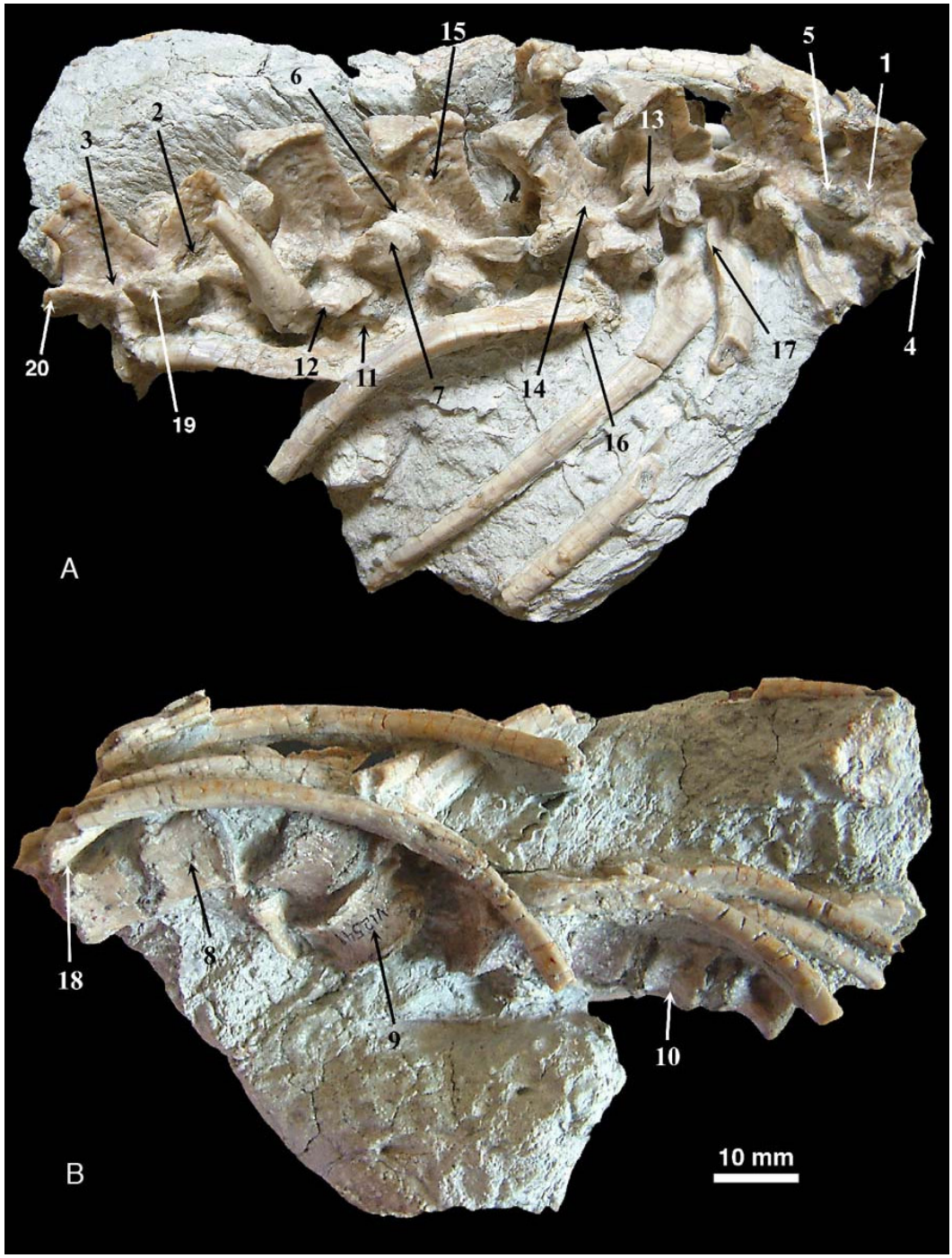

Figure 3-8

foramen of T14 is exposed anterior in V 12549, which is similar to those in middle thoracic region in the shape and size. V 12549 also has the vertebral foramen of L1 (first lumbar vertebra; figure 3-8: 3) exposed, which is semi-circular and larger than that on T14. Because the size and shape of L1 is similar to those of several posterior thoracics (T16-T20), the vertebral foramina on these thoracics are probably also large. It is possible that in the posterior thoracic region the vertebral foramen gradually increases size and changes shape from oval to semi-circular.

The pedicle, as those on more anterior thoracics, arises anteriorly on the lateral edge of the vertebral body (figure 3-7: 7). It is strongly grooved on the posterior edge, but, unlike on anterior vertebrae, it lacks distinct indentation on the anterior edge. The transverse process arises low on the pedicle near its junction with the vertebral body and is close to the cranial costal fovea (figure 3-8: 11). The dorsal projection of the transverse process (figure 3-8: 12), which shares the common base with the articular facet for rib tuberculum on more anterior thoracics, is now separated from the latter and highly located on the pedicle. On T14 the lateral projection is similar to those on the middle thoracic region but does not reach the level of the zygapophyses. On T15 and backwards the lateral projection reaches the posterior edge of the pedicel and points posterolaterally and slightly dorsally. The projection and postzygapophysis define a notch that receives the prezygapophysis of the successive vertebra. By the definition of Evans (1993: p 175), the projection on these thoracics (T15-T20) is the accessory process.

Except on T14, the prezygapophysis arises dorsolaterally and anteriorly from the junction of the pedicle and lamina and then turns anterodorsally (figure 3-8: 7). The process increases size from T15 backwards. The lateral surface of the process is strongly

convex and bears a low ridge, which probably represents the mamillary process (figure 3-8: 13). The postzygapophysis (figure 3-8: 6) is a little higher in position than the prezygapophysis, and arises mainly from the base of the spinous process, rather than the junction of the pedicle and lamina. The two postzygapophyses define a deep recess posteriorly on the base of the spinous process. The laminae form a thin plate between the prezygapophyses and bear articular facets extending from the latter (figure 3-8: 14). They are thickened posteriorly and form the bases for the postzygapophyses and spinous process.

The spinous process (figure 3-8: 15) arises from the whole length of the laminae. The process has a sharp anterior edge and thickens posteriorly. The cross section of the process is triangular. On T14 and T15 the anterior edge of the spinous process is straight and inclines posteriorly to a degree similar to that of the spinous process in the middle thoracic region. From T16 backwards the anterior edge of the spinous process is just slightly posteriorly oriented except the portion between the prezygapophyses, which is more horizontally oriented. The posterior edge of the process is bifurcated into two posterolateral margins that define a concave surface on the posterior aspect of the process. The posterior part of the spinous process is constricted just above the base for postzygapophysis, and from this point the process expands toward the apex. The constriction and expansion are obvious on T 14-T 19, and less so on T 20. In both V 12549 and V 14155, the exposed spinous processes in the posterior thoracic region have similar heights.

THORACIC RIBS (figures 3-6, 3-7, 3-8, and 3-9)**--**Ribs from different individuals complement to each other and together compose the whole suite of 20 thoracic ribs (R1-

R20), although some posterior ribs are only partially recognizable (figures 3-8, 3-9). At least the first thirteen ribs definitely have costal cartilages as distal ends of these ribs are expanded to various degrees and bear rough articular facets for cartilage (figure 3-6: 39; figure 3-7: 8; figure 3-9: 1). It is unclear whether more posterior ribs have costal cartilages because distal portions of these ribs are damaged in all known specimens. Curvatures of all ribs are small, indicating a deeper than broad thorax as in most extant therian mammals but different from the broad thorax of extant monotremes.

The first thoracic rib (figure 3-6: 34; figure 3-9: R1) is also the stoutest one and with the greatest curvature among thoracic ribs. The capitulum and tuberculum (figure 3-6: 40, 41) are well separated and protrude from the body of the rib; both heads are robust. The neck is long and well defined. The rib shaft is anteroposteriorly compressed and both anterior and posterior surfaces bear low ridges and shallow sulci. The cross section of the rib is ovate. The dorsal extremity (with both heads) is the (dorsoventrally) widest part of the bone. The rib body immediately distal to the neck is the most curved part of the bone, and the bone gradually widens ventrally. The capitulum, tuberculum and the rib body are roughly within the same imaginary plane. The costal fovea for the capitulum on T1 is anteroventral to the diapophysis for the tuberculum, so that the rib is positioned in a plane oblique, rather than perpendicular, to the longitudinal axis of T1 in life.

Figure 3-9. Left thoracic ribs of I *Repenomamus robustus*, IVPP V 13605, in ventral (A) and dorsal (B) views.

R1-R20, thoracic ribs; enclosed bony mass, remains of stomach content; 1, R2 articular facet for costal cartilage; 2, interclavicle; 3, middle sternal

elements; 4, most posterior sternal element; 5, suture between a pair of left and right middle sternal elements.

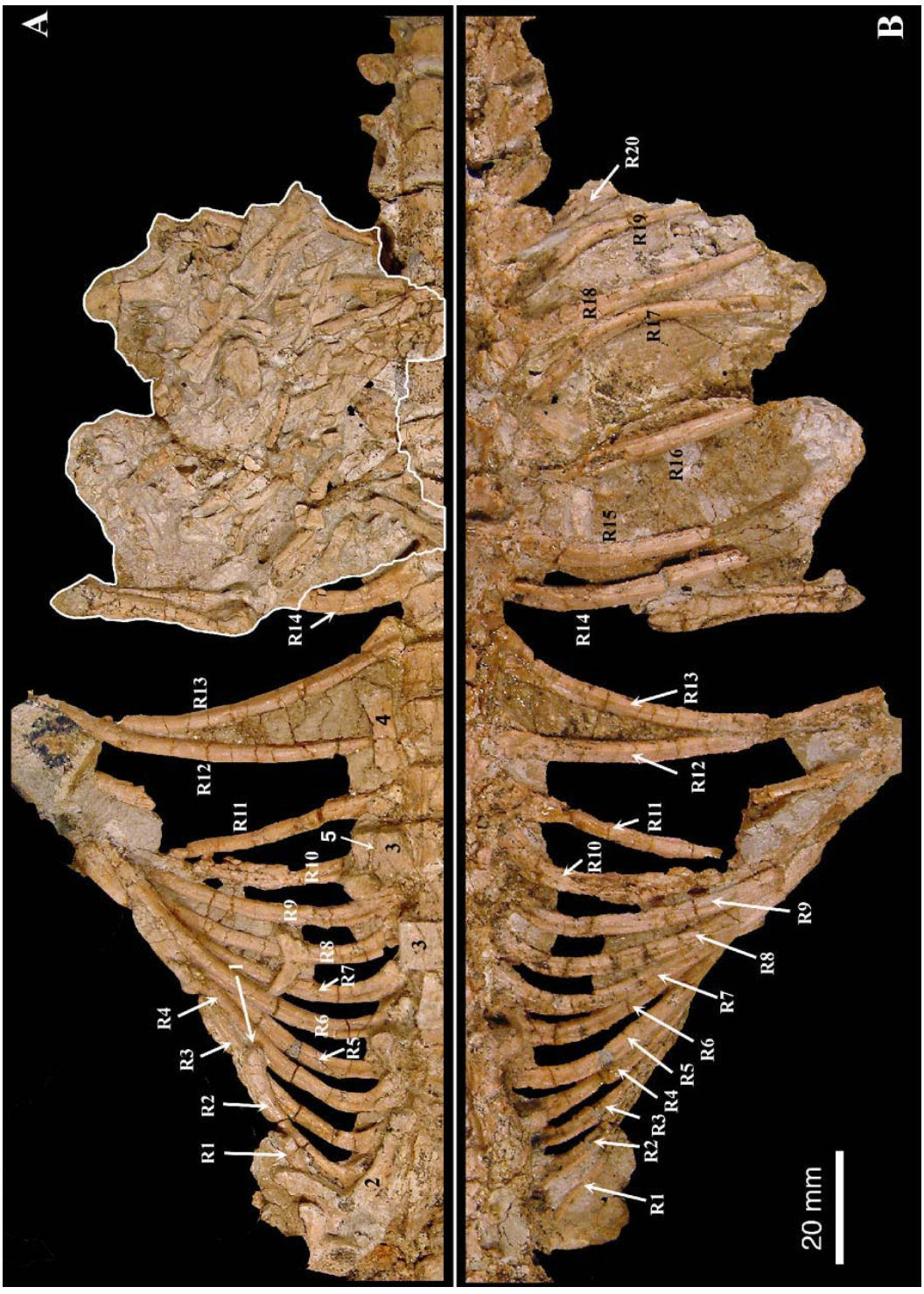

Figure 3-9

The rib morphology changes gradually from R1 backwards. The rib length increases from R1 to R13 (figure 3-9). The length differences between two neighboring ribs are salient from R1 to R5. From R5 to R13 the rib length increases mildly. The rib length decreases from R13 to R15, and probably continues so backwards to R20. The capitulum and tuberculum keep their identities (articulating with costal foveae and diapophyses, respectively) through all thoracic ribs, but they gradually approximate to each other in more posterior loci. The tuberculum is less protruding in more posterior ribs. From R2 backwards there are anterodorsal and posterodorsal ridges extending laterally from the tuberculum (figure 3-8: 16, 17). On the ventral side of the rib there is a ventral ridge on the neck connecting the capitulum and the rib body (figure 3-8: 18). Two dorsal ridges define a concavity on the dorsal side of the rib just distal to the tuberculum. There are shallow longitudinal sulci between ventral ridge and two dorsal ridges, respectively. The development of ridges, concavity and sulci gives the proximal portion of the rib a triangular shape in cross section. All three ridges and the dorsal concavity attenuate distally and disappear at the level where the rib has the largest curvature, except R20, where the ridges and dorsal concavity extends more than the half of the rib length. Two dorsal ridges become shaper and wider from R2 backwards and best developed on R15-R19, where the dorsal concavity is deep and broad. On R2-R14 the longitudinal sulci extend distally to the middle of the rib on anterior and posterior surfaces; and on more posterior ribs, the sulci are limited to the proximal portion of the rib as other structures (ridges and dorsal concavity). The rib becomes slenderer from R1 to R5; and from R5 backwards ribs have similar diameters, except last one (R20), which is slenderer than other ribs. From R2-R14 the middle part of the rib is (dorsoventrally) deeper than

(anteroposterior) wide in cross section; and that of the more posterior ribs, except R20, is roughly rounded.

3.1.4 LUMBAR SERIES

Material

V 12549 preserves the first and last lumbar vertebrae, articulating with thoracics and sacrals, respectively. V 13605 has the first three and last lumbar vertebrae preserved. In V 14155 all six lumbar vertebrae are preserved *in situ*.

Morphology

Repenomamus has six lumbar vertebrae (L1-L6; figures, 3-8, 3-10, and 3-11). The thoracolumbar transition in this taxon is demonstrated by the development of immobile ribs in lumbar vertebrae, in contrast to moveable ribs on thoracic vertebrae (figure 3-11).

The bodies of lumbar vertebrae are, similar to those of thoracics, constricted in the middle and concave on the ventral side; they also have a midventral crest (figure 3-11: 3) and lateral depressions, better developed than on T18-T20. The vertebral bodies seem slightly larger than those of the posterior thoracics and gradually increase size from L1 to T4; and those of L4 to L6 have similar sizes (figure 3-11). The anterior and posterior edges of the vertebral bodies are complete, not interrupted by the cranial and caudal costal foveae as seen in thoracics (figure 3-10: B-E and figure 3-11). The vertebral foramen (figure 3-10: 6) is semicircular and smaller on L6 than on L1.

Figure 3-10. Last lumbar vertebra (L6) of *Repenomamus robustus*, IVPP V 12549, in dorsal (A), lateral (B), dorsolateral (C), posterior (D), and anterior (E) views.

1, prezygapophysis; 2, postzygapophysis; 3, transverse process; 4, spinous process; 5, vertebral body; 6, vertebral foramen; 7, pedicle; 8, accessory process, 9, lamina; 10, bony ridge on posterior aspect of spinous process.

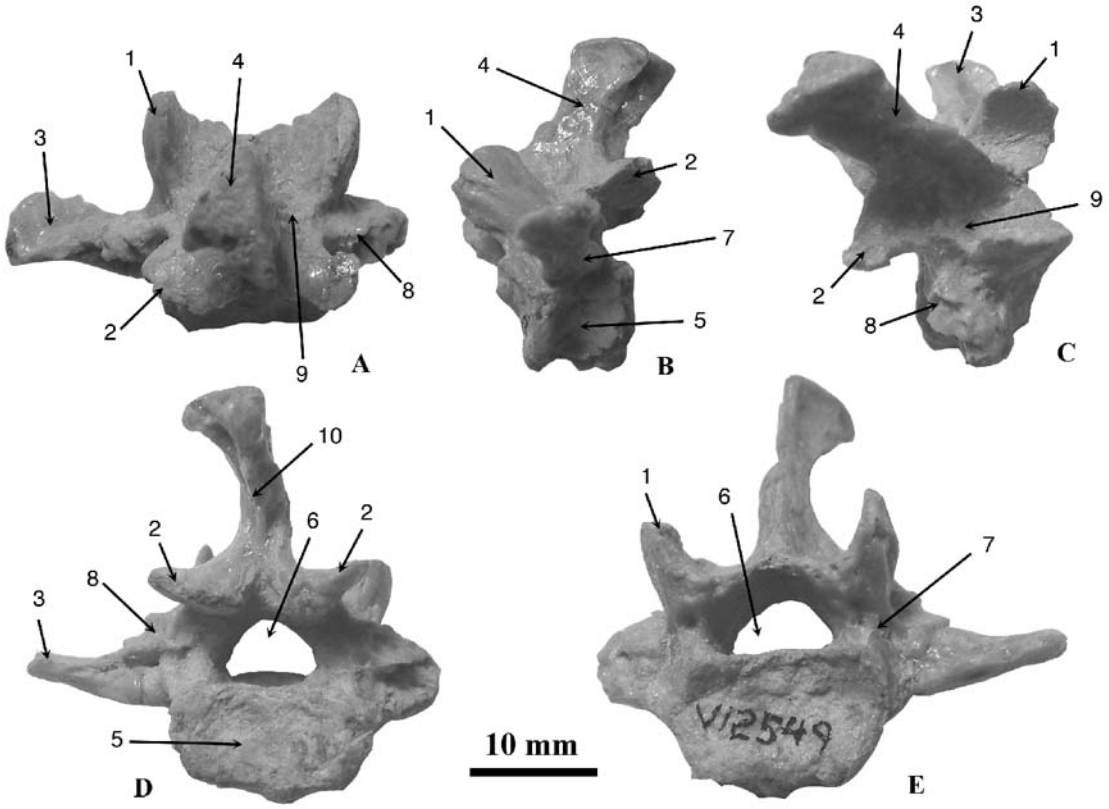

Figure 3-10

In V 12549 the pedicles of the lumbar vertebrae arise from the full length of the vertebral body, similarly indented at cranial and caudal edges, which are shallower than the indentation on the caudal pedicle edges of the thoracics (figure 3-10: 7). In V 14155 the pedicles of lumbar vertebrae arise anteriorly from the body and are strongly grooved posteriorly, more similar to those of thoracics in locations and indentations than those on V 12549 (figure 3-11: 4). The pedicles on lumbar vertebrae are lower on L6 than on L1, but it is unclear whether pedicles decrease in height from L1 to L6 or the pedicles on

middle lumbars are higher than on T1 and T6. In V 14155 all preserved transverse processes or lumbar ribs on lumbar vertebrae are broken at the bases, and all breakages are irregular (figure 3-11; Hu *et al*., 2005b: figure 2: Lr1). In L6 of V 12549, the transverse process has a suture with the pedicle and/or vertebral body (figure 3-10), which suggests that ribs in lumbar region are sutured with the vertebra and incorporated into the transverse process, rather than forming moveable lumbar ribs as seen in *Gobiconodon* (Jenkins and Schaff, 1988: p 11 and figure 12). The transverse process obliquely arises from both the body and pedicle (figure 3-10: 3). Anteriorly the transverse process is located on the body; posteriorly the base of the process extends posterodorsally onto the pedicle and reaches the accessory process (figure 3-10: 8; figure 3-11: 5) located high on the caudal edge of the pedicle. The transverse process itself is anteroposteriorly broad, tapering laterally, and slightly constricted at the base. On L6 of V 12549 the process is perforated at the base, but the foramen seems too small to be a transverse foramen (figure 3-10: D).

Both prezygapophyses of L1 and L6 are similar to those on the posterior thoracics in morphology and size (figure 3-8: 19; figure 3-10: 1). The main part of the articular

---

Figure 3-11. Lumbar series of *Repenomamus giganticus*, IVPP V 14155, in ventrolateral view. Scale bar is 50 mm.

L1, L3 and L6, the first, third and sixth lumbar vertebra; s1, the first sacral vertebra; T20, twentieth thoracic vertebra; 1, rib of T20; 2, transverse process of L1; 3, mid-ventral crest on the vertebral body of lumbar vertebra, 4, pedicle of L5; 5, accessory process on L5.

Figure 3-11

facet faces medially but the facet itself extends onto the dorsal surface of the lamina; therefore the whole articular facet forms a trough to receive the convex facet of the post-zygapophysis of the adjacent anterior vertebra. The accessory processes of lumbars are similar to those on the posterior thoracics, and form a deep notch with postzygapophyses. The postzygapophysis of L1 extends posteriorly from the lamina (figure 3-8: 20). The main part of the articular facet is vertical; the facet extends medially to underneath the process. Since L2-L5 are not preserved or not exposed dorsally, the zygapophyseal morphology is unclear on these elements. Judged by the morphology of the zygapophyses of L1 and prezygapophysis of L6, L2-L5 probably have similar zygapophyses. The postzygapophysis of L6 is different from those of more anterior lumbars (figure 3-10: 2). Its articular facet is flat, and not vertically oriented. As preserved, in V 12549 the left postzygapophysis of T6 faces ventrolaterally and nearly horizontally oriented, but the right postzygapophysis of T6 is nearly vertically oriented. See below (Section on Lumbar Vertebrae) for further discussion on this asymmetrical condition.

The laminae are nearly horizontally extended (figure 3-10: 9). Measured between pre- and postzygapophysis, the left plus right laminae are slightly narrower than the vertebral body at the same level. The anterior edges of the two laminae form a V-shaped notch between the prezygapophyses. Posteriorly, a deep recess is present between the postzygapophyses. The spinous processes of lumbars (figure 3-8: 3; figure 3-10: 4) are very similar to those of the posterior thoracics (T16-T20): steeply oriented and slightly posteriorly inclined, triangular in cross section, with a flat platform on the top of the apex, and with a median sulcus on the posterior aspect. The exception is the spinous process of L6, which has a thin vertical bony ridge in the middle of the sulcus on the posterior

aspect (figure 3-10: 10), suggesting that the sulcus itself cannot accommodate the anterior edge of the first sacral vertebra.

3.1.5 SACRAL SERIES

Material

V 12549 preserves the first sacral vertebra, which is associated with the last lumbar vertebra. The skeleton of V 13605 has a sacral series preserved and exposed dorsally. The sacrum of V 14155 is well preserved and exposed ventrally.

Morphology

The sacrum of *Repenomamus* is composed of three vertebrae (S1-S3), with their transverse processes contacting the iliac blade (figures 3-12, 3-13 and 3-14). The three vertebrae are partially ankylosed but not fully fused; the sutures between them are visible.

In V 12549 and V 14155, the body of S1 is similar to that of L6 in ventral aspect (constricted along the middle, with a mid-ventral crest), and longer than the latter (figures 3-8 and 3-14). In cross section, the vertebral body is oval, wider than high (figure 3-12: 5). In V 14155 the body of S2 is further longer than that of S1 and has stronger profile on the ventral aspect, with stronger mid-ventral crest and deeper lateral depressions (figure 3-14). The width of the body is similar in S1 and S2. The body of S3 is as long as that of S2 but narrower. Its ventral aspect is unknown for any specimen in the collection. The vertebral foramen of S1 is similar to that of L6 in the shape and size (figure 3-12: 6). The foramina of S2 and S3 are exposed laterally in V 13605 due to the damage of vertebral bodies and pedicles; their sizes and shapes are undetermined in this specimen. Since three sacral vertebrae are tightly associated, their vertebral foramina connect consecutively and form the sacral canal, as that of most recent mammals.

Figure 3-12. First sacral vertebra (S1) of *Repenomamus robustus*, IVPP V 12549, in dorsal (A), posterior (B) and anterior (C) views. Scale bar is 10 mm.

1, prezygapophysis; 2, postzygapophysis; 3, transverse process; 4, spinous process; 5, vertebral body; 6, vertebral foramen; 7, first sacral foramen, 8, pedicle; 9, wing-like plate of transverse process; 10, lamina.

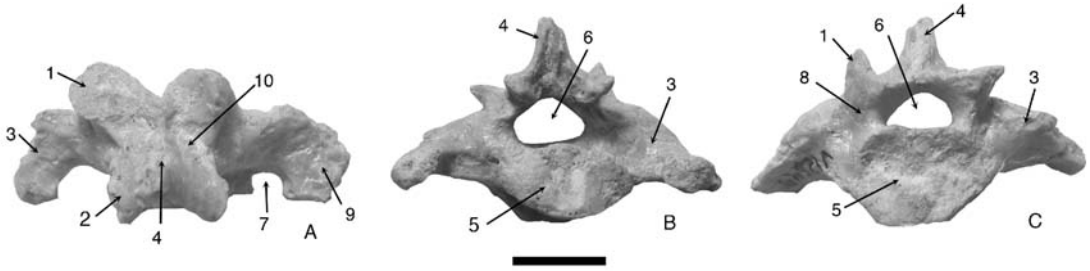

Figure 3-12

The pedicle of S1 arises dorsally from the lateral edge of the vertebral body (figure 3-12: 8) and has a distinct caudal notch and indistinct cranial notch. The transverse process projects laterally from the vertebral body and pedicle (figure 3-12: 3). Its base is stout, occupying all the lateral side of the pedicle and most that of the body. Laterally, the process expands anteroposteriorly and becomes a wing-like plate (figure 3-12: 9). The anterior edge of the plate extends beyond the edge of vertebral body; posteriorly, the plate reaches the same level as the posterior edge of the vertebral body, where it meet the transverse process of S2 and enclose the first sacral foramen with the latter (figure 3-12: 7; figure 3-14: 1). The pedicles of S2 and S3 are invisible in any specimen from our collection. The transverse processes of S2 and S3 are similar to that of S1, expanding into wing-like plates. All three plates join together to form the wing of the

sacrum (figure 3-14: 3). There are two pairs of sacral foramina between the transverse processes, the first and second sacral foramina, visible both ventrally and dorsally (figure 3-13: 1, 2; figure 3-14: 1, 2). The foramina are located lateral to the posterior part of vertebral bodies of their corresponding vertebrae, instead of at the level between two vertebrae. Evans (1993: p177) named the ventral and dorsal openings of the sacral foramina differently, which is followed in this study. The ventral openings are the pelvic sacral foramina, which are visible on the ventral side of the sacrum and presumably transmit the ventral branches of the sacral nerves and accompanying blood vessels (figure 3-14: 1, 2). The dorsal openings are the dorsal sacral foramina, transmitting dorsal branches of the sacral nerves and vessels (figure 3-13: 1, 2). The dorsal sacral foramina are larger and more open than their ventral counterparts, and intervertebral foramina between sacral vertebrae are visible through dorsal sacral foramina. The lateral edge of the sacral wing is expanded and forms the auricular surface for articulating with the ilium. None of the specimens has this part of the sacrum well preserved. Judged by the size of the articular facet on the ilium, the sacral auricular facet probably does not extend all the lateral edge of the sacral wing; at least posterior part of the transverse process of S3 does not contact the ilium.

The prezygapophysis of S1 (figure 3-12: 1; cranial articular process of the sacrum of Evans [1993: p 177]) forms a stout process, projecting anterolaterally and dorsally from the junction of the pedicle and lamina. The main part of its articular facet faces dorsally and slightly medially, and a small portion of the facet, as on the lumbars and the posterior thoracics, extends medioventrally onto the dorsal surface of the lamina. As preserved, the right prezygapophysis on S1 of V 12549 is nearly vertically oriented,

while the left one faces dorsally. The asymmetry of the prezygapophyses matches that of the postzygapophyses on L6 (figure 3-10) but it is unknown whether this is resulted from the postmortem deformation or trauma in life. The postzygapophysis of S1 (figure 3-12: 2) is much less laterally protruded than the prezygapophysis. Its articular facet faces ventrolaterally. Between the left and right postzygapophyses is a triangular concavity on the base of the spinous process. Anteroventral to the postzygapophysis and above the caudal notch of the pedicle is a small swelling, representing the vestige of the accessory process, but no true process is present. The zygapophyses of S2 and S3 (figure 3-13: 6, 7) form small projections protruding laterally from the junction of the pedicle and lamina. The processes align anteroposteriorly, forming the intermediate sacral crest. The articular facets on these processes face dorsomedially (on prezygapophyses) or ventrolaterally (on postzygapophyses).

The lamina of S1 is slightly longer than the vertebral body, even excluding the part forming the base for the postzygapophysis (figure 3-12: 10). The lamina has a thin and sharp anterior edge and thickens backwards. The anterior edges of the left and right

---

Figure 3-13. Sacral series of *Repenomamus robustus*, IVPP V 13605, in dorsal (A) and lateral (B) views.

Ca1, first caudal vertebra; L6, sixth lumbar vertebra; S1-S3, sacral vertebrae; 1, first dorsal sacral foramen; 2, second dorsal sacral foramen; 3, spinous process of S1; 4, spinous process of S2; 5, spinous process of S3; 6, zygapophyseal articulation between S1 and S2, part of intermediate sacral crest; 7, zygapophyseal articulation between S2 and S3, part of

intermediate sacral crest; 8, postzygapophysis of S3; 9, prezygapophysis of Ca1; 10, transverse process of Ca1; 11, right ischium.

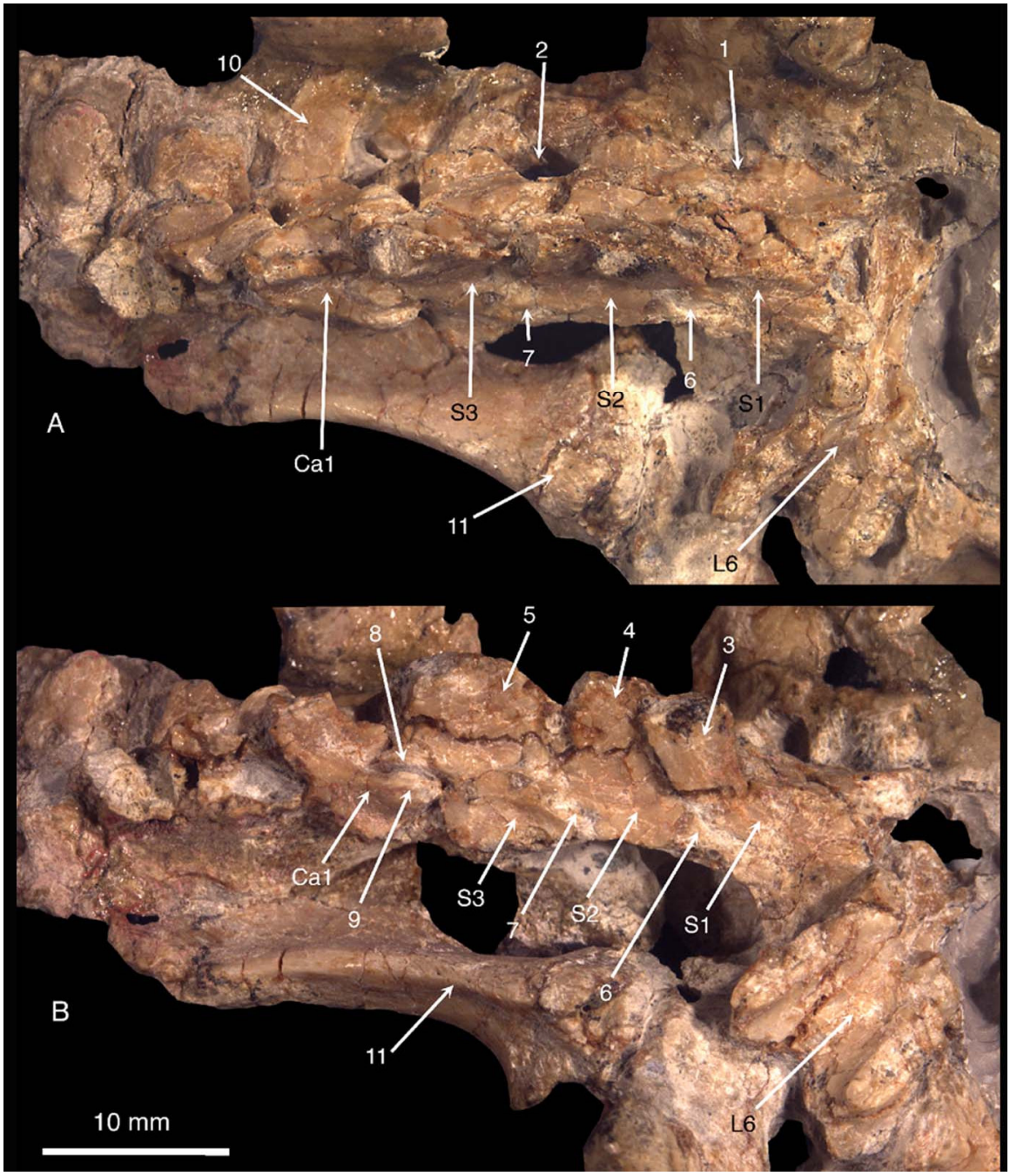

Figure 3-13

laminae converge into a V-shaped notch. The lengths and edges of laminae on S2 and S3 are unclear as no isolated vertebra at these positions is available for study. Laminae of

three sacrals tightly align to form the roof of sacral canal. Spinous processes of sacrals also tightly align and form the medial sacral crest (figure 3-12: 4; figure 3-13: 3, 4 and 5).

Figure 3-14. Sacral series of *Repenomamus giganticus*, IVPP V 14155, in lateroventral view. Scale bar is 20 mm.

Ca1, the first caudal vertebra; L6, sixth lumbar vertebra; S1-S3, lumbar vertebrae; 1, first pelvic sacral foramen; 2, second pelvic sacral foramen; 3, wing of sacrum.

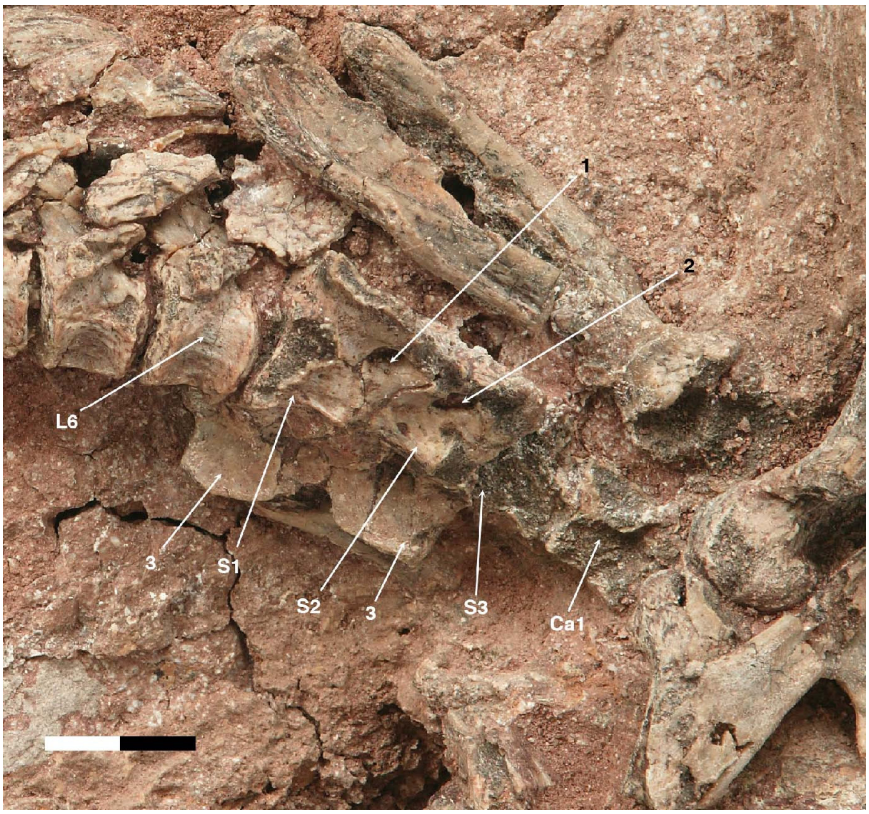

Figure 3-14

On every vertebra, the process arises along all the length of the merged laminae. It forms a posteriorly inclined thin plate for most of its length, only thickens in the posterior part, and has a shallow sulcus on the posterior aspect to accommodate the sharp anterior edge

of the spinous process of the next vertebra. The height of spinous process is undetermined due to the damage. It is also unclear whether there is a platform on the apex of the process, as seen in the posterior thoracics and lumbars.

3.1.6 CAUDAL SERIES

Material

V13605 preserves the first five caudal vertebrae, which are well exposed but most structures are not recognizable. V 14155 has the anterior seventeen caudal vertebrae preserved *in situ*, and most of them are exposed ventrally and laterally.

Morphology

The exact number of the caudal vertebrae of *Repenomamus* is unknown. V 14155 has the anterior seventeen caudals (figure 3-16: Ca1-Ca17) preserved, and the last one (Ca17) is still sizeable, which suggested that the animals must have at least a few more posterior caudals.

Figure 3-15. Anterior caudal vertebrae of *Repenomamus robustus*, IVPP V 13605, in ventral (A) and dorsal (B) view.

Ca1-Ca5, first five caudal vertebra; 1 transverse process of Ca1; 2, prezygapophysis of Ca1; 3, mamillary process on prezygapophysis of Ca1; 4, postzygapophysis of Ca1; 5, spinous process of Ca1; 6, hemal arch of Ca4; 7, hemal arch of Ca5; 8, right ischium.

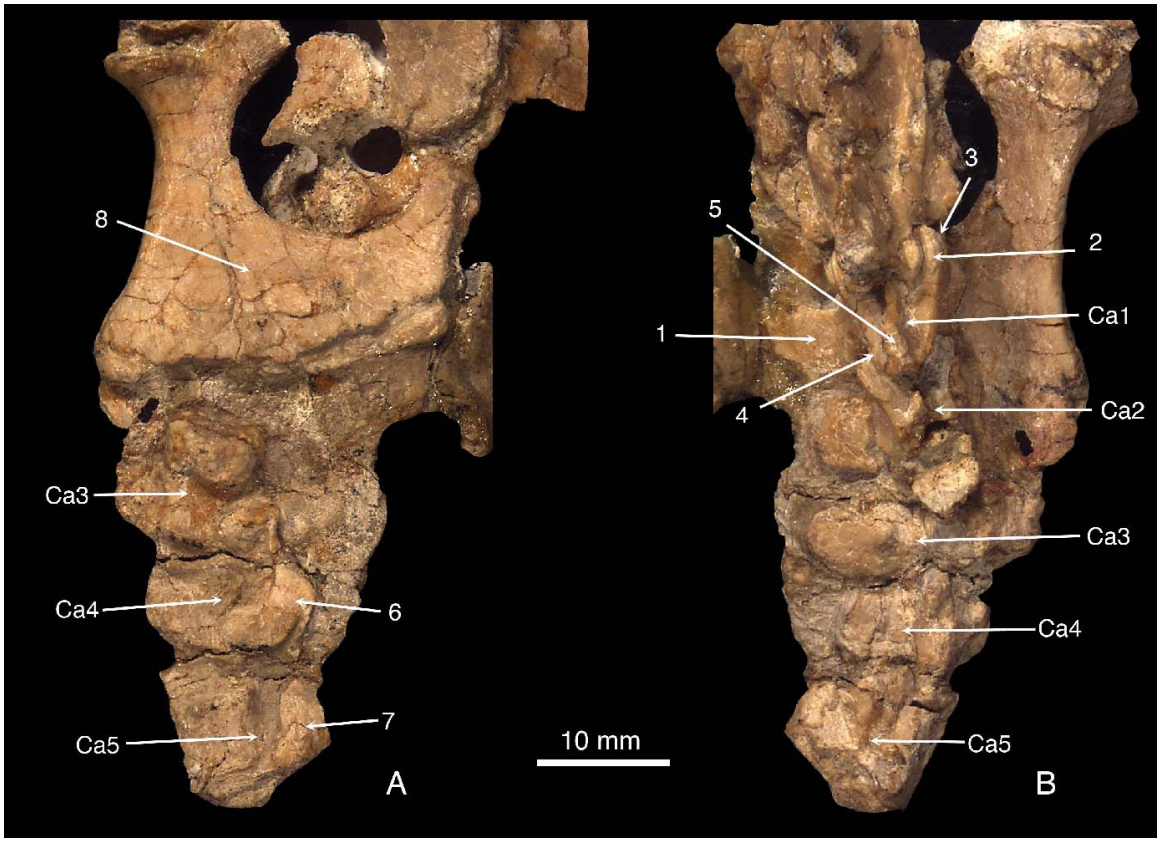

Figure 3-15

Ca1 is smaller than S3 in the length and width (figure 3-15: Ca1; figure 3-16: Ca1). Its transverse process is large, wing-like, and with the distal extremity pointing anterolaterally (figure 3-15: 1). The process arises from the junction of the vertebral body and pedicle. The prezygapophysis is stout and vertical, with the articular facet facing medially (figure 3-15: 2). There is a small mamillary process laterally on the prezygapophysis (figure 3-15: 3). The postzygapophysis (figure 3-15: 4) protrudes much less and smaller than the prezygapophysis. The spinous process (figure 3-15: 5) is posteriorly inclined and arises from the neural arch between the postzygapophyses. The neural arch is depressed compared to those of the sacrals. The vertebral canal is small. The vertebral body of Ca1 is either damaged or unexposed in specimens in the collection.

Posteriorly the caudals gradually decrease in the size and development of various processes, but increase in the length. Ca2-Ca6 (figure 3-15: Ca1-Ca5; figure 3-16: Ca1 and Ca6) either have a similar length of Ca1 or slightly increase length posteriorly. For Ca7-Ca16, the length increase between adjacent vertebrae becomes obvious (figure 3-16). Since the posterior caudal vertebrae are not preserved, it is unclear whether the terminal caudals reduce length, as normally seen in extant mammals.

Ca2 (figure 3-15: Ca2) has all the processes (the transverse process, zygapophyses, and mamillary process) and the vertebral canal similar to those on Ca1. Vertebral bodies of Ca3-Ca6 (figure 3-15: A and B) are short, concave in ventral side and slightly constricted about the middle. The transverse processes in these vertebrae are similar to those of Ca1-Ca2 in the shape, but arise from the lateral side of the vertebral body, rather than from the junction of the vertebral body and pedicle. The neural arches of Ca3-Ca5 are either partially damaged (in V 13605) or unexposed (in V 14155) on these vertebrae. They probably have the functional zygapophyses and spinous process because these structures are seen on Ca 6 of V 14155, which is exposed laterally and ventrally. It is unclear whether all these vertebrae (Ca3-Ca6) have vertebral foramen.

Posterior to Ca7, the vertebral body gradually becomes longer but narrower (figure 3-16: Ca7-Ca17). The body is constricted about the middle section. On Ca10-Ca13 there is a longitudinal sulcus on the ventral side of the body (figure 3-16: 1). On Ca7 and Ca8 the transverse processes arise from the posterior half of the vertebral body; and from Ca9 backwards the transverse process is reduced in its width but arises from the whole length of the vertebral body (figure 3-16: 2, 3). The process is thin and narrow in the middle, and thick and wide in anterior and posterior end. Ca7 is transitional in that it

has a functional prezygapophysis (figure 3-16: 4) and a reduced postzygapophysis, which does not articulate with the prezygapophysis of Ca8. From Ca7 backwards the articulation between zygapophyses disappears and the zygapophyses themselves are gradually reduces (figure 3-16: 5); and from Ca12 backwards the processes disappears. The spinous process is present on Ca7-Ca10 and disappears from Ca 11 backwards (figure 3-16: 6). From Ca11 backwards the vertebra itself is more or less cylindrical in shape with all processes reduced or gone.

The hemal arches are preserved in both V 13605 and V 14155. Ca4 and Ca5 of V 13605 have hemal arches preserved near the ventral sides of their vertebral bodies (figure 3-15: 6, 7). The arch of Ca4 is well preserved and Y-shaped. On V14155, there are two small hemal arches associated with Ca11 and Ca 13, respectively, which are similar to that of Ca4 in lateral view (figure 3-16: 7, 8). It is assumed here that at least those vertebrae in between Ca6-Ca10 and Ca 12 also have the hemal arches attached.

Figure 3-16. Caudal vertebrae of *Repenomamus giganticus*, IVPP V 14155, in ventral view. The scale bar is 20 mm.

Ca1-Ca17; caudal vertebrae; 1, longitudinal sulcus on ventral surface of vertebral body of Ca11; 2, transverse process of Ca8; 3, transverse process of Ca10; 4, prezygapophysis of Ca7, 5, reduced prezygapophysis of Ca 11; 6, spinous process of Ca9; 7, hemal arch of Ca 11; 8, hemal arch of Ca13.


Ca1
Ca5
Ca6
Ca7
Ca8
Ca9
Ca10
Ca11
Ca12
Ca13
Ca14
Ca15
Ca16
Ca17
1
2
3
4
5
6
7
8

Figure 3-16

3.1.7 STERNAL APPARATUS

Material

V 12728 has the interclavicle well preserved; only missing a small portion on the left side. It also preserves the sternal manubrium, second segment, and right piece of the third segment of the sternum. All are preserved on the ventral side of the vertebral column and have little deformation except for the broken anterolateral corner on the left side of the manubrium. V 13605 has the left half of the interclavicle preserved in situ and exposed ventrally. It also preserves the sternal manubrium and several other segments of the sternum, which are preserved on the ventral surface of the vertebral column and ribs. V 14155 has several segments of the sternum preserved in situ, but the sternal manubrium is either unexposed or damaged.

Morphology

INTERCLAVICLE (figures 3-9 and 3-17)--The sternal apparatus of *Repenomamus* includes the interclavicle, sternal manubrium and other sternal elements. The interclavicle of *Repenomamus* forms a fan-shaped structure with its handle attached to the sternal manubrium posteriorly (figure3-9: 2; figure 3-17: 1). The main body of the bone is a broad oval plate formed by two lateral wings (figure 3-17: 3). On the ventral surface of the lateral wing is the shallow concavity for articulation with the clavicle (figure 3-17: 4).

Figure 3-17. Interclavicle and sternal manubrium of *Repenomamus robustus*, IVPP V 12728, in ventral (A), dorsal (B), anterior (C), and lateral (D) views. Part of left first rib is attached to sternal manubrium and seen in A, B and C.

1, interclavicle; 2, sternal manubrium; 3, lateral wing of interclavicle; 4, concavity for clavicle; 5, anterior ridge of interclavicle; 6, posterior ramus of interclavicle; 7, vertical portion of posterior ramus of interclavicle; 8, horizontal portion of posterior ramus of interclavicle; 9, median ridge on ventral surface of sternal manubrium; 10, facet for R1; 11, facet for R2.

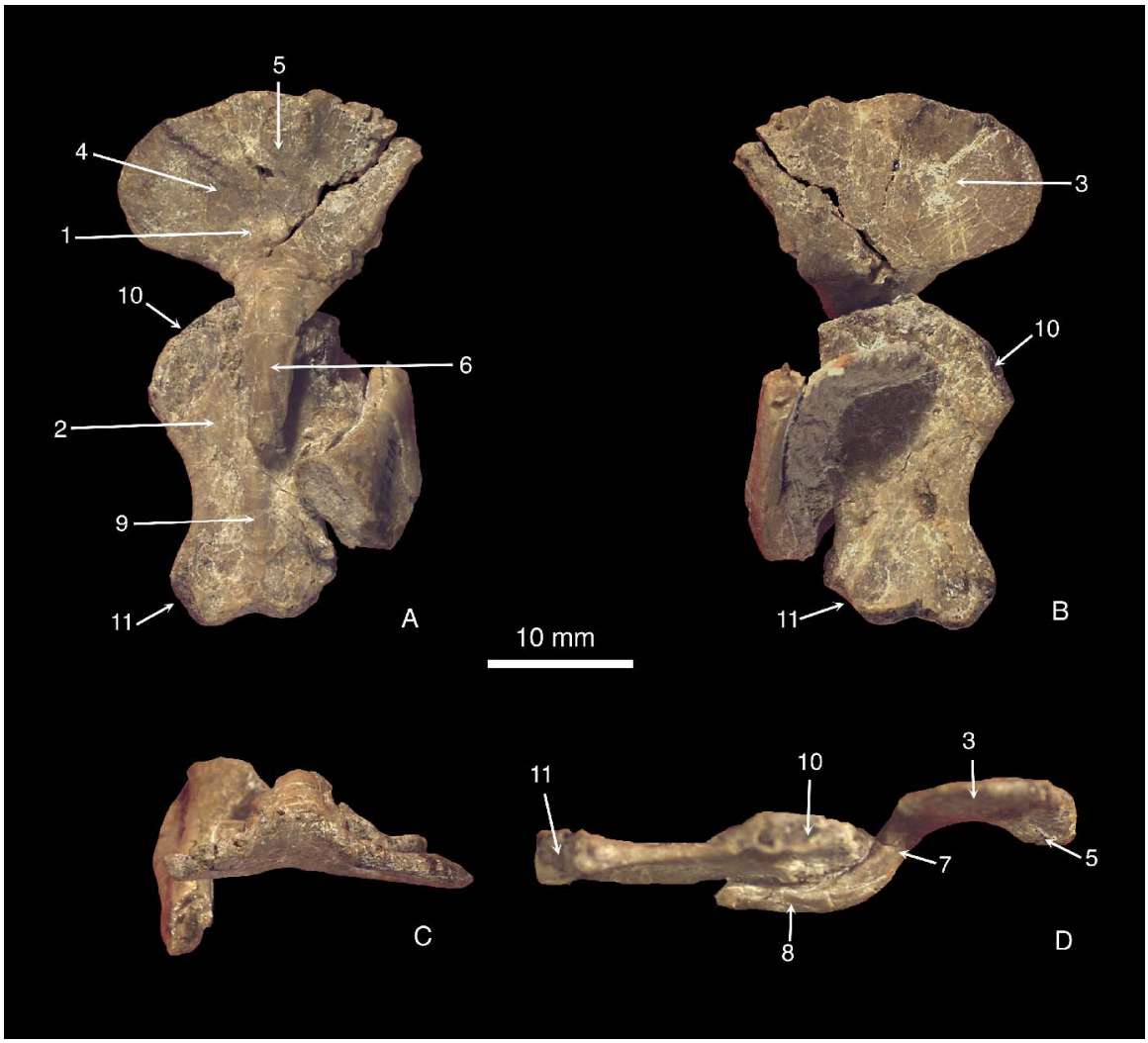

Figure 3-17

The floor of the concavity is smooth and bears no striations for the attachment of the cartilage or ligaments. The left and right concavities are confluent posteriorly. The anterior ridge between the lateral wings is low, broad, and short, just reaching the middle

of the plate (figure 3-17: 5). The dorsal surface of the bony plate, which is otherwise gently convex, forms a longitudinal shallow sulcus corresponding to the development of the anterior ridge. The anterior edge of the interclavicle is convex, except a small median indentation, where the anterior ridge begins.

The posterior ramus of the interclavicle (like the handle of the fan) is not in the same plane with the main body of the bone (figure 3-17: 6). It first turns ventrally (the vertical portion, figure 3-17: 7), and then extends posteriorly (the horizontal portion, figure 3-17: 8), forming a curved bony rod. The horizontal portion of the ramus attaches onto the ventral surface of the sternal manubrium. The contact between two bones is probably moveable, but ligaments connecting them may limit the mobility of the joint. The ventral surface of the ramus is convex, but no distinct ventral keel developed.

STERNAL ELEMENTS (figures 3-6, 3-9, 3-17, and 3-18)--The sternum of *Repenomamus* is composed of a series of broad and flat bony plates (figures 3-6, 3-9 and 3-18). The sternal manubrium is about twice as long as the bodies of anterior vertebrae and slightly narrower than the main body of the interclavicle (figure 3-17: 2). The dorsal and ventral surfaces of the bone are gently flat, but there is a low median ridge on the ventral surface, extending posteriorly from the place where the posterior ramus of interclavicle terminates (figure 3-17: 9). The manubrium narrows in the middle and therefore has concave lateral edges. The anterior edge is convex, with articular facets for the costal cartilages of the first pair of ribs on the anterolateral corners (figure 3-17: 10). The facets for the costal cartilages of the second pair of ribs are at the posterolateral corners of the bones (figure 3-17: 11). The posterior edge between the facets forms a median notch.

The segments of the sternum posterior to the manubrium, except for the most

posterior one, ossify in pairs (figures 3-6: 33; 3-9: 3; 3-18: 1-5). Their lengths are close to those of the bodies of the anterior thoracics. Each segment consists of two bony pieces, side by side, with a median fissure between them (figure3-6: 42; figure 3-9: 5; figure 3-18: 7). The second segment of the sternum, preserved in V 12728, widens posteriorly (figure 3-6: 33). The anterior edges of its two pieces form a median notch. Therefore, there is medial fontinelle between the manubrium and the second segment, which was probably filled by the intersternebral cartilage in life. The posterior edges are straight and transverse. The lateral edge is emarginated. Both the anterolateral and posterolateral corners of the segments are thickened, bearing articular facets for the costal cartilages of the second and third ribs, respectively (figure 3-6: 43, 44). The right piece of the third segment is preserved in V 12728. It is roughly rectangular in shape, slightly longer than wide and with the lateral edge a little concave. Its posterolateral corner bears a rough facet for articulation with the costal cartilage of the fourth rib, but the anterolateral corner of the bone is sharp, bearing no distinct facet for costal cartilage. Therefore, it is probable that the costal cartilages (except that of the first rib) mainly articulate with the posterolateral corners of the corresponding sternebrae, although they may also contact the anterolateral corners of the next sternebrae. Both V 13605 and V 14155 preserve some

---

3-18. Sternal elements of *Repenomamus giganticus*, IVPP V 14155, in lateroventral view. Scale bar is 20 mm.

1-5, five successive middle sternal elements; 6, most posterior sternal element; 7, median fissure between left and right pieces of a middle sternal element; 8, facet for costal cartilage of rib.

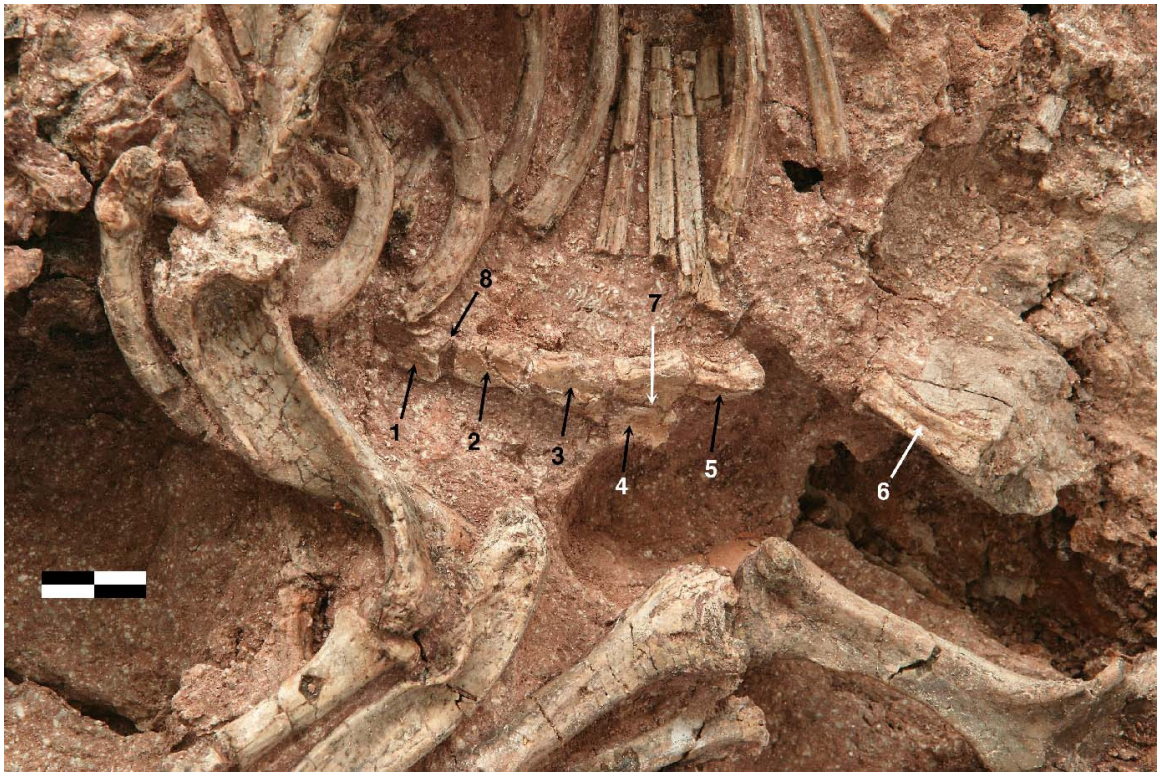

Figure 3-18

middle segments of the sternum (figure3-9: 3; figure 3-18: 1-5). Some of them preserve both the left and right pieces, with fissures between them, but most of them have only one side preserved. They are similar to the third segment of V 12728 in general morphology, but the bones in V 13605 are wider than those in V 12728 and V 14155, which may represent individual variations. The adjacent segments are tightly connected; therefore, the inter-sternebral cartilages between them, if existing, must be very small.

The most posterior segment of the sternum preserved in V 13605 and V 14155 is as twice long as the middle segments, but narrower (figure 3-9: 4; figure 3-18: 6). It has single element and probably did not ossify in pair in life. Most likely, the element is the xiphoid process of the sternum. Its posterior edge is straight and bears rough surface, suggesting the presence of the xiphoid cartilage in life. In both V 13605 and V 14155, the segment (xiphoid process) is preserved at the level of the 11th and 12th vertebrae, which

probably represented the end of the thorax floor in life. In V 14155, the direction of the sternebrae and the axis of the anterior thoracic vertebrae intersect at about 40° (figure 2-5). Since both structures are likely preserved in situ, the large intersecting angle suggests that the thorax deepens quickly and greatly as it extends posteriorly.

3. 2 FORELIMB

3.2.1 PECTORAL GIRDLE

Material

The pectoral girdle of *Repenomamus* is composed of the scapulocoracoid and clavicle. V 12549 preserves part of the right scapulocoracoid, with most of the scapular blade and the coracoid missing. V 12728 preserves both scapulocoracoids, just lost part of the scapular spine on the left side and part of scapular blade on the right side. Both clavicles of V 12728 are well preserved and suffer a little deformation. In V 14155 the left pectoral girdle is preserved in situ while the right one is either missing or unexposed.

Morphology

SCAPULOCORACOID (figures 3-19, 3-20)--The scapulocoracoid of *Repenomamus* is composed of the scapula and coracoid, the latter is reduced into a large process (figure 3-19: 1, 2). Since the scapulocoracoid is mobile, the orientation of the bone in life changed. Here the bone is positioned as the scapular spine directs laterally and vertically orientated (McKenna, 1961). The scapula is roughly semicircular in shape with the convex anterior and dorsal borders as the arc and a mostly straight posterior border as the diameter (figure 3-19: 3, 4, and 5; figure 3-20: 1, 2 and 3). The anterior border begins above the scapular notch (figure 3-19: 6), which marks the scapular neck, the constriction between the

scapular blade and the head (figure 3-19: 7; figure 3-20: 7). The anterior border continues dorsally with the dorsal border; together they form a large arc (about 170°). The boundary between two borders is unclear, and there is no distinct cranial angle between them. The posterior border of the scapula begins just above the glenoid. It is strongly reflected laterally except the most dorsal portion, which extends posteriorly and forms an acute caudal angle (about 60°) with the dorsal border (figure 3-19: 10).

The lateral surface of the scapular blade is slightly convex, with the scapular spine dividing it into the supra- and infraspinous fossa (figure 3-19: 8, 9; figure 3-20: 4, 5). Both fossae begin at the scapular neck. The supraspinous fossa first widens dorsally, reaches the widest point in its middle region, and then reduces its width as going further

---

Figure 3-19. Scapulocoracoids of *Repenomamus robustus*, IVPP V 12728: left scapulocoracoid in lateral (A), anterior (B), medial (C), posterior (D), and ventral (E) views; right scapulocoracoid in lateral (F), anterior (G), medial (H), posterior (I), and ventral (J) views.
1, scapula; 2, coracoid process; 3, anterior border of scapula; 4, dorsal border of scapula; 5, posterior border of scapula; 6, scapular notch; 7, scapular neck; 8, supraspinous fossa; 9, infraspinous fossa; 10, caudal angle of scapula; 11, scapular spine; 12, ventral edge of scapular spine, 13, lateral edge of scapular spine; 14, dorsal edge of scapular spine; 15, acromion; 16, acromioscapular notch; 17, subscapular fossa; 18, scapular head; 19, suture between scapula and coracoid process; 20, glenoid; 21, scapular portion of glenoid; 22, coracoid portion of glenoid.

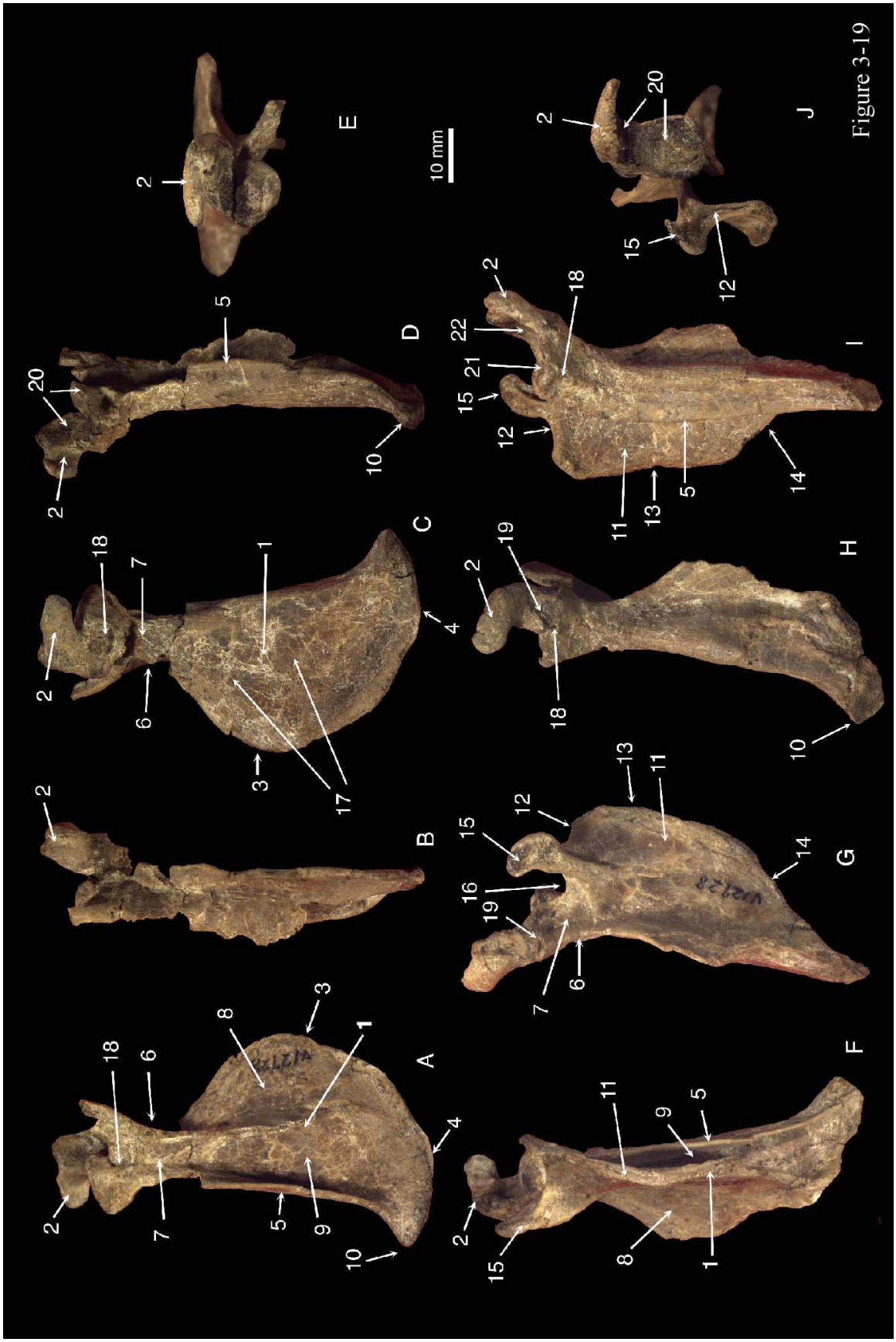

Figure 3-19

dorsally. The infraspinous fossa is very deep and widens moderately toward its dorsal end. It is larger than the supraspinous fossa in area and also slightly wider in every level.

The spine of the scapula forms a huge plate protruding laterally from the middle line of the scapular blade (figure 3-19: 11; figure 3-20: 6). It begins at the middle position of the lateral surface of the scapular neck, just several millimeters above the glenoid fossa. The spine does not reach the dorsal border of the scapula. At the point where the spine terminates a low ridge begins on the surface of the blade, extending posterodorsally, but it does not reach the dorsal border of the scapula. The spine has three edges, the ventral edge forms an L-shaped curve lying in a horizontal plane (figure 3-19: 12). In ventral view (figure 3-19: J) the plate of the spine is first perpendicular with the scapular blade, and then reflected posteriorly after passing the corner of the L-Shape. The corner is the location where the acromion arises from the spine. The lateral edge of the spine is nearly straight and roughly parallel to the baseline of the spine (figure 3-19: 13). The dorsal edge of the spine forms a slope from its lateral edge to the scapular blade (figure 3-19: 14).

As mentioned above, the acromion arises from the corner of the L-shaped ventral edge of the scapular spine, rather than as the ventral extension of its lateral edge as in most other mammals (figure 3-19: 15). The acromion extends anteroventrally from the spine. Its base, the bony thickening, is most obvious on the anterior aspect of the spine. The acromion itself is laterally compressed. The articular facet for the lateral end of the clavicle occupies most of the anterior surface of the acromion. The tip of the acromion extends ventrally (but not anteriorly) beyond the scapular part of the glenoid fossa. The acromioscapular notch, the gap between the acromion and the scapular head, is shallow

Figure 3-20. Left forelimb of *Repenomamus giganticus*, IVPP V 14155, in lateral view. Scale bar is 20 mm.

Cl, clavicle; Hu, humerus; Ra, radius; SC, scapulocoracoid; Ul, ulna; 1, anterior border of scapula; 2, dorsal border of scapula; 3, posterior border of scapula; 4, supraspinous fossa; 5, infraspinous fossa; 6, scapular spine; 7, scapular neck; 8, glenoid of scapula; 9, humeral head; 10, greater tubercle; 11, deltopectoral crest; 12, olecranon process of the ulna.

Figure 3-20

(figure 3-19: 16). Lateral to the notch on the medial aspect of the acromion is a deep fossa of unknown function. Another fossa is present on the lateral aspect of the acromion, which is slender and shallow, and extends onto the ventral edge of the spine.

The medial surface of the scapular blade forms the subscapular fossa, which is slightly concave, reflecting the relief of the lateral surface (figure 3-19: 17). The deepest part of the concavity corresponds to the base of the scapular spine. The lateral reflection of the posterior border of the scapula introduces a convexity to the posterior part of the medial surface.

The scapular notch marks the scapular neck, the narrowest part of the bone (figure 3-19: 6, 7; figure 3-20: 7). Beneath the neck is the scapular head (figure 3-19: 18; figure 3-20: 8), which thickens to support the coracoid and glenoid fossa.

The coracoid, which is a sizable bone in morganucodontids and monotremes, is reduced to a bony process attached to the scapula (figure 3-19: 2). Compared to therian mammals, the coracoid process in *Repenomamus* is stouter. It is ankylosed with the scapula, and the suture between two bones is distinct (figure 3-19: 19). On the right pectoral girdle of V 12529 the coracoid process has been detached from the scapula with the rough facet for the process exposed on the anteroventral extremity of the scapular head. The process protrudes ventrally from the anteroventral corner of the scapular head and forms the anterior wall of the glenoid fossa. After contributing to the glenoid fossa, the process strongly turns medially. The medially turned part of the process is as long as the glenoid part, but much slenderer than the latter.

The glenoid fossa is pear-shaped in ventral view (figure 3-19: 20). It has the scapular portion (figure 3-19: 21) and the coracoid portion (figure 3-19: 22), which form

a broad angle (about 120°), best visible in lateral view. The scapular portion of the glenoid fossa is perpendicular to the scapular blade. The surface of the glenoid fossa is gently concave. The coracoid portion of the glenoid fossa is slightly narrower than the scapular portion; and the former possesses one third the length of the glenoid. The lateral and medial margins of the scapular portion are more or less straight; and the posterior margin is gently convex.

CLAVICLE (figures 2-3, 2-4, 3-20, and 3-21)--The clavicle is the dermal bone bracing the pectoral girdle to the sternal apparatus. The element in *Repenomamus* forms an elongate S, which is moderately developed and strong enough to support the pectoral girdle. The bone is curved and bowed lateroventrally. Two ends of the bone are slightly flat and expanded (figure 3-21: 1 and 2). The shaft of the bone (figure 3-21: 3) is twisted at the middle and the medial half of the shaft (figure 3-21: 4) is slightly slenderer than the lateral half (figure 3-21: 5). The medial half has a flat posterior surface and convex anterior surface, which is otherwise elliptical (deeper than wide) in cross section. The lateral half of the shaft has three distinct surfaces. The ventral surface is concave and has a sulcus in the middle (figure 3-21: 6). As going medially the surface turns posteriorly and continues medially with the flat posterior surface of the medial half. Laterally there is a small notch that separates the ventral surface from the lateral end of the bone. The posterior surface of the lateral half of the shaft (figure 3-21: D) is also concave and much wider than the ventral surface. The surface narrows medially and fades out at the place where the shaft is twisted. The anterior surface (figure 3-21: A) of the lateral half of the shaft is gently convex and continues medially with the convex surface of the medial half.

Between three surfaces of the lateral half of the shaft are three ridges, among them the one between the anterior and posterior surfaces is the sharpest.

Figure 3-21. Clavicles of *Repenomamus robustus*, IVPP V 12728, in dorsal (A, right bone), anterior (B, left bone), medial (C, right bone), and posterior (D, left bone) views. Due to the postmortem deformation, the orientation of the bones is rough.

1, medial end of clavicle; 2, lateral end of clavicle; 3, shaft of clavicle; 4, medial half of clavicle shaft; 5, lateral half of clavicle shaft; 6, concavity on ventral surface of clavicle shaft; 7, facet for articulation with interclavicle; 8, nonarticular concavity on medial end of clavicle; 9, anterior surface of lateral end; 10, posterior surface of lateral end; 11, nonarticular concavity on posterior side of lateral end; 12, articular facet for acromion.

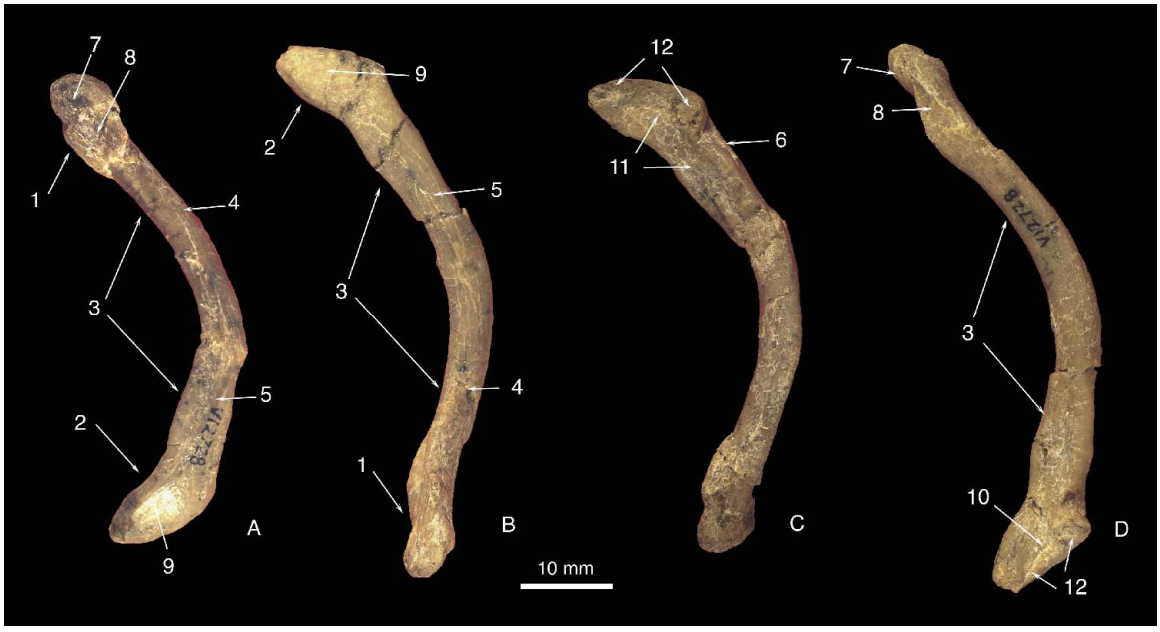

Figure 3-21

Two ends of the bone are oriented differently; the medial end (the sternal end, figure 3-21: 1) is expanded in a horizontal plane while the lateral end (the acromial end, figure 3-21: 2) is expanded in a vertical and transverse plane. The medial end is roughly oval in dorsal view. The medial one third of its dorsal surface has a flat and rough facet for articulation (synovial articulation) with the lateral concavity of the interclavicle (figure 3-21: 7). The lateral two-thirds of the surface form a shallow concavity, which does not contact the interclavicle (figure 3-21: 8). The extremity of the medial end is quite rough, suggesting the attachment of connective tissue. The lateral end of the clavicle tapers dorsally, which is best seen in anterior view. It has a convex and smooth anterior surface and a concave posterior surface (figure 3-21: 9 and 10). The concavity occupies most of its posterior surface and continues medially with the posterior surface of the shaft (figure 3-21: 11). The articulation with the acromion is actually on the lateral edge of the posterior surface, forming a narrow and vertically elongated facet, facing posteriorly and slightly laterally (figure 3-21: 12). The facet is much narrower than its counterpart on the acromion. This peculiar form of acromioclavicular articulation is not seen in other mammals.

3.2.2 HUMERUS

Material

V 12549 has only the distal portion of the right humerus preserved. V 12728 preserves both humeri, which are slightly damaged. V 13605 has both humeri preserved, which are crushed but still articulated with scapulae and forearms. V 14155 has the left humerus preserved *in situ* and exposed laterally.

Morphology

The position of the humerus probably changes constantly in movement. In this study the bone is described in an orientation assigned for that of *Gobiconodon* (Jenkins and Schaff, 1988: p14-15 and fig.14). In this position the intertubercular groove is on the ventral side of the humerus and the deltopectoral crest is on the lateroventral edge of the humeral shaft (figure 3-22). When the animal is standing, its limbs were probably crouched, and the humerus is obliquely oriented, pointing posterolaterally and ventrally (see below for more detail).

The humerus of *Repenomamus* is the sturdiest element of its postcranium. The humerus of V 12728 is about 70 mm long and 30 mm wide at the distal end. On both humeri of V 12728, the trace of the suture between the proximal epiphysis and the diaphysis is clearly visible although two parts are firmly fused (figure 3-22: 1). A fine line at the distal end indicates the fusion of distal epiphysis and the diaphysis (figure 3-22: 2). The humerus shows some degree of twisting. Measured with the method proposed by Kielan-Jaworowska and Gambaryan (1994: legend for fig. 46 on P. 61), the angle of twisting (the angle between the axes of flexor-extensors of the proximal and distal ends) is about 25°.

The humeral head forms an imperfect hemisphere, with the dorsoventral extension slightly bigger and more convex than the lateromedial one (figure 3-22: 3). The edge of the head between the tubercles, where the intertubercular groove begins, is concave. The articular surface of the humeral head faces proximally and dorsally. The extension and curvature of the humeral head are larger than those of the glenoid fossa in both the dorsoventral and lateromedial direction; the head is about twice wide as the scapular

portion of the glenoid fossa in lateromedial direction but only about one-sixth long in as the latter in the anteroposterior direction. The head overhangs the humeral shaft (diaphysis) prominently and about half of the articular surface (the portion of the surface facing dorsally) is above the shaft when the bone is positioned horizontally. The rough texture of the head surface indicates the presence of a cartilaginous cap in life.

Figure 3-22. Right humerus of *Repenomamus robustus*, V 12728, in Ventral (A), medial (B), lateral (C), dorsal (D), proximal (E), and distal (F) views.

1, suture between proximal epiphysis and diaphysis; 2, suture between distal epiphysis and diaphysis;3, humeral head; 4, greater tubercle of humerus; 5, lesser tubercle of humerus; 6, notch separating greater tubercle from head; 7, notch separating lesser tubercle from head; 8, deltopectoral crest; 9, ventral extremity of deltopectoral crest; 10, ridge at junction of deltopectoral crest and humeral shaft; 11, crest of lesser tubercle; 12, tuberosity for teres major; 13, intertubercular groove; 14, ridge on the dorsal side of humeral shaft; 15, ridge from tuberosity for teres major to entepicondyle; 16, ridge from deltopectoral crest to entepicondyle; 17, entepicondylar foramen; 18, entepicondyle; 19, sulcus separating entepicondyle from ulnar condyle; 20, ectepicondyle; 21, ectepicondoid crest; 22, radial condyle; 23, radial fossa; 24, lateral edge of trochlea; 25, ulnar condyle; 26, olecranon fossa; 27, trochlea.

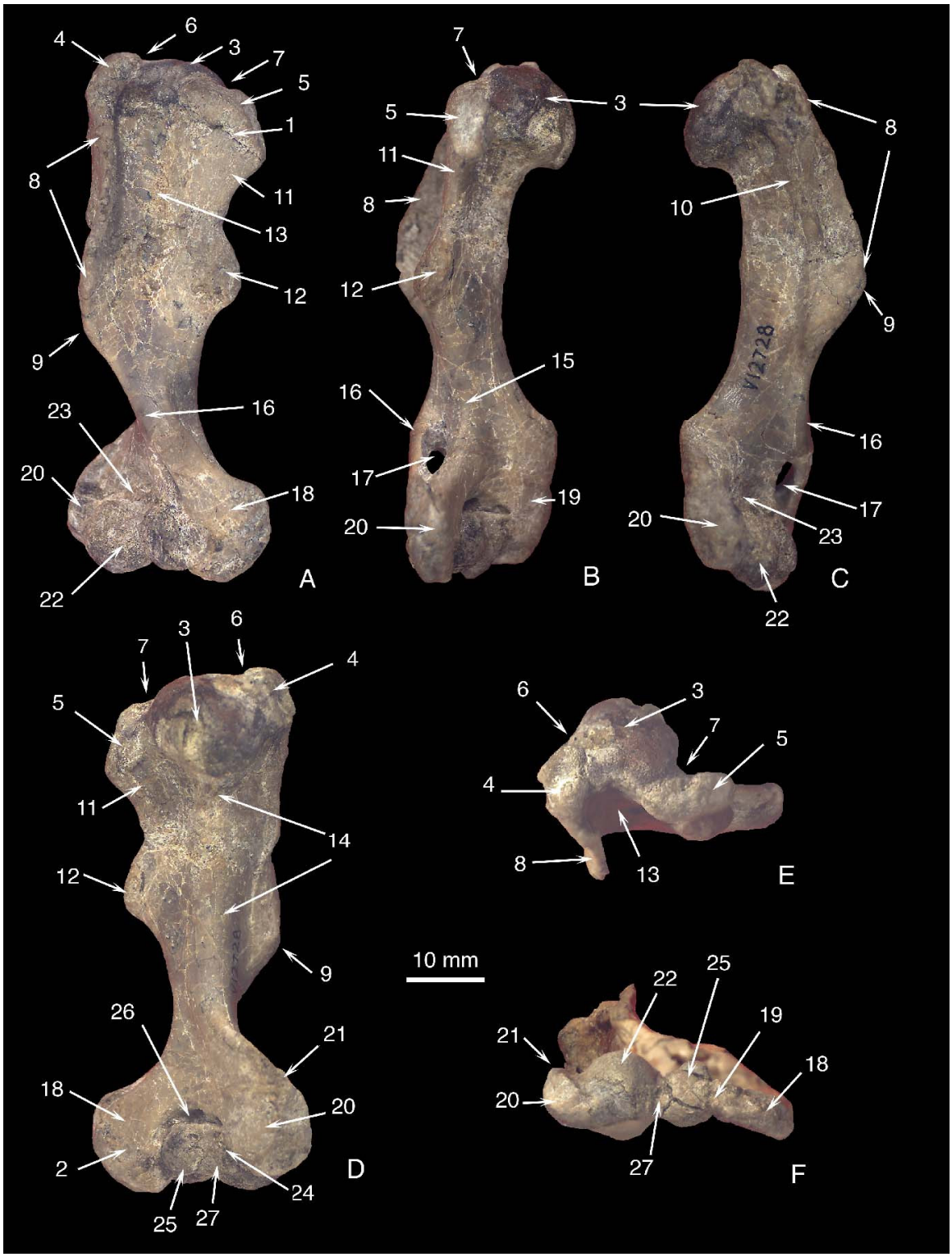

Figure 3-22

The greater and lesser tubercles are separated from the humeral head by shallow

notches, respectively (figure 3-22: 4, 5, 6, and 7). Both tubercles are prominent, the lesser tubercle about twice as wide (lateromedial direction) as the greater one. The greater tubercle projects lateroventrally from the ventrolateral corner of the head, and is irregular in shape. Its summit protrudes proximally beyond the humeral head. The pits and ridges on the summit indicate the attachments of muscles. The tubercle is supported by a strong deltopectoral crest (figure 3-22: 8). The lesser tubercle arises from the ventromedial corner of the head, and then turns medially. It has a rough texture and forms a wide and thick protuberance. The lesser tubercle does not protrude proximally beyond the head, therefore is lower than the greater one. The lesser tubercle is buttressed by its distal elongation.

The shape of the humeral shaft is irregular and its shape in cross section changes proximodistally. The shaft is nearly straight, does not show the dorsal flexure (of the proximal shaft), a character common in humeri of nonmammalian cynodonts (Jenkins, 1971: p 113). The proximal portion of the shaft is flat on the ventral side and convex on the dorsal side, but its exact shape is difficult to describe due to the development of the deltopectoral crest and distal prolongation of the lesser tubercle. The convexity of the dorsal side, which forms a low and broad ridge on the dorsal side of the proximal shaft, buttresses the overhanging head. Just distal to the deltopectoral crest the humeral shaft is roughly triangular in cross section. More distally, the shaft is expanded in an oblique (dorsolateral-to-ventromedial) direction.

The deltopectoral crest forms a robust flange extending distally from the greater tubercle and along the lateroventral edge of the humeral shaft (figure 3-22: 8). The crest thickens at its ventral extremity (figure 3-22: 9), which is beyond the midpoint of the

shaft (in V 12728, the ventral extremity reaches a point 40 mm from the proximal end and the humerus is 70 mm long). The margin of the crest is rugose and reflected ventrally. The lateral surface of the crest is slightly concave due to the presence of a low ridge at the junction of the crest and shaft (figure 3-22: 10). In V 12728 the length of this ridge is different on two humeri, on left humerus the ridge is 30 mm long and does not reach the ventral extremity of the crest while the one on right humerus reaches. The ridge probably represents the tricipital line and the lateral surface of the crest represents the deltopectoral surface (Muizon, 1998: p 58).The medial surface of the deltopectoral crest, the lateral wall of the intertubercular groove, is concave. The ventromedial side of the proximal half of the shaft presents a prominent ridge extending from the lesser tubercle. The ridge is thicker and wider than the deltopectoral crest and protrudes medially with its margin slightly reflected dorsally. Distally the ridge reaches the midpoint of the shaft. The ridges can be divided into two components, proximodistally aligned; the notch on the margin indicates the division between them. The proximal portion of the ridge is the distal prolongation of the lesser tubercle, called the crest of the lesser tubercle (Evans, 1993: p 188); its margin has a smooth texture (figure 3-22: 11). The distal portion represents the tuberosity for the teres major (figure 3-22: 12). The roughened texture on the tuberosity indicates the attachment of the teres major muscle. The tuberosity is slightly thicker than the crest. The ventral surface of the whole ridge (the crest plus tuberosity) is smooth and convex. The dorsal side of the ridge is concave, especially that of the crest for lesser tubercle, which presents a large shallow fossa. A similar fossa is present in some marsupials, which has been suggested for the origin of the accessory head of triceps muscle (Muizon, 1998: p 58).

The intertubercular groove (Evans, 1993: p. 187) extends distally from the edge of the humeral head on the ventral side of the bone (figure 3-22: 13). The groove is delimited laterally by the deltopectoral crest and medially by the crest for the lesser tubercle plus the tuberosity for teres major. It is very broad, facing ventromedially. The groove reaches its deepest point at the position between the distal deltopectoral crest and the tuberosity for teres major; then it quickly fades out as the crest and tuberosity terminate. The intertubercular groove is also called the bicipital groove (Jenkins and Parrington, 1976: p 400) as it accommodates the tendon of the biceps muscle. But in *Repenomamus* the groove would be too wide if the tendon was the only occupant. It is unclear what else was in the groove in life.

The middle portion of the shaft best displays the twisting nature of the bone. After passing the midpoint of the shaft the broad ridge on the dorsal side of the bone (figure 3-22: 14) gradually turns dorsolaterally and connects to the ectepicondoid crest at the level where the distal humerus begins to expand. A second ridge extends distally from the tuberosity for the teres major to the entepicondyle along the medial edge of the distal humeral shaft (figure 3-22: 15). The ridge is low and thick. A third ridge is on the ventral surface of the shaft, extending obliquely from the distal extremity of the deltopectoral crest toward the entepicondyle. The ridge is very prominent as leaving the deltopectoral crest; then it becomes flattened and broadened at the level where the shaft begins to expand. Three ridges and the surfaces between them shape the triangular configuration of the humeral shaft between the midpoint and the expanded distal humerus.

In the distal portion of the humerus the above mentioned second and third ridges enclose a large oval entepicondylar foramen, which is positioned just above the condyle

for the ulna and penetrates the base of the entepicondyle (figure 3-22: 17). The entepicondyle strongly projects distomedially with its margin slightly reflects dorsally. Its edge is thickened and protrudes distally beyond the condyles for the forearm bones (figure 3-22: 18). A shallow and narrow sulcus separates the entepicondyle from the condyles (figure 3-22: 19). The width of the entepicondyle is about one-third of the distal humeral width. The ectepicondyle slightly protrudes distally (figure 3-22: 20). Due to the spirality of the condyles the width of the ectepicondyle is different in ventral and dorsal sides; it is as wide as the entepicondyle in the dorsal side but only half the width of the latter on the ventral side. The lateral margin of the ectepicondyle is relatively sharp. It is ventrally reflected and extends proximally to form an ectepicondoid crest. The proximal extremity of the crest marks the beginning of the expansion of the humerus at the distal end. In the distal view the entepicondyle protrudes medially while the ectepicondyle extends lateroventrad.

The radial condyle (capitulum humeri of Evans, 1993: p 188) forms a large hemisphere, limited on the ventral side of the distal humerus (figure 3-22: 22). A shallow groove separates the condyle and the ectepicondyle. A large radial fossa is present above the condyle; it is wider than high (figure 3-22: 23). The condyle reaches the distal aspect of the humerus and protrudes well beyond the margins of epicondyles, but does not further wrap onto the dorsal side of the bone. Instead, there is a low and narrow ridge on the dorsal side of the distal humerus, extending proximally from the ventral extremity of the radial condyle. The medial aspect of the ridge has a smooth surface. The ridge is indeed not the dorsal prolongation of the radial condyle; it represents the lateral edge of the trochlea, which articulates with the trochlear notch of the ulna. A shallow fossa

separates the ridge from the ectepicondyle. The ridge and condyle together have a spiral appearance in distal view.

The ulnar condyle is less prominent and narrower than the radial condyle in the ventral side; it is only half as wide as the latter (figure 3-22: 25). The medial edge of the ulnar condyle is prominent; and there is a shallow fossa separating it from the entepicondyle. The articular facet of the condyle does not exceed medially over the ridge. The condyle wraps around the distal aspect of the humerus but does not protrude beyond the distal margins of the epicondyles. The condyle further extends onto the dorsal side of the distal humerus; here the condyle is wider than its component on the ventral side and there is not a distinct medial ridge defining the articular facet. It appears that on the dorsal side of the bone the articular facet extends onto the medial aspect of the condyle. In the distal view the axis of the ulnar condyle intersects with the axis of the distal humerus at a large angle (near 90°). The olecranon fossa is present on the dorsal side of the distal humerus. The fossa is proximodistally short and lateromedially wide, above both the ulnar condyle and the trochlea.

The trochlea forms a shallow and wide sulcus, between the two condyles (on ventral side), wrapping around the distal humerus and extending onto the dorsal side of the distal humerus (figure 3-22: 27). The axis of the trochlea is nearly perpendicular with that of the distal humerus.

3.2.3 ULNA AND RADIUS

Material

V 12549 has both left and right ulnae and radii well preserved. V 12728 only preserves the right ulna and radius, which suffer little deformation. Both ulnae of radii of

V 13605 are preserved in articulation, and both are partially damaged during the excavation. The left ulna and radius in the skeleton of V 14155 is well preserved and exposed laterally.

Morphology

ULNA (figures 2-4, 3-20 and 3-23)--The ulna of *Repenomamus* is nearly as long as the humerus. It is compressed transversely and slightly sigmoidal in shape, as that of most other mammals. In most previous studies on postcrania of nonmammalian cynodonts and Mesozoic non-therian mammals (Kühne, 1956; Jenkins, 1971; Jenkins and Parrington, 1976; Krause and Jenkins, 1983; Jenkins and Schaff, 1988; Kielan-Jaworowska and Gambaryan 1994), the ulna is often oriented as the trochlear notch faces anteriorly and the radial notch is anterolaterally located, and therefore the bone has an anterior (or cranial), a posterior (or caudal), a lateral, and a medial side. But for these extinct Mesozoic taxa, the ulna is more likely positioned obliquely as the proximal end points posterolaterally and dorsally, the trochlear notch faces anteromedially and the radial notch nearly faces anteriorly. For descriptive purposes, here the ulna is positioned as the trochlear notch faces cranially and therefore the bone has a cranial, a caudal, an anterolateral and a posteromedial side (figure 3-23: A, B, C, and D). The cranial side is the equivalent of the anterior in previous studies, caudal that of posterior, anterolateral that of lateral, and posteromedial that of medial.

The olecranon is massive, occupying the proximal one-sixth of the bone (figure 3-23: 1). Its proximal extremity (epiphysis) has a rough texture (figure 3-23: 2). The suture between the epiphysis and the shaft is fused, but the trace is visible in all available specimens. The proximal surface of the olecranon is slightly asymmetrical, higher

posteromedially than anterolaterally. The anterolateral and posteromedial surfaces of the olecranon are divided by a sharp ridge, which forms the cranial border of the olecranon (figure 3-23: 3). The distal end of this cranial border does not project cranially to form a prominent beak; therefore, the anconeal process (Evans, 1993: p191) is weak (figure 3-23: 4). Both surfaces bear concavities, which extend distally onto the proximal part of the

---

Figure 3-23. Right ulna and radius of *Repenomamus robustus*, IVPP V 12728, in cranial (A), caudal (B), anterolateral (C), posteromedial (D), proximal (E), and distal (F) views. Scale bar is 10 mm.

1, olecranon; 2, proximal epiphysis; 3, cranial border of olecranon; 4, anconeal process; 5, flexor fossa; 6, extensor fossa; 7, trochlear notch; 8, facet for ulnar condyle; 9, radial notch; 10, anterolateral wing of trochlear notch; 11, medial projection of coronoid process; 12, lateral projection of coronoid process; 13, cranial border (or interosseous border) of ulna; 14, caudal border of ulnar shaft; 15, anterolateral surface of ulnar shaft; 16, posteromedial surface of ulnar shaft; 17, fossa for brachialis and biceps muscles; 18, concavity on distal ulna to accommodate distal radius; 19, ulnar facet for carpals; 20, radial head; 21, radial articular facet for radial condyle of humerus; 22, radial facet articulating with radial notch of ulna; 23, ridge for forearm flexors; 24, cranial side of distal radius; 25, caudal side of distal radius; 26, anterolateral surface of distal radius; 27, posteromedial surface of distal radius; 28, distal end of radius; 29, radial facet for carpals.

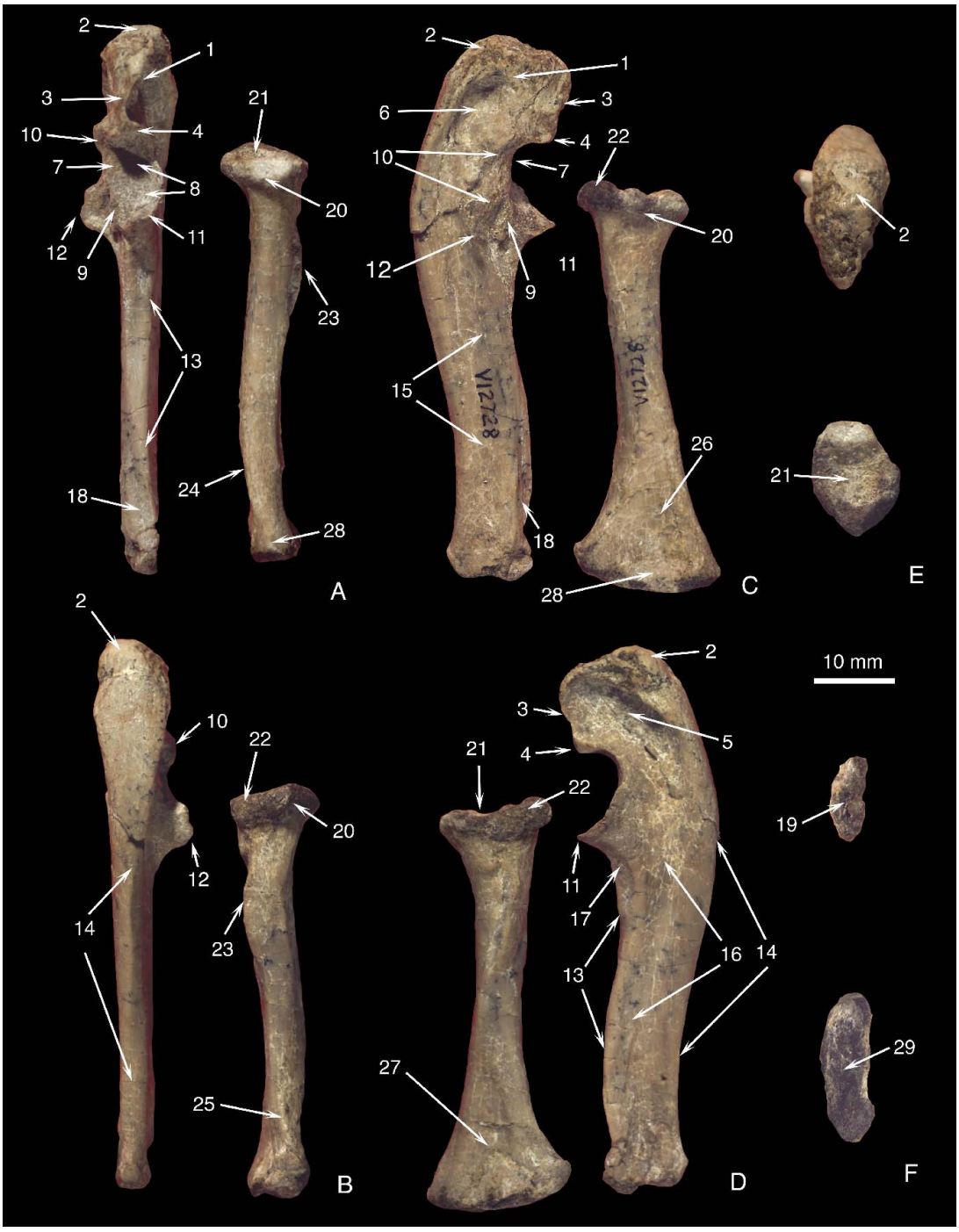

Figure 3-23

ulnar shaft. The concavity on the posteromedial surface (figure 3-23: 5; flexor fossa of Muizon [1998: p 61]) is probably for the origin of the flexor musculature of the hand, while that on the anterolateral surface (figure 3-23: 6; called extensor fossa in following

text) for the extensor musculature (Jenkins, 1971: p123-124 and fig. 31, 32; Jenkins and Parrington, 1976: p 402; Muizon, 1998: p 61). The flexor fossa is limited posteriorly by a strong crest, which is slightly curved cranially. Similar crest is present in marsupials, which is suggested "for the attachment of the posterior and transverse parts of ulnar collateral ligament" (Muizon, 1998: p 61). The extensor fossa on the anterolateral surface is also limited posteriorly by a crest, which is sharper than the one on the posteromedial side and markedly curved anteriorly. Between two crests is the caudal surface of the olecranon, which is slightly convex and has a smooth texture. The surface diminishes distally and two crests merge at the level of the coronoid process. The olecranon is recurved cranially and more so in anterolateral view than in posteromedial view due to the different curvatures of the above mentioned crests.

The proximal articular surface of the ulna has three components: the trochlear notch, the facet for the ulnar condyle and the radial notch (figure 3-23: 7, 8 and 9). The trochlear notch is wide open and semi-oval in shape. It has a fine ridge in the middle and two wings extending posteromedially and anterolaterally, respectively. The ridge fits into the trochlea of the humerus. It extends from proximolateral to distomedial and intersects with the long axis of the ulna at a small angle (about 10-15°, estimated on right ulna of V 12549). The anterolateral wing is slightly convex lateromedially; it is narrow proximally and widens distally (figure 3-23: 10). The posteromedial wing of the trochlear notch also forms the lateral half of the facet for the ulnar condyle. The facet has the similar orientation and proximodistal curvature as the trochlear notch. It is slightly concave lateromedially. Proximally the facet begins at the weak anconeal process and distally it narrows and terminates onto the proximal side of the medial projection of the coronoid

process (figure 3-23: 11). The radial notch of the ulna, which articulates with the ulnar facet on the head of the radius, is distal to the anterolateral wing of the trochlear notch (figure 3-23: 9). A fine ridge separating two facets is visible on the right ulna of V 12549, but not on other specimens. The radial notch is gently concave, facing anteriorly, and embraced by two projections (medial and lateral) of the coronoid process. Both projections contact the humerus and radius, respectively; therefore they "increase the surface area of the elbow joint without contributing materially to its weight-bearing function" (Evans, 1993: p 191). The medial projection is lateromedially extended and points cranially (figure 2-23: 11). The lateral projection is proximodistally extended and directs laterally (figure 3-23: 12). Both projections are salient and both have a fine prolongation extending distally onto the surface of the ulnar shaft.

The ulnar shaft distal to the proximal articular surface is strongly compressed transversely and therefore has a cranial and caudal border and an anterolateral and a posteromedial surface (figure 3-23: 13, 14, 15, and 16). The cranial border is also the interosseous border. Just distal to the medial projection of the coronoid process and posteromedial to the cranial border on the ulnar shaft is a shallow fossa with the rough texture (figure 3-23: 17). Similar fossae are seen in multituberculates (Krause and Jenkins, 1983: p 214 and fig. 14) and some fossil marsupials (Marshall and Sigogneau-Russell, 1995: p 125; Muizon, 1998: p 62). The location of the fossa corresponds to the insertion position of the brachialis and biceps muscles in extant therian mammals (Evans, 1993: fig. 6-55; Muizon, 1998: p 62). Distal to the radial notch and lateral to the cranial border presents another fossa, which is short and shallow. Its lateral border is the short prolongation of the lateral projection of the coronoid process. A similar but long fossa

and a distinct crest lateral to the fossa (supinator crest) are present in fossil marsupial *Mayulestes*, which has been suggested for the origin of the supinator muscle (supinator brevis; Muizon, 1998: p 62 and figs. 23, 24). The fossa of *Repenomamus* and its lateral border appear smaller and less distinct than those of *Mayulestes*, and they were concealed by the radius in life. Therefore, the supinator muscle, if present in *Repenomamus*, does not originate from the fossa and ridge on the ulna. The cranial border of the ulnar shaft distal to the proximal articular surface is first blunt, low and slightly concave; then, as reaching the distal half of the shaft, the border gradually becomes sharper, higher and slightly convex. On the distal quarter of the shaft the cranial border becomes a sharp crest slightly deflected medially. Lateral to the crest is a longitudinal concavity, which is bounded laterally by a low ridge. The concavity accommodates the distal radius (figure 3-23: 18), while the low ridge and crest are probably for the attachment of interosseous membrane. The caudal border of the ulnar shaft is the distal prolongation of the caudal surface of the olecranon. It is low and blunt. The proximal portion of the border is convex while its distal half is concave. The posteromedial surface of the ulnar shaft has a fine line, which extends obliquely, from the middle of the surface (at the level of the coronoid process) to the cranial border of the shaft (at the level where the border becomes the medially deflected crest). Caudal to the line on the posteromedial surface is a depression, which becomes a shallow and wide concavity in distal quarter of the shaft. On the anterolateral surface of the shaft the distal extremity of the extensor fossa reaches the midpoint of the shaft and another shallow depression appears at the distal quarter of the shaft; otherwise the surface is gently flat. The distal portion of the shaft slightly expands craniocadually and transversely. The distal epiphysis is only preserved on the right ulna

of V 13605. It is partially fused with the diaphysis (shaft) with the suture between them clearly visible. The articular surface (with carpals) of the distal epiphysis is smooth and gently convex (figure 2-23: 19). There is no ulnar styloid process.

RADIUS (figures 2-4, 3-20 and 3-23)**--**The radius is the major weight-supporting element of the forearm. It is slightly sigmoidal in shape (in lateral or medial views) and expands on both ends. The bone is shorter and much slenderer than the humerus. Compared to the ulna, the radius is slightly slenderer at the proximal end but greatly expanded at the distal end. When articulated, the radius is in front of the ulna and crosses over the latter with the proximal end anterolaterally and the distal end anteromedially positioned.

The proximal epiphysis is fused to the diaphysis in all specimens without visible suture. The rough texture of the radial head indicates the presence of articular cartilage in life. The radial head is oval in proximal view (figure 3-23: 20). The long axis of the radial head is obliquely oriented (anteromedial to posterolateral) if the ulna is positioned obliquely as stated before. The rim of the radial head is slightly oblique to, rather than perpendicular with, the axis of the bone, lower medially than laterally. The articular facet for the radial condyle of the humerus is concave and spheroid in the contour (figure 3-23: 21). The facet occupies most, but not all, of the proximal surface of the head. Both anteromedial and lateral parts of the surface have a convex nonarticular facet. Around posterolateral quarter of the radial head margin is the facet articulating with the radial notch of the ulna (figure 3-23: 22; the ulnar facet of Jenkins and Parrington [1976: p401] and Muizon [1998: p64]; the articular circumference of Evans [1993: p 188]). The facet is slightly convex, as long as the radial notch.

The shaft of the radius first narrows distally from the head toward the midpoint;

then expands distally. On the posterior aspect of the shaft is a ridge passing from the ulnar facet down to the middle of the shaft (figure 3-23: 23). The ridge reaches its highest point in the middle portion and curves medially as attenuating distally. The lateral surface of the ridge continues with the surface of the shaft smoothly; the medial surface of the ridge is rough. A similar ridge is seen in nonmammalian cynodonts (Jenkins, 1971: p 119), morganucodontids (Jenkins and Parrington, 1976: p 401) and multituberculates (Krause and Jenkins, 1983: p 215). It is probably associated with the attachment of forearm flexors, including the biceps muscle, and the interosseous ligament. If so, the ridge includes (but is not restricted to) the radial tuberosity (Evans, 1993: p 190; the bicipital tuberosity of Muizon [1998: p 64]). The latter is commonly seen in therian mammals and serves for the insertion of the biceps muscle. Excluding the ridge the proximal half of the shaft has a smooth surface and is nearly circular in cross section.

Passing the midpoint, the shaft begins to expand greatly lateromedially and slightly posteriorly; therefore, the distal radius has broad anterolateral and posteromedial surfaces and narrow cranial and caudal sides. The anterolateral surface is smooth and gently convex (figure 3-23: 26). The posteromedial surface is flat in the lateromedial direction and gently concave in the proximodistal direction (figure 3-23: 27). The different curvatures of the anterior and posterior surfaces make the distal radius slightly bending posteriorly in the lateral or medial view. The cranial and caudal sides of the distal radius are convex craniocadually and concave proximodistally (figure 3-23: 24, 25). On the caudal side at the junction of the third and fourth quarter of the shaft is a fine ridge extending obliquely. When articulated, the ridge is next to the low ridge on the anterolateral surface of the distal ulna and probably, as the latter, serves for the

attachment of the interosseous membrane. At the distal extremity of the caudal side, next to the epiphysis, is a raised facet with rough texture. This facet contacted the distal ulna in life.

The distal end of the radius is strongly expanded and elongate ovoid in cross section (figure 3-23: 28). It is about twice as wide as the distal end of the ulna and much thicker (anteroposteriorly). In the distal view the distal end is slightly twisted anticlockwise relative to the proximal end; and its long axis is nearly lateromedially oriented when the ulna is positioned obliquely as stated before. The distal epiphysis is sutured with the shaft. The articular surface for the carpals is gently flattened lateromedially and slightly concave anteroposteriorly with fine marginal rim (figure 3-23: 29).

3.2.4 MANUS

Material

V 12549 has two isolated metacarpals preserved. They are identified as the left metacarpal II (Mc II) and the left Mc V. V 12728 preserves the right trapezium and Mc I in articulation, another distal carpal bone, probably the right trapezoid, and a proximal phalange of some middle finger (II, III, or IV), and a second (middle) phalange of some middle finger. V 13605 has both manus preserved in articulation, but only some elements are identifiable, including several metacarpals and phalanges, but no carpal bone could be positively identified.

Morphology

CARPALS--Among preserved carpals only the right trapezium of V 12728 is preserved together with the Mc I *in situ* and positively identified (figure 2-3 and 3-24). The bone

has an irregular shape. In dorsal view, the bone is widest at distal end and narrowest about the middle where the bone is constricted. A smooth and concave surface occupies both the dorsal and medial aspect of the bone and forms a steep valley opening medially (figure 3-24: 1). The lateral edge of the valley is concave in lateral view; the edge is the highest part of the bone. The distal edge is straight (figure 3-24: 2); here the distal articular facet extends beyond the edge onto the dorsal aspect. The proximal edge is divided into two parts, the proximolateral part extending distolaterally and proximomedial part extending distomedially; both are straight and the latter with a fine margin and longer (figure 3-24: 3 and 4). On the medial aspect of the bone, distal to the opening of the valley is a tuberosity with a rough texture, which probably served for attachment of ligaments and/or tendons in life (figure 3-24: 5).

The distal aspect of the bone has a wide and flat surface articulating with metacarpal I (figure 3-24: 6). The surface is widest in the middle, which is the widest part of the bone. The articular facet itself extends onto the dorsal aspect of the bone. Beneath the articular facet is a prominent tubercle (the distoventral tubercle of the trapezium) protruding distally (figure 3-24: 7). Lateral to the tubercle the ventral edge of the distal aspect bears a shallow notch (figure 3-24: 8). When articulated, the tubercle fits into the space between the tuberosities on the ventral side of the proximal head of Mc I while the notch accommodates the lateral proximal tuberosity of Mc I.

The proximal aspect of the bone is deeper but narrower than the distal one. It can be divided into two parts, a proximomedial facet and a proximolateral facet (figure 3-24: 9 and 10). Both facets are wider (lateromedially) dorsally than ventrally; the proximo-lateral facet is about twice wide as the proximolateral one at dorsal side but as wide as the

latter at the ventral side. The angles between two facets are larger on the dorsal aspect (about 90°) than on the ventral aspect (about 45°). The corner between two facets is blunt; the ridge at the corner is the deepest part of the bone, about twice as deep as the distal aspect of the bone. Both facets and the corner have smooth textures and probably contacted other carpals in life. The proximomedial facet probably articulates with the scaphoid and/or prepollex, and the proximolateral facet with the proximal part of the trapezoid. It is unclear whether the proximal corner of the bone contacts the centrale and/or lunate.

Except the proximolateral facet, the lateral aspect of the trapezium is concave and uneven, with pits and nodes. The distal portion of the bone protrudes laterally; the protrusion probably contacted the trapezoid in life (figure 3-24: 11). In lateral view (also in medial view), the proximal end of the bone is deepest; the bone is gradually shorter distally, but deepens again as distal tubercle appears. The ventral aspect is narrower than the dorsal aspect, and extends proximomedial-to-distolaterally. Its proximal half is smooth and convex. Distally, the protruding base of aforementioned distal tubercle occupies the distolateral corner of the ventral aspect; and medial to the base are fine sulci and ridges.

Figure 3-24. Right trapezium of *Repenomamus robustus*, IVPP V 12728, in dorsal (A), ventral (B), medial (C), lateral (D), distal (E), and proximal (F) views.

1, valley occupying dorsal and medial aspect of bone; 2, distal edge of dorsal aspect; 3, proximolateral edge of dorsal aspect; 4, proximomedial

edge of dorsal aspect; 5, distal tuberosity on the medial aspect; 6, facet for metacarpal I (Mc I); 7, distoventral tubercle; 8, notch accommodating lateral tuberosity of Mc I; 9, proximomedial facet; 10, proximolateral facet; 11, protrusion on lateral aspect.

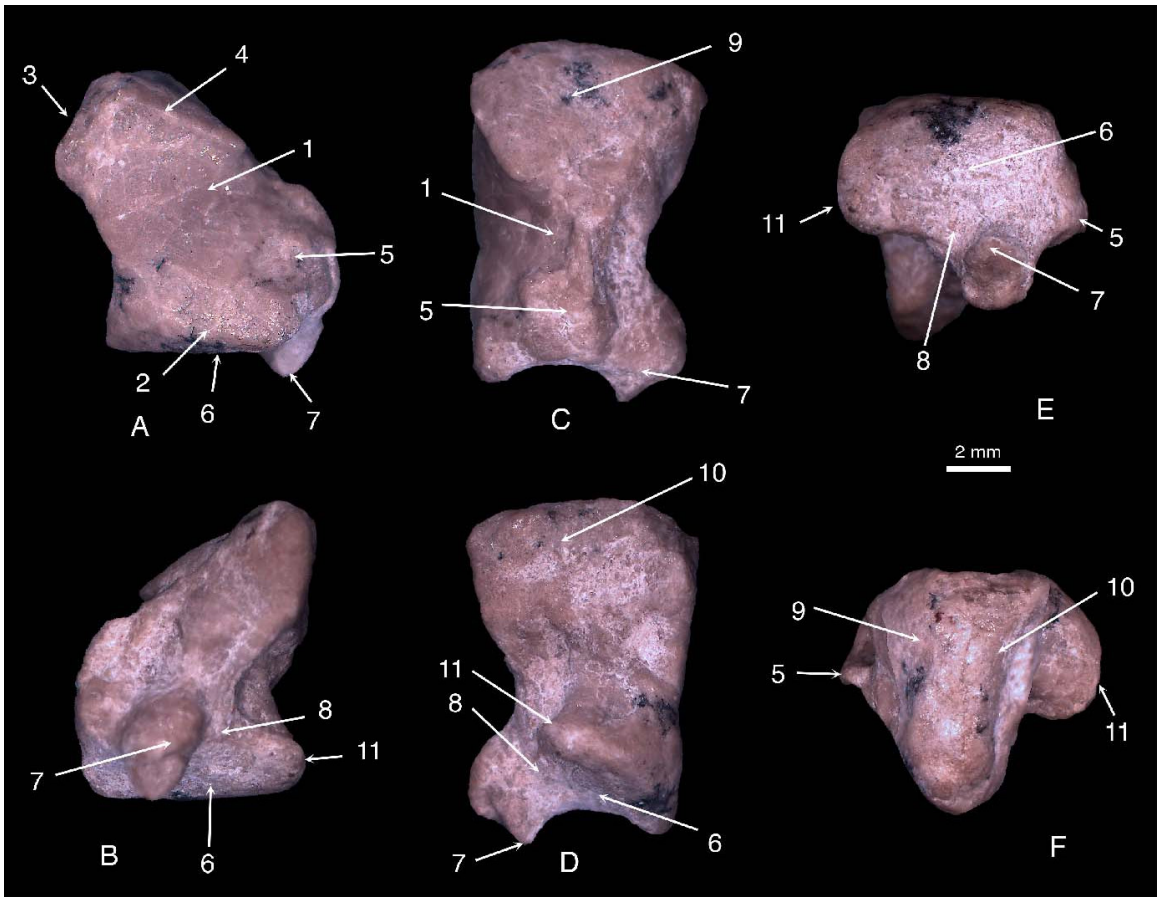

Figure 3-24

V 12728 preserves a second carpal bone, which is not associated with the other manual elements when discovered (figure 3-25). The bone unlikely belongs to the proximal row of the carpal bones as it has only one distinct articular facet, which is convex and does not match the flat surfaces of the distal radius or ulna. The bone is most likely the right trapezoid because it perfectly fits when positioned next to the trapezium. The bone is roughly quadrilateral in lateral (or medial) view and wedge-shaped in dorsal

view (thickening distally). The bone is smaller than the trapezium in overall size. It is deepest in its distal part, longest in dorsal side and widest at the disto-dorsal corner. The dorsal aspect of the bone is gently concave, with a few pits and otherwise featureless (figure 3-25: A). The distal aspect possesses a large smooth facet, which is convex lateromedially and flat dorsoventrally. The facet articulates with the Mc II; and the medial edge of the facet may also contact the lateral protrusion of the trapezium (figure 3-25: 1 and 2). The ventromedial corner of the distal aspect is concave, rough and nonarticular (figure 3-25: 3). The medial aspect of the bone has a sulcus extending proximoventral-to-distodorsally (figure 3-25: 4). The sulcus is deepest at its proximoventral end and gradually fades out distodorsally. A facet occupying proximodorsal quarter of the medial aspect articulated with the proximolateral facet of the trapezium in life (figure 3-25: 5).

In lateral aspect the bone is rough in the texture, with pits and sulci (figure 3-25: C). It is gently concave and probably contacted the hamate in life, but a distinct articular facet is not present. The proximal aspect of the bone is shorter and much narrower than the distal aspect (figure 3-25: F). It has several swellings and pits, but no obvious facet for articulating with other carpals. The ventral aspect of the trapezoid is narrower and shorter than the dorsal aspect, and slightly expands distally (figure 3-25: B). It has three tuberosities, the largest one occupying the proximal end, a smaller and lower one on the distomedial corner, and the smallest but sharpest one on the distolateral corner (figure 3-25: 6, 7 and 8).

The right manus of V 13605 has fragments of several carpal bones preserved, but none of them can be identified.

Figure 3-25. Right trapezoid of *Repenomamus robustus*, IVPP V 12728, in dorsal (A), ventral (B), lateral (C), medial (D), distal (E), and proximal (F) views.

1, articular facet for metacarpal II (Mc II); 2, facet contacting lateral protrusion of trapezium; 3, nonarticular area of distal aspect; 4, sulcus on medial aspect; 5, facet contacting proximolateral facet of trapezium; 6, proximal tuberosity on ventral aspect; 7, distomedial tuberosity on ventral aspect; 8, distolateral tuberosity on ventral aspect.

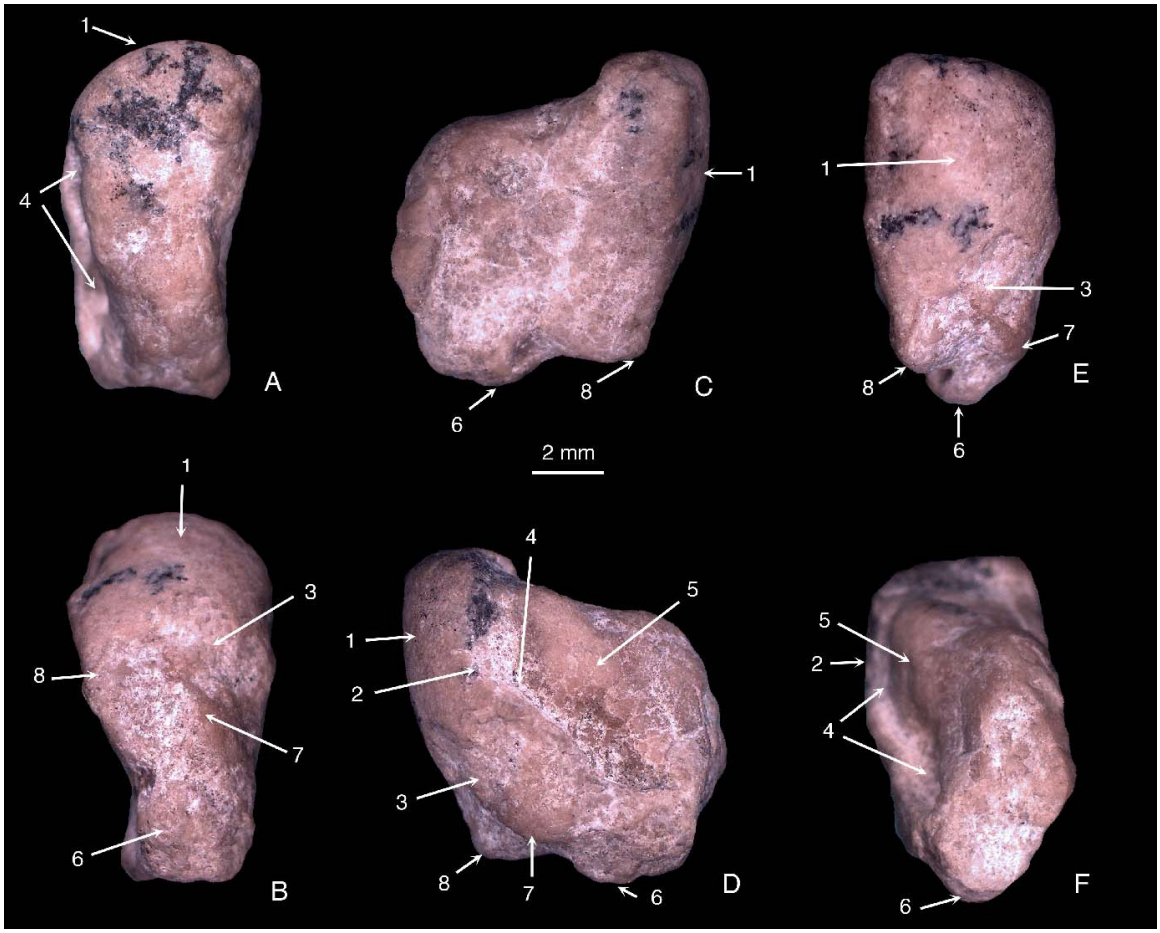

Figure 3-25

METACARPALS (figures 3-26 and 3-27)--The right Mc I of IVPP V 12728 is well preserved (figures 2-3 and 3-26). Mc I is a stout element and longer than trapezium. The proximal end is obviously asymmetrical and has a lateral protuberance due to the great lateral expansion (figure 3-26: 1). The end does not expand medially. The proximal articular facet forms a large smooth surface occupying most area of the proximal aspect, which is slightly convex in both dorsoventral and lateromedial directions and faces proximodorsally and slightly laterally (figure 3-26: 2). The facet is lateromedially wider than dorsoventral deep, and deeper on the lateral, than on the medial, side. The margin of the facet is distinct in dorsal, lateral and medial sides; and the facet does not further extend onto these aspects, but it does extend onto the ventral aspect of the bone (see below). The facet matches the size of the distal articular facets of the trapezium and does not contact the trapezoid at all. The edge of the lateral protuberance (i.e. the lateral rim of the articular facet) may contact the Mc II, but a distinct facet is not present. The dorsal and lateral aspects of the proximal end are smooth and continuous with the surface of the shaft. The medial aspect of the end bears a small pit in the center (figure 3-26: 3). The rugose area surrounding the pit is probably for the attachment of ligaments and muscles. The ventral aspect of the proximal end has two proximal ventral tuberosities. The medial one is small, pointing ventrally (figure 3-26: 4). The lateral tuberosity is much more prominent than the medial one; it points proximally and extends beyond the proximal articular facet (figure 3-26: 5). Both tuberosities have ridge prolonging distally onto the ventral surface of the shaft. Between two tuberosities is the notch where the proximal articular facet extends and articulates with the dorsal surface of the distoventral tubercle of the trapezium (figure 3-26: 6). Distal to the edge of the notch is a concavity laterally

delimited by the prolongations of the tuberosities. The shaft of the Mc I has no distinct boundary with expanded ends. It is round in cross section. Its surface is smooth and featureless. In dorsal view, the medial wall of the shaft is slightly concave while the lateral wall is strongly concave due to the distinct lateral expansion of both ends. The distal end of the bone is much less expanded than the proximal one. Similar to the latter, it is also asymmetrical, expanded laterally but not medially. On the ventral aspect of the distal end are two distal ventral tuberosities (figure 3-26: 7 and 8). They are also asymmetrical, the lateral one wider but less ventrally protruding than the medial one. Between the tuberosities is a shallow concavity, which accommodated a large sesamoid bone in life (figure 3-26: 9). The distal articular facet (for the proximal phalange) is convex in both lateromedial and dorsoventral directions. The facet extends onto the dorsum of bone as well as the ventral side of both tuberosities. The convexity in dorsoventral direction is asymmetrical, greater on the lateral than on the medial side. On the dorsal aspect, proximal to the articular facet, is a small pit, the sesamoid fossa (figure 3-26: 11), also found in the dog and probably for accommodating a small dorsal sesamoid bone (Evans, 1993: p194). The distal articular facet also extends onto the medial and lateral aspects of the distal end, to a lesser degree than onto the dorsal and ventral aspects. On the medial aspect a vertical sulcus delimits the facet proximally (figure 3-26: 12). Proximal to the sulcus is a broad but low medial protuberance (figure 3-26: 13; Bernor *et al*., 1997: p 103). On the lateral aspect proximal to the articular facet is a depression, roughly semicircular in contour and with rugose surface (figure 3-26: 14). Further proximal is a low and vertical ridge, representing the lateral protuberance, which is less prominent than the medial protuberance. These structures on medial and lateral aspects,

as seen in placental mammals (Evans, 1993; Bernor *et al*., 1997), are probably for attachments of collateral and sesamoid ligaments.

Figure 3-26. Metacarpals of *Repenomamus robustus*: right Mc I of IVPP V 12728 in dorsal (A), medial (B), ventral (C), lateral (D), distal (E), and proximal (F) views; left Mc II of IVPP V 12549 in dorsal (G), medial (H), ventral (I), lateral (J), distal (K), and proximal (L) views; left Mc V of IVPP V 12549 in dorsal (M), medial (N), ventral (O), lateral (P), distal (Q), and proximal (R) views.

1, lateral protuberance of Mc I; 2, proximal articular facet of Mc I; 3, pit on the medial aspect of proximal end of Mc I; 4, medial proximal ventral tuberosity; 5, lateral proximal ventral tuberosity; 6, notch between proximal ventral tuberosities; 7, medial distal ventral tuberosity; 8, lateral distal ventral tuberosity; 9, sesamoid bone on ventral side of distal end of Mc I; 10, distal articular facet; 11, sesamoid fossa; 12, sulcus on medial aspect of distal end of Mc I; 13, medial protuberance on distal end of Mc I; 14, depression on lateral aspect of distal end of Mc I; 15, proximal articular facet of Mc II; 16, notch on dorsal margin of proximal articular facet of Mc II; 17, facet for articulating with trapezium; 18, semilunar groove on dorsal aspect of proximal end of Mc II; 19, articular facet for proximal end of Mc III; 20, tubercle on shaft of Mc II; 21, distal articular facet of Mc II; 22, sesamoid bone residing in sesamoid fossa of Mc II; 23, depression and protuberance on medial aspect of distal end of Mc II; 24, depression and

protuberance on lateral aspect of distal end of Mc II; 25, proximal articular facet of Mc V; 26, nonarticular portion on the proximal side of Mc V; 27, intermetacarpal facet of Mc V for Mc IV; 28, depression and protuberance on lateral aspect of distal end of Mc V; 29, depression and protuberance on medial aspect of distal end of Mc V; 30, distal articular facet of Mc V; 31, sulcus on distal articular facet of Mc V; 32, sesamoid fossa of Mc V.

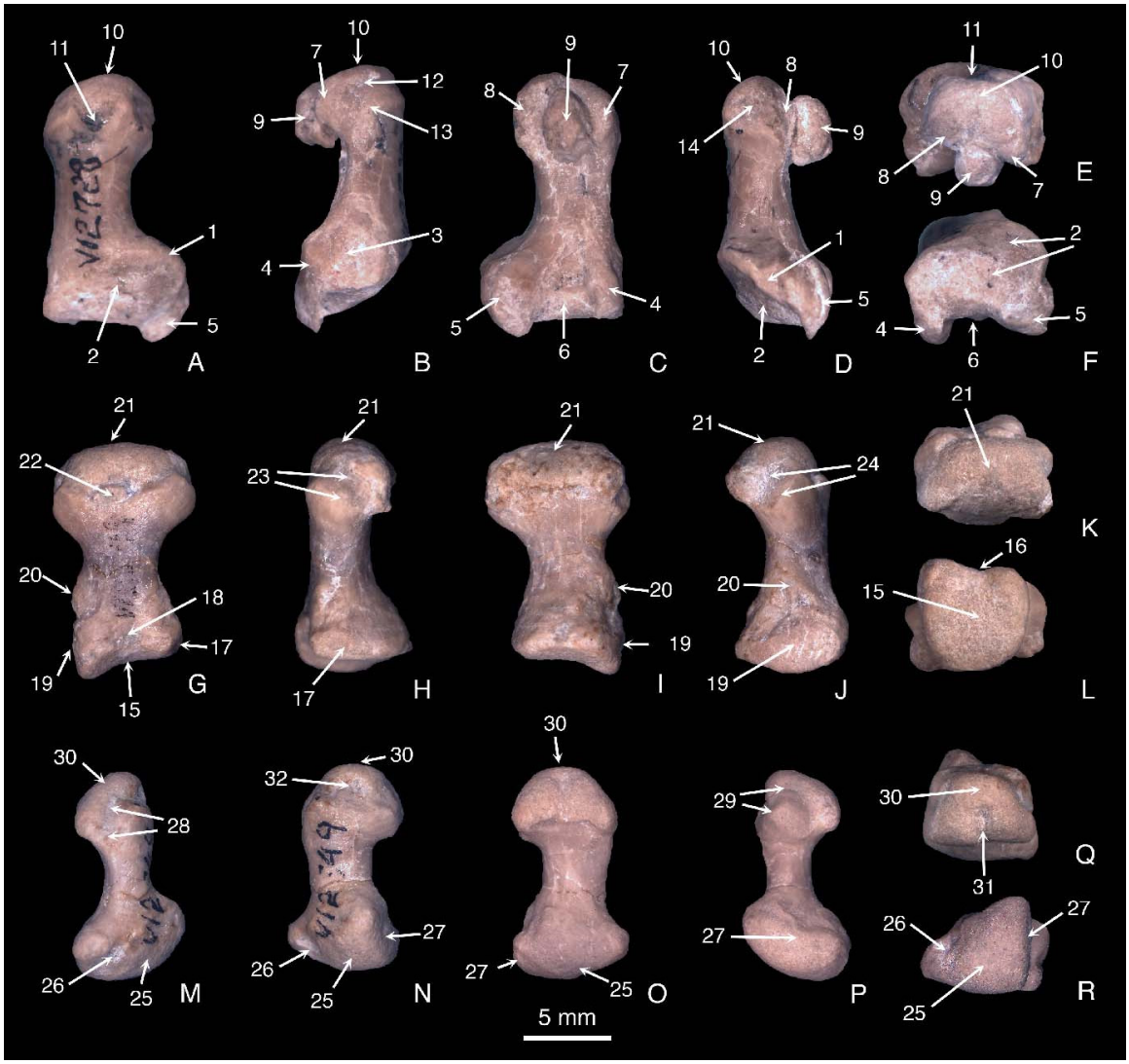

Figure 3-26

An isolated metacarpal of V 12549 is identified as the left Mc II (figure 3-26: G-

L). The bone is similar to other middle metacarpals seen in the manus of V 13605 but bears the intermetacarpal facet only on one side, which matches the morphology of Mc II I expect (see below for detail). Mc II is similar to Mc I in length and stoutness. It is slightly expanded proximally and greatly distally. The proximal end is slightly compressed on lateral side and deeper than high. The articular facet occupies the whole proximal aspect of the bone (figure 3-26: 15). The facet does not extend onto other aspect of the bone. It is lateromedially concave and slightly dorsoventrally convex, matching the distal articular facet of the trapezoid. The margin of the facet is complete on lateral, medial and ventral sides; a notch indents the middle of the dorsal portion of the margin (figure 3-26: 16). The lateral rim is more prominent and proximally protruding than the lateral one. A narrow strip of the facet along its medial edge is gently flat, which may contact the distolateral corner of the trapezium when articulated. The notch on the dorsal rim of the proximal articular facet extends onto the dorsal aspect of the proximal end, where, distal to the rim, is a semi-lunar groove, possibly for the attachment of extensor tendon (figure 3-26: 18; Jenkins and Parrington, 1976: p 413). The medial aspect of the proximal end is smooth, bearing no distinct facet for Mc I. Two bones may not contact as Mc I bears no facet for Mc II either. The ventral aspect of the proximal end is rugose, but otherwise featureless, without proximal ventral tuberosities seen on Mc I. The lateral aspect of the proximal end bears a flat facet for articulation with Mc III (figure 3-26: 19). Compared to proximal end, the shaft is markedly shortened dorsoventrally but only slightly narrows lateromedially. The dorsal aspect of the shaft is gently flat while other three aspects are concave. In the middle the shaft is ovoid in cross section, wider than deep. The surface of the shaft is smooth except that a tubercle on the lateral aspect, just

distal to the facet for Mc III (figure 3-26: 20). The distal end is greatly expanded mediolaterally and, to a lesser degree, dorsoventrally. It is wider but shorter than the proximal end. The distal articular facet is convex dorsoventrally and flat lateromedially (figure 3-26: 21). The facet extends proximally onto the dorsal and ventral aspects of the distal end. On dorsal aspect proximal to the facet is the sesamoid fossa, in which a small sesamoid bone resides (figure 3-26: 22). On the ventral aspect a lip delimits the facet proximally; and small swellings are present on both lateral and medial ends of the lip. On both lateral and medial aspects a shallow depression and prominent protuberance indicate the attachment of collateral and sesamoid ligaments (figure 3-26: 23 and 24).

Mc III (based on left one of V 13605) is similar to Mc II on the whole (figure 3-27). The major differences include that Mc III has an intermetacarpal facet on both lateral and medial aspects of the proximal end (figure 3-27: 1 and 2), the shaft of Mc III is relatively slender and longer, and the distal end of Mc III is less expanded. Mc IV (based on left one of V 13605) is more similar to MC III than to Mc II in length and general morphology. The major difference is that the proximal end of Mc IV is lateromedially compressed and its proximal articular facet is convex dorsoventrally (figure 3-27: 5).

V 12549 also preserved one other metacarpal, which is asymmetrical and different from Mc I-IV in morphology. Here the bone is identified as the left Mc V (figure 3-26: M-R). Mc V is much slenderer and smaller than other metacarpals. Its proximal and distal halves are twisted to each other and therefore the dorsal aspect of the distal half continues with the laterodorsal aspect of the proximal half. Both ends are expanded, the proximal one stouter. The proximal end is triangular with medial, ventral and dorsolateral edges. The proximal articular facet (figure 3-26: 25) occupies most of the proximal aspect of the

bone and extends onto the ventral aspect of the proximal end, where the marginal rim of the facet is indistinct. The dorsal portion of the facet faces proximodorsally. The lateroventral corner of the proximal end is nonarticular (figure 3-26: 26); there are a small tubercle at the corner, pointing ventrolaterally, and small pits dorsal to the tubercle. The medial aspect of the proximal end bears a strip-shaped facet for articulation with Mc IV (figure 3-26: 27). The shaft of Mc V is ovoid in cross section; it has a smooth surface, devoid of the protuberance, ridge, pit, and sulcus. The distal end is slightly narrower and shorter than the proximal end. Similar to on Mc II-VI, the lateral and medial aspects of the distal end have distinct depressions and protuberances for collateral and sesamoid ligaments (figure 3-26: 28 and 29). The distal articular facet (for proximal phalange) is convex dorsoventrally and lateromedially (figure 3-26: 30). The convexity is greater on dorsal than on the ventral portion; therefore the dorsal portion is more distally protruding. The facet is triangular, widened ventrally. A sulcus extends ventrally from the center of the facet, dividing the ventral portion of the facet into the medial and lateral halves (figure 3-26: 31). The facet extends onto the dorsal and ventral aspects of the bone, more proximally extended on ventral aspects. On dorsal aspect, a small sesamoid fossa is present proximal to the facet (figure 3-26: 32). On the ventral aspect an elevated lip marks the edge of the facet; two ends of the lip have small swellings, a condition also seen on Mc II.

MANUAL PHALANGES (figures 3-27 and 3-28)--V 12728 has two isolated phalanges well preserved. They are different in size, and probably represent one proximal phalange of some middle finger (II, III or IV) and one proximal phalange of side finger (Mc I or V). V 13605 preserved several proximal and middle phalanges, which are similar to those of

V 12728 in general morphology. No terminal phalange is preserved in the collection.

Figure 3-27. Partially preserved left manus of *Repenomamus robustus*, IVPP V 13605, in ventral view.

Mc III, metacarpal III; Mc IV, metacarpal IV; PP III, proximal phalange of digit III; 1, intermetacarpal facet of Mc III for Mc II; 2, intermetacarpal articulation Between Mc III and IV, 3, proximal articular facet of Mc III; 4, intermetacarpal facet of Mc IV for Mc V; 5, proximal articular facet of Mc IV.

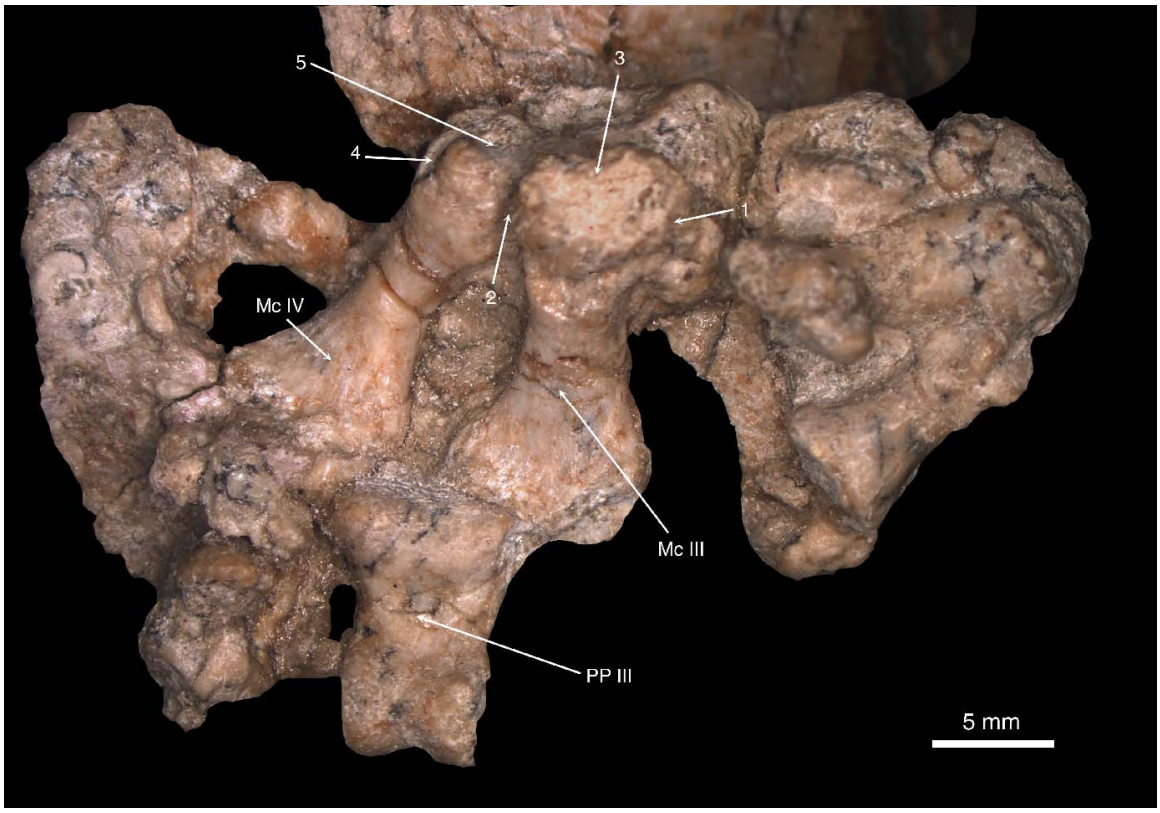

Figure 3-27

The larger phalange of V 12728 is very similar to proximal phalanges of middle fingers of V 13605 (figure 3-28: A-E). Here the element is identified as a proximal phalange of some middle finger (II, III or IV). The following description is mainly based

on this bone. The proximal phalange of a middle finger is a stout element, with the length about 80% of the metacarpal. The proximal end is moderately expanded lateromedially. The proximal articular facet is concave and shallow, facing proximal (figure 3-28: 1). The dorsoventral length of the facet is less than that of the distal facet of the metacarpal, indicating large range of the dorsoventral extension/flexion at the metacarpophalangeal joint. The dorsal margin of the facet is well defined. The bone misses the lateral or medial corner of the proximal end. The preserved corner bears a strip-shaped and convex facet facing medially (or laterally), which is either for the contact between proximal phalanges of middle fingers or the attachment of an articular cartilage (figure 3-28: 2). The ventral margin of the proximal facet is hardly distinguishable; where a furrow along the border is most likely for the attachment of articular cartilage (Bernor *et al*., 1997: p 114).The ventral aspect of the proximal end has a shallow notch in the middle. The shaft is wider than deep. The dorsal, lateral and medial aspects are gently smooth, devoid of distinct structure for the attachment of the soft tissue. The ventral aspect of the shaft has a groove in the middle, which deepens distally (figure 3-28: 3). On the side of the groove are furrows and sulci. Along the ventrolateral and ventromedial margins of the distal half of the shaft is a low flange (figure 3-28: 4), similar to that seen on the metatarsals of *Megazostrodon* and probably for the attachment of flexor tendons (Jenkins and Parrington, 1976: p 415). The distal end is slightly expanded dorsoventrally. The distal articular facet is saddle-shaped, with a convex lateral and medial portion and a central groove (figure 3-28: 5 and 6). The facet extends onto the dorsal and, more proximally, ventral aspect of the bone. On the dorsal aspect and proximal to the central groove of the facet is a depressed area. On the ventral aspect there is a rugose strip proximal to the

articular facet. The lateral and medial aspects of the distal end are nearly vertically oriented, bearing depressions and protuberances for collateral ligaments (figure 3-28: 7).

Figure 3-28. Proximal manual phalanges of *Repenomamus robustus*, IVPP V 12728: proximal phalange of a middle digit in dorsal (A), side (B), ventral (C), distal (D) and proximal (E) views; proximal phalange of digit I in dorsal (F), side (G), ventral (H), distal (I), and proximal (J) views. 1, proximal articular facet; 2, facet on the side of proximal end; 3, groove on the ventral aspect of shaft; 4, flange on the ventrolateral and ventromedial margins of shaft; 5, distal articular facet; 6, central groove of distal articular facet; 7, scars on sides of distal end; 8, swelling on the ventral lip of proximal articular facet; 9, rugose facet on ventral aspect of proximal end.

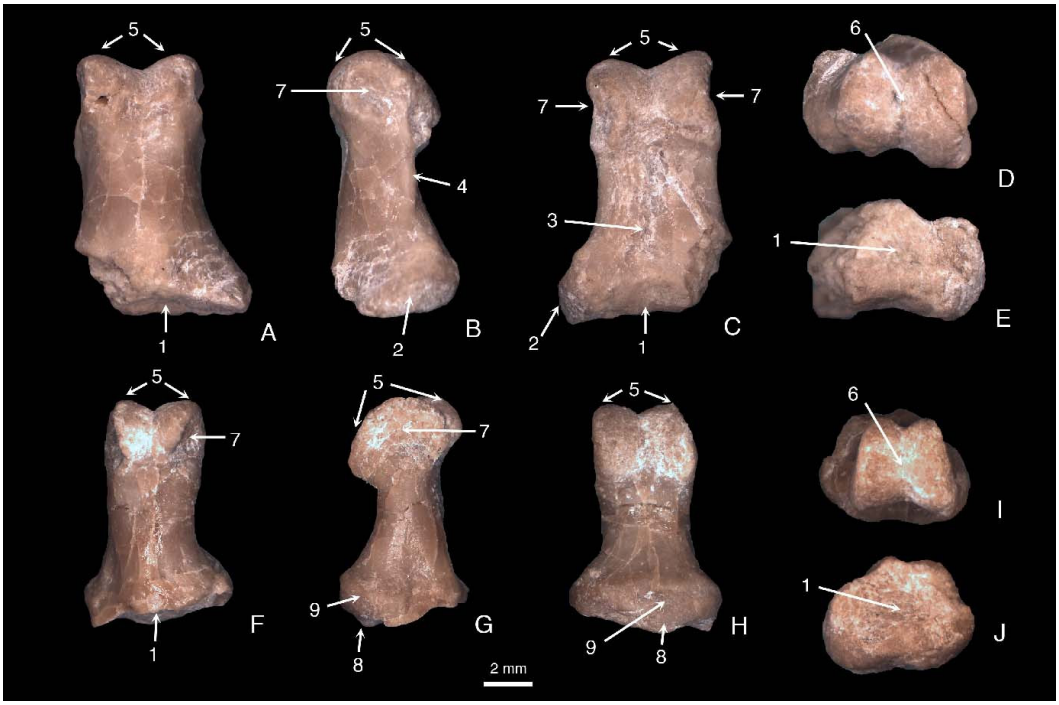

Figure 3-28

The smaller phalange preserved in V 12728 is not a middle phalange, as its proximal articular facet is gently concave and does not match the saddle-shaped distal facet seen in a proximal phalange of some middle finger described above, and presumably for all fingers. The bone is slenderer than the proximal phalanges of the middle digits, and most likely is the proximal phalange of a side finger (I or V). Here it is tentatively identified as the proximal phalange of digit I since it matches the distal facet of Mc I. The proximal end is moderately expanded lateromedially. The concave proximal articular facet faces proximally and slightly laterally, therefore the facet is not perpendicular with the axis of the bone (figure 3-28: 1). Several small tubercles and notches interrupt the dorsal lip of the facet. The ventral lip of the facet has a swelling medial to the midpoint, which fits into the notch between the distal ventral tuberosities of Mc I (figure 3-28: 8). Distal to the ventral lip of the facet is a strip of a rugose surface (figure 3-28: 9). The shaft is slightly compressed dorsoventrally and becomes slenderer distally. The surface of the shaft is smooth. The distal end is expanded dorsoventrally. Its dorsal portion is compressed lateromedially; therefore, the side walls of the distal end are not vertically oriented. The distal articular facet is saddle-shaped, similar to those of middle fingers (figure 5). The facet, as a whole, widens ventrally; its medial portion is convex, and slightly narrower but more ventrally protruded than the lateral one. The depressions on both sides of the distal end are proximodorsally located, with a notch open dorsally; proximal to the depression there is a protuberance (figure 3-28: 7).

3.3 HINDLIMB

3.3.1 PELVIC GIRDLE

Material

V 12549 has the right ilium, left ilium (missing the body), left pubis, and left ischium well preserved. The skeleton of V 13605 preserves both sides of the pelvic girdle, which are exposed both dorsally and ventrally, only lacking the left epipubic bone. In the skeleton of V 14155 the pelvic girdle is exposed ventrally.

Morphology

The pelvic girdle is composed of the ilium, ischium, and pubis, which are sutured, and epipubic bone, which articulates with the pubis.

ILIUM (figures 3-29 and 3-30)--The ilium is about 60% of the total length of the girdle. The bone can be divided into the blade-like wing in the anterior and the rod-shaped body in the posterior. The anterior extremity of the bone, the iliac crest (Evans, 1993: p 202), has a convex profile, thickened ventrally, and with a rugose surface (figure 3-29: 3). The anterodorsal angle of the wing is rounded; therefore, the anterodorsal iliac spine is virtually absent. The anterodorsal portion of the wing, which is anterodorsal to the iliosacral articulation, is everted. The dorsal edge of the iliac wing is slightly concave. In dorsal view, the edge first thickens backwards, then, as approaching the posterodorsal iliac spine, thins again. The posterodorsal iliac spine, located posteriorly between the third and forth quarter of the dorsal edge, is well developed (figure 3-29: 4). It marks the boundary between the iliac wing and iliac body on the dorsal side. Posterior to the spine, the dorsal edge of the iliac body is markedly notched, forming the greater ischiatic notch (figure 3-29: 5). The posterior end of the dorsal edge of the bone is slightly thickened and elevated. It continues with the dorsal edge of the ischium and forms a low convexity dorsal to the acetabulum. This convexity represents a weak ischiatic spine (figure 3-29: 6).

The anteroventral angle of the iliac wing is better marked than the anterodorsal one and forms a blunt anteroventral iliac spine (figure 3-29: 7). The ventral edge of the wing is thinner than the dorsal one. It forms a fine crest terminated posteriorly into a thin eminence, the posteroventral iliac spine (figure 3-29: 8), which is less prominent and more anteriorly located than the posterodorsal iliac spine. The posteroventral spine is in the middle of the ventral edge of the bone, marking the boundary between the wing and body ventrally. The ventral edge of the body is rounded, concave and much thicker than that of the wing. As approaching the acetabulum, the ventral edge expands lateromedially into a ventral surface. The surface continues posteroventrally with the anterior surface of the pubis; and there is no distinct iliopubic eminence at the junction of two bones.

Figure 3-29. Right half of pelvic girdle of *Repenomamus robustus*, IVPP V 12549 in lateral (A), dorsal (B), medial (C), and ventral (D) views. The epipubic bone is not preserved; the ilium is mirror image of left side. 1, wing of ilium; 2, body of ilium; 3, iliac crest; 4, posterodorsal iliac spine; 5, greater ischiatic notch; 6, ischiatic spine; 7, anteroventral iliac spine; 8, posteroventral iliac spine; 9, acetabular surface; 10, ridge on lateral surface of ilium; 11, gluteal fossa; 12, iliac fossa; 13, tuberosity for the rectus femoris; 14, auricular facet; 15, ischiatic process of ilium; 16, pubic process of ilium; 17, body of ischium; 18, neck of ischium; 19, blade of ischium; 20, acetabular facet of ischium; 21, iliac process of ischium; 22, pubic process of ischium; 23, acetabular notch; 24, lesser ischiatic notch; 25, obturator foramen; 26, dorsomedial surface of ischial blade; 27,

ventrolateral surface of ischial blade; 28, ridge on ventrolateral surface of ischial blade; 29, ischiatic tuberosity; 30, posterior edge of ischial blade; 31, symphysis facet of pelvis; 32, body of pubis; 33, ramus of pubis; 34, acetabular facet of pubis; 35, notch on posterior edge of the pubis; 36, facet for epipubic bone; 37, suture between pubic ramus and ischial blade; 38, pubic tubercle.

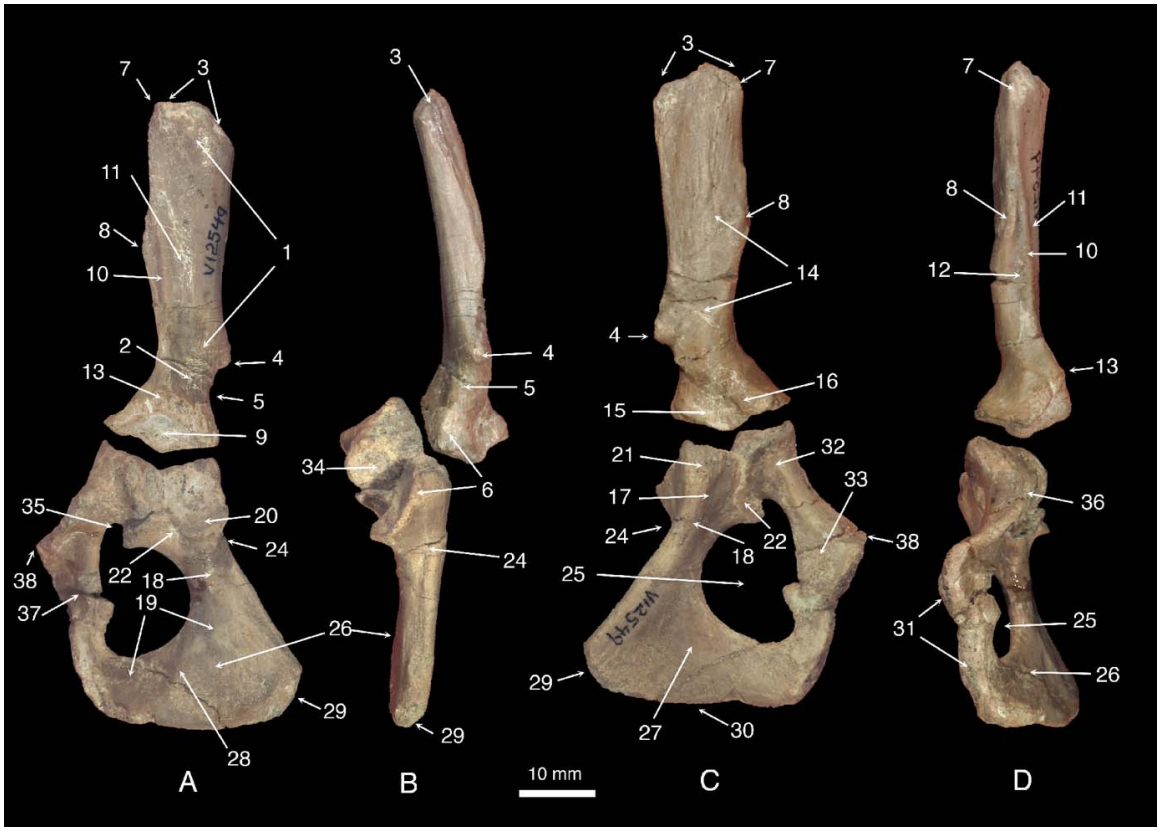

Figure 3-29

In lateral view, the ilium is roughly rectangular in shape. The boundary between the wing and the body is indistinct on the lateral side. Instead, a low and rounded ridge extends anteriorly from near the edge of the acetabular surface, reaches the ventral edge of bone just in front of the posteroventral spine and joins the fine crest on the ventral edge of the wing (figure 3-29: 10). The ridge divides the lateral side of the bone into two

shallow fossae. The larger superior fossa, most obvious just above the ridge, faces laterally; and the smaller inferior fossa faces lateroventrally (figure 3-29: 11 and 12). In therian, the superior fossa is mainly for the insertion of the gluteal muscles and called the gluteal fossa and the inferior fossa, for iliacus, the iliac fossa (Muizon, 1998: p 67). The fossae on the ilium of *Repenomamus* probably have the similar function. Posterior to the iliac fossa and near the acetabulum, the lateral surface of the body continues ventrally with its ventral surface; and there is no distinct boundary between two aspects. Just in front of the acetabulum and below the low ridge as the lateral surface turns around is a small and elevated area with a rugose surface. The elevation probably represents the tuberosity for the rectus femoris, a structure commonly seen in therians (figure 3-29: 13). In morganucodontids, the corresponding area is a depression (Jenkins and Parrington, 1976: p 404).

On the medial side of the bone there is a low and rounded ridge, extending posterodorsally from the posteroventral iliac spine to the middle of the medial surface, right below the posterodorsal iliac spine. The ridge represents the boundary between the wing, which has the rugose surface on the medial aspect, and the body, which has the smooth surface. Above the ridge is the auricular facet for articulation with the sacrum (figure 3-29: 14). The facet has numerous furrows, which are parallel to the axis of the bone. However, the axis of the facet itself is oblique to the bone axis, in a direction from the posterodorsal to anteroventral iliac spine; two axes form an angle of about 20°. Dorsally, a low crest separates the articular facet from the nonarticular and everted anterodorsal portion of the wing. The medially surface of the iliac body is smooth and slightly convex in its front portion. Posteriorly, the surface expands dorsoventrally and

becomes concave medial to the acetabulum.

Figure 3-30. Pelvic girdle of *Repenomamus robustus*, IVPP V 13605, in ventral view.

EP, epipubic bone; FE, femur; IL; ilium; IS, ischium; OF, obturator foramen; PU, pubis; 1, wing of ilium; 2, body of ilium; 3, acetabular facet of ilium; 4, body of ischium; 5, neck of ischium; 6, blade of ischium; 7, ischiatic tuberosity; 8, symphysis facet of pelvis; 9, acetabular notch; 10, base of epipubic bone; 11, ventral edge of epipubic bone; 12, dorsal edge of epipubic bone; 13, dorsal emargination of acetabulum.

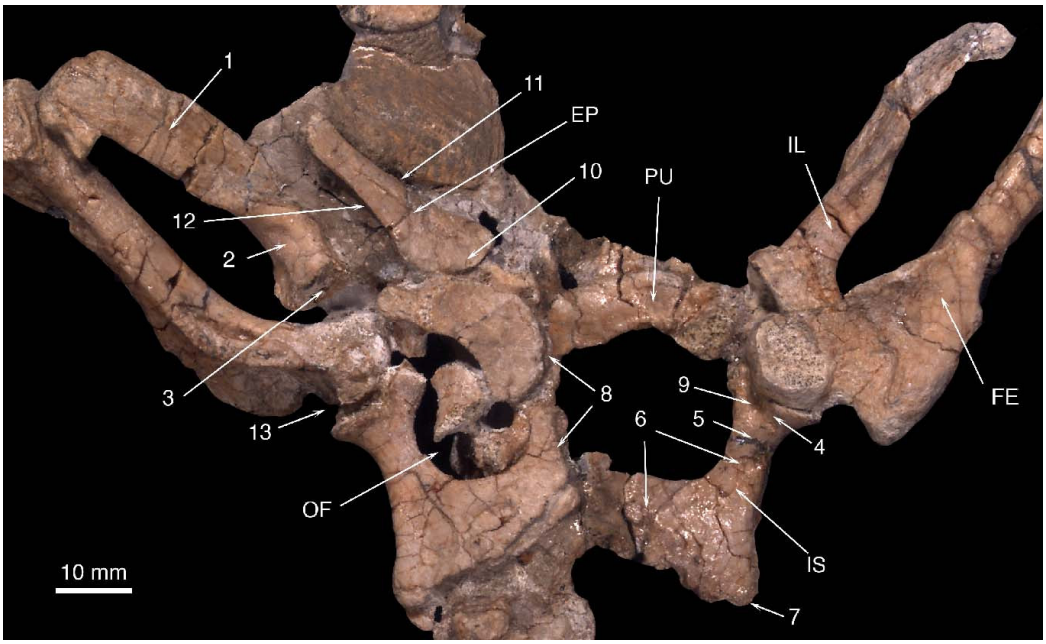

Figure 3-30

The acetabular facet forms a shallow concave fossa laterally on the posterior extremity of the ilium, facing posterolaterally (figure 3-29: 9; figure 3-30: 3). The surface of the facet is rough and was probably coved by the articular cartilage in life. The

marginal rim of the facet is elevated, more so ventrally than dorsally. Dorsomedial to the facet is the process for articulation with the ischium (figure 3-29: 15). The process is laterally compressed and thickened toward the dorsal edge. The contacting surface for the ischium is vertically oriented, facing posteriorly. The process for the contact with the pubis is anteroventral and medial to the acetabular facet (figure 3-29: 16). It is much thicker than the dorsomedial process for the ischium. The contacting surface for pubis is roughly triangular in outline and faces posteroventrally.

ISCHIUM (figures 3-29 and 3-30)--The ischium consists of a body and blade, and a neck between them (figure 3-29: 17, 18 and 19; figure 3-30: 4, 5 and 6). The body of the ischium is its anterodorsal part of the bone, which supports the acetabular facet and processes for the contact with the ilium and pubis. It is the stoutest part of bone and triangular in cross section with stocky corners. The dorsomedial corner of the body forms the iliac process, which is sutured with ilium (figure 3-29: 21). The dorsal edge of the process continues proximally with the dorsal edge of the ilium and together forms a low ischiatic spine above the acetabulum. The process itself is laterally compressed and slightly thickened dorsally. The dorsolateral corner of the body supports the posterior part of the acetabular facet (figure 3-29: 20). The facet itself extends proximally onto the lateral side of the iliac process. It is kidney-shaped, oriented in an anteromedial to distolateral direction. The surface of the facet is shallow and concave, facing anterolaterally and slightly ventrally. The posterior margin of the facet is much more elevated than the dorsal one. The ventral corner of the body is the pubic process for the contact with the pubis (figure 3-29: 22). The process is rounded, and stouter than the iliac process. The process also forms the anterodorsal boundary of the obturator foramen. On

the lateroventral surface of the body between the pubic process and the acetabular facet is a deep incision, the acetabular notch (figure 3-29: 23; figure 3-30: 9). The dorsal surface of the body is flat; its lateral edge disappears at the neck, and the medial edge (= dorsal edge of the iliac process) continues posteriorly as the dorsal margin of the ischial blade. The medial surface of the ischial body is gently concave and dorsoventrally deep.

The ischial neck is the constricted part of the bone posterior to the body (figure 3-29: 18; figure 3-30: 5). The constriction is obvious both dorsally and ventrally. The dorsal edge of the neck is concave and forms a notch on the dorsal edge of the bone, the lesser ischiatic notch (figure 3-29: 24). The ventral edge of the neck forms the concave dorsal boundary of the obturator foramen.

The blade of the ischium forms a broad bony plate, which is twisted relative to the body with the ventral part turning medially (figure 3-29: 19; figure 30: 6). Therefore, the blade has a dorsomedial and ventrolateral surface, instead of a medial and lateral surface (figure 3-29: 26 and 27). Both surfaces have a smooth texture. The dorsomedial surface is gently concave. On the ventrolateral surface there is a low and curved ridge extending from the dorsal margin of the obturator foramen to the junction of the middle and ventral third of the posterior edge of the blade (figure 3-29: 28). The ridge divides the surface into a dorsolateral and ventromedial fossa, both very shallow. The dorsal edge of the blade, which continues with that of the neck, is straight in lateral view and slightly inflected medially, visible in dorsal view. The posterior edge of the blade is convex for the dorsal two thirds and straight for the ventral third. The dorsal and posterior edge meet at a rounded angle, which is thickened and rugose at the tip, forming the ischiatic tuberosity (figure 3-29: 29). The posterior edge of the blade also meets its counterpart to

form an ischial arch (figure 3-29: 30). The anterior edge of the blade forms the posterior boundary of the obturator foramen, but the inferior portion of blade also forms most of the ventral boundary of the foramen. This inferior portion of the blade is sutured with the ventral ramus of the pubis (figure 3-29: 37). Together, tow bones meet their counterparts and form the pubic symphysis; and the ischium portion forms the posterior three-fifths length of the symphysis. The symphysis facet (figure 3-29: 31) is perpendicular with the inferior portion the ischial blade, which indicates a broad and shallow U-shaped ischial arch, visible in posterior view. This is in contrast with the deep V-shaped ischial arch of multituberculates (Kielan-Jaworowska and Gambaryan, 1994: p62 and references therein).

PUBIS (figures 3-29, 3-30)--The pubis can be roughly divided into a body, which supports the acetabular facet, and a ramus, which forms the anteroventral border of the obturator foramen (figure 3-29: 32 and 33). The body is the thickened part of the bone. It has a iliac and ischial facet for the contact with the corresponding bones. The iliac facet faces anterodorsally, and the ischial facet posterodorsally. Between these two facets is the acetabular facet of the pubis, which is gently concave and dorsolaterally oriented (figure 3-29: 34). There is no distinct (iliopubic) tubercle at the junction of the pubis and ilium, but the junction of the pubis and ischium presents an eminence protruding posteriorly into the obturator foramen. Below the eminence is a notch on the posterior edge of the pubis, which is probably for transmitting the obturator nerve and vessels (figure 3-29: 35; Jenkins and Schaff, 1988: p 16).

The ramus extends ventromedially and posteriorly from the body (figure 3-29: 33). It is much thinner than the latter. Its anterior edge is strongly everted. Therefore, the

mediodorsal surface of the ramus is convex, and the anterodorsal portion of the surface actually faces anteriorly. Along the anterior edge is the facet for the epipubic bone, which is directed ventrally and anterolaterally, more laterally than anteriorly (figure 3-29: 36). The posterior edge of the ramus is slightly concave, forming the anteroventral border of the obturator foramen. The ventral portion of the ramus turns medially. It meets its fellow along the pelvis symphysis and is sutured with the ventral portion of the ischial blade (figure 3-29: 37). The anteroventral corner of the ramus, the pubic tubercle, is not thickened (figure 3-29: 38).

EPIPUBIC BONE (figures 2-5 and 3-30)--The epipubic bone of *Repenomamus* is a large element. It is triangular in shape, with a stout base, a long ventral edge and a shorter dorsal edge (figure 3-30: 10, 11 and 12). Its minimal length (along the dorsal edge) is loner than the length of the ischium. Its base is slightly thickened, sitting at the anterior edge of the pubis in life. The tip of the bone points dorsally and anterolaterally, probably more laterally than anteriorly (figure 2-5). The posterolateral surface of the bone is slightly convex while the anteromedial surface has a longitudinal sulcus.

ACETABULUM AND OBTURATOR FORAMEN (figures 3-29, 3-30)**--**The acetabulum is shallower than a hemisphere. The ilium, ischium and pubis are sutures but not fused within the acetabulum. Among three bones, the ilium has the largest acetabular facet and the pubis the smallest. The margin of the acetabulum protrudes laterally, but it is incomplete at the junction of the ilium and ischium, where a broad V-shaped notch, the dorsal emargination of acetabulum, is present (figure 3-30: 13). The surface of the acetabulum is rugose, and can not be divided into the surrounding lunate surface and the nonarticular acetabular fossa in the center. In life, the surface was probably covered with

articular cartilage and the dorsal emargination may be completed by the fibrocartilaginous tissue, as suggested for *Gobiconodon* (Jenkins and Schaff, 1988: p 17). As a whole, the acetabulum probably faces laterally and slightly ventrally.

The obturator foramen is imperfectly circular in shape (figure 3-29: 25; figure 3-30: OF). Most of its border is formed by the edge of the ischium, and only the anteroventral border is that of the pubis. The foramen is larger than the acetabulum and located posteroventral and slightly medial to the latter.

3.3.2 FEMUR

Material

V 12549 has both femora well preserved, among which the left one suffers some postmortem deformation. V 12728 preserves the right femur, which misses part of the distal shaft. V 13605 has both femora preserved in articulation but crushed in same plane as the pelvic girdle. In V 14155 both femora are well preserved *in situ* and exposed ventrally.

Morphology

The femur is about 10% longer than the humerus and appears a little slenderer than the latter. Both the proximal and distal epiphysis are fused with the diaphysis, and the trace of sutures is still visible (figure 3-31: 1). The proximal third of the bone turns dorsally and slightly medially; the feature is further exaggerated by the femoral head, which is oriented proximally and dorsomedially (figure 3-31: 2). A low rounded and curved ridge on the dorsal aspect of the bone (figure 3-31: 3), extending from the head through the neck onto the surface of the shaft, well indicates this continuous turning of the proximal structures.

The femoral head is globular in its general morphology, but slightly flattened in its ventromedial quarter, where a small depressions is present on the surface, probably for the attachment of the ligament of the head (figure 3-31: 4; Muizon, 1998: p 71; = ligamentum capitis femoris of Jenkins and Parrington [1976: p 407]). The articular surface of the head is smooth. On the dorsal aspect, the margin of the surface is along a semicircular line, which demarcates the head from the neck; on the ventral aspect, the surface has a tongue protruding distolaterally beyond the semicircular line onto the neck (figure 3-31: 5 and 6). The femoral neck is short, broad lateromedially and compressed dorsoventrally (figure 3-31: 5). A low ridge fills the gap between the neck and the greater trochanter (figure 3-31: 7). The latter appears as a prominent process, arising from the lateroventral aspect of the bone (figure 3-31: 8). Proximally, the trochanter is much lower than the head. The apex of the trochanter points proximolaterally. The lateral edge of the trochanter is thickened proximally and slightly reflected dorsally. The trochanter becomes slender distally. Near its distal extremity, the lateral edge of the greater trochanter presents a small eminence protruding laterally, which represents the third trochanter (figure 3-31: 9). The lesser trochanter arises from medioventral aspect of the shaft (figure 3-31: 10), just distal to the neck. It is triangular in outline, and smaller and lower than the greater trochanter. The edge of the lesser trochanter is thin and slightly reflected dorsally. On the dorsal aspect of the trochanter, adjacent to the shaft, is a shallow fossa of unknown function. A similar but deeper fossa is present in specimens of *Gobiconodon ostromi* (Jenkins and Schaff, 1988: p 17). On the ventral aspect of the bone, between the greater and lesser trochanter, is a broad and shallow intertrochanteric fossa (figure 3-31: 11). The fossa is distally delimited by a low intertrochanteric crest (figure 3-

31: 12). The distal extremity of the lesser trochanter reaches the same level as the third trochanter.

Figure 3-31. Right femur of *Repenomamus robustus*, IVPP V 12549, in dorsal (A), lateral (B), ventral (C), medial (D), proximal (E), and distal (F) views. Scale bar is 10 mm.

1, suture between epiphysis and diaphysis; 2, femoral head; 3, ridge on dorsal aspect of shaft; 4, nonarticular depression on the femoral head; 5, femoral neck; 6, margin of articular facet on femoral head; 7, ridge connecting femoral neck and greater trochanter; 8, greater trochanter; 9, third trochanter; 10, lesser trochanter; 11, intertrochanteric fossa; 12, intertrochanteric crest; 13, medioventral edge of shaft; 14, lateroventral edge of shaft; 15, patellar groove; 16, lateral condyle; 17, medial condyle; 18, intercondylar fossa; 19, lateral epicondyle.

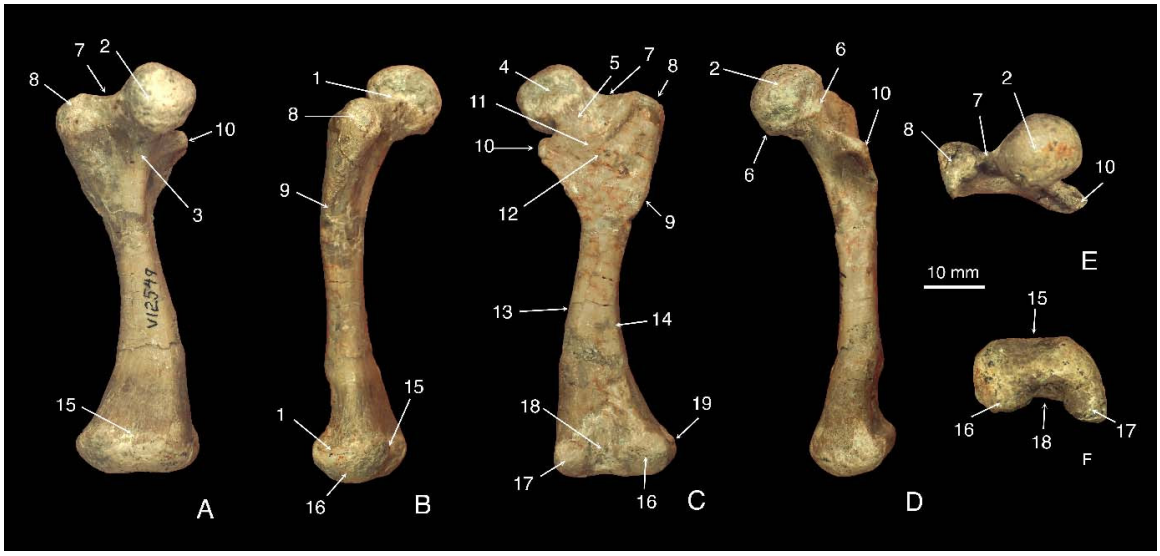

Figure 3-31

The femoral shaft can be roughly divided into three segments, which have

different profiles. The proximal third is between the trochanters. As described above, it has a longitudinal ridge on the dorsal aspect and the intertrochanteric fossa and crest on the ventral aspect. The femoral shaft narrows at the level of distal extremity of trochanters. The middle segment of the shaft is roughly oval in cross section. Here the medial, dorsal and lateral aspects are convex and not demarcated from each other while the ventral aspect is gently flat, with a low and rounded medioventral edge and a fine lateroventral edge (figure 3-31: 13 and 14). On the right femur of V 12728, the medioventral edge has a small eminence, oriented ventrally; the condition is not seen on other specimens in the collection. Both edges are most distinct in the middle segment of the bone, but extend along the whole length of the shaft. The medioventral edge is continuous from the lesser trochanter to the medial condyle of the distal end, and the lateroventral edge from the greater trochanter to the lateral condyle. The distal segment of the shaft gradually expands laterally toward the distal end of the bone. The cross section of this portion of the shaft is somewhat kidney-shaped as the dorsal aspect is gently flat while the ventral aspect slightly concave.

The distal end of the femur is asymmetrical. It is lateromedially wider than dorsoventrally deep and protrudes laterally and slightly ventrally. In dorsal view, the lateral condyle strongly protrudes laterally while the medial one not protruding medially (figure 3-31: 16 and 17). The patellar groove is broad and shallow, without a lateral or medial crest (figure 3-31: 15). Its central line is on the dorsal aspect of the lateral condyle, rather than between the condyles. Distally, the groove becomes the flat facet extending onto the ventral aspect of the lateral condyle. In distal view, the lateral condyle is about twice as wide as the medial one but much less ventrally protruding than the latter.

Between the condyles is the intercondylar fossa (figure 3-31: 18), which is slightly narrower than the medial condyle. A small facet lateroventral on the lateral condyle is possibly for articulation with the head of the fibular. In ventral view, the intercondylar fossa widens proximally and continues with the concavity on the ventral aspect of the distal shaft. The surface of the lateral condyle for articulation with the tibia is gently convex while that of the medial one distinctly convex. The lateral aspect of the femur presents a protruding lateral epicondyle with a rugose appearance (figure 3-31: 19). The medial aspect of the distal femur is gently flat, only the fine wrinkles on the side of the medial condyle indicating the present of an indistinct medial epicondyle.

3.3.3. TIBIA AND FIBULA

Material

Tibiae and fibulae are well preserved in V 12549; the left fibula losses the distal epiphysis while the right one misses part of the shaft in the middle. V 13605 and V 14155 have both tibiae and fibulae preserved in articulation, which suffer some damages. Together, they allow us the reconstruct the morphology of both bones.

Morphology

TIBIA (figure 3-32)--Both proximal and distal epiphyses are fused to the diaphysis on all specimens in the collection. The bone is gently straight and shorter than the femur and ulna, but longer than the radius. The proximal end is transversely expanded, forming a subtriangular plateau with posterolateral and posteromedial corners protruding beyond the shaft. The medial condyle is obliquely oriented, in anterolateral to posteromedial direction; and the lateral condyle is nearly anteroposteriorly oriented (figure 3-32: 1 and 2). Both condyles are slightly concave and longer than wide, the medial one longer.

Between the condyles is the nonarticular surface, including an anterior intercondyloid area, a posterior intercondyloid area and a deep fossa between them (figure 3-32: 3, 4 and 5). Both areas are slightly convex, the anterior one larger. In front of the anterior intercondyloid area is the tibial tuberosity, which has the rugose surface and moderately projects (figure 3-32: 6). The posterolateral corner of the tibial plateau presents a small convex facet for articulation with the head of the fibula (figure 3-32: 7).

The proximal half of the tibial shaft is subtriangular in cross section and gradually narrows distally. The tibial crest is low and rounded, with smooth surface (figure 3-32: 8). The crest quickly fades out as reaching the second quarter of the shaft, where the shaft is anteroposteriorly thick as transversely wide. The anteromedial surface of the proximal half of the shaft is broad and flat. The anterolateral surface is narrow and concave, presenting a shallow lateral tibia fossa beneath the plateau (figure 3-32: 9; Muizon, 1998: p 75). The posterior surface has a low crest in middle, extending only quarter length of the bone. Lateral and medial to the crest are shallow fossae, the lateral one about twice as wide as the medial one. The distal half of the tibial shaft is slightly compressed lateromedially. It has a flat lateral surface, a flat posterior surface and a convex anteromedially surface. In third quarter of the shaft the edge between the lateral and anteromedial surfaces presents a thickened eminence.

Figure 3-32. Right tibia and fibula of *Repenomamus robustus*, IVPP V 12549, in anterior (A), posterior (B), medial (C), lateral (D), proximal (E), and distal (F) views. Scale bare is 10 mm.

1, medial condyle of tibia; 2, lateral condyle of tibia; 3, anterior

intercondyloid area; 4, posterior intercondyloid area; 5, fossa in intercondyloid area; 6, tibial tuberosity; 7, articular facet for fibular head; 8, tibial crest; 9, lateral tibial fossa; 10, distal articular facet; 11, tibial malleolus; 12, fibular head; 13, facet on top of fibular head; 14, flange posterior to fibular head; 15, lateral surface of fibula; 16, medial surface of fibula; 17, distal articular facet of fibula.

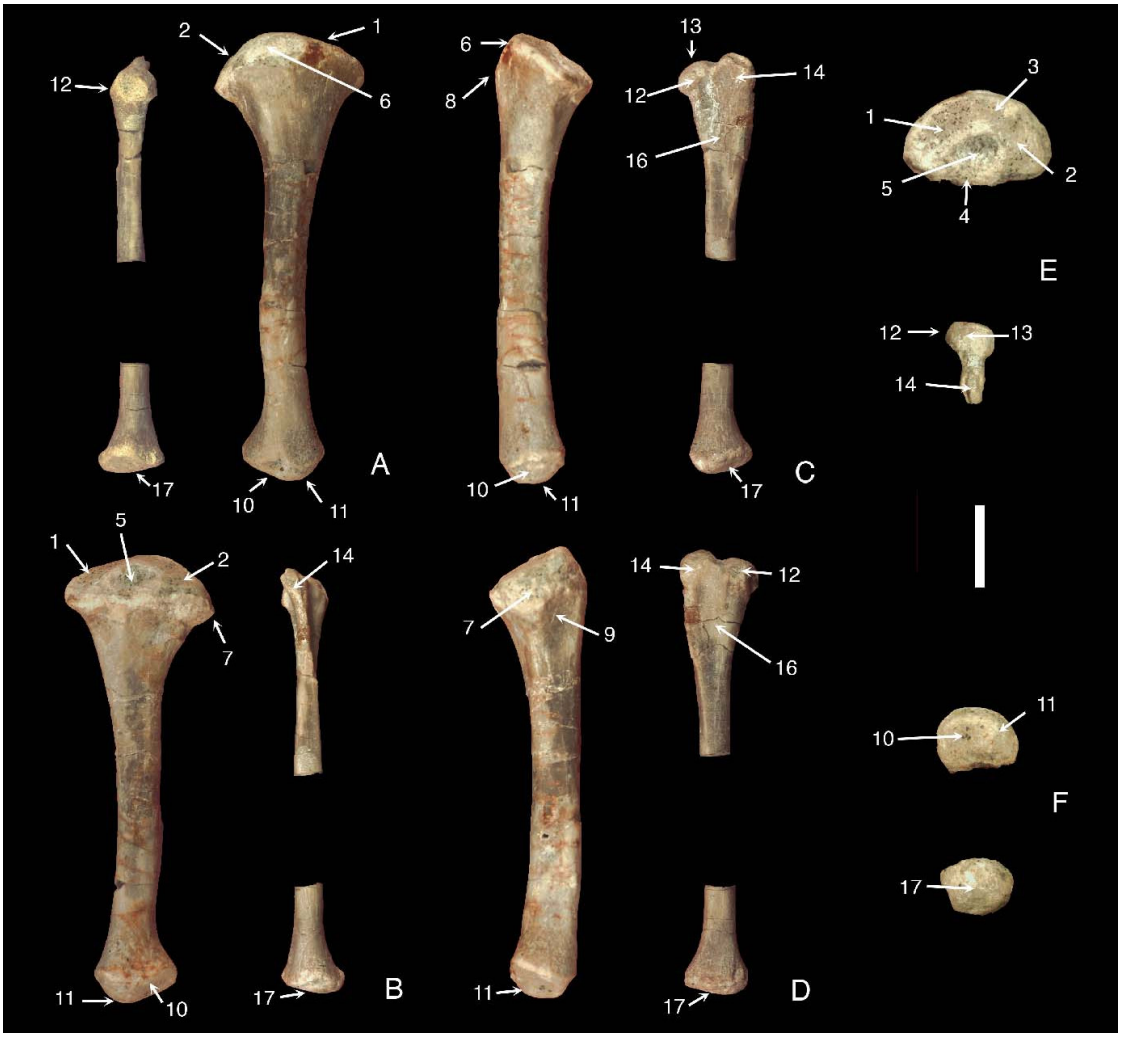

Figure 3-32

The distal end of the tibia expands laterally and slightly medially. The distal articular facet (for the astragalus) is slightly concave, facing distally and slightly laterally

(figure 3-32: 10). Medial to facet is a low and blunt tibial malleolus (figure 3-32: 11). The lateral aspect of the distal end protrudes laterally beyond the surface of the shaft, but no distinct facet for the fibula present.

FIBULA (figure 3-32)--The fibula of *Repenomamus* is a slender and rod-shaped element. The bone roughly has the same length as the tibia, as shown in articulated skeleton of V 14155 (figure 2-5). The fibular head is bulbous (figure 3-32: 12). The top of the head has a convex facet, proximomedially oriented (figure 3-32: 13). The facet is probably for articulation with the femur. Lateral to the facet, on the lateral side of the head is a small depression. It is unclear whether there is a parafibula present and contacting the fibular head anteriorly or laterally. A bony fragment is preserved in the skeleton of V 14155, on the lateral side of the right fibula; and a smaller bony piece is also seen on the left side of the skeleton, lateral to between the fibula and femur. Since the bones are somewhat crushed, it is difficult to identify these two fragments. Posterior to the fibular head is a flange separated from the head by a shallow notch (figure 3-32: 14). The flange is anteroposteriorly oriented. Its tip is convex with sulci and ridges, extending proximally slightly beyond the head. Similar flange on the fibula of *Morganucodon* has been interpreted as for the musculotendinous attachment, like that of monotremes (Jenkins and Parrington, 1976: p411). The flange in *Repenomamus* probably has the similar function.

The proximal half of the fibular shaft is flattened lateromedially and gradually thins anteroposteriorly from the proximal end. The lateral surface of the proximal half is convex anteriorly and concave posteriorly (figure 3-32: 15). Correspondingly, the medial surface is concave anteriorly and convex posteriorly (figure 3-32: 16). The posterior edge of the proximal half is straight and everted while the anterior edge is concave and turning

medially. The distal half of the shaft is roughly cylindrical, but its lateral surface is flat.

The distal end of the bone is moderately expanded anteroposteriorly and medially. It may contact the lateral side of the distal tibia, but there is no distinct facet for the articulation. The distal articular facet is convex (figure 3-32: 17). Its medial part probably articulates with the astragalus while the lateral part with the calcaneus, but facet is continuous and has not boundary between two parts. There is no fibular malleolus. The left fibula of V 12549 lost the distal epiphysis. As preserved, a piece of bony fragments attaches the distal end of the shaft. It is unclear whether it is part of the distal epiphysis or some other element, such as external pedal spur. Other than this ambiguous evidence, there is no remains in our collection indicating the presence of a pedal spur.

3.3.4 PES

Material

V 12549 has all tarsals, metatarsals and proximal phalanges of digit II-IV of the left pes preserved in articulation. Except proximal phalanges of digit III and IV, all these elements are perfectly preserved. V 13605 has both pedes partially preserved, which supplement some information not seen in the V 12549. The following description is mainly based on V 12549 (figure 3-33).

Morphology

ASTRAGALUS (figures 3-33, 3-34)--The astragalus is the stoutest element of the pes. The bone is irregular in shape. The anterior part of the bone slightly narrows and forms an incipient head (figure 3-34: 1), but there is no distinct neck (constricted part behind the head). In dorsal view, the bone is roughly ovoid and longer than wide. The dorsal aspect is bulbous. The articular facet for the tibia occupies most of this aspect and faces dorsally

(figure 3-34: 2). It is smooth, convex and not further divided into the lateral and medial facet. A fine ridge medially on the dorsal aspect delineates the medial boundary of the articular facet (figure 3-34: 3). Medial to the ridge, the surface is rugose and nonarticular. The articular facet for the fibula is posterolateral to that for the tibia and faces laterodorsally (figure 3-34: 4). It continues with the latter; a rounded and indistinct ridge marks the boundary between two facets (figure 3-34: 5). The medial aspect of the bone presents a shallow and broad sulcus in the middle, extending anteroposteriorly (figure 3-34: 6). The surface of the medial aspect is rugose, with pits and swellings, which are probably for the attachment of ligaments. Also visible in medial view is the astragalar medial plantar tuberosity, which protrudes ventrally (figure 3-34: 7). The tuberosity has a hook-like process (figure 3-34: 8) directing anteriorly and enclosing a foramen. This structure is never seen in other mammals.

Figure 3-33. Left pes of R*enomamus robustus*, IVPP V 12549: articulated foot in dorsal (A) and ventral (B) views; articulated astragalus and calcaneus in lateral (C), distal (D) and medial (E) views.
As, astragalus; Ca, calcaneus; Cu, cuboid; Ec, ectocuneiform; En, entocuneiform; Me, mesocuneiform; Mt I-Mt V, first to fifth metatarsals; PP II-PP IV, proximal phalanges of second to fourth digits; Se1-Se4, sesamoid bones; 1, tuberosity of calcaneus; 2, calcaneocuboid facet; 3, sustentaculum tail; 4, astragalonavicular facet; 5, medial plantar tuberosity of astragalus.

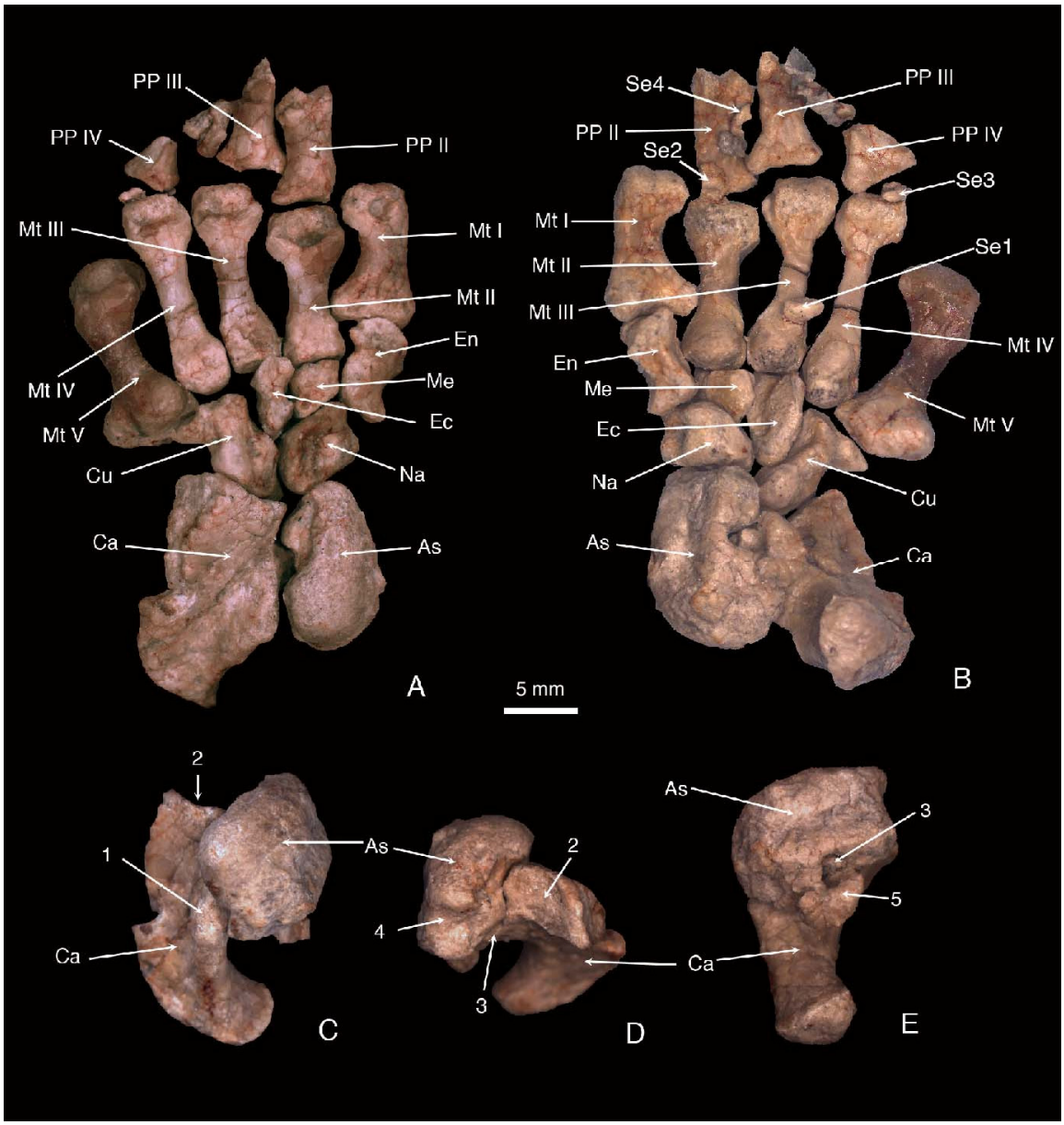

Figure 3-33

The lateral aspect of the astragalus has a complex contour. There is a deep and large concavity posteroventrally located (figure 3-34: 9). In life, the concavity accommodated the sustentaculum tail of the calcaneus. The concavity is posteroventrally delimited by the medial plantar tuberosity and its process. The anterior wall of the concavity is flat, facing posteriorly, it presents the facet for the sustentaculum tail (figure 3-34: 10). The facet itself extends medially onto the medial aspect of the bone. The dorsal

margin of the concavity bears the astragalocalcaneal facet (figure 3-34: 11). The facet forms a strip around the margin, extending from the dorsal wall of the concavity (facing ventrally) to the medial aspect of the bone (facing medially). As a whole, the facet is convex, oriented in an anterolateral to posteromedial direction. Between the astragalo-calcaneal facet and the facet for the sustentaculum tail, on the anterodorsal corner of the concavity, is a shallow sulcus. Posteroventral to the astragalocalcaneal facet is another shallow sulcus. Both sulci probably represent trace of the sulcus astragali (Szalay, 1994: p 5), the astragalus part of the astragalar canal (figure 3-34: 12). In *Repenomamus*, the canal does not penetrate the astragalus. Adjacent to the anterior margin of the concavity, anteroventral to the facet for the sustentaculum tail is a small lateral protrusion of the bone, which presents the facet for the cuboid, the astragalocuboid facet, facing laterally and slightly anteriorly (figure 3-34: 13). The presence of the astragalocuboid contact separates the calcaneus and navicular.

Figure 3-34. Left astragalus of *Repenomamus robustus*, IVPP V 12549, in dorsal (A), ventral (B), distal (C), proximal (D), medial (E), and lateral (F) views.

1, incipient head of astragalus; 2, articular facet for tibia; 3, medial boundary of articular facet for tibia; 4, articular facet for fibula; 5, ridge between facet for tibia and fibula; 6, sulcus on medial aspect; 7, medial plantar tuberosity of astragalus; 8, hook-like process on the medial plantar process; 9, concavity accommodating sustentaculum tail; 10, facet for sustentaculum tail; 11, astragalocalcaneal facet; 12, sulcus astragali; 13,

astragalocuboid facet; 14, medioventral edge of astragalus; 15, astragalonavicular facet; 16, posterior end of sulcus astragali.

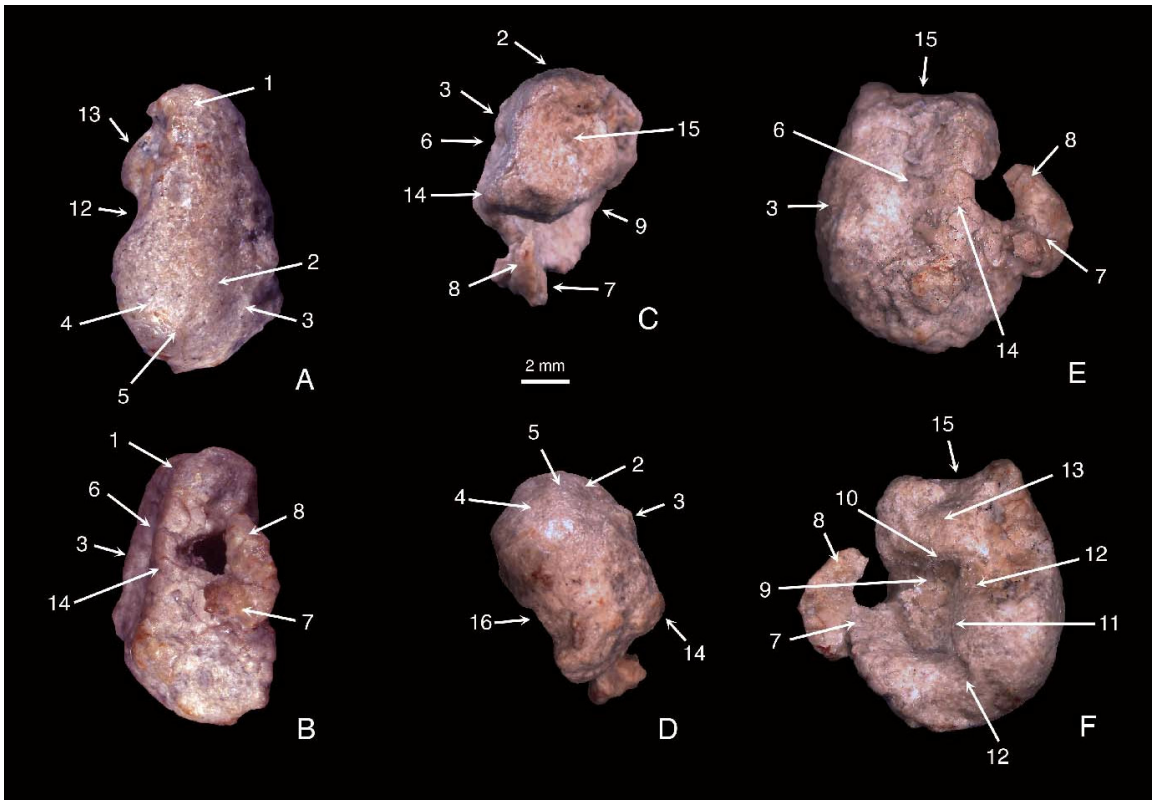

Figure 3-34

The ventral (plantar) aspect of the astragalus is peculiar. The medioventral edge of the bone is rounded and distinct, and roughly straight, forming the medial border of the ventral aspect (figure 3-34: 14). The astragalar medial planter tuberosity occupies the posterior porting of the ventral aspect. It arises from the medioventral and posteromedial edges of the bone, and forms a thick bony plate with free anterior and lateral edges. In front of the plate is a deep notch, which communicates the concavity seen in medial view and the ventral side of the bone. From the anterolateral corner of the tuberosity arises a hook-like process, which directs anterodorsally, nearly close the above mentioned notch. When articulated, the tip of the sustentaculum tail of the calcaneus directs toward the

nearly enclosed notch. In life, the astragalus was probably obliquely oriented with its medial aspect facing medially and slightly ventrally so that both the lateral edge of the medial plantar tuberosity and its hook-like process contact the substrate.

The anterior end of the astragalus forms an incipient head, which is narrower and shorter than the posterior part of the bone. The anterior aspect is taller than wide. The astragalonavicular facet occupies the surface of the anterior aspect (figure 3-34: 15). It is saddle-shaped, dorsoventrally concave and mediolaterally convex. As a whole, the facet is perpendicular with the long axis of the bone. The facet is slightly visible in medial view, in front of the astragalocuboid facet. Between two facets is a small pit of unknown function. The posterior end of the bone is the widest part of the bone. The posterior aspect is generally convex. Its dorsal half has a smooth surface, which is the posterior extension of the articular facet for the upper ankle joint. The ventral half has a rugose appearance. In the middle of the medial border of the posterior aspect is a shallow notch, which represents the posterior end of the sulcus astragali (figure 3-34: 16).

CALCANEUS (figure 3-35)**--T**he calcaneus is the largest element of the pes. It is dorsoventrally compressed, lateromedially broad and proximodistally elongate. As a whole, the bone forms an arch bowed both dorsally and laterally. The proximal extremity of the bone is the calcaneal tuber (figure 3-35: 1). The tuber is stout and strongly reflected ventromedially. In proximal view, the tuber is droplike, with its tail laterodorsally directed. The tip of the tuber (facing posteriorly) is generally convex, with some pits in the center. Around the edge of the convex surface is a fine suture, indicating that the tip of the calcaneal tuber was developed from a separate ossification center and

Figure 3-35. Left calcaneus of *Repenomamus robustus*, IVPP V 12549, in dorsal (A), ventral (B), proximal (C), distal (D), medial (E), and lateral (F) views.

1, calcaneal tuber; 2, peroneal process of calcaneus; 3, tuberosity of calcaneus; 4, sustentaculum tail; 5, calcaneoastragalar facet; 6, calcaneofibular facet; 7, sustentacular facet of calcaneus; 8, sulcus on posterior side of sustentaculum tail; 9, calcaneocuboid facet.

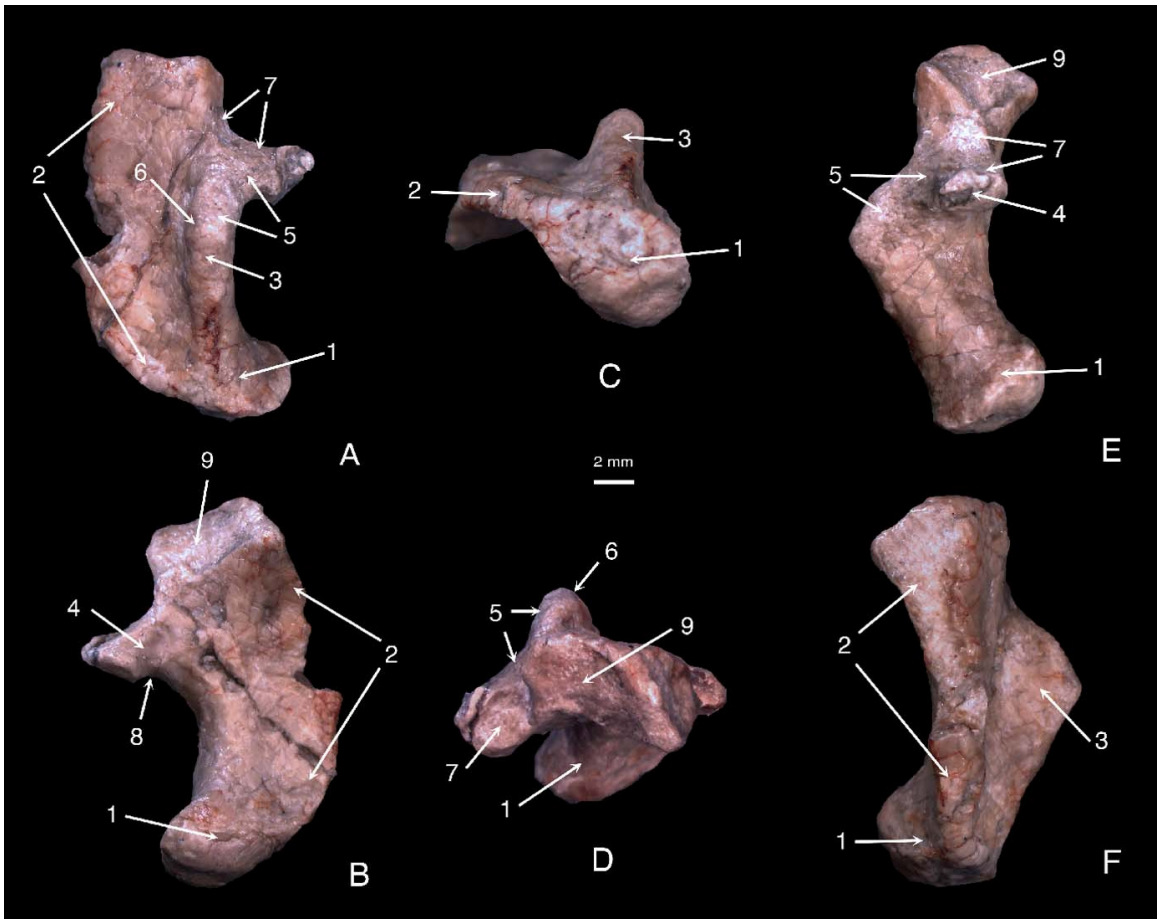

Figure 3-35

fused with the other part of the bone during ontogeny. Seen in dorsal view, the tuber forms the posterior fifth of the calcaneus. Much of the remaining part of the bone forms a

broad lateral flange, the peroneal process of the calcaneus (figure 3-35: 2). The process extends along the entire lateral side of the bone, thickened distally and reaching its broadest point near the distal extremity. The lateral edge is convex and slightly deflected ventrally. In life, the plate of the process was probably inclined lateroventrally to allow the lateral edge contacting the substrate rather than horizontally oriented.

Along posterior two thirds of the medial margin of the bone stands an elongate tuberosity (figure 3-35: 3). In lateral view, the tuberosity forms a low triangle with a broad base, a gentle posterior slope and a steeper anterior slope. The highest point of the process is at near the transverse midline of the bone. Anteroventral to the tuberosity is the sustentaculum tail, extending medially and slightly ventrally from the medial margin of the bone (figure 3-35: 4). The tail is slightly dorsoventrally deeper than anteroposteriorly thick. The medial wall of the bone anterior to the sustentaculum tail is flat and nearly vertically oriented. Both the tuberosity and the sustentaculum tail bear articular facet for the astragalus. Anteromedially on the anterior slope of the tuberosity is the calcaneoastragalar facet, which extends onto the dorsal side of the sustentaculum tail (figure 3-35: 5). As a whole, the facet forms a strip-like concave surface, facing mediodorsally. Posterolateral to the calcaneoastragalar facet on the top of the tuberosity is the calcaneofibular facet (figure 3-35: 6). The facet is convex, facing dorsally. Two facets are continuous, with no distinct boundary between them. Distoventral to the calcaneoastragalar facet on the anterior side of the sustentaculum tail presents the sustentacular facet of the calcaneus, which articulates with its counterpart on the astragalus (figure 3-35: 7). The facet extends onto the medial wall of the calcaneus anterior to the sustentaculum tail and reaches the anteromedial edge of the bone. As a

whole, the facet is vertically oriented, concave and faces anteromedially. Between the calcaneoastragalar and sustentacular facet is a fine crest on the anterodorsal edge of the sustentaculum tail. The posterior side of the sustentaculum tail presents a vertical sulcus (figure 3-35: 8). It is unclear whether the sulcus is the part of the sulcus calcanei (Szalay, 1994: p 5), but there is no sulcus separating the calcaneoastragalar and sustentacular facet, as that seen in some African middle Triassic cynodonts (Jenkins, 1971: p 194 and fig. 61), *Oligokyphus*, morganucodontids, monotremes, multituberculates and some therians (Szalay, 1994).

The anterior aspect of the calcaneus bears the calcaneocuboid facet (figure 3-35: 9). The facet is dorsoventrally flat and lateromedially concave, wider than deep. It faces ventrodistally and intersects with the long axis of the bone in an angle of about 40°. In life, the facet faced more anteriorly than ventrally. The dorsal aspect of the bone is slightly concave lateral to the tuberosity. The ventral aspect of the bone is strongly concave anteroposteriorly and slightly so lateromedially. Both dorsal and ventral aspects present several small foramina of unknown function.

NAVICULAR (figure 3-36)**--**The navicular is roughly a cuboidal bone, but narrows and thins ventrally. In proximal view, the bone is roughly quadrilateral, with a straight dorsal and ventral edge, a convex lateral edge and a concave medial edge. The proximal aspect articulates with the astragalus (figure 3-36: 1). The articular facet (astragalonavicular facet) is shallowly saddle-shaped, matching its counterpart on the distal aspect of the astragalus.

Figure 3-36. Left navicular of *Repenomamus robustus*, IVPP V 12549, in

proximal (A), distal (B), dorsal (C), ventral (D), medial (E), and lateral (F) views.

1, astragalonavicular facet; 2, nonarticular portion of distal aspect; 3, articular facet for entocuneiform; 4, articular facet for mesocuneiform; 5, articular facet for ectocuneiform; 6, naviculocuboid facet; 7, concavity on dorsal aspect of navicular; 8, tubercle at proximomedial corner of dorsal aspect; 9, ventral tuberosity of navicular; 10, fossa at medial aspect of navicular.

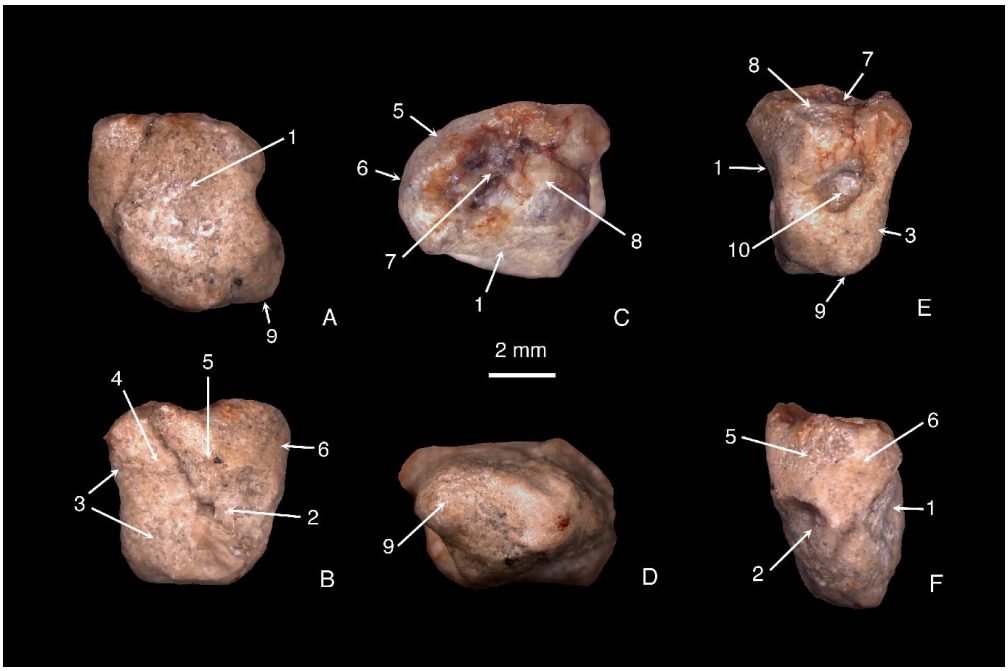

Figure 3-36

The distal aspect of the bone is gently flat, articulating with all four distal tarsals. Its ventrolateral quarter is nonarticular; a fine ridge separates it from the articular part (figure 3-36: 2). Medial to this nonarticular surface is the articular facet for the entocuneiform, which extends dorsally and occupies the medial portion of the distal aspect (figure 3-36: 3). The facet is convex; its ventral portion extends medially around

the distomedial corner of the bone. Lateral to the facet for the entocuneiform and above the nonarticular surface is the facet for the mesocuneiform (figure 3-36: 4). The facet is flat, faces distally and occupies most of the dorsomedial quarter of the distal aspect. The boundary between facets for the entocuneiform and mesocuneiform is hardly recognizable. More lateral is the facet for the ectocuneiform, which is flat, faces distolaterally, and separated from the facet for the mesocuneiform by a fine ridge (figure 3-36: 5). It is shorter than the latter. Continuous laterally from the facet for the ectocuneiform is the one for the cuboid (naviculocuboid facet), and there is no distinct boundary between two facets (figure 3-36: 6). The latter extends onto the lateral aspect of the bone and, as a whole, is convex.

The dorsal aspect of the navicular is roughly pentagonal in outline, with a proximal, medial, distal, distolateral, and lateral edge. The proximal edge is straight and the longest. The medial edge extends distomedially and has a notch in the middle. The distal edge is only half as long as the proximal one and parallels with the latter. The distolateral edge is nearly as long as the distal edge and intersects with the latter in an angle of 135°. The lateral edge is the shortest. Five edges enclose an irregular and concave area in the center (figure 3-36: 7). The proximomedial corner of the dorsal aspect presents a tubercle (figure 3-36: 8). The ventral aspect of the bone is narrow and forms a prominent tuberosity directing ventrally and slightly proximally (figure 3-36: 9).

The medial aspect of the bone has a reversed trapezoid outline, narrowing ventrally. It has a circular fossa in the middle, surrounded by low and blunt rim (figure 3-36: 10). The lateral aspect is convex proximodistally and flat dorsoventrally. It is constricted in the middle. Above the constricted area is the lateral part of the

naviculocuboid facet.

CUBOID(figure 3-37)--The cuboid is the largest among distal tarsals and overall slightly larger than the navicular. With a large plantar process, the bone has an irregular shape. The process is the most peculiar feature of the bone (figure 3-37: 1). It is lateromedially compressed and extends all along the length of the bone. The edge of the process is thick. In lateral view, the process is low triangular in outline, with its apex located proximal to the transverse midline of the bone.

The lateral aspect of the bone presents a large concavity above the edge f the plantar process and open distolaterally (figure 3-37: 2). At the bottom of the concavity is a small foramen, probably a nutrition foramen. Proximodorsal to the concavity the bone is thick, where the proximal articular facet of the bone (calcaneocuboid facet) extends. Distal to the concavity is a lateral transverse process (figure 3-37: 4), similar to that in multituberculates (Kielan-Jaworowska and Gambaryan, 1994: p 16). The medial aspect of the bone is relatively flat. In the middle there is a triangular facet for the contact with the lateral surface of the ectocuneiform (figure 3-37: 5). Proximal to this triangular facet is the medial extension of the calcaneocuboid facet; a fine ridge separates two facets. The distal edge of the medial aspect slightly protrudes medially, contacting the distolateral edge of the ectocuneiform.

Figure 3-37. Left cuboid of *Repenomamus robustus*, IVPP V 12549, in dorsal (A), ventral (B), distal (C), proximal (D), lateral (E), and medial (F) views.

1, plantar process of cuboid; 2, concavity on lateral aspect of cuboid; 3,

calcaneocuboid facet; 4, lateral transverse process; 5, articular facet for ectocuneiform; 6, ridge on dorsal aspect of cuboid; 7, articular facet for Me IV; 8, articular facet for Mt V.

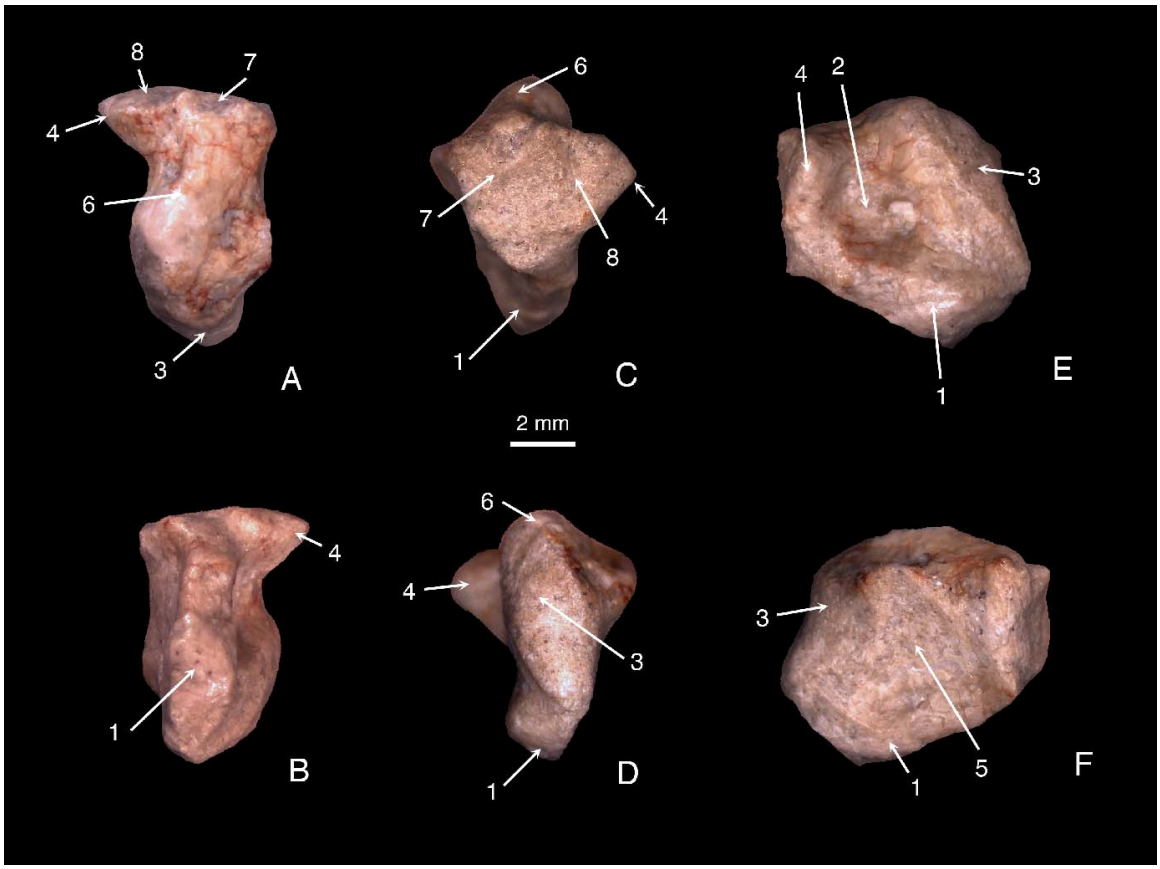

Figure 3-37

In dorsal view, the bone is roughly rectangular, longer than wide (figure 3-37: A). The dorsal aspect has a low rounded ridge extending from the proximolateral to distomedial corner (figure 3-37: 6). On both sides of the ridge are shallowly concave surfaces with small nutrition foramina. The distal edge of the dorsal aspect (also the dorsal edge of the distal aspect, see below) has a small tubercle in the middle, marking the boundary between the facets for Mt IV and Mt V.

The distal aspect of the bone is triangular in outline. It has flat articular facets for

Mt IV and V, respectively (figure 3-37: 7 and 8). A fine ridge, extending from the tubercle on the middle of the dorsal edge to the middle of the surface, separates two facets. Therefore, much of the facet for Mt V is on the distal aspect of the lateral transverse process. The proximal aspect of the bone is much narrower than the distal aspect. It is convex lateromedially and slightly concave dorsoventrally. The calcaneo-cuboid facet fully occupies the proximal aspect and extends onto both lateral and medial aspects of the bone (figure 3-37: 3). In fact, more than half of the articular facet is on the lateral aspect of the bone, and this portion of the facet extends in a proximoventral to distodorsal direction. The facet is convex on the lateral aspect and slightly concave on the medial aspect. As a whole, the facet forms a strip of a smooth surface around the proximal end of the bone.

ECTOCUNEIFORM (figure 3-38)--The ectocuneiform is lateromedially compressed. The ventral portion of the bone has a large plantar process, which presents a tuberosity at the extremity (figure 3-38: 1). The lateral and medial aspects of the bone are broad and roughly pentagonal in outline, with a dorsal, proximal, distal, proximoventral, and distoventral edge. The lateral aspect contacts the cuboid. A vertical sulcus anteriorly on the surface divides the facet into a broad posterior and a narrow anterior part (figure 3-38: 2, 3 and 4). The medial aspect contacted the mesocuneiform in life. There are two strip-like facets for the articulation (figure 3-38: 5). The proximal one is along the proximal edge, facing distomedially; the distal on the distal edge, facing medially. Between two facets is a shallow concavity. The proximal aspect of the bone has a flat facet; it faces proximomedially and articulated with the navicular in life (figure 3-38: 6). The distal aspect of the bone presents the articular facet for Mt III (figure 3-38: 7). The facet is

Figure 3-38. Left ectocuneiform of *Repenomamus robustus*, IVPP V 12549, in dorsal (A), ventral (B), lateral (C), medial (D), distal (E), and proximal (F) views.

1, plantar process of ectocuneiform; 2, sulcus on lateral aspect of ectocuneiform; 3, anterior part of articular facet for cuboid; 4, posterior part of articular facet for cuboid; 5, facets for articulation with mesocuneiform; 6, articular facet for navicular; 7, articular facet for Mt III; 8, lip dorsal to articular facet for Mt III.

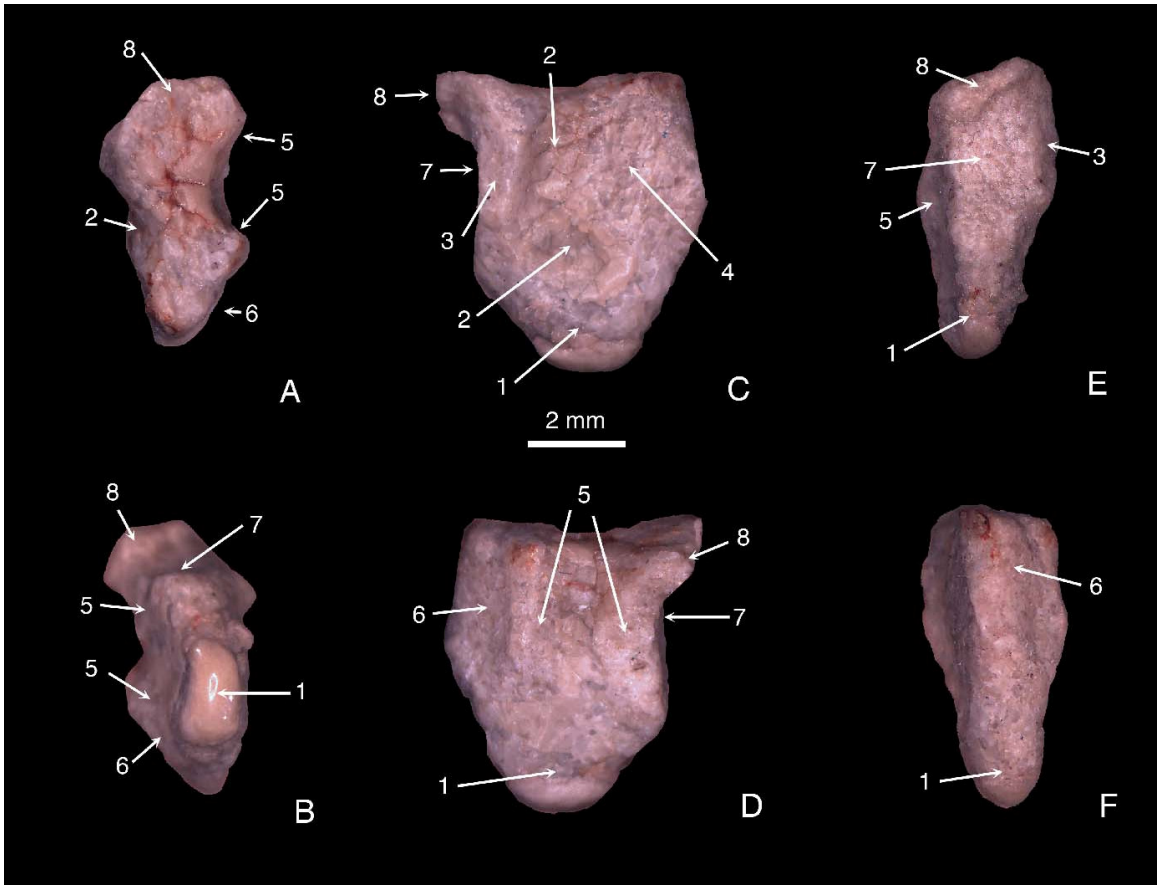

Figure 3-38

concave due to a distally protruding lip on its dorsal edge (figure 3-38: 8). In dorsal

view the ectocuneiform is dumbbell-shaped, convex proximally and distally and concave laterally and medially. The dorsal aspect is gently flat.

MESOCUNEIFORM (figure 3-39)--The mesocuneiform is the smallest among tarsals. It is wider and shorter than the ectocuneiform. The bone forms a tetrahedron with a dorsal, lateral, distal, and proximomedial aspect. The latter three aspects converge ventrally into a plantar process, which has a tip directed distally (figure 3-39: 1). The dorsal aspect is triangular in outline and has a smooth and convex surface (figure 3-39: C). The distal aspect forms a concave facet for articulating with Mt II, deeper than wide (figure 3-39: 2). The lateral aspect contacts the ectocuneiform. It has two small facets; the proximal one is flat while the distal slightly convex (figure 3-39: 3 and 4). Between two facets is a furrow. The proximomedial aspect is the largest among four aspects (figure 3-39: A). It is convex and articulates with the navicular and entocuneiform. The facet for the navicular occupies the laterodorsal third of the surface, facing proximomedially (figure 3-39: 5). The facet for the entocuneiform occupies the distodorsal corner of the surface and faces medially (figure 3-39: 6). Between two facets is a low ridge. Two facets have a continuous ventral border, which separates them from the nonarticular portion of the surface (figure 3-39: 7).

Figure 3-39. Left mesocuneiform of *Repenomamus robustus*, IVPP V 12549, in proximomedial (A), lateral(B), dorsal (C), ventral (D), distal (E), and proximal (F) views.

1, plantar process of mesocuneiform; 2, articular facet for Mt II; 3, proximal facet for ectocuneiform; 4, distal facet for ectocuneiform; 5, articular facet for navicular; 6, articular facet for entocuneiform; 7, nonarticular portion of

proximomedial aspect of mesocuneiform.

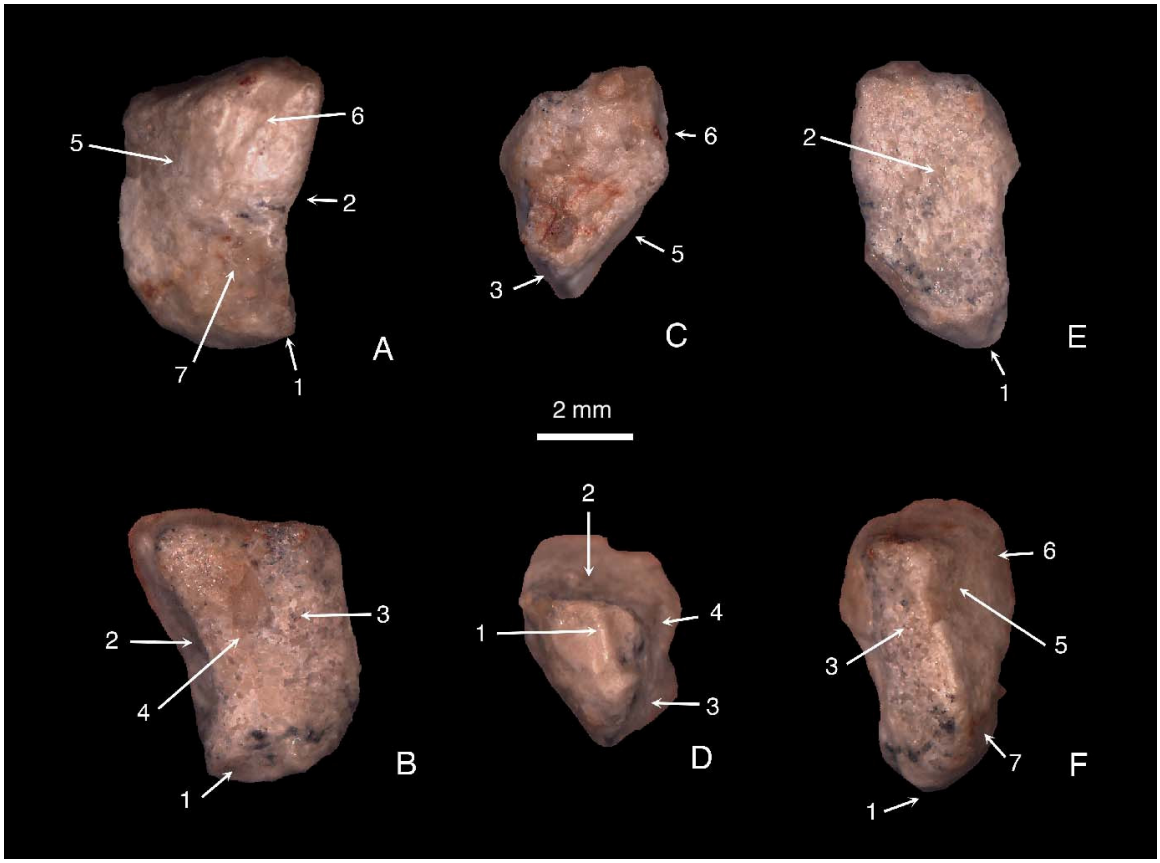

Figure 3-39

ENTOCUNEIFORM (figure 3-40)--The entocuneiform is much larger than the ectocuneiform and mesocuneiform and, overall, slightly smaller than the navicular. Its distal half extends beyond the distal margins of other distal tarsals and contacts the medial side of the Mt II. The bone is roughly cuboidal in shape, longer than wide, and roughly deep as long. The dorsal aspect is gently convex (figure 3-40: A). Its distal margin is sharp and convex. The lateral margin is also prominent and has a notch in the distal part. The medial margin is low and indistinct; therefore, the dorsal aspect continues with the medial aspect. The proximal end of the dorsal aspect presents a tuberosity, directing proximally (figure 3-40: 2). The ventral aspect is quadrilateral in outline (figure

3-40: B). The proximal and distal margins are straight but not strictly parallel. The lateral and medial margins are concave; the medial margin is longer and most curved in its distal part while the lateral one slightly shorter and most curved in the middle. The middle of the ventral aspect bears a longitudinal sulcus (figure 3-40: 3). The medial aspect has a smooth surface (figure 3-40: E). It is concave in the center. Proximally there is a vertically oriented tuberosity (proximal medial tuberosity; figure 3-40: 4). Another tuberosity (distal medial tuberosity; figure 3-40: 5) is horizontally oriented and located near the distoventral corner of the medial aspect. The lateral aspect is gently flat and was probably obliquely oriented in life (figure 3-40: F). The ventral half of the lateral aspect is nonarticular (figure 3-40: 6), which is separated from the articular part by a low ridge. The articular facet for the mesocuneiform occupies the proximodorsal quarter of the surface; it is slightly convex (figure 3-40: 7). The distodorsal quarter of the lateral aspect presents the facet for contacting the medial side of the Mt II. A deep sulcus divides the facet into a dorsal and ventral portion (figure 3-40: 8, 9 and 10).

Figure 3-40. Left entocuneiform of *Repenomamus robustus*, IVPP V 12549, in dorsal (A), ventral (B), proximal (C), distal (D), medial (E), and lateral (F) views.

1, notch on the lateral margin of dorsal aspect of entocuneiform; 2, proximal tuberosity on dorsal aspect of entocuneiform; 3, sulcus on ventral aspect of entocuneiform; 4, proximal medial tuberosity of entocuneiform; 5, distal medial tuberosity; 6, nonarticular surface of lateral aspect; 7, articular facet for mesocuneiform; 8, dorsal portion of articular facet for Mt

II; 9, ventral portion of articular facet for Mt II; 10, sulcus on lateral aspect of Mt II; 11, articular facet for navicular; 12, articular facet for Mt I.

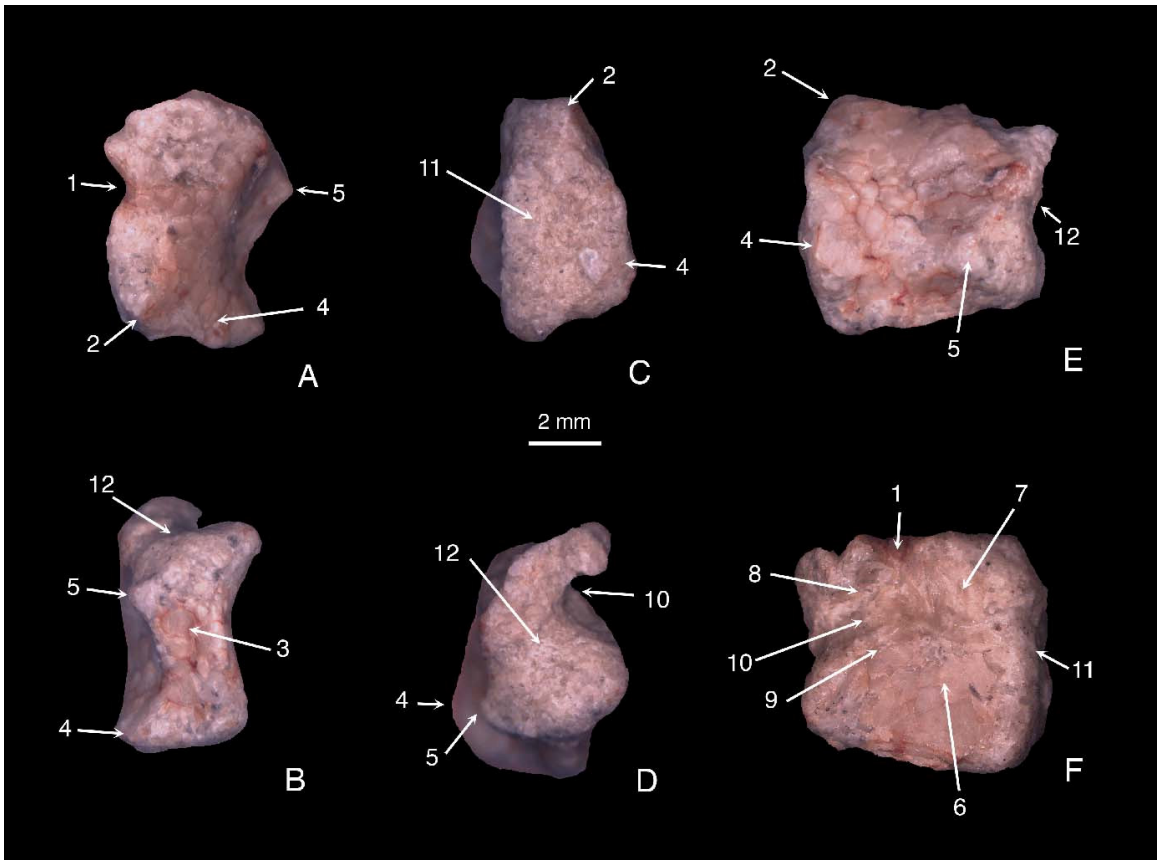

Figure 3-40

The proximal aspect of the bone is much taller than wide and slightly widens ventrally (figure 3-40: C). Its lateral half bears the articular facet for the navicular. The medial half is also the proximal aspect of the proximal medial tuberosity; it is convex and nonarticular. The distal aspect has the articular facet for Mt I (figure 3-40: 12). In distal view, the facet looks like a comma, with the head on the bottom and the tail directing laterodorsally. The notch between the head and tail is also the anterior opening of the deep sulcus of the lateral aspect of the bone (see above). Overall, the facet is saddle-shaped, concave dorsoventrally and convex lateromedially.

METATARSALS (figures 3-33 and 3-41)--Mt I is the shortest among metatarsals (figure 3-41: A). The bone is somewhat flattened dorsoventrally and slightly bowed dorsally. Both ends of the bone are expanded lateromedially and asymmetrical, therefore the lateral edge of the bone is much more concave than the medially one. The proximal facet for the ectocuneiform is saddle-shaped, convex dorsoventrally and concave lateromedially (figure 3-41: 1 in A). The facet extends onto the dorsal aspect of the proximal end. On the ventral aspect of the proximal end are two proximoventral directed tuberosities (proximal ventral tuberosities; figure 3-41: 2 in A), the medial one slightly more prominent. On the dorsal aspect distal to the dorsal extension of the articular facet is a semi-lunar sulcus (figure 3-41: 3 in A), possibly for the attachment of an extensor tendon, as that in morganucodontids (Jenkins and Parrington, 1976: p 413). The medial aspect of the proximal end bears a pit and small protuberance distal to the pit (figure 3-41: 4 in A). The lateral aspect of the proximal end is smooth, contacting the medial side of the Mt II in life. The shaft of Mt I is roughly ovoid in cross section. The ventral aspect of the shaft is concave proximodistally while the dorsal aspect is slightly convex in the same direction. The distal articular facet is convex dorsoventrally and extends onto the dorsal aspect of the bone (figure 3-41: 5 in A). The facet has an indistinct sulcus in the middle and therefore slightly concave lateromedially. On the dorsal aspect proximal to the articular facet is a rounded pit, possibly representing a sesamoid fossa (figure 3-41: 6 in A). The lateral aspect of the distal end presents a prominent protuberance and several small pits (figure 3-41: 7 in A). The medial aspect of the distal is flat with a rugose surface.

Mt II is slightly longer than Mt I (figure 3-41: B). In dorsal view, the bone is nearly symmetrical, slightly expanded at proximal end and moderately at the distal end.

The proximal end has a huge plantar process directing ventrally (figure 3-41: 8 in B). The proximal articular facet (for the mesocuneiform) has two parts, the dorsal part slightly concave while the ventral part slightly convex; between two parts is a fine ridge (figure 3-41: 1 in B). The dorsal aspect of the proximal end is flat. Distally on the lateral and medial edges of the dorsal aspect are small swellings and pits, possibly for the insertion

---

Figure 3-41. left metatarsals of *Repenomamus robustus*, IVPP V 12549: Mt I in dorsal (A1), medial (A2), ventral (A3), lateral (A4), distal (A5), and proximal (A6) views; Mt II in dorsal (B1), medial (B2), ventral (B3), lateral (B4), distal (B5), and proximal (B6) views; Mt III in dorsal (C1), medial (C2), ventral (C3), lateral (C4), distal (C5), and proximal (C6) views; Mt IV in dorsal (D1), medial (D2), ventral (D3), lateral (D4), distal (D5), and proximal (D6) views; Mt V in dorsal (E1), medial (E2), ventral (E3), lateral (E4), distal (E5), and proximal (E6) views.

1, proximal articular facet; 2, proximal ventral tuberosities; 3, semilunar sulcus; 4, protuberance and pit on medial aspect of proximal end; 5, distal articular facet; 6, sesamoid fossa; 7, protuberance in lateral aspect of distal end; 8, plantar process of proximal end; 9, protuberance and pit on lateral aspect of proximal end; 10, intermetatarsal facet on lateral aspect of proximal end; 11, sulcus on dorsal aspect of distal end; 12, protuberance in medial aspect of distal end; 13, intermetatarsal facet on medial aspect of proximal end; 14, shallow sulcus on distal articular facet.

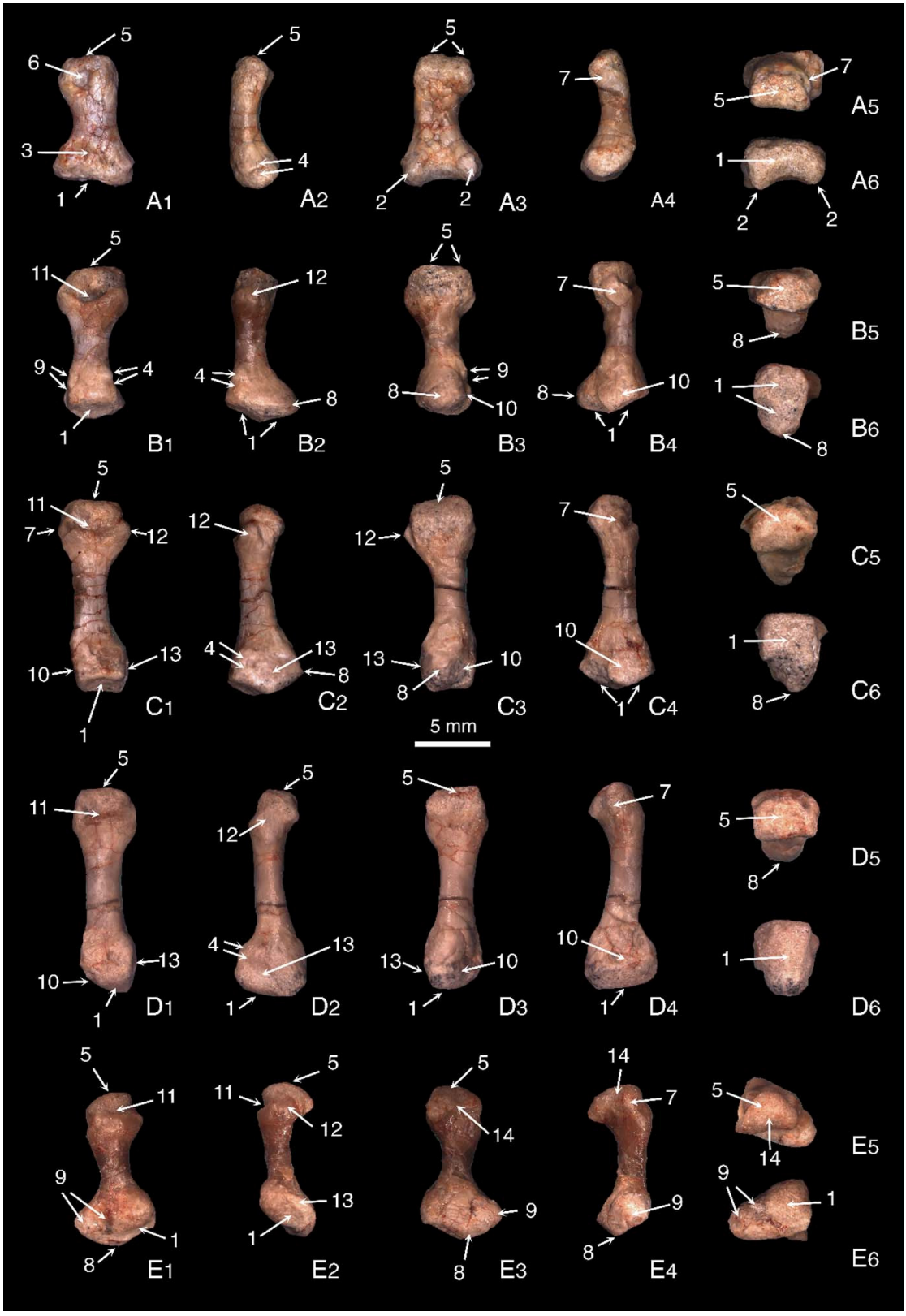
A1
A2
A3
A4
A5
A6
B1
B2
B3
B4
B5
B6
C1
C2
C3
C4
C5
C6
5 mm
D1
D2
D3
D4
D5
D6
E1
E2
E3
E4
E5
E6

Figure 3-41

of the peroneal musculature (figure 3-41: 4 and 9 in B). The medial aspect of the proximal end contacts the entocuneiform and Mt I, but with no distinct facet. The lateral aspect has a small raised intermetatarsal facet for the contact with Mt III (figure 3-41: 10 in B). Distal to the facet is a vertical sulcus. The shaft of Mt II is oval in cross section. Distal to the transverse midline on the junction of the lateral and ventral aspect is a small eminence of unknown function. The distal end of Mt II has a distinct depression and protuberance on both medial and lateral aspect (figure 3-41: 7 and 12 in B). The distal articular facet is convex dorsoventrally and flat mediolaterally (figure 3-41: 5 in B). The facet extends onto the dorsum of the distal end. Proximal to the facet is a transverse sulcus, which is deep in the middle and separates the articular facet from the nonarticular dorsal surface of the bone (figure 3-41: 11 in B).

Mt III and IV are similar to Mt II in the general morphology, but longer and slenderer; Mt IV is the longest among metatarsals. Other differences include that they have intermetatarsal facets on both the medial and lateral aspects of the proximal end (figure 3-41: 10 and 13 in C and D); and their sulci on the dorsum of distal end are deeper near lateral protuberances (figure 3-41: 11 in C and D). Mt IV is further different from Mt II and III in having a convex proximal articular facet (figure 3-41: 1 in D), and with its distal articular facets extending onto the ventral aspect medially (figure 3-41: 5 in D).

Mt V is slightly shorter and stouter than Mt IV (figure 3-41: E). The proximal end greatly expands laterally and ventrally. It has a huge lateral protuberance; a sulcus on the proximal aspect separates the protuberance from the proximal articular facet (figure 3-41: 1 and 9 in E). The latter is slightly concave, articulating with the cuboid. Mt V does not contact the calcaneus. The plantar process is continuous with the lateral protuberance

(figure 3-41: 8 in E). The shaft is oval in cross section. The distal end expands moderately. It is asymmetrical. The protuberance on the medial aspect is more prominent than the one on the lateral aspect (figure 3-41: 7 and 11 in E). The distal articular facet is convex and extends onto the dorsum of the bone, where a transverse sulcus separates the facet from the smooth surface of the shaft (figure 3-41: 5 and 11 in E). The facet is triangular, widening ventrally. A shallow sulcus (figure 3-41: 14 in E) divides the ventral part of the facet into a lateral and medial portion; the medial is wider and further extends onto the ventral aspect of the bone. Proximal to this ventral extension of the articular facet is a shallow fossa; it is unclear whether there was a sesamoid bone resides in the fossa in life. Because the Mt V is deviated from other metatarsals, the asymmetry of its distal end allows the proximal phalange of digit V to flex/extend in the same vertical plane as those of other digits.

PEDAL PHALANGES (figures 3-33 and 3-42)--The proximal phalange of digit II (PP II) is well preserved in V 12549, only missing the medial corner of the proximal end (figure 3-42: A-F). Its length is about 75% of that of Mt II. Its proximal end is moderately expanded. The proximal articular facet is gently concave, facing proximally and

---

Figure 3-42. Pedal phalanges of *Repenomamus robustus*, IVPP V 12549: left proximal phalange of digit II in dorsal (A), medial (B), ventral (C), lateral (D), distal (E), and proximal (F) views; left proximal phalange of digit III in dorsal (G), medial (H), ventral (I), lateral (J), and proximal (K) views.

1, proximal articular facet of PP II; 2, trochlea of PP II; 3, medial edge of

trochlea of PP II; 4, lateral edge of trochlea of PP II; 5, sulcus and protuberance on lateral aspect of distal end of PP II; 6, sulcus and protuberance on medial aspect of distal end of PP II; 7, proximal articular facet of PP III.

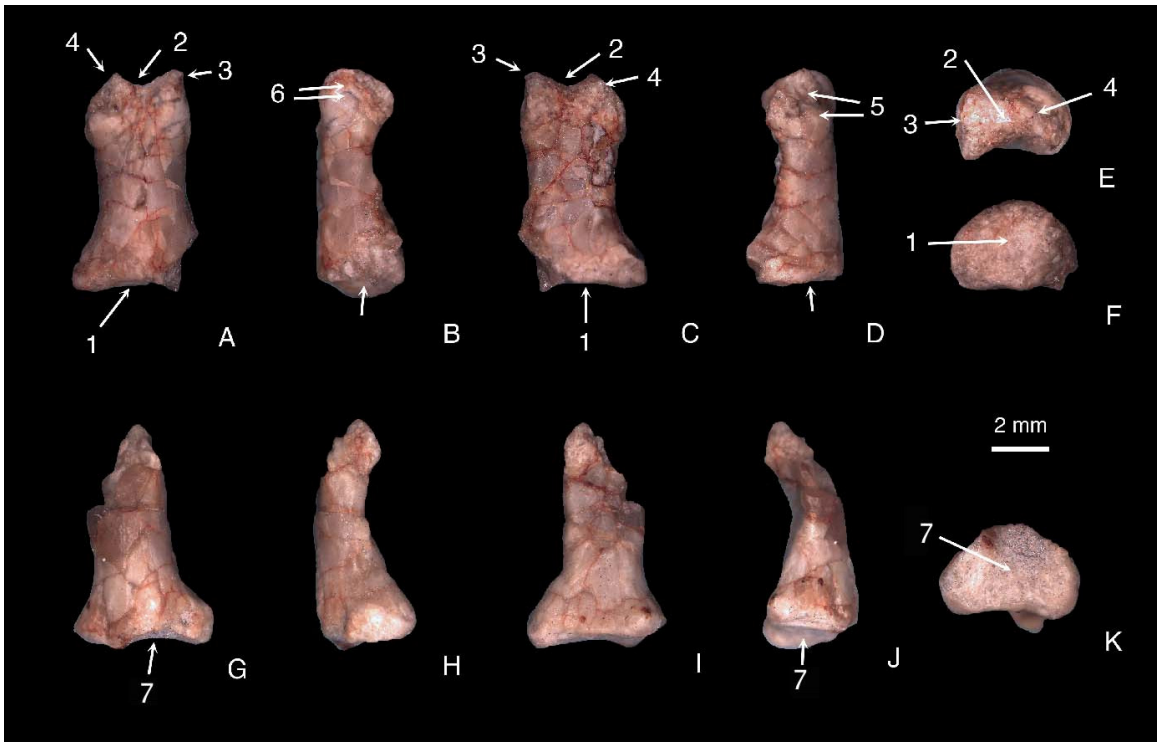

Figure 3-42

perpendicular with the long axis of the bone (figure 3-42: 1). The shaft of the bone is slightly wider than deep and roughly semicircular in cross section. The ventral aspect of the shaft is slightly concave with distinct lateral and medial margins. There are some furrows and swellings on the proximal part of the ventral aspect. The three other aspects of the shaft are continuous, rounded and smooth. The distal end has a trochlea for the middle phalange; the articular facet of the trochlea extends onto the dorsal and ventral aspects of the bone (figure 3-42: 2). Two edges of the trochlea are not parallel; the medial one is nearly vertical while the lateral is oriented in a dorsomedial to ventrolateral

direction (figure 3-42: 3 and 4). The medial and lateral aspects of the distal end bear sulci and protuberances for the attachment of collateral ligaments, those on the lateral aspect are more prominent (figure 3-42: 5 and 6).

The left proximal phalange of digit III of V 12549 misses the distal end (figure 3-42: G-K); that of digit IV preserves the proximal end. The preserved parts of these two phalanges are similar to the corresponding parts of the proximal phalange of digit II in the morphology and size, which indicates that in *Repenomamus* proximal phalanges of middle digits are probably quite similar in general.

Other phalanges of the pes are not recognizable in the collection.

SESAMOID BONES (figure 3-33: B)--Four sesamoid bones are preserved on the ventral surface of the left pes of V 12549. A relatively large sesamoid is preserved proximally on the ventral aspect of the Mt III (figure 3-33: Se1). Two small one are preserved between the metatarsal and proximal phalange, on digit II and IV, respectively (figure 3-33: Se2 and Se3). The fourth element is preserved on the ventral side of the proximal phalange of digit II, near the distal trochlea (figure 3-33: Se4). All four bones have smooth surface and irregular shape. Because no sesamoid bone is preserved in pair, it is most likely that *Repenomamus* does not have paired sesamoid bones.

4. CHARACTER ANALYSIS AND PHYLOGENETIC ANALYSIS

4.1 CHARACTER ANALYSIS

Character analysis illustrates similarities and differences among taxa. In this study, comparison of postcranial features of *Repenomamus* and related cynodont (nonmammalian and mammalian) taxa is conducted in the format of the character analysis, which is also the first step of the phylogenetic analysis.

Many characters in this study are modified from those employed in the previous studies, which are indicated in parentheses following character definitions. Some characters, which either have been discussed in previous studies, or have self-explanatory definitions, are listed but not discussed in this study, and the conditions in *Repenomamus* and some other taxa are indicated. Taxa included in the analysis are *Repenomamus*, other Mesozoic mammals with the postcranial skeleton at least partially known, selected extant mammals, and selected nonmammalian cynodonts with postcranial skeletons preserved. The major data source for each taxon is listed here:

Procynosuchus: Kemp, 1980

Thrinaxodon: Jenkins, 1971

Chiniquodon (including *Probelesodon*): Romer and Lewis, 1973

Tritylodontids (represented by *Oligokyphus*, *Bienotheroides*, *Bienotherium*)**:**

Kühne, 1956; Sun and Li, 1985; Hu *et al*., unpublished data

Pachygenelus: Gow, 2001

Morganucodon: Jenkins and Parrington, 1976

Megazostrodon: Jenkins and Parrington, 1976

Haldanodon: Krusat, 1980; Lillegraven and Krusat, 1991; Martin, 2005

Tachyglossus: personal observation on AMNH, # 77856, 179983

Ornithorhynchus: personal observation on AMNH, VP teaching collection #2945

Cimolodontan multituberculates: Krause and Jenkins, 1983; Kielan-Jaworowska, 1989; Kielan-Jaworowska, and Gambaryan, 1994

Gobiconodon: Jenkins and Schaff, 1988; Hu *et al*., unpublished data

Repenomamus: Hu *et al*., 2005b; this study

Jeholodens: Ji *et al*., 1999

Zhangheotherium: Hu *et al*., 1997, 1998; Luo and Ji, 2005

Henkelotherium: Krebs, 1991

Vincelestes: Rougier, 1993

Asiatherium: Szalay and Trofimov, 1996

Pucadelphys: Marshall and Sigogneau-Russell, 1995

Didelphis: personal observation on AMNH, VP teaching collection #635

Sinodelphys: Luo *et al.*, 2003

Eomaia: Ji *et al*., 2002

Ukhaatherium: Horovitz, 2001, 2003; Novacek *et al*., 1997

Kennalestes: Kielan-Jaworowska, 1977

Asioryctes: Kielan-Jaworowska, 1977

Zalambdalestes: Kielan-Jaworowska, 1978; Novacek *et al*., 1997

Erinaceus: personal observation on AMNH # 41296, 42563, 69553

VERTEBRAL COLUMN AS A WHOLE(2 CHARACTERS)

Ch 1. <u>Vertebral centra: (0) amphicoelous; (1) platycoelous</u> (Rowe, 1988: Ch 108; Sidor and Hopson, 1998: Ch 123; Hopson and Kitching, 2001: Ch 101).

Sidor and Hopson (1998) coded Tritheledontidae having amphicoelous centra, but Hopson and Kitching (2001) coded *Pachygenelus*, a genus of Tritheledontidae, having platycoelous centra. In this study, I follow Hopson and Kitching (2001). *Repenomamus*, as most other mammals, has platycoelous vertebral centra.

Ch 2. <u>Neural arches synostosed with the centrum: (0) absent; (1) present</u>.

In primitive cynodont, *Procynosuchus*, neural arches are sutured with the centrum (Kemp, 1980: p220). *Repenomamus* and other taxa studied here have the neural arched synostosed with the centrum.

ATLAS-AXIS COMPLEX (20 CHARACTERS)

Ch 3. <u>The facet for the proatlas on the atlas: (0) present at the atlantal neural arch; (1) the atlantal neural arch bearing no facet for the proatlas</u> (modified from Rowe, 1988: Ch 92; Hu *et al*., 1997: Ch 1; Ji *et al*., 1999: Ch 1; Luo *et al*., 2002: Ch 1**1**9).

The proatlas is a pair of small bony elements between the atlas and occipital region of the skull. In extant vertebrates, it develops in *Sphenodon*, alligator and a few mammals (Evans, 1939). It is also present in many nonmammalian cynodonts (Jenkins, 1971). In those fossil vertebrates, the elements, if present, are often missing. Since the proatlas articulates with the atlas, the facet on the atlantal neural arch could indicate the presence of the element. In previous studies (Rowe, 1988; Hu *et al*., 1997; Ji *et al*., 1999; Luo *et al*., 2002), the presence vs. absence of the proatlas constitutes a character. But as

Jenkins (1971) indicated, the intact proatlas is rare in fossil record; therefore, a more appropriate and operable character is the presence vs. absence of the facet on the atlas for the proatlas. The atlas of *Thrinaxodon* has the facet. In *Oligokyphus* and *Bienotheroides* the facet is absent. None of mammalian taxa compared here and with atlantal neural arches known, including *Repenomamus*, has the facet in adult.

Ch 4. Fusion of the atlantal intercentrum with the neural arch in adult: (0) unfused; (1) fused (modified from Rowe, 1988: Ch 93; and Hu *et al*., 1998: Ch 2; Luo *et al*., 2002: Ch 120).

The cynodont atlas has four separate ossifications: the intercentrum, the centrum, and two halves of the neural arch (Jenkins, 1971). The atlantal centrum joins that of the axis to form the body of the axis, and other three elements form the atlas in adult. In nonmammalian cynodonts and many mammals studied here, i.e. morganucodontids, multituberculates, *Repenomamus*, *Jeholodens*, *Vincelestes*, *Kennalestes*, and *Pucadelphys*, the atlantal intercentrum is not fused with the neural arch in adult. The intercentrum and neural arches are fused in *Didelphis*, *Erinaceus*, and extant monotremes.

Ch 5. The articular facet for the occipital condyle on the atlantal intercentrum: (0) present; (1) absent.

In nonmammalian cynodonts with the atlantal intercentrum known (*Thrinaxodon*--Jenkins, 1971: p20 and Fig 1E; *Oligokyphus*--Kühne, 1956: Fig 42D) there are facets on the atlantal intercentrum for the occipital condyles, but mammals, including *Repenomamus*, lack such facets, which is probably due to the lateral displacement of the occipital condyles.

Ch 6. Fusion of two halves of the atlantal neural arch in adult: (0) not fused; (1) fused.

Jenkins (1971: p17) stated that two halves of the atlantal neural arch are not fused, even do not contact, in some nonmammalian cynodonts including *Thrinaxodon*. Similar condition is present in *Procynosuchus* and tritylodontids. In mammals with the atlas adequately known, including *Repenomamus*, two halves of the atlantal neural arch are fused in adult. In a subadult individual of *Repenomamus robustus* (IVPP V 13606) two halves of the atlantal neural arch are indeed not yet fused .

Ch 7. Anteroposterior length of the atlantal neural arch of the atlas: (0) long; (1) short.

Sues (1985: p 210) pointed out that the neural arch in tritylodontids and morganucodontids is anteroposteriorly short, while that in more primitive cynodonts, such as *Procynosuchus* and *Thrinaxodon,* is much longer anteroposteriorly. Kemp (1983: figs. 8A-C) illustrated both two conditions in cynodonts. Kemp (1980) did not mention the feature in *Procynosuchus*, but his figure 1 showed a long neural arch. The atlases of mammals, including that of *Repenomamus*, have a short neural arch. The short atlantal neural arch probably facilitates movements of the head and neck.

Ch 8. Atlantal rib in the adult: (0) present; (1) absent (Rowe 1988: Ch 9; Hu *et al*., 1997: Ch 3; Luo *et al*., 2002: Ch 121).

The atlantal rib is present in nonmammalian cynodonts, morganucodontids, multituberculates, and *Jeholodens*. In other mammals studied here, including *Repenomamus*, there is not trace of separate rib attached to the atlantal transverse process, which is probably incorporated into the latter during development.

Ch 9. Development of the atlantal transverse process (including the rib): (0) more vertically than transversely oriented, narrow and not expanded; (1) more transversely than vertically oriented, wing-like and anteroposteriorly expanded.

Jenkins (1971) suggested that the evolution of mammalian oblique muscles is in conjunction with that of the atlas-axis complex. The mammalian M. obliqus capitis caudalis spans between the axial spinous process and the atlantal transverse process. But in nonmammalian cynodonts with the atlantal transverse process know (*Procynosuchus*: Kemp, 1980; *Galesaurus* and *Thrinaxodon*: Jenkins, 1971; *Oligokyphus*: Kühne, 1956), the process and associated rib is more or less vertically oriented. Jenkins (1971: p44) argued that this feature is difficult to account for in terms of mammalian musculature arrangement, which implies that the latter did not yet evolve in nonmammalian cynodonts. In mammals, the process is more transversely than vertically oriented.

Ch 10. Posterior extension of the atlantal transverse process or rib: (0) beyond the caudal facets for axis; (1) not beyond the caudal facets (modified from Horovitz and Sánchez-Villagra, 2003: Ch 4)

The posterior extension of the atlantal transverse process is most distinct in monotremes, but the condition is also present in some early cynodonts (*Procynosuchus* and *Thrinaxodon*), some eutherians and metatherians. In *Repenomamus*, as well as in morganucodontids, multituberculates, *Vincelestes*, and *Ukhaatherium*, the atlantal transverse process does not extend posteriorly beyond the facet for the axis.

Ch 11. Prezygapophysis on the axis: (0) present; (1) absent.

Jenkins (1971: p41-42) discussed the reduction of the zygapophyseal articulation between the atlas and axis in cynodonts, which is necessary for the rotation of atlanto-axial joint. In most taxa discussed here, including *Repenomamus*, the lamina of the atlantal neural arch lacks the postzygapophysis and there is no articular facet on the axial prezygapophysis either; but the articulation is present in *Procynosuchus* and *Thrinaxodon*. Rowe (1988) coded that tritylodontids have the prezygapophysis on axis. Most of other students followed Rowe's coding. But *Oligokyphus* and *Bienotherium* do not preserved the axial neural arch, neither other tritylodontids.

Ch 12. Enlargement of the second intervertebral foramen: (0) slightly; (1) moderately; (2) greatly.

Jenkins (1971: p42) indicated that the enlargement of the second, or atlanto-axial, intervertebral foramen relative to other cervical intervertebral foramen is a characteristic of nonmammalian cynodonts and most mammals who could rotate the atlas on the axis. The enlargement of the atlanto-axial intervertebral foramen is related to the evolution of rotation between two vertebrae, which provides enough space for the passage of the second spinal nerve and associated vessels when the caudal intervertebral notch of the rotating atlas is displaced relative to the cranial intervertebral notch of the axis. Most authors ignore this feature. Here the assessment on the enlargement of the foramen in nonmammalian cynodonts and mammals is mainly based on the dorsoventral width (or depth) of cranial intervertebral notch of the axis relative to those of more caudal cervicals as an indication of the relative enlargement of the second intervertebral foramen. In *Procynosuchus*, the notch is slightly wider than the more caudal ones (Kemp, 1980: figs. 1, 2). The foramen in *Thrinaxodon* is enlarged, but the presence of axial prezygapophysis

reduces its amount. The wide axial cranial intervertebral notch in *Repenomamus* and other mammals indicates the great enlargement of the atlanto-axial intervertebral foramen in these taxa, further suggesting a greater range of atlantal rotation than in nonmammalian cynodonts.

Ch 13. Atlantal and axial centra: (0) sutured; (1) fused with no suture.

The body of axis is composed of the centrum of the atlas, the centrum and intercentrum of the axis, which could be sutured or fused in adult. In most mammals, including *Repenomamus*, the atlantal centrum is fused with the axial centrum in adult; two structures are not fused in nonmammalian cynodonts, morganucodontids, and *Jeholodens*. The development of axial intercentrum is discussed in Ch 16.

Ch 14. Shape of the axial body (atlantal and axial centra): (0) more or less round in cross section; (1) dorsoventrally flattened.

The axial body is dorsal ventrally compressed in mammals and tritylodontids, which is probably an adaptation for the enlargement of the vertebral canal to accommodating the enlarged spinal cord in the cervical region (Jenkins and Parrington, 1976: p416). In *Procynosuchus* (Kemp, 1980: fig. 1) and *Thrinaxodon* (Jenkins, 1971: fig. 2) the axial body retains the round contour in the cross section and does not flatten dorsoventrally. The condition is unclear in *Pachygenelus* and other nonmammalian cynodonts studied here.

Ch 15. Development of the dens: (0) as anterior extension of the atlas centrum, without constriction at the base; (1) as small protuberance from the atlas centrum, with constriction at the base; (2) tongue-like or tooth-like and with constriction at its base (modified from Sidor and Hopson, 1998: Ch 128).

Jenkins (1971: p28-49) thoroughly discussed the origin, evolution and function of the dens in nonmammalian cynodonts and mammals. His major argument is that the dens originally arises from, and never completely replaces, the atlantal centrum, and therefore is a neomorph in the evolution of cynodonts. Jenkins made his case based on the substantial evidence from paleontology, osteology and embryology. The primary function of the dens, according to him, is to work together with ligaments, i.e. transverse ligament and apical ligament, to prevent the atlas and the head from flexing on the axis. The secondary function of the dens is to act as a pivot for the atlas rotation, but "the mammalian atlanto-axial joint without dens and transverse ligaments would be no less mechanically suited for rotation" (Jenkins, 1971: p40).

Luo *et al*. (2002) have a character (Ch 123; duplicated in Kielan-Jaworowska *et al*., 2004) dealing with the fusion of dens with the axis: "123. Fusion of dens to axis: (0) Unfused; (1) Fused". If Jenkins' argument is correct, it is the atlantal centrum, not the dens, could either be sutured or fused with the axial centrum; and the latter (dens) is only the anterior protrusion of the atlantal centrum.

Watson (1981, cited by Evens, 1993: fig. 4-52 and p 174) argued that in the dog the atlantal centrum forms the dens and the centrum of the proatlas forms the apical tip of the dens. But as shown in Evens (1993: figs. 4-51 and 4-52), the part of the atlantal centrum posterior to the dens is wider and deeper than the dens itself, this part is the main body of the atlantal centrum while the dens is just the anterior projection of the latter. The dens-atlantal centrum-axial centrum relationships are more clearly demonstrated in extant monotremes, juvenile marsupials (Jenkins, 1971: p 33-38) and many fossil mammals. In these taxa, the dens occupy a small portion of the anterior part of the axial body, and the

suture between the anterior and posterior parts of the axial body is behind the cranial articular facets, not the dens, of the axial body. The axial cranial articular facets articulate with the neural arches of the atlas, and this articulation is equivalent to the centrum-arch contact in posterior vertebrae, and the cranial articular facets are mainly on the centrum of the atlas. It is evident that the atlantal centrum (anterior part of the axial body) is more than the dens.

Among taxa discussed here, *Procynosuchus* has the dens continuous with the vertebral body without constriction at the base, *Thrinaxodon* has the dens as a small anterior protrusion of the atlas centrum, and other taxa, including *Repenomamus*, have the dens a tongue-like process from the atlas centrum.

Ch 16. Axial intercentrum: (0) sutured to the axial centrum; (1) fused with the axial centrum or lost (modified from Sidor and Hopson, 1998: Ch 126).

In the dog, the axial intercentrum appears in the early postpartum stage, and then it fused with the axial centrum (Evans, 1993: p173-174 and figs. 4-51 to 4-53). It is probably also the case for fossil mammals, including *Repenomamus*, in which no separate axial intercentrum is visible; the element is probably fused with the axial centrum early in the development. In *Procynosuchus* and *Thrinaxodon*, the axial intercentrum is not fused to the centrum and visible in adult specimens.

Ch 17. Anterior articular facets of the axis: (0) extended ventrally to atlantal centrum and connecting; (1) posterolateral to the dens and not linked to each other (modified from Horovitz and Sánchez-Villagra, 2003: Ch 12).

Jenkins (1971: p34) indicated that the anterior articular surface of the axis in monotremes has a ventromedial component, which is also present in nonmammalian

cynodonts. Morganucodontids and *Vincelestes* have the similar condition. In *Repenomamus* and most other mammals discussed here, two anterior articular facets are not linked.

Ch 18. Rib of axis in adults: (0) present; (1) absent (Hu *et al*., 1997: Ch 5; Luo *et al*., 2002: Ch 124; Horovitz and Sánchez-Villagra, 2003: Chs 9, 13).

The axial rib is present in nonmammalian cynodonts and most mammal taxa discussed here, including *Repenomamus*. Only in eutherians and metatherians, the axial rib is absent, which is probably incorporated into the transverse process during development.

Ch 19. Lateroventral lamella of the axial body: (0) absent; (1) present.

The ventral part of the axial body in *Procynosuchus* and *Thrinaxodon* is void of lamella. In mammals, including *Repenomamus*, there are thin plates along the lateroventral edges of the axial body ,which form the bases of ventral branch of the axial transverse processes or ribs. Tritylodontids are similar to mammals in this character (Sun and Li, 1985; fig. 1)

Ch 20. Anapophysis of the axis: (0) absent; (1) present.

The anapophysis is a small process below the postzygapophysis on the lateral side of the pedicle. In taxa discussed here, only *Thrinaxodon* has the anapophysis on the axis.

Ch 21. Anterior extension of the axial spinous process relative to anterior articular facets: (0) not extended, the spinous process mainly posterodorsal to the facets; (1) extended, the process over the facets.

Jenkins (1971) suggested that the evolution of mammalian oblique muscles is in conjunction with that of the atlanto-axial complex. The mammalian M. obliqus capitis

caudalis spans between the axial spinous process and the atlantal transverse process. The anterior extension of the axial spinous process increases the transverse component of the oblique muscles, which further increases the efficiency of the atlanto-axial rotation. Jenkins (1971: P43) indicated that nonmammalian cynodonts and monotremes retain in primitive condition: the anterior articular facets well ahead the spinous process. Multituberculates have the similar condition. In *Repenomamus*, *Vincelestes*, and eutherians and metatherians discussed here the spinous process of axis extends anteriorly over the articular facets .

Ch 22. Posterior extension of the axial spinous process: (0) not extended beyond the centrum; (1) beyond the centrum (modified from Horovitz and Sánchez-Villagra, 2003: Ch 10).

The spinous process of the axis does not extend beyond the axial centrum in monotremes, multituberculates and *Didelphis*. The condition is different in *Repenomamus*, *Vincelestes*, *Pucadelphys*, *Zalambdalestes*, and *Asioryctes*, in which the process posteriorly extends. *Procynosuchus* and *Thrinaxodon* also have posteriorly extended spinous process on the axis.

POSTAXIAL CERVICAL VERTEBRAE (12 CHARACTERS)

Ch 23. Postaxial cervical ribs in adult: (0) present; (1) absent (Rowe, 1988: Ch 101; Hu *et al*., 1997 Ch 6; Luo *et al*., 2002: Ch 125).

The ribs of postaxial cervicals are present in nonmammalian cynodonts and many Mesozoic mammals, including morganucodontids, multituberculates, eutriconodonts (*Repenomamus* and *Jeholodens*), and *Zhangheotherium*. In *Vincelestes*, monotremes,

eutherians and metatherians, the cervical ribs are absent, either lost or incorporated into transverse processes.

Ch 24. Attachment of the head of postaxial ribs: (0) margins of the vertebral centra; (1) ventral lamellae.

In *Procynosuchus* (Kemp, 1980: fig.2) and *Thrinaxodon* (Jenkins, 1971: p50) heads of cervical ribs attach the vertebral centra directly, a condition similar to that of thoracic ribs. In *Oligokyphus* and mammals (including *Repenomamus*) in which the cervical ribs are present, there are lateroventral lamellae on the centra for supporting the cervical ribs. In terms of differentiation of vertebral column, the latter condition is derived.

Ch 25. Articulation of the postaxial cervical rib with the vertebral body: (0) mobile articulation; (1) immobile.

In *Procynosuchus* (Kemp, 1980) and *Thrinaxodon* (Jenkins, 1971), the articulation between the cervical rib and vertebra is essentially similar to that in the thoracic region, as a mobile joint, although the mobility is probably more restriction than in the thoracic region. Neither of the above authors mentioned the mobility of rib-vertebra joint in cervical region, but both (Kemp, 1980: p219 and 229; Jenkins, 1971: p57-58) indicated the mobility in thoracic region and the similarity and gradual transition between cervical and thoracic ribs. Therefore, it is reasonable to suggest that the cervical ribs in both taxa are mobile. In *Oligokyphus*, monotremes, multituberculates, and *Repenomamus* the cervical rib-vertebra contact is immobile, with sutures between them.

Ch 26. Shape of vertebral bodies of postaxial cervicals: (0) circular in cross section; (1) dorsoventral flattened.

The flattening of the vertebral body in cervical region is related to the enlargement of vertebral canal in this region, which is probably associated with increasing neuromuscular control of the forelimbs and the freedom of the neck during the evolution of mammals (Jenkins and Parrington, 1976: p416). The flattened condition is present in mammals (including *Repenomamus*) and tritylodontids, but not early cynodonts, i.e. *Procynosuchus*, *Thrinaxodon* and *Chiniquodon*, in which the vertebral bodies of cervical vertebrae are circular in the cross section.

Ch 27. Lateroventral lamellae of postaxial cervical vertebrae (0) absent; (1) present.

The lateroventral lamellae are plate-like projections extending lateroventrally from the lateroventral edges of the vertebral body in cervical region. The lamellae are present in taxa with flattened cervical vertebral bodies (see Ch 26).

Ch 28. Midventral keel on the bodies of postaxial cervicals: (0) ventral surface is gently round without distinct midventral keel and lateral concavities; (1) prominent midventral keel and associated lateral concavities present on ventral surface of centra.

The development of the midventral keel and associated lateral concavities in *Oligokyphus* and many mammals, including *Repenomamus*, probably facilitates attachment of hypoaxial musculature.

Ch 29. Length of the neural lamina relative to the centrum in postaxial cervicals: (0) not shortening; (1) shortening, narrow and thin.

The shortening of the neural lamina in cervical vertebrae facilitates the dorsal flexion and therefore the ascending of the neck. The condition is typical of mammals, present in morganucodontids and later mammals (Jenkins and Parrington, 1976). But

Repenomamus, similar to nonmammalian cynodonts, has (anteroposteriorly) wide neural laminae in cervical region, suggesting a less ascending posture of the head and neck.

Ch 30. Development of cervical spinous processes: (0) large, with the height equal or larger than the length of vertebral bodies; (1) reduced, with the height less than the length of the vertebral bodies.

Narrow and thin laminae and reduced spinous processes in postaxial cervicals of generalized mammals are probably related to an ascending posture of the neck (Jenkins and Parrington, 1976: p 416). But two characters are not always associated, for example, a typical cervical vertebra of *Oligokyphus* (Kühne, 1956: p101 and figs. 44 A-C) has a short spinous process, but the lamina is not shortened. The reduced spinous process and short lamina are seen in *Megazostrodon* (Jenkins and Parrington, 1976: p416 and figs 6 a-c) and multituberculates (Kielan-Jaworowska and Gambaryan, 1994: figs. 8E-F and 9). It is interesting that *Repenomamus* is similar to *Thrinaxodon* in both features, which indicates a less ascending posture than in other mammals mentioned here.

Ch 31. Prezygapophyses and postzygapophyses of postaxial cervicals: (0) as distinct processes on neural laminae; (1) reduced to be facets on laminae (Modified from Horovitz and Sánchez-Villagra, 2003: Ch 22).

The zygapophyses are normally developed as distinct processes from the neural laminae, but in extant monotremes the zygapophyses are reduced and become facets on laminae. *Repenomamus* has the normal condition in this character.

Ch 32. Vertebral anapophysis in postaxial cervicals: (0) absent; (1) present (modified from Sidor and Hopson, 1998: Ch 124)

In *Thrinaxodon* and morganucodontids postaxial cervicals have anapophyses. *Repenomamus* and other taxa discussed here don't have anapophysis on cervical vertebrae.

Ch 33. Number of cervical vertebrae: (0) more than seven; (1) seven.

Nearly all mammals have seven cervical vertebrae, no matter whether they have shortening or elongate necks (Flower, 1870). In nonmammalian cynodonts studied here, P*rocynosuchus* has nine cervicals while *Thrinaxodon* has seven.

Ch 34. Postaxial intercentra of cervical vertebrae in adults: (0) sutured with centra; (1) fused with centra.

In *Procynosuchus* and *Thrinaxodon* the intercentra are not fused with the centra in postaxial cervical vertebrae while in other nonmammalian cynodonts and mammals discussed here, the intercentra are absent, which are probably fused with the centra during development.

THORACIC VERTEBRAE (8 CHARACTERS)

Ch 35. Transition from the cervical to thoracic region: (0) gradual; (1) distinct.

Kemp (1980: p222) observed that there is no definable distinction between cervical and thoracic vertebrae in *Procynosuchus*. But marked change does exist in *Thrinaxodon* (Kemp, 1980: p222 cited Jenkins [1971] and Jenkins, 1971: p49-50), which is reflected in the shift in orientation of the zygapophyses and transverse processes and a change in the morphology of the spinous processes (but see Jenkins, 1971 [p53]: " The morphological transition between the cervical and thoracic series in gradual and not extensive. …The abrupt change in zygapophyseal orientation is the only definite marker separating thoracic from cervical vertebrae."). The contact between thoracic ribs, not cervical ribs, and the sternums is the best criterion for demarcate two vertebral regions,

but the ribs and sternal apparatus are poorly preserved in nonmammalian cynodonts and early mammals. *Repenomamus* is exceptional in that it well preserves the cervical and thoracic vertebrae and ribs in both regions, which indicate the distinct transition from the cervical to thoracic region. in the orientation of the zygapophyses, morphology of the transverse processes and ribs (See Ch 36 for the transition in rib morphology).

Ch 36. Transition from the cervical to thoracic ribs: (0) gradual; (1) distinct.

In *Procynosuchus* (Kemp, 1980: p219) and *Thrinaxodon* (Jenkins, 1971: p 58), the morphological transition from the cervical to thoracic ribs is gradual, and no abrupt change occurs at the boundary. In other taxa discussed here, including *Repenomamus*, the thoracic ribs are easily discerned from cervical ribs. The cervical ribs are slender, with no articular facet on the distal end; but the anterior thoracic ribs are stout and have articular facets for sternal elements on the distal end.

Ch 37. Number of thoracic vertebrae: (0) 15 or less; (1) 16 or more (modified from Luo *et al*., 2002: Ch 126).

The majority of extant therian mammals have 13 thoracic vertebrae (Flower, 1870; Sliper, 1946). Two extant monotremes have 16 and 17 thoracics, respectively. *Repenomamus* has 20 thoracics, which is rare among mammals.

Ch 38. Shape of the thoracic vertebral body: (0) roughly circular or oval in cross section; (1) strongly dorsoventrally flattened.

Ch 39. Development of spinous processes of thoracics: (0) well developed; (1) reduced.

(Discussion for Ch 38 and 39) In extant monotremes, the vertebral bodies of thoracics are dorsoventrally flattened, and the spinous processes are reduced, with the

height less than the length of bodies. *Repenomamus*, as other taxa discussed here, has the bodies of the thoracics circular/oval in the cross section and the spinous processes relatively high.

Ch 40. Vertebral anapophysis in thoracics: (0) absent; (1) present (modified from Sidor and Hopson, 1998: Ch 124).

Anapophyses in the thoracic region are present in several nonmammalian cynodonts and many mammals discussed here, i.e. *Thrinaxodon*, tritylodontids, morganucodontids, multituberculates, *Gobiconodon*, *Repenomamus*, *Vincelestes*, *Ukhaatherium*, and *Pucadelphys*. the process is absent in *Procynosuchus*, monotremes and *Henkelotherium*.

Ch 41. T1 transverse process: (0) present; (1) absent (modified from Horovitz and Sánchez-Villagra, 2003: Ch 24).

Repenomamus: (0) present.

Ch 42. Intervertebral foramen in thoracic region: (0) intervertebral; (1) enclosed by the caudal edge of the neural arches. (Modified from Horovitz and Sánchez-Villagra, 2003: Ch 28)

(Discussion for Ch 41 and 42) Extant monotremes don't have a distinct transverse process on the first thoracic vertebra, and their intervertebral foramina in thoracic region are enclosed by the caudal edge of the neural arches, rather than truly intervertebral in position.

THORACIC RIBS (3 CHARACTERS)

Ch 43. <u>Thoracic ribs: (0) at least anterior ribs double-headed with capitulum and tuberculum separated; (1) single-headed.</u>

Mammalian ribs in the anterior thoracic region generally have two heads, the tuberculum and capitulum, which articulate with the transverse process and vertebral body, respectively. In posterior thoracics, two heads may be fused together, articulating with the transverse process. But in extant monotremes, all thoracic ribs have only one head, which is articulated with the vertebral body only, although the transverse process does exist (Flower, 1870). The double-head condition is well demonstrated in *Repenomamus*.

Ch 44. <u>Sternal ribs of the thoracic ribs: (0) cartilage; (1) ossified</u> (Modified from Horovitz and Sánchez-Villagra, 2003: Ch 34).

The sternal rib is the ventral portion of the thoracic rib, which contacts the sternum. In extant monotremes the cartilage is ossified (Flower, 1870). In fossil taxa, including *Repenomamus*, the element is not preserved, its presence is inferred from the distal extremity of the anterior ribs, which are rough and bear articular facets.

Ch 45. <u>Anterior Thoracic ribs' (true ribs) articulation with sternum: (0) with single sternebra; (1) with two sternebrae</u> (modified from Horovitz and Sánchez-Villagra, 2003: Ch 35).

In extant therian mammals the anterior thoracic ribs, also called the true ribs, articulate with two successive sternal elements. But this is not the case of monotremes, in which every true rib articulates with a single sternebra (Flower, 1870). *Oligokyphus* is probably similar to monotremes in rib-sternum articulation, judged by the morphology of

the sternubrae as seen in Kühne (1956: fig. 51). Judged by the articular facets on sternal elements, each true rib articulates with two successive sternal elements in *Repenomamus*.

LUMBAR VERTEBRAE (4 CHARACTERS)

Ch 46. <u>Demarcation between the thoracic and lumbar vertebral series based on rib/transverse process morphology: (0) gradually; (1) distinct.</u>

Among taxa discussed here only *Procynosuchus* has the thoracic and lumbar regions continuous in rib morphology. In *Repenomamus* and other taxa, the lumbar ribs are either different from thoracic ribs in morphology (lumbar ribs are often shorter, broader than the thoracic ones and have one head sutured to the vertebral body) or further incorporated into the transverse processes.

Ch 47. <u>Lumbar ribs: (0) present and sutured with transverse process; (1) synostosed to transverse process without suture.</u> (Modified from Luo *et al*., 2002: Ch 127)

Lumbar ribs are present in nonmammalian cynodonts, early mammals, such as *Repenomamus*, *Gobiconodon* and *Jeholodens*, and extant monotremes. In these taxa, the lumbar ribs are sutured with vertebrae and have very limited mobility. Separate lumbar ribs are not seen in multituberculates, *Vincelestes*, metatherians, and eutherians, which are probably incorporated into transverse processes during development. Luo and Wible (2005: 106) suggested an enigmatic late Jurassic mammal, *Fruitafossor windscheffeli,* having mobile lumbar ribs and declared that as a feature of nonmammalian cynodonts and monotremes. Recently, Li and Luo (2006) announced the presence of mobile lumbar ribs in a new spalacotheriid symmetrodont. Unfortunately, both authors do not illustrate the articulation relationships between the ribs and lumbars on original specimens, which makes it difficult to judge the mobility lumbar ribs in these taxa.

Ch 48. Articulation between the lumbar ribs and vertebrae: (0) with an intervertebral capitular articulation; (1) no intervertebral articulation.

The intervertebral capitular articulation is present in the anterior lumbar region of T*hrinaxodon (*Jenkins, 1971: p60). It is probably the primitive condition because it is similar to that of thoracic region and suggests less differentiation between two regions. In other taxa studied here, including R*epenomamus,* the lumbar ribs only articulate with corresponding vertebrae.

Ch 49. Zygapophyseal articulation in lumbar region: (0) nearly horizontal; (1) more vertical than horizontal.

The horizontal orientation of zygapophyses in the lumbar region allows the lateral flexion of the vertebral column, which is present in many extant reptiles and probably represents primitive condition in amniotes. In mammals, including *Repenomamus*, the lumbar zygapophyses have more or less vertical orientation, facilitating the dorsoventral flexion of the vertebral column. In *Procynosuchus*, the horizontal orientation of the lumbar zygapophyses is obvious (Kemp, 1980). Jenkins (1971: p55) did not mention directly the orientation of zygapophyseal articulation of the lumbar region in *Thrinaxodon* but his figure 12 showed a continuation in the change of the orientation from thoracic to lumbar series. The zygapophyses in the thoracic region of *Thrinaxodon* have a more vertical than horizontal orientation, as seen in *Galesaurus* (Jenkins, 1971: p 64). Therefore, the lumbar series probably also have more vertically oriented zygapophyses. Kemp (1980: p256) stated that horizontal lumbar zygapophyses of *Procynosuchus*, among several other features, is not found in other cynodonts. Jenkins' musculature reconstruction (1971: P.87) suggested some degree of the lateral flexion of

the axial skeleton, but did not implied the horizontal (or near so) orientation of lumbar zygapophyses in *Thrinaxodon* and other nonmammalian cynodonts.

SACRAL VERTEBRAE (3 CHARACTERS)

Ch 50. Number of sacral vertebrae: (0) five or more; (1) four; (2) three or less.

Repenomamus has four sacral vertebrae, a condition also found in multituberculates and *Zhangheotherium*. Other mammalian taxa discussed here have only three or less sacrals. Nonmammalian cynodonts, i.e. *Thrinaxodon*, *Chiniquodon* and tritylodontids, have more than four sacrals.

Ch 51. Development of sacrum: (0) sacral vertebrae articulated; (1) sutured or synostosed.

In nonmammalian cynodonts discussed here, sacral vertebrae, similar to other regions of the vertebral column, are articulated to each other. In mammals, sacrals are sutured or synostosed to form a sacrum.

Repenomamus (1) sutured.

Ch 52. Sacral rib development: (0) not fused with vertebral body; (1) fused

(modified from Sidor and Hopson, 1998: Ch 125).

Sacral ribs are not fused to sacral vertebrae in nonmammalian cynodonts discussed in this study. In mammals, including *Repenomamus*, there is no separate ribs on sacrals.

CAUDAL VERTEBRAE (1 CHARACTER)

Ch 53. Caudal ribs: (0) present in at least some anterior caudals; (1) absent.

In *Thrinaxodon*, caudal vertebrae have ribs (Jenkins, 1971: p 57). The condition in *Procynosuchus* is unclear, but posterior caudals don't have ribs. Mammals, including *Repenomamus*, don't have caudal ribs.

STERNAL APPARATUS, INCLUDING INTERCLAVICLE (7 CHARACTERS)

Ch 54. <u>Interclavicle as separate element in the adult: (0) present; (1) absent.</u> (Rowe, 1988: Ch 110 and 113; Hu *et al*., 1997: Ch 8; Luo *et al*., 2002: Ch 128; Horovitz and Sánchez-Villagra, 2003: Ch 39)

The interclavicle is a distinct element in extant monotremes, many Mesozoic mammals, i.e. *Sinoconodon*, morganucodontids, multituberculates, *Gobiconodon*, *Repenomamus*, *Jeholodens*, and *Zhangheotherium*, and nonmammalian cynodonts. In extant therians, there is no interclavicle in the adult, but the homologous structure of the interclavicle does appear early in development, which is incorporated into the sternal manubrium (Klima, 1973, 1987). *Vincelestes* and *Eomaia*, have no interclavicle preserved, which is probably, as in extant therians, incorporated into the sternal manubrium.

Ch 55. <u>Anterior part (articulating with clavicle) of the sternal manubrium/interclavicle: (0) with short and narrow lateral process; (1) as broad and expanded plate; (2) with extra elongated lateral process.</u>

The interclavicle or the sternum manubrium articulates with the clavicle. In nonmammalian cynodonts, including *Thrinaxodon*, the interclavicle bears a pair of concavities defined by the short lateral and anterior median processes. The concavities are for articulating with the medial ends of the clavicles (Jenkins, 1971). In extant therians, similar facets and processes are present on the anterior portion of the sternal

manubrium. In some fossil mammals (*Zhangheotherium*, *Repenomamus*, and multituberculates) the processes on the interclavicle are indistinct; the plate supporting the concavities for clavicles are expanded. In extant monotremes, *Morganucodon* and tritylodontids, there are extra elongate processes, which articulate with not only the medial end of the clavicle but also medial portion of the claviclar shaft.

In extant mammals different morphologies in the anterior part of the interclavicle/sternal manubrium in monotremes and therians have developmental background (Klima, 1973, 1987). In monotremes, the interclavicle develops out of two elements, a paired exoskeletal lateral element (pars desmmalis interclaviculae, consisting of membranous tissue) and an unpaired endoskeletal element (pars chondralis interclaviculae, consisting of cartilaginous tissue). The paired element forms the pair of extra processes and the anterior part of the median portion of the interclavicle. The clavicle of monotremes only articulates with these exoskeletal elements. The endoskeletal element is probably equivalent to the "pro-osteon" of Parker (1868), which was proposed by Parker as the pre-costal portion of the sternal manubrium (the element was erroneously identified as the dorsal epiphysis of the interclavicle by Cave [1970: p306]).. This endoskeletal element is fused to the sternal manubrium in extant therians. More than that, the sternal manubrium of extant therians also incorporates the medial part of the paired chondral elements of the coracoid-scapular plate, which form the procoracoid and coracoid in monotremes (Klima, 1973, 1987). But the exoskeletal element of the interclavicle (pars desmmalis interclaviculae) never appears in extant therians.

The nonmammalian cynodonts and fossil mammal taxa don't have the development information available, the composition of their interclavicle/sternal

manubrium can only be speculated based on their similar morphologies to those of extant taxa, assuming that the general developmental pattern of the girdle-breast region is similar in fossil and extant cynodonts. When preserved, the sternal manubrium in fossil therians is narrow, very similar to that of extant therians; it is quite possible the similar development pattern of sternal manubrium has occurred in these fossil taxa. In *Morganucodon* (Jenkins and Parrington, 1976: p395 and fig. 3) and tritylodontids (Sun and Li, 1985: p 139 and fig. 4) the "T"-shaped interclavicle is similar to that of monotremes in morphology, and articulates with not only the medial end but also the shaft of the clavicle. It is possible that, as seen in monotremes, the medial part of the interclavicle develops out of the cartilaginous tissue but extra elongate lateral processes of the interclavicle are from the membranous tissue. The narrow interclavicles of other cynodonts, e.g. *Thrinaxodon* (Jenkins, 1971) and *Pachygenelus* (Gow, 2001), are similar to that of extant therians. The main portion of the bone probably develops out of the endoskeletal element of the interclavicle (pars chondralis interclaviculae), which is the common element of interclavicle/sternal manubrium in all extant mammals. It seems unlikely that there is membranous tissue participating in the development of the interclavicle as no extra lateral processes are present in these animals and the interclavicle only articulates with the medial head of the clavicle. It is difficult to assess whether there is any tissue from coracoid-scapular plate participating in the formation of interclavicle in these cynodonts. Nonmammalian Cynodonts have large procoracoid and coracoid, but these bones do not, as in monotremes, contact the interclavicle. One possibility is that, as in monotremes, the coracoid-scapular plate only develops into the scapulocoracoid and procoracoid and does not contribute to the formation of interclavicle.

Another possibility is that the medial part of the coracoid-scapular plate contributes to the formation of the interclavicle while the lateral part develops into the shoulder girdle; similar pattern is seen in extant therians, but in the latter the interclavicle itself is further incorporated into the sternal manubrium, the coracoid is reduced and the procoracoid never develops. The expanded plate seen in the interclavicles of several Mesozoic mammals, e.g. *Repenomamus*, multituberculates and *Zhangheotherium*, is also difficult to explain given that no similar morphology is seen in extant mammals. It is different from the extra processes of monotremes in morphology and articulation with the clavicle. One possibility is that the plate is simply the expanded lateral process. But more likely the plate incorporates tissues from the medial part of the coracoid-scapular plate. The shape of the plate is more similar to the procoracoid/coracoid of the monotremes than the extra process. In many extant therians, the articular part of the sternal manubrium also develops from the coracoid-scapular plate (Klima, 1987). In other words, the interclavicle in these fossil mammals probably has both the unpaired and paired chondral element, but no membranous tissue.

Ch 56. <u>Articulation between the interclavicle and sternal manubrium (0) posterior edge of the interclavicle contacting the anterior edge of the sternal manubrium; (1) posterior process of the interclavicle overlapping ventral side of the sternal manubrium.</u> (Modified from Luo *et al*., 2002: Ch 129).

Luo *et al* (2002) have one character (Ch 128) dealing with the presence vs. absence of the interclavicle in adult, and the other (Ch 129) on the contact relationships between the interclavicle and the sternal manubrium in adult. The distribution of the absence of the interclavicle (Ch 128 state 1) and the fusion of the interclavicle and sternal

manubrium (Ch 129 state 2) among different taxa are the same, which indicates that they treat two states as identical, which I agree with; but they use one feature (absence of the interclavicle = the fusion of interclavicle and sternal manubrium) twice, which I don't follow in this study. Among taxa with the interclavicle and sternal manubrium well preserved, *Repenomamus*, *Jeholodens* and *Zhangheotherium* have the interclavicle overlapping the manubrium, while multituberculates, monotremes, *Sinoconodon*, and tritylodontids have the interclavicle abutting the manubrium.

Ch 57. Posterior portion of the interclavicle: (0) much longer than anterior portion (clavicle articulation); (1) equal to or less than the anterior portion in length (modified from Sidor and Hopson, 1998: Ch 140).

Repenomamus: (1) equal to or less than the anterior portion in length.

Ch 58. Interclavicle posterior process shape: (0) uniformly broad; (1) paddle-like; (2) narrow (Sidor and Hopson, 1998: Ch 141).

Repenomamus: (2) posterior process of the interclavicle narrow.

Ch 59. Anterior median process of sternal apparatus: (0) present; (1) absent

(Modified from Luo *et al*., 2002 Ch 130).

The anterior median process is the small process between the clavicle articular facets of the interclavicle (when the interclavicle is present) or sternal manubrium (when interclavicle fused with sternum). The process is present in *Jeholodens*, *Vincelestes*, eutherians, and metatherians, and absent in morganucodontids, monotremes, *Repenomamus*, and *Zhangheotherium*.

Ch 60. Size of the anterior-most element of the sternal apparatus relative to the more posterior sternebrae: (0) wider; (1) similarly narrow (Hu *et al*., 1997: Ch

15; Luo *et al*., 2002: Ch 140).

The anterior-most element of the sternal apparatus is either the interclavicle, if the bone is present, or the sternal manubrium, if the interclavicle is incorporated into the latter. In eutherian and metatherian, the sternal apparatus, including the anterior-most element, is narrow. In other mammals discussed here, including *Repenomamus*, and nonmammalian cynodonts, the anterior-most element is wider than other sternal elements.

SHOULDER GIRDLE (19 CHARACTERS)

Ch 61. Scapular blade: (0) narrow and high, dorsal part not distinctly expanded compared with ventral part of the blade; (1) dorsal part distinctly expanded.

The scapular blade in nonmammalian cynodonts is narrow and high (Jenkins, 1971; Kemp, 1980), in contrast with that of typical mammalian scapula, which is gradually expanded dorsally. *Repenomamus* has the typical mammalian condition.

Ch 62. Lateral surface of the scapular blade: (0) gently flat anteroposteriorly; (1) concave and forming distinct supracoracoideus fossa or infraspinous fossa.

The supracoracoideus fossa is present on the lateral surface of the scapular blade in some nonmammalian cynodonts (*Thrinaxodon*--Jenkins, 1971: 94 and fig. 18; tritylodontids—Kühne, 1956: p 117 and fig. 53; Sun and Li 1985: p 141 and fig. 6). The fossa is defined by laterally reflected anterior and posterior edges of the blade. It provides the origin for the M. supracoracoideus, the homologous of mammalian spinati muscles; and the fossa itself is the homolog of the mammalian infraspinous fossa (Jenkins, 1971: p94 and fig. 17). In a primitive cynodonts, *Procynosuchus*, the scapular blade does not have the supracoracoideus fossa, and its anterior and posterior edges do not reflected

laterally. In monotremes, the anterior edge of the scapula is not everted. There is a lower ridge in the middle of the lateral surface of the scapular blade, in front of which a shallow supracoracoideus fossa is evident (Jenkins, 1971: fig. 19g). In other mammals, including *Repenomamus*, there is well defined infraspinous fossa on scapular blade.

Ch 63. Scapular blade: (0) laterally bowed; (1) not bowed and flat in dorsoventral direction.

Primitive tetrapods have massive pectoral girdle, especially the ventrally components (coracoids, clavicle, and interclavicle), to resists the compressive forces generated by sprawling limb posture. In nonmammalian cynodonts, the ventral components of the pectoral girdle become reduced, but their scapulas are bowed laterally with dorsal portion inclined medially, which makes the serratus musculature obliquely oriented . Such an arrangement helps resisting the compressive forces (Jenkins, 1971: p 135). Monotremes have a similar inclination of the scapula. Other mammals, including *Repenomamus*, have the scapular blade not bowed but flat in dorsoventrally direction.

Ch 64. Twist of the scapular blade: (0) twist; (0) not twist.

In *Procynosuchus* and *Thrinaxodon*, the ventral part of the scapular blade and the coracoid plate are pointed anteromedially when the dorsal edge of the blade is positioned parallel to the body axis (Kemp, 1980: p 230, and fig. 7; Jenkins, 1971: fig. 18c). In mammals, the coracoid process is often turned anteromedially, but the scapular blade itself is not twisted.

Ch 65. Acromial process of the scapula: (0) absent; (1) weakly developed as a short process above the glenoid; (2) as a long hook-like process extending ventrally beyond the glenoid process (Modified from Rowe, 1988 Ch 115; Hu *et al*., 1997:

Ch 11; Sidor and Hopson, 1998: Ch 134; Hopson and Kitching, 2001: Ch 85; Luo *et al*., 2002: Ch 135; Horovitz and Sánchez-Villagra, 2003: Ch 37).

The acromial process is the place where the clavicle articulates with the scapulocoracoid. In *Procynosuchus*, the anterior edge of the scapula is thin, with no sign of the acromial process (Kemp, 1980: p 231 and fig. 7). In *Thrinaxodon*, the thickening on the everted anterior edge of the scapula probably represents the location of acromioclaviclar articulation, but a distinct acromial process does not develop (Jenkins, 1971: p 94 and fig. 18). A weakly developed acromial process is seen in some late nonmammalian cynodonts, such as tritylodontids and tritheledontids, in which a robust but short process is evident ventrally on the anterior edge of the scapula, above the glenoid; the process normally does not extend ventrally beyond the glenoid fossa (Kühne, 1956; Sun and Li, 1985; Gow, 2001). The scapula of primitive mammals, including *Morganucodon*, *Megazostrodon*, and monotremes, has the acromial process similarly developed (Jenkins and Parrington, 1976). A more established acromial process, with hook-like morphology and extending ventrally beyond the glenoid, is seen in multituberculates (Kielan-Jaworowska and Gambaryan, 1994), eutriconodonts including *Repenomamus*, symmetrodonts (Hu *et al*., 1997) and late therian mammals.

Ch 66. <u>The neck of the scapula: (0) not developed; (1) as short constriction below the acromial process; (2) moderate or elongated constriction between the acromial process and glenoid</u> (modified from Sidor and Hopson, 1998: Ch 135 and 136; Hopson and Kitching, 2001: Ch 86 and 87; Bonaparte *et al*., 2003: Ch 41).

The scapular neck is the constriction between the scapular blade and glenoid and below the base of the acromial process, marked by the scapular notch (Muizon, 1998: p 55). In the taxa without acromial process, such as *Procynosuchus* and *Thrinaxodon*, there is no constriction above the glenoid. In tritylodontids and *Chiniquodon*, the acromion arises at the level just above the glenoid, and the scapular neck is very short. In *Pachygenelus* and mammals, the base of the acromion (either on the anterior edge of the scapula or from the spine) is well above the glenoid, leaving a well defined neck between them.

Ch 67. <u>Development of supraspinous fossa: (0) absent; (1) incipiently developed; (2) weakly developed; (3) fully developed</u> (Modified from Rowe, 1988: Ch 114; Hu *et al*., 1997: Ch 10; Luo *et al*., 2002: Ch 134).

In extant therians the infra- and supraspinous fossae provide the origins for infra- and supraspinatus muscles, respectively (Evens, 1993). The infraspinous fossa is equivalent to the original concave lateral surface of the nonmammalian cynodonts, the supracoracoideus fossa, while the supraspinous fossa is a neomorph structure evolved in mammals. Nevertheless, the initiation of the supraspinous fossa can be traced back into nonmammalian cynodonts. The supraspinous fossa does not appear in *Procynosuchus* (Kemp, 1980), which has a flat scapular blade. *Thrinaxodon* does not have supraspinous fossa either (Jenkins, 1971: p94-96). The concave lateral surface of the scapulocoracoid provides the origin for M. supracoracoideus, the homolog of mammalian spinati muscles. The concavities along the anterior borders of the scapula and procoracoid provide the origin for the anteroventral division of the M. scapulocoracoideus, where the anterior edge of the scapula is directed anteriorly or anteromedially although the more dorsal part

of the edge is everted (Jenkins, 1971: fig. 18C). This is initial stage in the differentiation of the supra- and infraspinatus muscles. But the supraspinous fossa does not appear, as all parts of the scapulocoracoideus muscle originate from the lateral side of the scapular blade and posterior to the acromion and the edge of the scapular blade. The scapulocoracoid of *Chiniquodon* (Romer and Lewis, 1973) is similar to that of *Thrinaxodon*. In tritylodontids the anterior edge of the scapula (with the acromion) strongly everts laterally, the internal surface of the scapular blade is convex with the anterior portion facing anteriorly or anterolaterally (Kühne, 1956; Sun and Li, 1985; Sues, 1986). A portion of the scapulocoracoideus muscle originates from this portion of the internal surface, which passes beneath the clavicle and inserts onto the humerus (Sun and Li, 1985: fig. 8). The development of the scapular neck and the reduction of the procoracoid provide the space for the path of the muscle. The muscle is regarded homologous with mammalian supraspinatus muscle and its origination site represents the initial supraspinous fossa (Sun and Li, 1985). However, the fossa itself is not well defined in this taxon. Its surface is flat or convex rather than concave as that of infraspinous fossa. It does not have clear boundary with the subscapular fossa except a small dorsal portion, where a thin bony plate marks the border. Sun and Li (1985: p 140 and fig. 8, sp-small piece of protuberance) suggested that this small bony plate represents the secondary anterior edge of the scapular blade. Similarly, everted anterior scapular edge (with an acromion) and anteriorly facing supraspinous fossa are present in tritheledontids, *Morganucodon* and *Megazostrodon*. A more established supraspinous fossa is found in multituberculates (Kielan-Jaworowska, 1989; Kielan-Jaworowska and Gambaryan, 1994; Sereno and McKenna, 1995). In the scapulocoracoid of

multituberculates, the acromion is positioned lateral to and above the glenoid fossa. A lower spine, which is homologous with the anterior edge of the scapulocoracoid of nonmammalian cynodonts, *Morganucodon* and *Megazostrodon*, extends dorsally from the acromion. The supraspinous fossa is in front of the acromion and spine, and faces anterolaterally. But the fossa isn't yet fully developed as the new anterior margin of the scapula, which separates the fossa from the internal surface of the scapular blade, does not extend the full depth of the scapular blade. The edge is lower, attenuates ventrally and disappears above the scapular neck (Kielan-Jaworowska and Gambaryan, 1994: fig 13H, I, J; Note: Sereno and McKenna's [1995: fig. 3a] reconstruction of the scapula did not show the presence of the anterior margin of the scapula), and the separation of supraspinous fossa from the internal surface of the scapula is incomplete. The supraspinous fossa is fully developed in extant therians, symmetrodonts (Hu *et al*., 1997, 1998), and eutriconodonts, i.e. *Jeholodens* and *Repenomamus* (Ji *et al*., 1999; Hu *et al*., 2005b and this study). In these taxa the lateral surface of the scapular blade has two fossae, the supraspinous fossa in front and the infraspinous fossa in behind, separated by the high scapular spine; and the anterior edge of the scapula completely separates the supraspinous fossa from the internal surface of the scapula.

Monotremes represent an exception in the evolution of mammalian supraspinous fossa outlined here. The lateral surface of the scapular blade in monotremes has a lower ridge in the middle, the acromion is on the anterior edge of the scapular blade, which is not everted. There is no trace of the supraspinous fossa. Howell (1937: p203-204, cited by Jenkins, 1971: p96) and Jenkins (1971: p 96 and fig. 19) believed that the shoulder

musculature of monotremes is specialized and the arrangement of infra- and supraspinatus muscles seen in therians does not occur, even initially, in monotremes.

Luo *et al*. (2002: Ch 134) coded among others *Morganucodon*, Megazostrodon and multituberculates as having weakly developed supraspinous fossa present only along a part of the scapula and with the acromion positioned lateral to the glenoid. As shown in Jenkins and Parrington (1976: figs. 4a and 7a), the acromion and the anterior edge of the scapula in *Morganucodon* and *Megazostrodon* is anterior not lateral to the glenoid. The edge separating the supraspinous fossa and the internal surface is not seen in the preserved part of the scapula either, which is evident and well developed on the scapula of multituberculates. The development of the supraspinous fossa in *Morganucodon* and *Megazostrodon* is similar to that in tritylodontids and tritheledontids. But Luo *et al* coded absence of the fossa for tritylodontids, tritheledontids and monotremes. As discussed above, the condition in monotremes is incomparable with that in other taxa.

Ch 68. <u>Development of the scapular spine: (0) absent; (1) low bony ridge; (2) high bony plate.</u>

The scapular spine is the bony plate arising in the middle of lateral aspect of the scapular blade. It separates the supraspinous fossa from the infraspinous fossa. In extant mammals, the scapular spine is present only in therians, not in monotremes. As a distinctive structure, the spine probably evolved within mammals. Primitive mammals, such as morganucodontids and sinoconodontids, don't have a spine. The spine in multituberculates forms a low ridge extending dorsally from the well-developed acromion (Sereno and McKenna, 1995). The fully developed spine is seen in *Repenomamus*, symmetrodonts, eupantothere, metatherians, and eutherians. The

mammalian scapular spine was regarded as the homologue of the anterior edge of the scapular blade of nonmammalian cynodonts (Kemp, 2005: p 113).

Ontogenetic data of extant therians indicate that there is an appositional bone, an ossification in the intermuscular septum, between the infra- and supraspinatus muscles or an ossified dorsal cartilaginous process from the acromion dorsal to the scapular spine (Grossmann, Sánchez-Villagra and Maier, 2002; Sánchez-Villagra and Maier, 2002, 2003). Sánchez-Villagra and coauthors proposed that only the ventral portion of the spine (the acromial portion) in extant therians originates from the anterior margin of the scapular blade, while the major dorsal portion of the spine is a neomorphic structure. Sánchez-Villagra and coauthors did not explicitly explain whether the anterior margin of the therian scapula is original or secondary, but they proposed that the floor of the supraspinous fossa is already present at the beginning of scapular development, which implies that the major portion of the original anterior margin of the scapular blade remains as the anterior margin in therians (Sánchez-Villagra and Maier, 2002: fig. 1c).

The fossil evidence of nonmammalian cynodonts and early mammals is not fully consistent with all these claims, contrary to what Sánchez-Villagra and Maier (2002: p461) suggested. The scapula in late nonmammalian cynodonts and morganucodontids has an everted anterior margin with the supraspinatus muscle anterior to it, a relationship equivalent to that of the spinatus muscle and spine in extant therians. Such equivalency favors the homologue between the spine of extant therians and the original anterior margin of the cynodont scapula. The scapula of multituberculates provides further evidence for such homology. It has a well-developed acromion, a low spine extending dorsally from the acromion, and an incipient anterior margin anterior to the weak

supraspinous fossa (Kielan-Jaworowska and Gambaryan, 1994; Sereno and McKenna, 1995). Referring to their relationships with the supraspinous fossa, the acromion and low spine in multituberculates are corresponding to the everted anterior scapular margin of the nonmammalian cynodonts and morganucodontids, and the incipient anterior scapular margin of the multituberculates is a secondary structure. The presence of an appositional bone or an ossified cartilaginous process on the scapular spine in extant therians does not necessarily mean the whole dorsal portion of the spine is neomorphic. It is also possible that in extant therians the anterior margin of the scapular blade is neomorphic while the acromion and the base of the spine is homologous with the original anterior margin of scapula blade of nonmammalian cynodonts, the latter (the spine) is further enhanced by the development of an appositional bone or cartilaginous process. The base of the spine in dorsal portion could even be reduced and the dorsal portion of the spine is totally replaced by the neomorphic structure. Compared to hypothesis of Sánchez-Villagra and coauthors, this alternative opinion on the homology of scapular spine is more consistent with the fossil evidence and relationships among bony structures and muscles.

Ch 69. <u>Development of the Procoracoid: (0) present as a separated element in adult, contact with scapula greater than coracoid; (1) present, contact with scapula less than coracoid; (2) present, no contact with scapula; (3) absent in adult as individual element</u>. (Modified from Rowe, 1988: Ch 117; Hu *et al*., 1997: Ch 12; Sidor and Hopson, 1998: Ch 138; Hopson and Kitching, 2001: Ch 89; Luo *et al*., 2002: Ch 137; Bonaparte *et al*., 2003: Ch 43).

This character combines two characters used in previous studies: (1) presence vs. absence of procoracoid in adults (Rowe, 1988: Ch 117; Hu *et al*., 1997: Ch 12; Luo *et al*.,

2002: Ch 137), and (2) procoracoid contact with scapula (Sidor and Hopson, 1998: Ch 138; Hopson and Kitching, 2001: Ch 89; Bonaparte *et al*., 2003: Ch 43). The great majority of tetrapods have only a single coracoidal ossification, which is called coracoid. But synapsids and a few anapsids have two coracoidal ossifications, called coracoid (posterior one) and procoracoid (anterior one), respectively (Romer, 1956: p 308-309). In primitive synapsids, the procoracoid is larger than the coracoid, but the element is gradually reduced in late synapsids. Accordingly, its contact with scapula is also reduced in the evolution of synapsids. In primitive cynodonts, such as *Procynosuchus*, *Thrinaxodon* and *Chiniquodon*, the scapular facet for the procoracoid is larger than that for the coracoid. The reverse is true for tritylodontids, tritheledontids, *Sinoconodon*, *Morganucodon* and *Megazostrodon*. The procoracoid of monotremes losses contact with the scapula. Its contact with the interclavicle probably represents a specialized condition. All other mammals in which the pectoral girdle is adequately known, including *Repenomamus*, don't have a separate procoracoid. Development data of all three clades of extant mammals (Klima, 1973, 1987) suggest that in the early developmental stage the corresponding element (medial part of the chondral coracoid-scapular plate) appears in all of these clades, but in therians it fused with the sternum manubrium. This is probably also the case for those fossil mammals without procoracoid, in which the element is either fused with the interclavicle, or incorporated into the sternal manubrium.

Ch 70. <u>Procoracoid participating in the glenoid: (0) present; (0) absent</u>. (Sidor and Hopson, 1998: Ch 137; Hopson and Kitching, 2001: Ch 88; Bonaparte *et al*., 2003: Ch 42)

In *Procynosuchus* and *Thrinaxodon*, the posterodorsal corner of the procoracoid forms a small segment of the glenoid lip between the scapula and coracoid (Kemp, 1980: fig 7a; Jenkins, 1971: p101). In other taxa mentioned above, the procoracoid is excluded from the glenoid. The character is inapplicable to *Repenomamus* and other mammals with the procoracoid absent.

Ch 71. Procoracoid foramen: (0) present; (1) absent (Luo *et al*., 2002: Ch 13).

The procoracoid foramen, also called the supracoracoid foramen or coracoid foramen, transmits the supracoracoid nerve and accompanying blood vessels in tetrapods (Goodrich, 1930: p 174; Jenkins, 1971: p 107). In nonmammalian cynodonts, the foramen often perforates the procoracoid, but in *Chiniquodon minor* (originally *Probelesodon lewisi*), the foramen is between the procoracoid and the coracoid (Romer and Lewis, 1973: fig 7). Monotremes, although having the procoracoid, don't have the procoracoid foramen. The character is coded as absent for *Repenomamus* and other mammals with the procoracoid absent.

Ch 72. Morphology of the coracoid: (0) as a large bone with a posterior process; (1) as a large coracoid process of the scapulocoracoid, well contributing to the glenoid fossa and without posterior process; (2) as a small hook-like coracoid process, barely or not contributing to the glenoid (Modified from Rowe, 1988: Ch 118; Hu *et al*., 1997: Ch 13; Luo *et al*., 2002: Ch 139; Horovitz and Sánchez-Villagra, 2003: Ch 36).

Similar to the procoracoid, the coracoid is gradually reduced in size during the evolution of synapsids, especially in mammals, which is probably related to the transition of the posture and gait from non-mammalian to mammalian condition (Jenkins, 1971).

Although much reduced compared to that in primitive synapsids, the coracoid in nonmammalian cynodonts, and primitive mammals, such as *Sinoconodon*, *Morganucodon* and *Megazostrodon*, is still a separate bone with a large posterior process (Jenkins, 1971; Jenkins and Parrington, 1976). The extremity of the process forms the tuberosity for the coracoid head of the triceps muscle (Jenkins, 1971: p101 and fig. 18). Monotremes have a similar large coracoid with a posterior process, which even contacts with the interclavicle. In multituberculates (Kielan-Jaworowska and Gambaryan, 1994; Krause and Jenkins, 1983) eutriconodonts, including *Repenomamus*, (Jenkins and Schaff, 1988; Ji *et al*., 1999; this study), symmetrodonts (Hu *et al*., 1997, 1998) and eupantotheres (Krebs, 1991), the coracoid is further reduces in size and become a large process (coracoid process) anteroventral to the scapula and has no posterior process. In these taxa, the coracoid process contributes to the glenoid fossa substantially (1/2 to 1/3 of the length of the glenoid surface). In late therians, the coracoid process is further reduced into a small hook-like process or pedicle with little or no contribution to the glenoid surface, most or all parts of the process departs anteromedially from the glenoid.

Ch 73. Articulation of the coracoid with the sternal apparatus (including interclavicle): (0) not articulating; (1) articulation.

In extant monotremes, the coracoid has a large posterior process articulating with the sternal apparatus (the interclavicle and sternal manubrium). The feature probably represents a derived condition, which is related to the fossorial habit.

Ch 74. Orientation of scapular portion of the glenoid relative to the plane of scapula: (0) facing posterolaterally and ventrally; (1) facing ventroposteriorly or

facing ventrally; (2) facing laterally (modified from Hu *et al*., 1997: Ch16; Sidor and Hopson, 1998: Ch 131).

The orientation of the glenoid is estimated by the direction of the glenoid surface relative to the plane of scapular blade. In nonmammalian cynodonts and primitive mammals, such as *Morganucodon*, *Megazostrodon*, *Sinoconodon*, the scapular portion of the glenoid surface faces posterolaterally and ventrally, and the portion on the coracoid(s) faces dorsally and posterolaterlly, the result is that the glenoid as a whole faces posterolaterally. In monotremes, the glenoid surface is further turned laterally, probably related to the abducted posture of the humerus for the fossorial habit (Jenkins and Parrington, 1976: p 418). In multituberculates, eutriconodonts, including *Repenomamus*, symmetrodonts, and eupantotheres the scapular portion of the glenoid surface is more or less perpendicular to the scapular blade and faces ventrally, and the coracoid portion of the surface often faces posteriorly; combined, the glenoid surface faces ventroposteriorly. In eutherians and metatherians, the glenoid is mostly on the bottom of the scapula and faces ventrally.

Ch 75. Contour of the scapular surface of the glenoid: (0) lateromedially convex and dorsomedially concave; (1) gently flat with the out lip convex; (2) concave

(Modified from Hu *et al*. 1997: Ch 17 and Luo *et al*., 2002: Ch 142).

Procynosuchus has the scapular surface of the glenoid lateromedially convex and dorsomedially concave, which is gently flat and only with the out lip convex in later nonmammalian cynodonts (Kemp, 1980: p232). *Morganucodon*, *Megazostrodon* and monotremes are similar to these later nonmammalian cynodonts in this aspect. The scapular surface of the glenoid is concave in other mammals, including *Repenomamus*.

Ch 76. Contour of coracoid surface of the glenoid: (0) gently convex or saddle-shaped (lateromedially convex and dorsomedially concave); (1) concave (Modified from Hu *et al*. 1997: Ch 17 and Luo *et al*., 2002: Ch 142).

In those taxa with a saddle-shaped glenoid, including nonmammalian cynodonts, *Morganucodon*, *Megazostrodon*, and monotremes, the coracoid surface of the glenoid is also saddle-shaped (lateromedially convex and dorsomedially concave). In multituberculates, eutriconodonts, including *Repenomamus*, symmetrodonts, and eupantotheres, the surface is concave.

Ch 77. Medial surface of the scapula (in anteroposterior direction): (0) slightly convex; (1) distinctly convex; (2) flat (Modified from Hu *et al*. 1997: Ch 18; Luo *et al*., 2002: Ch 143).

Procynosuchus has the medial surface of the scapula slightly convex, which probably represent the primitive condition. In other nonmammalian cynodonts, *Sinoconodon*, morganucodontids, *Haldanodon*, and multituberculates, the medial surface of the scapular blade is distinctly convex due to everting of both anterior and posterior edges. In *Repenomamus*, *Jeholodens*, *Zhangheotherium, Henkelotherium Vincelestes*, eutherians, and metatherians, the medial surface of the scapular blade is mainly flat.

Ch 78. Morphology of the clavicle: (0) medial end expanded in to a plate; (1) the medial end not expanded and the whole bone rod-like.

Clavicles of nonmammalian cynodonts are morphologically alike (Jenkins, 1971: p 109). The medial two-third of the bone forms an expanded plate with numerous striations. In mammals discussed here the clavicle is not expanded medially. The condition in tritylodontids and tritheledontids is similar to that in mammals.

Ch 79. <u>Mobility of clavicle-sternal apparatus joint: (0) immobile; (1) mobile</u> (Hu *et al*., 1997: Ch 9; Luo *et al*., 2002: Ch 131).

Slender striations on the expanded plate of the nonmammalian cynodont clavicle indicate extensive ligamentous or other connective tissue bonding the clavicle and interclavicle (Jenkins, 1971: p 109). The mobility at such a joint is probably quite limited. In tritylodontids, Morganucodontids, and particularly in monotremes, the shaft of the clavicle articulates with eh extra process of the interclavicle, suggesting the immobile clavicle-interclavicle joint in these taxa. In multituberculates, eutriconodonts, including *Repenomamus*, symmetrodonts, and late therian, the medial end of the clavicle have smooth surface contacting the similarly smooth surface of the interclavicle or sternal manubrium, suggesting a mobile joint.

HUMERUS (20 CHARACTERS)

Ch 80. <u>Humeral head: (0) elongate oval; (1) subspherical and weakly inflected dorsally; (2) nearly spherical and strongly inflected dorsally</u> (modified from Rowe, 1988: Ch 120; Hu *et al*., 1997: Ch 19; Sidor and Hopson, 1998: Ch 144; Luo *et al*., 2002: Ch 144; Horovitz and Sánchez-Villagra, 2003: Ch 55)

Repenomamus has (1) a subspherical humeral head, which is weakly inflected dorsally.

Ch 81. <u>The development of greater and lesser tubercles: (0) no actual tubercle visible; (1) distinct tubercles.</u>

In nonmammalian cynodonts the insertions of muscles on the proximal end of the humerus are not marked by actual tubercles, which are confluent with the humeral head (Jenkins, 1971: p 113; Kühne, 1956: fig. 54; Sun and Li, 1985: fig. 9 and plate 1). Jenkins

and Parrington (1976: p400) pointed out that in *Morganucodon* (their *Eozostrodon*) and *Megazostrodon* the greater tubercle is confluent with the humeral head, but their figures and photos of humeri (figs. 5, 7c-d and 8a-b) showed that there is a shallow furrow separating two structures. The greater and lesser tubercles are well developed in other mammals (including *Repenomamus*) except monotremes.

Ch 82. <u>Intertubercular groove: (0) broad; (1) narrow</u> (Modified from Rowe, 1988: Ch 121, Ch 122, Ch 123; Hu *et al*., 1997: Ch 20; Luo *et al*., 2002: 145)

Gambaryan and Kielan-Jaworowska (1997: p30) indicated that a wide intertubercular groove is present in tetrapods with the sprawling stance, providing the pathway for several muscles from the coracoid and sternum, while a narrow groove in therians, which have parasagittal stance, has only the tendon of M. biceps brachii caput longum passing along. The intertubercular groove in nonmammalian cynodonts, morganucodontids, monotremes, multituberculates, and eutriconodonts (including *Repenomamus*) is broad. The groove becomes narrow only in therians.

Ch 83. <u>Size of lesser tubercle of humerus relative to the greater tubercle: (0) wider than the greater tubercle; (1) narrower</u> (Hu *et al*., 1997: Ch 21; Luo *et al*., 2002: Ch 146).

Gambaryan and Kielan-Jaworowska (1997: p30) observed that the lesser tubercle is wider than the greater one in nonmammalian cynodonts, morganucodontids and monotremes, in which the forelimb is primarily abducted, while in mammals with parasagittal limbs the lesser tubercle is narrower and smaller than the greater tubercle. The condition in *Repenomamus* is similar to that in nonmammalian cynodonts, morganucodontids and monotremes.

Ch 84. The orientation of the greater tubercle and deltopectoral crest: (0) extending lateroventrally from the humeral head and shaft; (1) reflected anteromedially from the anterolateral corner of the humeral head and shaft.

In *Repenomamus* the deltopectoral crest of the humerus is reflected anteromedially (1).

Ch 85. Distal extension of the deltopectoral crest on the humeral shaft: (0) reaching the midpoint of the humeral shaft or beyond; (1) not reaching the midpoint of the humeral shaft (Modified from Hu *et al*., 1997: Ch 23; Sidor and Hopson, 1998: Ch 146; Luo *et al*., 2002: Ch 1148; Horovitz and Sánchez-Villagra, 2003: Ch 50).

In *Repenomamus* the deltopectoral crest of the humerus extends beyond the midpoint of the shaft (0)

Ch 86. Width of the deltopectoral crest: (0) broad, about one third width of the proximal shaft of the humerus or broader; (1) narrow, much less than one third width of the proximal humeral shaft.

Repenomamus has a broad deltopectoral crest on humerus (0).

Ch 87. The dorsal flexure of the proximal half of the humeral shaft: (0) distinct; (1) indistinct (See Jenkins, 1971: p113).

Jenkins (1971: p 113) indicated that in nonmammalian cynodonts the proximal half of the humeral shaft is flexed dorsally. The condition is obvious in *Procynosuchus*, *Chiniquodon* and *Thrinaxodon*, and less so in Tritheledontids and tritylodontids. In most mammals the dorsal flexure of humerus is not distinct. the exception is extant monotremes, which have distinctly dorsal flexed humerus.

Ch 88. <u>The tuberosity distal to the lesser tubercle, on the medial aspect of the humeral shaft, for the teres major muscle: (0) prominent; (1) weak or absent.</u>

Jenkins and Parrington (1976: p 400) indicated that in nonmammalian cynodonts and primitive mammals a prominent tuberosity is present on the medial side of the humeral shaft, opposite to the deltopectoral crest, which probably represents the attachment site of the teres major muscle. The tuberosity is present in tritylodontids, morganucodontids, monotremes, *Haldanodon*, multituberculates, *Gobiconodon*, and *Repenomamus*. In therians discussed here, the tuberosity is weak.

Ch 89. <u>Torsion between the proximal and distal ends of humerus: (0) strong (>= 30°); (1) moderate 15°-30°); (2) weak (< 15°)</u>. (Hu *et al*., 1997: Ch 22; Luo *et al*., 2002: Ch 147).

The humeri of nonmammalian cynodonts, morganucodontids, and monotremes are distinctly twisted. Symmetrodonts and eupantotheres have less twisted humeri. The presence vs. absence of the humeral torsion was regarded as important indicator of sprawling vs. parasagittal stance in fossil mammals (Simpson, 1928; Kielan-Jaworowska and Gambaryan (1994); Sereno and McKenna, 1995), but Gambaryan and Kielan-Jaworowska (1997: p 28) indicated that humeral torsion may or may not be present in fossorial placentals, which presumably secondarily acquire sprawling stance. In eutriconodonts, *Gobiconodon* and *Jeholodens* have the humerus strongly twisted, but that of *Repenomamus* is moderately twisted.

Ch 90. <u>Relative breadth of the distal humerus: (0) broad; (1) moderate; (2) slender; (3) extremely broad.</u>

The relative breadth of the distal humerus here is measured by the ratio of distal width (maximal width between the epicondyles) of the humerus with the length of the bone. In nonmammalian cynodonts, the distal width is about one-half of the length of the bone (Jenkins, 1991: p112-113), which indicates a broad humerus. In terms of distal humeral width, extant monotremes have a more robust humerus than that in nonmammalian cynodonts. The distal humeral width in monotremes is more than 80% of the length of the bone. *Haldanodon*, similar to monotremes, has a humerus with a very broad distal end. Other early mammals, including morganucodontids, multituberculates, eutriconodonts, have the ratio about 0.30, indicating a moderately broad distal humerus. Later mammals have the ratio < 0.20.

Ch 91. <u>Humero-ulnar articulation of the distal humerus: (0) condylar; (1) trochlea with vestigial condyle; (2) trochlea</u> (modified from Rowe, 1988: Ch 126; Hu *et al*., 1997: Ch 24; Sidor and Hopson, 1998: Ch 147; Luo *et al*., 2002: Ch 149; Horovitz and Sánchez-Villagra, 2003: Ch 51).

Jenkins (1973) investigated the functional anatomy and evolution of humero-ulnar articulation from pelycosaurs to mammals. The nonmammalian synapsids possessed a condylar, rather than trochlear, articulation between the humerus and ulna. This condylar humero-ulnar articulation was largely retained in early mammals and extant monotremes. The trochlea of therians evolved by the enlargement of the intercondylar groove into the trochlea and by partial retention of the ulnar condylar mechanism. Hu *et al*. (1997 and 1998) further recognized an intermediate condition in the evolution of therian trochlea presenting in eutriconodonts, symmetrodonts and eupantotheres, in which both the trochlea and vestigial ulnar condyle are present. Luo *et al*. (2002: Ch 149) indicated that

the intermediate condition was recognized by the combination of cylindrical trochlea in posterior view and vestigial condyle in anterior view at the humero-ulnar joint. This is not what Hu *et al*. (1997, 1998) originally suggested; and if this was true, it would be difficult for the ulna to rotate smoothly at the joint. As Jenkins (1971) has indicated, the trochlea evolved from the intercondylar groove, which is lateral, not posterior, to the ulnar condyle. In multituberculates the groove on the humerus is narrow (Krause and Jenkins, 1983: figs. 11, 12; Kielan-Jaworowska and Gambaryan, 1994: fig. 14B); and the ulna has a distinct ridge, which is lateral to the articular surface for ulnar condyle, for fitting into the groove (Kielan-Jaworowska and Gambaryan, 1994: fig 14C-E). In symmetrodonts (*Zhangheotherium*: Hu *et al*., 1998: p 119 and fig. 3), eutriconodonts (*Repenomamus*: this study) and therians (Jenkins, 1973: figs. 20, 23), the intercondylar groove seen on the distal humerus of multituberculates becomes a shallow and wide trochlea with smooth articular surface, the ridge present on the ulna of multituberculates disappears in these taxa and is replaced by saddle-like trochlear notch. The retention of the vestigial ulnar condyle is indicated by the facts that articular surface of the ulnar condyle on the humerus extends to its medial side and that there is bony wing on the ulna for articulating this medial portion of the condyle (for *Zhangheotherium* see structure 2 in: Hu *et al*., 1998: fig. 3).

Sidor and Hopson (1998: Ch 147) coded that *Thrinaxodon* has a notch on the distal humerus for articulating with the ulna while some other nonmammalian cynodonts (*Procynosuchus, Chiniquodon*, and Tritheledontidae) and *Morganucodon* have condylar articulation. Since the articulating portion of the distal humerus in small nonmammalian cynodonts such as *Thrinaxodon* and *Galesaurus* is not well ossified (Jenkins, 1971: 118),

the condylar structure is not well preserved, but the concave articular surface on the proximal ulna (Jenkins, 1971: fig. 32) indicates the presence of a bulbous ulnar condyle on the distal humerus.

Jenkins (1971: p118) used the term “trochlea” to describe the humero-ulnar articulation in nonmammalian cynodonts. But Jenkins (1973) changed the terminology and discussed the condylar articulation at the humero-ulnar articulation of cynodonts. He (Jenkins, 1973: p 284) also indicated that a low ridge on ulna, between articulating surfaces for ulnar and radial condyles, represents only the initial stage of mammalian trochlear notch in cynodonts, implying the absence of true trochlear articulation in nonmammalian cynodonts.

Ch 92. <u>The radial condyle (capitulum) of the humerus: (0) bulbous; (1) spindly</u>

(Modified from Luo *et al*., 2002: Ch 150 and Horovitz and Sánchez-Villagra, 2003: Ch 45).

The humerus has a capitulum (or radial condyle) to articulate the proximal surface of the radius. The capitulum is mainly located on the ventral (or anterior) aspect of the distal humerus and extends to around the distal aspect. In nonmammalian cynodonts and mammals except therian the capitulum is often bulbous or rounded. The condition is well demonstrated in *Repenomamus* (figure 3-23). In therians, the capitulum becomes more or less spindle-like.

Lou *et al*. (2002: Ch 150) further distinguished two conditions for the bulbous capitulum (their condyle) based on the morphology of the dorsal (posterior) aspect of the condyle, which implied that the humor-radial articulation extends to the dorsal aspect of the humerus. Jenkins and Parrington (1976: p 400) also proposed that the bulbous

capitulum on the humerus of morganucodontids has the articulator surface extending to the dorsal aspect of the bone. But in fact, the capitulum and its articular surface could only be present on the ventral (or anterior) and distal aspects of the humerus. If the radius articulated with the dorsal aspect of the humerus, the elbow joint would have overextended and the unlar-radial joint would have disarticulated in proximodistal direction. Moreover, the contour of the capitulum is only limited on the ventral and distal aspects of the humerus, as shown in multituberculates (Krause and Jenkins, 1983: figs. 11 and 12), morganucodontids (Jenkins and Parrington, 1976: fig. 8c) and *Repenomamus* (this study, figure 3-23). In these taxa, the dorsal aspect of the humerus adjacent to and above the capitulum has a low ridge, which is narrower than the rounded capitulum and does not match the concave articular surface on the proximal end of the radius (Krause and Jenkins, 1983: fig. 15; Jenkins and Parrington, 1976: fig. 8f). This ridge actually represents the lateral edge of a groove (extension of the intercondylar groove), which articulates with the low ridge on the ulna (Jenkins, 1973: p284; see discussion for Ch 91). The state 2 of the Ch 150 in Luo *et al*. (2002) described the condition of the capitulum present in therians, in which both anterior and posterior aspects of the capitulum are cylindrical. But in therians, the convex capitulum is only on the anterior (or ventral) and distal aspects of the humerus; the posterior (or dorsal) aspect of the distal humerus has the posterior part of the trochlea, which is concave and articulates the trochlear notch of the ulna. In conclusion, the dorsal aspect of the distal humerus only articulates with the ulna. It is improper to distinguish different morphologies of the radial articulation with the structure in this aspect of the humerus.

Ch 93. The separation vs. conjoining of ulnar and radial articulations on humerus: (0) separation; (1) conjoining.

In extant monotremes, the ulnar and radial articulations on humerus join together to form a singly ulnar-radial condyle (Gambaryan and Kielan-Jaworowska, 1997: p30; Pridmore *et al*., 2005: p 374). The evolutionary origin of this configuration is still poorly understood.

Ch 94. The ectepicondylar foramen on humerus: (0) present; (1) absent (Sidor and Hopson, 1998: Ch 143; Hopson and Kitching, 2001: Ch 90; Bonaparte *et al*., 2003: Ch 44).

The ectepicondylar foramen provides the pathway for a branch of the radial nerve. The development of the ectepicondylar foramen in synapsids is probably related to the distal migration of the origination site of supinator musculature (Romer, 1922: p 538-539 [also cited in Jenkins, 1971: p117-118]). The foramen is absent in most pelycosaurs in which the supinator tuberosity and the ectepicondyle are separated by a groove. In later nonmammalian synapsids the distal migration of the supinator tuberosity enclosed an ectepicondylar foramen. In most mammals, including *Repenomamus*, the foramen disappears, probably due to the further distal migration and/or reduction of the supinator tuberosity.

Ch 95. The entepicondylar foramen on humerus: (0) present; (1) absent (Modified from Horovitz and Sánchez-Villagra, 2003: Ch).

The entepicondylar foramen is enclosed by a bony ridge, which is the distal extension of the deltopectoral crest (Jenkins, 1971: p 118). The foramen encloses the median nerve. The development of the foramen is related to the proximal expansion of

the flexor musculature in tetrapods (Romer, 1922: p 557; also cited in Jenkins, 1971: 118). The foramen is lost in many extant therians, probably indicating the reduction of hand flexor musculature. The foramen is present in nearly all taxa discussed in this study and with distal humerus known; the exception is *Erinaceus*, in which the foramen is absent.

Ch 96. Epicondyles of the humerus (0) robust; (1) weak (Rowe, 1988: Ch 124; Hu *et al*., 1997: Ch 25; Luo *et al*., 2002: Ch151; Horovitz and Sánchez-Villagra, 2003: Ch 53)

Nonmammalian cynodonts, morganucodontids, *Haldanodon*, monotremes, multituberculates, *Gobiconodon*, *Repenomamus*, *Henkelotherium*, and *Vincelestes* have robust epicondyles on humerus. In *Jeholodens*, *Zhangheotherium*, eutherians and metatherians discussed here, the epicondyles of the humerus are weak.

Ch 97. Entepicondyle of the humerus: (0) much less than one-half width of the distal humerus; (1) about one half of the distal humerus width.

In extant monotremes, the entepicondyle is hypertrophied, extending about one-half of the distal humerus width (Gambaryan and Kielan-Jaworowska, 1997: p23). In other taxa discussed here, including *Repenomamus*, the entepicondyle has less than half width of the distal humerus.

Ch 98. Ectepicondoid crest (supinator crest): (0) well developed with proximal extremity confluent with the humeral shaft; (1) well developed with marked notch separating the crest from the shaft (2) weak or absent. (Modified from Luo *et al*., 2002: Ch 152; Horovitz and Sánchez-Villagra, 2003: Ch 48).

Repenomamus has the ectepicondoid crest well developed, which is confluent with humeral shaft proximally (0).

Ch 99. Olecranon fossa: (0)shallow fossa; (1) deep fossa; (2) perforated (Modified from Horovitz and Sánchez-Villagra, 2003: Ch 47).

Repenomamus has a relatively deep olecranon fossa, similar to that seen in morganucodontids, *Gobiconodon*, and *Zhangheotherium*. The fossa is poorly defined in *Haldanodon,* monotremes and nonmammalian cynodonts.

FOREARM (5 CHARACTERS)

Ch 100. Olecranon process of the ulna: (0) absent or unossified; (1) present or ossified (Modified from: Sidor and Hopson, 1998: Ch 149; Hopson and Kitching, 2001: Ch 91; Bonaparte *et al*., 2003: Ch 45).

The olecranon process is unossified in early nonmammalian cynodonts, such as *Procynosuchus*, *Thrinaxodon* and *Chiniquodon*. It is well ossified in tritylodontids, *Pachygenelus* and mammals.

Ch 101. The coronoid process of the ulna: (0) absent or weakly developed; (1) prominent (Modified from Horovitz and Sánchez-Villagra, 2003: Ch 59).

The coronoid process is a process on the ulna distal to the trochlear notch (Evans, 1993: p 191). The process is divided into two projections, with the medial one often more prominent than the lateral. Tow projections extend the radial notch, but also articulate with the humerus proximally. The presence of the coronoid process on the ulna increases area of its articular surfaces. In nonmammalian cynodonts, morganucodontids, *Haldanodon*, and monotremes, the process is not well developed. The process is prominent in multituberculates, eutriconodonts (including *Repenomamus*) and therians.

Ch 102. Ulnar flange: (0) high and prominent; (1) low and weak.

The ulnar flange (Jenkins and Parrington, 1976: p 402; =ulnar crest of Jenkins, 1971: p 123 and figs. 31 and 32), presumably for the attachment of the radio-ulnar interosseous ligaments is much narrower in mammals than in nonmammalian cynodonts (*Morganucodon*-- Jenkins and Parrington, 1971: p402; *Thrinaxodon*-- Jenkins, 1971: p 123; tritylodontids-- Kühne, 1956: p121)

Ch 103. Radial tuberosity for m. biceps brachii: (0) indistinct or as a swelling on a low ridge; (1) as a tuberosity distal to ulnar facet.

In *Repenomamus*, the tuberosity appears as a swelling on a low ridge extending distal from the radial head (0).

Ch 104. Styloid process of the radius: (0) weak or absent; (1) prominent (Modified from Rowe, 1988: Ch 129; Hu *et al*., 1997: Ch 26; Luo *et al*., 2002: Ch 153).

Repenomamus: (0) weak or absent.

MANUS (12 CHARACTERS)

Ch 105. The size of the scaphoid: (1) smaller than triquetrum; (1) larger than triquetrum.

Repenomamus: unknown.

Ch 106. The proximal articular surface of the scaphoid: (0) mainly on the dorsal aspect of the bone; (1) extending medially.

Repenomamus: unknown.

Ch 107. Morphology of the triquetrum: (0) roughly rectangular; (1) roughly triangular.

The name of the triquetrum implies a triangular morphology, which is true for that of most mammals with the lateral aspect of the bone joining the proximal articular

surface. A triangular shape of the bone probably facilitates the unlar deviation of the hand, as seen in extant carnivores (Yalden, 1970) and primates (Jouffroy and Medina, 2002). The triquetrum in nonmammalian cynodonts is rough rectangular with the lateral side probably separated from the proximal articular surface (Jenkins, 1971: fig 33; Kemp, 1980: p 235 and fig 11; Hopson, 1995: fig. fig. 2).

Repenomamus: unknown.

Ch 108. Distomedial process of the scaphoid: (0) absent; (1) present (Modified from Luo *et al*., 2002: Ch 154).

Repenomamus: unknown.

Ch 109. Distal carpal V: (0) present; (1) fused with carpal IV to form the hamate or absent (Modified from Sidor and Hopson, 1998: Ch 151).

Procynosuchus (Kemp, 1980: p 235 and fig. 235) and *Thrinaxodon* (Jenkins, 1971: fig 33 and p 128) have five distal carpals, one for each digit. Mammals normally have four distal carpals; presumably the carpals for digit IV and V are fused and become the hamate during ontogeny (Walker and Liem, 1994: fig. 8-29).

Repenomamus: unknown.

Ch 110. Size of the triquetrum vs. hamate: (0) triquetrum larger; (1) subequal; (2) hamate larger (Modified from Luo *et al*., 2003: Ch 192; Luo and Wible, 2005: Ch 209)

Repenomamus: unknown.

Ch 111. Size ratio between the trapezium and trapezoid: (0) trapezium larger; (1) subequal; (2) trapezoid larger (modified from Luo *et al*., 2003: Ch 193; Luo and Wible, 2005: Ch 210).

Repenomamus: (0) trapezium larger.

Ch 112. Development of centrale (Centralia) in carpus: (0) two; (1) one centrale; (2) no separated centrale present.

Repenomamus: unknown.

Ch 113. Phalanx number of manual digit III: (0) four; (1) three (Hopson and Kitching, 2001: Ch 92; Modified from Sidor and Hopson, 1998: Ch 152).

Repenomamus: unknown.

Ch 114. Phalanx number of manual digit IV: (0) four; (1) three (Hopson and Kitching, 2001: Ch 93; Modified from Sidor and Hopson, 1998: Ch 153).

Repenomamus: unknown.

Ch 115. Length ratio of the metacarpal II to metacarpal IV: (0) Mc II much shorter than Mc IV (ratio < 0.8); (1) roughly equal in length (ratio > 0.8).

In the manus of primitive amniotes the digit length increases from I to IV (Romer, 1956: p 405). Two factors contribute to this length increase, one is the number of phalanges (Ch 114), the other is that the length of the metacarpals increase from digit I to IV. During the evolution toward mammals, there is a trend toward equalization of metacarpal length (Hopson, 1995: p 633). This trend is correlated to the evolution of the limb posture from sprawling to parasagittal. *Repenomamus*, similar to most other mammals, has the Mc II and Mc IV subequal. The exception is extant monotremes, in which Mc II is shorter than Mc IV.

Ch 116. Length of the metacarpal III: (0) Mc III shorter than Mc IV; (1) longer than Mc IV or roughly equal in length.

Nonmammalian cynodonts have the Mc III shorter than Mc IV (Hopson, 1995: fig. 2), while extant therians normally have the Mc III the longest metacarpal. The condition in symmetrodonts (Hu *et al*., 1998: fig. 4) and eutriconodonts (including *Repenomamus*) is similar to that of extant therians. Increase of the length of Mc III subequal to or beyond Mc IV is probably also related to the evolutionary transition of the limb posture from sprawling to parasagittal. The elongate Mc III (relative to Mc IV) contributes to the elongation of the digit III and therefore gives the manus a more symmetrical appearance, which is better adapted for moving in a parasagittal track than the more asymmetrical manus with the digit IV the longest. In monotremes, the Mc III is shorter than Mc IV.

PELVIC GIRDLE (18 CHARACTERS)

Ch 117. Development of the posterior process of the ilium (measured by its length relative to the diameter of the acetabulum: (0) well-development (> 0.5 time of the acetabular diameter); (1) weak or absent (<= 0.5 time of the acetabular diameter) (Modified from Sidor and Hopson, 1998: Ch 156; Hopson and Kitching, 2001: Ch 95; Bonaparte *et al*., 2003: Ch 47, Luo *et al*., 2003: Ch 196; Luo and Wible, 2005: Ch 213).

Repenomamus: (1) weak or absent.

Ch 118. Relative length of the anterior process of ilium anterior to the acetabulum (relative to the diameter of the acetabulum): (0) less than 1.0; (1) 1.0-1.5; (2) greater than 1.5 (Hopson and Kitching, 2001: Ch 94).

Repenomamus: (2) greater than 1.5.

Ch 119. Orientation of the acetabular facet of the ilium: (0) facing lateroventrally; (1) facing posteriorly or posteroventrally.

Repenomamus: (1) facing posteriorly of posteroventrally.

Ch 120. Dorsal profile of the ilium: (0) strongly convex; (1) flat to concave (Hopson and Kitching, 2001: Ch 96).

Repenomamus: (1) flat to concave.

Ch 121. Longitudinal ridge on the lateral aspect of the ilium: (0) absent; (1) present.

Kemp (1983: p367) pointed out that the ilium in tritylodontids and morganucodontids has a longitudinal ridge, which divides the lateral side of the bone into dorsal and ventral components (fossae). Similar condition appears in many mammals (including *Repenomamus*), but more primitive cynodonts such as *Procynosuchus* and *Thrinaxodon* don't have the ridge. In extant therians, the dorsal fossa is called gluteal fossa, mainly for the origin of m. gluteal muscles, and the ventral one iliac fossa, for m. iliacus (Muizon, 1998: p 67)

Ch 122. Anterior extension of the pubis: (0) anterior process beyond the acetabulum; (1) ventral or posteroventral to acetabulum, no anterior process.

The primitive condition for cynodonts is that the anterior margin of the pubis projects anteriorly well beyond the acetabulum (Jenkins, 1971). In late nonmammalian cynodonts, such as tritylodontids, and mammals the pubis is posteriorly displaced to a position posteroventral to the acetabulum.

Ch 123. Total length (or anteroposterior width) of the pubis relative to acetabular diameter: (0) much greater than 1; (1) subequal or less than 1 (Modified from Sidor and Hopson, 1998: Ch 161; Hopson and Kitching, 2001: Ch 97).

Repenomamus: (1) subequal or less than 1.

Ch 124. <u>The acetabular facet of the pubis: (0) facing posterodorsally; (1) facing dorsally.</u>

Repenomamus: (1) facing dorsally.

Ch 125. <u>Development of the ischial tuberosity: (0) rounded tuberosity, thicker than the ischial blade; (1) hypertrophied protuberance projecting posterodorsally</u>

(modified from Luo *et al*., 2002: Ch 158).

In Luo *et al*. (2002) Ch 158 (ischiatic dorsal margin and tuberosity) has three states: (0) dorsal margin concave (emarginated) and ischiatic tuberosity present; (1) dorsal margin concave and ischiatic tubercle hypertrophied; (2) dorsal margin straight and ischiatic tubercle small. Due to the presence of the convexity above the acetabulum and the lesser ischiatic notch on the dorsal edge of the ischium, the dorsal margin is more or less concave in most taxa. It is also hard to distinguish "ischiatic tubercle small" from "ischiatic tubercle present". In fact, the taxa Luo *et al*. coded with state 2 have no obvious difference from those with state 0. For examples, the ischiatic dorsal margin and tuberosity are similar in *Gobiconodon* (Jenkins and Schaff, 1988: figs. 16 C, D, G, and H) and *Morganucodon* (Jenkins and Parrington, 1976: figs 11 c and d); *Pucadelphys* has a concave ischiatic dorsal edge (Marshall and Sigogneau-Russell, 1995: figs. 31 and 42). Here the character is simplified with two states. Among taxa discussed here only monotremes and multituberculates have a hypertrophied ischiatic tuberosity.

Ch 126. <u>Development of the ischiatic spine: (0) absent or indistinct; (1) present</u>

(Modified from Luo *et al*., 2003: Ch 200).

The ischiatic spine is a small process present on the dorsal margin of the ischium, anterior to the lesser ischiatic notch. Luo *et al*. (2003) Ch 200--posterior spine of the

Ischium has two states: (0) elongate; (1) short and blunt. Here I define two states in a way different from that of Luo *et al*'s: if the dorsal ischiatic margin anterior to the lesser ischiatic notch is smooth, the character is coded as spine absent or indistinct; otherwise it is coded as spine present.

Repenomamus: (0) absent or indistinct.

Ch 127. Development of the iliopubic eminence: (0) small, low and rounded eminence; (1) hypertrophied broad process (Modified from Horovitz and Sánchez-Villagra, 2003: Ch 73).

The iliopubic eminence is the small tuberosity on the ventral side of the pubis at the point corresponding to the junction of the pubis and the ilium. In extant therians, the eminence marks the insertion of the tendon of psoas, a flexor muscle of the lumbar vertebrae (Muizon, 1998: p 67). By definition, the protuberance at the junction of the pubis and ilium in some nonmammalian cynodonts (Jenkins, 1971: 45 and 46) is the iliopubic eminence, but it is difficult to assess the muscle attachment in these cynodonts as their pelvic girdles are quite different from those of mammals. In monotremes, the iliopubic eminence is hypertrophied.

Repenomamus: 0) small, low and rounded eminence.

Ch 128. Fusion of the ilium, ischium and pubis in adult: (0) unfused; (1) fused (Modified from Ji *et al*., 1999: Ch 36; Luo *et al*., 2002: Ch 157; Luo *et al*., 2003: Ch 198; Luo and Wible, 2005: Ch 215)

Repenomamus: (0) unfused.

Ch 129. Epipubic bone: (0) absent; (1) present. (Horovitz and Sánchez-Villagra, 2003: Ch 76; (Luo *et al*., 2003: Ch 201; Luo and Wible, 2005: Ch 218).

The epipubic bone is present in extant monotremes and marsupials but absent in placentals. It is also developed in many fossil mammals (*Zhangheotherium*: Hu *et al*., 1997; *Henkelotherium*: Krebs, 1991: p 78 and fig. 9; multituberculates: Kielan-Jaworowska, 1979; some fossil eutherians: Novacek *et al*., 1997). The epipubic probably functions in both locomotion and reproduction; and its absence in living eutherians (placentals) suggested that evolution of placental reproduction probably evolved within eutherians (Novacek *et al*., 1997: p485). The bone could also help to stiffen the trunk between the diagonal limbs that support the body in locomotion, which probably represents the primitive condition for mammals (Reilly and White, 2003: p 400). But it is difficult to assess which function, reproduction or locomotion, is the primary one of the epipubic during evolution.

The bone has been reported present in tritylodontids (Fourie, 1962). Its presence in other nonmammalian cynodonts is unknown (Jenkins, 1971: p 163). Hopson suggested that the epipubic in tritylodontids may have been cartilaginous, that is probably why it is not found in other cynodonts (Sues, 1985: p 211). In nonmammalian cynodonts other than few advanced groups (including tritylodontids) the pubis extends anteriorly well beyond the acetabulum. Vaughn (1956: p260; cited in Jenkins, 1971: p 163 and Sues, 1985: p 211) suggested the epipubic element is the replacement or retention of this anterior portion of the primitive pelvic girdle, which happened as the pubis itself shifted posteriorly. Therefore, the epipubic element (bone or cartilage) is probably not developed in those taxa with the pubis anteriorly extending.

Repenomamus: (1) present.

Ch 130. Acetabulum position relative to auricle facet: (0) ventral; (1) posteroventral

(Modified from Sidor and Hopson, 1998: Ch 165)

Repenomamus: (1) posteroventral.

Ch 131. Acetabular dorsal emargination between ilium and ischium: (0) open; (1) closed. (Modified from Rowe, 1988: Ch 134; Hu *et al*., 1997: Ch 27; Luo *et al*., 2002: Ch 156; Luo *et al*., 2003: Ch 197; Luo and Wible, 2005: Ch 214).

Repenomamus: (0) open.

Ch 132. Development of the acetabular notch: (0) between iliac and ischial parts of the acetabulum; (1) between the acetabular surface and the pubic process of the ischium; (2) absent. (Modified from Horovitz and Sánchez-Villagra, 2003: Ch 75)

Several authors (Broili, 1908: p 3-4; Romer, 1922: p 581; Jenkins, 1971: p 160) mentioned the presence of a deep recess posterior to the supra-acetabular buttress of the ilium in early nonmammalian cynodonts. The recess is probably covered by a transverse ligament and provides pathway for nerves and vessels supplying the femoral head and joint capsule. It was regarded as the homolog of the mammalian acetabular notch, which is developed on the ischium. The notch is absent in monotremes.

Repenomamus: (1) between the acetabular surface and the pubic process of the ischium.

Ch 133. Obturator foramen position relative to the acetabulum: (0) ventral; (1) posteroventral.

Repenomamus: (1) posteroventral.

Ch 134. Size of the obturator foramen: (0) smaller than that of the acetabulum; (1)

larger than or equal to that of the acetabulum (Rowe, 1988: Ch 139; Hu *et al*., 1997: Ch 28; modified in Horovitz and Sánchez-Villagra, 2003: Ch 72).

Repenomamus: (1) larger than or equal to that of the acetabulum.

FEMUR (14 CHARACTERS)

Ch 135. Morphology of the Femoral shaft: (0) proximal portion turns dorsomedially; (1) roughly straight.

Jenkins (1971: p 167) pointed out that the proximal portion of the femoral shaft in nonmammalian cynodonts turns dorsomedially. The condition is also seen in morganucodontids (Jenkins and Parrington, 1976: fig. 12) and eutriconodonts (*Gobiconodon*: Jenkins and Schaff, 1988: fig. 17; *Jeholodens*: Ji *et al*., 1999; *Repenomamus*: this study). On the other hand, multituberculates, symmetrodonts, eupantotheres and most therians have nearly straight femora.

Ch 136. Femoral head: (0) oval; (1) nearly spherical. (Modified from Sidor and Hopson, 1998: Ch 168)

An oval femoral head is seen in nonmammalian cynodonts (Jenkins, 1971: p 167; Kemp, 1980: fig. 14), but those in tritylodontids have a spherical head, a condition common in mammals (Kühne, 1956: fig. 58; Sun and Li, 1985: p 147 and fig. 11).

Repenomamus: (1) nearly spherical.

Ch 137. Development of the neck below the femoral head: (0) absent, no constriction below the head; (1) incipient neck indicated by faint constriction; (2) well defined neck, well constricted (Modified from Rowe, 1988: Ch 141, 142; Hu *et al*., 1997: Ch 29; Sidor and Hopson, 1998: Ch 172; Hopson and Kitching, 2001: Ch 98; Luo *et al*., 2002: Ch 159; Bonaparte *et al*., 2003: Ch 49).

Kühne (1956: p 125) pointed out that in *Oligokyphus* the presence of a faint constriction on the medial side (his anterior side) below the femoral head marks an incipient neck. In fact, the constriction is also visible on the dorsal and ventral sides. Similar condition is seen in *Bienotheroides* (Sun and Li, 1985: fig. 11), morganucodontids (Jenkins and Parrington, 1976: p 408 and Figs. 12, 13b, c, and e) and eutriconodonts (*Gobiconodon*: Jenkins and Schaff, 1988: fig. 17; *Repenomamus*: this study). A well-defined neck is the distinct constriction below the head; the head offsets medially from the femoral shaft for a distance and normally at an acute angle, and the neck separates and also connects the head and the shaft. Such a neck has been seen in multituberculates (Krause and Jenkins, 1983: figs. 20, 21; Kielan-Jaworowska and Gambaryan, 1994: figs. 16A-C), symmetrodonts (*Zhangheotherium*: personal observation), eupantotheres (*Henkelotherium*: Krebs, 1991: figs. 10, 11), eutherians and metatherians. Most nonmammalian cynodonts don't have a neck separating the femoral head from the shaft (Jenkins, 1971; Kemp, 1980).

Luo *et al*. (2002) Ch 159 and other previous studies (Rowe, 1988; Hu *et al*., 1997) did not distinguish incipient neck from absence of the neck. Lou *et al*. coded *Probainognathus*, tritylodontids, tritheledontids, *Sinoconodon*, *Morganucodon*, *Megazostrodon*, *Haldanodon*, *Ornithorhynchus*, *Jeholodens* and *Gobiconodon* with neck absent. The condition in *Chiniquodon* (Romer and Lewis, 1973: p 25 and figs. 16, 17) is similar to that in *Thrinaxodon* and *Procynosuchus*, and quite different from those in taxa with the incipient neck as discussed above.

Ch 138. <u>Separation between the greater trochanter and the femoral head: (0) greater trochanter and head confluent; (1) a distinct notch separating two</u>

structures (Sidor and Hopson, 1998: Ch 172; Hopson and Kitching, 2001: Ch 98; Bonaparte *et al*., 2003: Ch 49).

Repenomamus: (1) a distinct notch separating two structures.

Ch 139. Ridge connecting the greater trochanter and the femoral head: (0) present; (1) absent (Hopson and Kitching, 2001: Ch 99).

Hopson and Kitching (2001) coded tritylodontids and *Morganucodon* without the ridge, but Jenkins and Parrington (1976: p 407) mentioned "a ridge between the head and greater trochanter" in *Morganucodon*. The condition in tritylodontids (Kühne, 1956: fig. 58; Sun and Li, 1985: fig. 11) is similar to that of *Morganucodon*. In fact, a ridge connecting the greater trochanter and the femoral head is also present in most mammal taxa, with the trochanter fossa behind (or below) the ridge. Only in multituberculates the connecting ridge is absent (Krause and Jenkins, 1983: figs. 20, 21; Kielan-Jaworowska and Gambaryan, 1994: figs. 16A-C).

Repenomamus: (0) present.

Ch 140. Orientation of the greater trochanter: (0) directed proximolaterally; (1) directly proximally (Modified from Rowe, 1988: Ch 143; Hu *et al*., Ch 30; Luo *et al*., 2002: Ch 161).

The orientation of the greater trochanter is coded based on the direction of the tip (or the most convex portion) of the trochanter.

Repenomamus: (0) directed proximolaterally.

Ch 141. Dorsal reflection of the greater trochanter: (0) present; (1) absent.

Jenkins (1971: p 167 and figs. 48 and 49)) observed the greater trochanter in *Thrinaxodon* and ?*Diademodon* is reflected dorsally. A similar but less distinct condition

is seen in tritylodontids (Kühne, 1956: fig. 58 A, D) and morganucodontids (Jenkins and Parrington, 1976: 408). The dorsal reflection of the greater trochanter is not obvious in most late mammals with the structure known.

Repenomamus: (1) absent.

Ch 142. Development of trochanteric fossa: (0) large, shallow and rounded fossa; (1) small, deep and irregular fossa.

In nonmammalian cynodonts (Jenkins, 1971: p 170 and figs. 48, 49, intertrochanteric fossa; Kemp, 1980: fig. 11d; Kühne, 1956: fig. 58B; Sun and Li 1985: fig. 11B), morganucodontids (Jenkins and Parrington, 1976: p 408 and figs. 12b and 13c), docodonts (Krusat, 1991: fig. 1), and eutriconodonts (*Gobiconodon*: Jenkins and Schaff, 1988: fig. 17D; *Repenomamus*: this study), a large roughly rounded and shallow fossa is present between the femoral head and the greater trochanter. In multituberculates and therians the fossa is small, deep and irregular in shape.

Ch 143. Position of the lesser trochanter: (0) on the ventral surface of the femoral shaft; (1) on the ventromedial aspect of the femoral shaft; (2) on the medial aspect of the femoral shaft. (Modified from Rowe, 1988: Ch 144; Hu *et al*., 1997 Ch 31; Sidor and Hopson, 1998: Ch 174; Hopson and Kitching, 2001: Ch 100; Luo *et al*., 2002: Ch 162; Bonaparte *et al*., 2003: Ch 50).

Luo *et al*. (2002) Ch 162 did not distinguish "the lesser trochanter on the ventral surface" from "on the ventromedial surface". Sidor and Hopson (1998: Ch 174) coded that *Procynosuchus* and *Thrinaxodon* have the internal trochanter (= the lesser trochanter, See Jenkins [1971: p178-186] for the discussion on the homology of the mammalian lesser trochanter with the synapsids internal trochanter) on the ventral surface of the

femur, but Hopson and Kitching (2001: Ch 100) coded the same taxa having the lesser trochanter on the ventromedial surface of the femur. But positions of the lesser trochanter in two taxa are different. In *Thrinaxodon* the lesser trochanter is on the ventromedial aspect (Jenkins' anteroventral aspect) of the femur (Jenkins, 1971: p 170 and fig. 49), while in *Procynosuchus* the trochanter arises on the ventral surface of the femur (Kemp, 1980: p 245 and fig. 14). All previous authors coded tritylodontids and morganucodontids having the lesser trochanter on the medial surface of the femur, but well-preserved femur of tritylodontids (IVPP specimen, uncatalogued) shows that the lesser trochanter is indeed on the ventromedial surface of the femur, similar to that seen in other nonmammalian cynodonts (Jenkins, 1971) except *Procynosuchus*. Morganucodontids probably have the same condition as tritylodontids (Jenkins and Parrington, 1976: p408 and figs. 12, 13b, c). A medially positioned lesser trochanter is only observed in monotremes. *Repenomamus* and *Gobiconodon* have the lesser trochanter on the ventromedial aspect of the femoral shaft.

Ch 144. Size and shaper of the less trochanter: (0) elongate bony wing extending more than 1/3 of the femoral length; (1) triangular bony wing about 1/4 to 1/5 of the femoral length; (2) triangular bony wing less than 1/6 of the femoral length; (3) nearly rounded eminence. (Modified from Rowe, 1988: Ch 144; Hu *et al*., 1997 Ch 32; Luo *et al*., 2002: Ch 163).

Luo *et al*. (2002) and other previous studies only distinguished small vs. large size of the lesser trochanter.

Repenomamus: (1) triangular bony wing about 1/4 to 1/5 of the femoral length.

Ch 145. Shape of femur at cross section: (0) rounded or rectangular; (1) dorsoventrally compressed.

Monotremes have the femur dorsoventrally compressed.

Repenomamus: (0) rounded or rectangular.

Ch 146. Patellar facet the femur: (0) flat, no groove; (1) shallow groove; (2) deep groove with lateral and medial ridges. (Modified from Rowe, 1988: Ch 145; Hu *et al*., 1997: Ch 33; Luo *et al*., 2002: Ch 164)

Repenomamus: (1)shallow groove.

Ch 147. Patella: (0) absent; (1) present.

Repenomamus: (0) absent.

Ch 148. Development of intercondylar fossa of the femur: (0) indistinct; (1) distinct.

Kühne (1956: p 125) pointed out that in *Oligokyphus* the condyles of the femur are not separated by a notch and the popliteal fossa is shallow. Jenkins (1971: p172) did not mentioned the intercondylar fossa in his description of distal femur of South African nonmammalian cynodonts. Judged by his drawings the intercondylar fossa is indistinct in *Thrinaxodon* (Jenkins, 1971: fig. 49B). Kemp (1980: p 245 and fig. 14f) found that *Procynosuchus* has a deep fossa for flexor muscle on the ventral surface of the distal femur, and the fossa extends distally as a deep intercondylar fossa and separates the lateral and medial condyles. Mammals normally have a well-defined intercondylar fossa separating the lateral and medial condyles.

Repenomamus: (1) distinct intercondylar fossa.

LOWER HINDLIMB (8 CHARACTERS)

Ch 149. Dimension of the tibia at the cross section: (0) anteroposterior flattening; (1) not flattening anteroposteriorly.

In most nonmammalian cynodonts the tibia is flattened anteroposteriorly (Jenkins, 1971, p 186; Kemp, 1980: fig. 15). In tritylodontids (Kühne, 1956: fig. 59; Young, 1947: p 587-588) and mammals (Jenkins and Parrington, 1976: fig. 15; Kielan-Jaworowska and Gambaryan, 1994: fig. 6C, 17F-I) the tibia is anteroposteriorly deeper than mediolaterally wide. The curvature of the tibia shaft is also different in two types of tibia. It is unclear whether such differences are related to difference in the posture or gait.

Repenomamus: (1) not flattening anteroposteriorly.

Ch 150. Lateral margin of the tibia: (0) markedly concave along the whole length; (1) concave at the proximal 1/3 of the shaft; (2) concave near the proximal end.

The shaft of a nonmammalian cynodont tibia (except that of tritylodontids) is slightly bowed medially but lateral margin of the bone is markedly concave due to the expansion of both end of the bone (Jenkins, 1971: p 186; Kemp, 1980: fig. 245). In tritylodontids (Kühne, 1956: fig. 59) only the proximal portion (about 1/3) of the shaft is concave on lateral side. In mammals (Jenkins and Parrington, 1976: fig. 15; Kielan-Jaworowska and Gambaryan, 1994: fig. 6C, 17F-I) only a small portion of the shaft at the nearly proximal end (less than 1/5 length of the tibia) is concave due to the expansion of the proximal end.

Repenomamus: (2) concave near the proximal end.

Ch 151. Proximolateral process of the tibia: (0) distinct laterally projecting process; (1) indistinct; (2) hook-like process. (Modified from Luo *et al*., 2002: Ch 165).

The process on the proximolateral corner of the tibia is most likely for articulating with the proximal end of the fibula. Luo *et al*. (2002: Ch 165) coded tritylodontids, *Morganucodon*, *Megazostrodon*, *Haldanodon*, *Gobiconodon*, *Jeholodens*, *Ornithorhynchus* and cimolodontans with the proximolateral tubercle or tuberosity of the tibia large and hook-like. In fact, only multituberculates has the process hook-like (Krause and Jenkins, 1983: fig. 23; Kielan-Jaworowska and Gambaryan, 1994: p 28 and figs. 6F-I). In all other taxa, the process is simply laterally projecting, as Jenkins and Parrington (1976: p 140) described for *Morganucodon*.

Repenomamus: (0) distinct laterally projecting process.

Ch 152. The tibial tuberosity and cnemial crest: (0) indistinct; (1) distinct.

The tibial tuberosity is for the insertion of patellar ligament. Distally, the tuberosity is normally continued as a cnemial crest. The tuberosity and crest are well-developed in mammals and tritylodontids, but more primitive cynodonts don't have a distinct tibial tuberosity and cnemial crest, and the anterior surface of the proximal tibia is gently flat (Jenkins, 1971: p 186).

Repenomamus: (1) distinct.

Ch 153. Articulation between femur and fibula: (0) present; (1) absent. (Modified from Luo *et al*., 2002: Ch 167; Horovitz and Sánchez-Villagra, 2003: Ch 84)

Repenomamus: unknown.

Ch 154. Proximal head of the fibula: (0) not extending beyond the knee joint; (1) well beyond the knee joint. (Modified from Horovitz and Sánchez-Villagra, 2003: Ch 85).

Jenkins (1971: p 189) pointed out that in nonmammalian cynodont the flange at the proximal head of the fibula may participate in the femoro-tibial joint and serve as the musculotendinous process. It is presumably homologous with the expanded fibular head in monotremes, which extends well beyond the knee joint. In most mammals, the flange, if present, does not extend beyond the knee joint.

Repenomamus: (0) not extending beyond the knee joint.

Ch 155. Tibial medial malleolus (0) indistinct; (1) distinct (Modified from Hu *et al*., 1997: Ch 34; Luo *et al*., 2002: Ch 166; Horovitz and Sánchez-Villagra, 2003: Ch 88).

Repenomamus: (0) indistinct.

Ch 156. Fibular external malleolus (0) absent or indistinct; (1) distinct (Modified from Hu *et al*., 1997: Ch 34; Luo *et al*., 2002: Ch 168).

Repenomamus: (0) indistinct.

PES (18 CHARACTERS)

Ch 157. Calcaneofibular articulation: (0) well-developed; (1) reduced or absent (Modified from Hu *et al*., 1997: Ch 35; Horovitz, 2000: Ch 4; Luo *et al*., 2002: Ch 169; Horovitz and Sánchez-Villagra, 2003: Ch 125).

The presence of the calcaneofibular articulation in mammals represents the retention of the primitive tricontact upper ankle joint condition of nonmammalian cynodonts. Szalay (1994: p 104) pointed out that primitive cynodonts, tritylodontids, morganucodontids, monotremes, multituberculates, and primitive therians have extensive calcaneofibular contact. The contact in marsupials is reduced or disappears.

Eutriconodonts, including *Repenomamus*, have well developed calcaneofibular articulation.

Ch 158. Astragalofibular facet of astragalus: (0) separated from lateral astragalotibial facet by a nonarticular groove; (1) continuous with lateral astragalotibial facet without distinct angle; (2) forming an obtuse angle with lateral astragalotibial facet; (3) forming a right angle with lateral astragalotibial facet (Modified from Horovitz, 2000: Ch 14; Horovitz and Sánchez-Villagra, 2003: Ch 99).

Szalay (1994: p114 and fig. 9.11) noticed that in *Oligokyphus*, morganucodontids and *Ornithorhynchus* the astragalofibular facet is separated from the lateral astragalotibual facet by a nonarticular groove. Previous studies (Horovitz, 2000: Ch 14; Horovitz and Sánchez-Villagra, 2003: Ch 99) did not distinguish this condition from that in most marsupials in which two facets are continuous. In *Repenomamus*, the astragalofibular facet is continuous with lateral astragalotibial facet without distinct angle.

Ch 159. Astragalotibial facet(s) of astragalus: (0) lateral and medial facets continuous; (1) a ridge separating lateral and medial facets. (Horovitz and Sánchez-Villagra, 2003: Ch 107)

Repenomamus: (0) lateral and medial facets continuous.

Ch 160. Lateral astragalotibial facet of the astragalus: (0) gently flat or slightly convex; (1) as trochlea (Luo *et al*., 2002: Ch 173; Horovitz, 2000: Ch 14).

Repenomamus: (0) gently flat or slightly convex.

Ch 161. Astragalar neck: (0) absent; (1) present (Modified from Ji *et al*., 1999: Ch 46; Horovitz, 2000: Ch 12, 16; Luo *et al*., 2002: Ch 172; Horovitz and Sánchez-Villagra, 2003: Ch 100).

Repenomamus: (0) absent.

Ch 162. Astragalar head: (0) absent; (1) present as the narrowed distal extremity; (2) present as expanded distal extremity (Modified from Horovitz, 2000: Ch 13).

(Discussion for Ch 161 and 162) Szalay (1994: p 130) defined the astragalar neck as the narrowed distal portion of the astragalus, which is present in tritylodontids and morganucodontids, as well as in therians. He (Szalay, 1994: p 130) also defined the astragalar head as the convex distal articulation of the astragalus, which is only developed in therians. In this study the astragalar neck is defined as the constricted part of the astragalus between the head and the body, and the astragalar head is defined as the distal extremity of the bone which can be distinguished from the posterior part of the bone, either narrowed or expanded. With such definition, multituberculates have neither head nor neck; *Repenomamus* has the head but no neck.

Ch 163. Astragalonavicular facet extension on medial side of the bone: (0) absent; (1) present (Modified from Horovitz and Sánchez-Villagra, 2003: Ch 95).

The medial extension of the astragalonavicular facet on the medial side of the astragalus reflects the loading of habitual inversion on the astragalus. The condition is present in some eutherians and metatherians.

Repenomamus: (0) absent.

Ch 164. Astragalonavicular facet extension on the ventromedial area of the bone: (0) absent; (1) present. (Modified from Horovitz and Sánchez-Villagra, 2003: Ch 96)

Repenomamus: (0) absent.

Ch 165. <u>Superposition (overlapping) of the astragalus over the calcaneus: (0) slight overlapping; (1) partially superposition; (2) well-developed; (3) absent.</u>

(Modified from Hu *et al*., 1997 Ch 36; Luo *et al*., 2002: Ch 170).

In extant therian mammals the astragalus overlaps the calcaneus, which allows two bone act as a unit in a parasagittal plane and the forces is transmitted to distal part of the foot mainly through the tabioastragalar joint and calcanoastragalar complex (Horovitz, 2000: p 547). The condition seen in extant therians is the end of the long transformation initiated in early cynodonts, in which the astragalus just slightly overlaps the calcaneus, two bones lies mostly side by side and both directly transmit weight to the substrate. The arrangement in nonmammalian cynodonts maintains the stability of the leg through double column of bones but not efficient in transmitting forces exerted on the calcaneal tuber to the front of the foot (Schaeffer, 1941). Similar, but not identical, slight overlapping condition is observed in morganucodontids. In eutriconodonts (*Repenomamus*: this study), multituberculates, symmetrodonts, and *Vincelestes*, the astragalus is partially overlaps the calcaneus. The fully overlapping condition probably develops within therians (Szalay, 1993: p 123-124; Szalay, 1994: p129-130; Horovitz, 2000: p 553-554). In monotremes, the astragalus does not overlap the calcaneus at all and the lower ankle joint is sagittally oriented (Szalay, 1993: p 120 and figs. 9.6, 9.7 and 9.11), which probably represents a specialization evolved within the clade.

Ch 166. <u>Development of the sustentaculum tail of the calcaneus: (0) blunt protuberance; (0) acute process; (2) absent.</u> (Modified from Horovitz and Sánchez-Villagra, 2003: Ch 111)

The sustentaculum tail bears a calcaneal sustentacular facet for articulating with the counterpart on astragalus. In nonmammalian cynodonts, morganucodontids, and multituberculates the sustentaculum tail is a blunt protuberance, which is different from relatively acute process seen in eutriconodonts (including *Repenomamus*), symmetrodonts, *Vincelestes*, and therians. Monotremes lack the sustentaculum tail and the sustentacular facet is on the body of the calcaneus. Szalay (1993: p122; 1994: p125) claimed that multituberculates, as monotremes, don't have the sustentaculum tail (his sustentacular shelf). Here I follow Krause and Jenkins (1983: p 239) and Kielan-Jaworowska and Gambaryan (1994: p14) in recognizing in multituberculates the protuberance bearing the sustentacular facet as the sustentaculum tail.

Ch 167. <u>Orientation of the sustentacular facet of the calcaneus: (0) nearly vertical (medial or anteromedial); (0) oblique (dorsomedial); (2) nearly dorsal.</u>

(Modified from Horovitz, 2000: Ch 1; Luo *et al*., 2002: Ch 171; Horovitz and Sánchez-Villagra, 2003: Ch 118).

In nonmammalian cynodonts, morganucodontids, monotremes, multituberculates, and eutriconodonts (including *Repenomamus*), the sustentacular facet faces medially or anteromedially (Szalay, 1993: figs. 9.3-9.8; this study). In *Vincelestes* and some primitive metatherians the facet is oblique, and a nearly dorsal facing facet is seen in marsupials and eutherians (Horovitz, 2000: p 533). Horovitz (2000: Ch 1) didn't distinguish an intermediate state (oblique) for the orientation of the sustentaculum fac*et al*though she (p 533) noticed that in *Vincelestes* a small posterior portion of the facet is nearly dorsally oriented while the anteriormost region of facet is oblique (having a 67º angle with the horizontal plane), and the condition in some primitive metatherians (*Deltatherium*,

Pucadelphys, and *Mayulestes*) is similar to that in *Vincelestes*. She coded all these taxa, as *Oligokyphus,* morganucodontids, *Jeholodens, Ornithorhynchus,* and multituberculates, having medially oriented sustentacular facet. On the other hand, Luo *et al*. (2002: Ch 171) did not distinguish the oblique condition from the "nearly dorsal facing" condition and coded *Vincelestes*, *Pucadelphys*, and *Deltatheridium*, as *Didelphis*, *Erinaceus*, and *Asioryctes,* having dorsally oriented sustentacular facet.

Ch 168. Calcaneal tuber (0) with tip ventromedially pointed; (1) with a terminal swelling dorsally pointed (Modified from Rowe, 1988: Ch 151; Hu *et al*., 1997: Ch 37; Sidor and Hopson, 1998: Ch 175; Horovitz, 2000: Ch 3; Luo *et al*., 2002: Ch 174)

Repenomamus: (0) with tip ventromedially pointed.

Ch 169. Calcaneus body cross-section at level of calcaneoastragalar facet: (0) dorsoventrally depressed; (1) mediolaterally compressed (Horovitz, 2000: Ch 2).

Repenomamus: (0) dorsoventrally depressed.

Ch 170. Peroneal process of the calcaneus: (0) as broad and laterally directed shelf; (1) as anteriorly positioned process with shallow or no groove at the base; (2) as anteriorly positioned process with deep groove at the base. (Modified from Hu *et al*. 1997: Ch 38; Horovitz, 2000: Ch 10; Luo *et al*., 2002: Ch 175; Horovitz and Sánchez-Villagra, 2003: Ch 115 and 116).

Repenomamus: (0) as broad and laterally directed shelf.

Ch 171. <u>Calcaneocuboid facet of the calcaneus: (0) facing distoventrally and medially; (1) facing distomedially; (2) facing distally.</u> (Modified from Horovitz, 2000: Ch 8; Luo *et al*., 2002: Ch 176).

Repenomamus: (0) facing distoventrally and medially.

Ch 172. <u>Approximation between the Metatarsal V and the peroneal process of the calcaneus: (0) absent; (1) present.</u>

In extant monotremes the peroneal process of the calcaneus approaches the Metatarsal V (Szalay, 1993: p 117 and fig. 9.2), a condition not seen in other mammals and nonmammalian cynodonts. Kielan-Jaworowska and Gambaryan (1994: p74 and figure 54) reconstructed the pes of a multituberculates, K*ryptobaatar dashzevegi,* with the Mt V articulating with the calcaneus. Luo *et al*. (2002: Ch 178) followed Kielan-Jaworowska and Gambaryan's reconstruction and coded that cimolodontan multituberculates, similar to *Ornithorhynchus*, has the Mt V offsetting from the cuboid and contacting the calcaneus. The specimen Kielan-Jaworowska and Gambaryan based on is the right pes of *Kryptobaatar dashzevegi* (ZPAL MgM-I/41, Kielan-Jaworowska and Gambaryan, 1994: Figs. 6A-C and 7A-G), in which, as preserved, the peroneal process of the calcaneus approaches the Mt V. But that specimen probably suffers postmortem deformation and the calcaneus is in a plane nearly perpendicular with metatarsals. If restored, the calcaneus does not contact the Mt V, and the latter only articulates with the cuboid, a condition had been shown in previous studies on multituberculates pes (Granger and Simpson, 1929: fig. 23; Krause and Jenkins, 1983: figs, 24 and 30; Szalay, 1993: fig. 9.10). A recently found specimen of eobaatarid

multituberculate from Jehol Biota (Hu and Wang, 2002) also showed the similar condition.

Repenomamus: (0) metatarsal V not approaching peroneal process of calcaneus.

Ch 173. <u>Orientation of calcaneus relative to the long axis of the foot: (0) nearly aligned; (1) calcaneus transversely oriented</u> (Modified from Luo *et al*., 2002: Ch 179).

Luo *et al*.'s original character dealt with the angle of Mt III to the calcaneus. Assuming Mt III roughly representing the axis of the pes, the character indeed discussed the orientation of the calcaneus relative to the axis of the pes. They coded *Ornithorhynchus*, *Jeholodens* and cimolodontans having the metatarsal III oriented oblique to an imaginary line through the long axis of the calcaneus in contrast to the aligned condition in *Megazostrodon*, *Vincelestes*, *Didelphis*, *Pucadelphys*, *Erinaceus*, and *Asioryctes*. But the condition in *Jeholodens* and cimolodontans is much closer to aligned condition than to that of *Ornithorhynchus*, in which the calcaneus, with the calcaneal tuber laterally positioned, is actually transversely oriented. This condition is only seen in monotremes and probably represents the specialization evolved within the group. Kielan-Jaworowska and Gambaryan (1994: p 7 and figs. 54 and 57) first reconstructed the pes of multituberculates with the Mt III abducted about 30° with respect to the calcaneal tuber. They cited Krause and Jenkins (1983) to suggest that the longitudinal axis of the foot (through third digit) deviate 30-40° from the sagittal plane. But this does not necessarily mean that these authors (Krause and Jenkins) believed that the Mt III should be abducted relative to the calcaneus. In fact, Krause and Jenkins (1983: p 236) also proposed that the femur of the multituberculates lay at about 45° to the sagittal plane, and their

reconstruction showed that the calcaneus is aligned with Mt III (Krause and Jenkins, 1983: figs. 24 and 30), a conclusion also reached by Granger and Simpson, (1929: fig. 23) and Szalay (1993: fig. 9.10). Kielan-Jaworowska and Gambaryan's suggestion is related to their believing in the contact between the calcaneus and Mt V, which, as discussed above, is probably not the case. In *Repenomamus*, the calcaneus is nearly aligned with the axis of the foot in dorsal view.

Ch 174. Phalangeal number of pedal digital IV: (0) four; (1) three (modified from Sidor and Hopson, 1998: Ch 179).

Repenomamus: (1) three.

OTHER POSTCRANIAL FEATURES (2 CHARACTERS)

Ch 175. Sesamoid bones in flexor tendons: (0) absent; (1) present, single; (2) present, paired (modified from Rowe, 1988: Ch 158; Hu *et al*., 1997: Ch 39; Luo *et al*., 20002: Ch 180).

Repenomamus: (1) present, single.

Ch 176. External pedal (tarsal) spur: (0) absent; (1) present (Hu *et al*., 1997 Ch 40; Luo *et al*., 2002: Ch 181).

Repenomamus: (0) absent.

4.2 PHYLOGENETIC ANALYSIS

The past 26 years (since the publication of Lillegraven *et al*., 1979) has witnessed a great increase in the knowledge of Mesozoic mammals. Among nearly 300 genera of Mesozoic mammals, more than three fifths were described in the past 26 years (Kielan-Jaworowska *et al*. [2004] summarized information of Mesozoic mammals prior to 2003

and listed references prior to 2005; for the latest information, see: Averianov and Archibald, 2005; Averianov *et al*., 2005; Butler and Hooker, 2005; Datta, 2005; Hu *et al*., 2005a, b; Kemp, 2005; Li *et al*., 2005; Li and Luo 2006; Lopatin *et al*., 2005; Luo and Ji, 2005; Luo and Wible, 2005; Martin, 2005; Martin and Rauhut, 2005; Meng *et al*., 2005; Maisch *et al*., 2005; Pfretzschner *et al*., 2005; Pridmore *et al*., 2005; Rich *et al*., 2005). Our knowledge on the diversity, morphology, distribution, and evolution of Mesozoic mammals has grown so dramatically.

Lillegraven *et al*. (1979) summarized our knowledge, including our understanding of the relationships, of Mesozoic mammals in the pre-cladistic era. McKenna (1975) published the first high-level cladogram of mammals including Mesozoic mammals, but he did not include a dataset from which his cladogram was built. Prothero (1981) studied the interrelationship of non-tribosphenic mammals and published a cladogram of these mammals based on a dozen dental and lower jaw characters. Rowe (1988, published version of Rowe [1986], Ph. Dissertation) is the first cladistic study of Mesozoic mammal phylogeny with substantial morphological data. Since then, there are at least nineteen studies that performed phylogenetic analyses of Mesozoic mammals with substantial morphological characters (Wible, 1991; Wible and Hopson, 1993; Rougier, 1993; Wible *et al*., 1995; Rougier *et al*, 1996a, b; Hu *et al*., 1997; Ji *et al*., 1999, 2002; Lou *et al*., 2001a and b, 2002, 2003; Wang Y.-q. *et al*., 2001; Rauhut *et al*., 2002; Woodburne, 2003; Woodburne *et al*, 2003; Luo and Wible, 2005; Li and Luo, 2006). With extensive sampling of taxa and characters, these studies have greatly deepened our understanding of the phylogenetic relationships of Mesozoic mammals.

The present study incorporates much of the information from previous

phylogenetic studies. The dataset employed in this study is composed of 435 osteological characters (176 postcranial, 151 cranial and 108 dental characters) and 57 taxa. The postcranial characters are analyzed in the previous section and all characters are listed in appendix I. The appendix II is the data matrix employed in the phylogenetic analysis. All characters are unordered.

The phylogenetic analysis of the 57X435 data matrix using PAUP V 4.0b10 for Macintosh™ (Swofford, 2002) generates 48 equally most parsimonious trees (all character are unordered; tree length= 1336 steps; Consistency index = 0.4648; Retention index = 0.7415). The strict consensus tree of these trees is showed below in figure 4-1.

Figure 4-1. Strict Consensus tree of 48 equally most parsimonious trees (Scores of the most parsimonious trees: length = 1336 steps; consistency index = 0. 465; retention index = 0.751. Scores of the strict consensus tree: length = 1369; consistency index = 0.454; retention index = 0. 740). Node A, Mammalia; node B, crown Mammalia; Node C, Monotremes plus allotherians; node D, monotremes; node E, allotherians; node F, eutriconodonts plus trechnotheres; node G, eutriconodonts; node H, trechnotheres; node I, symmetrodonts; node J, Gondwanan mammals with tribosphenic-like lower molariforms; node K, northern continent tribosphenic mammals. Values attached to nodes are bootstrapping values (the nodes with no number attached have bootstrapping value less than 50%).

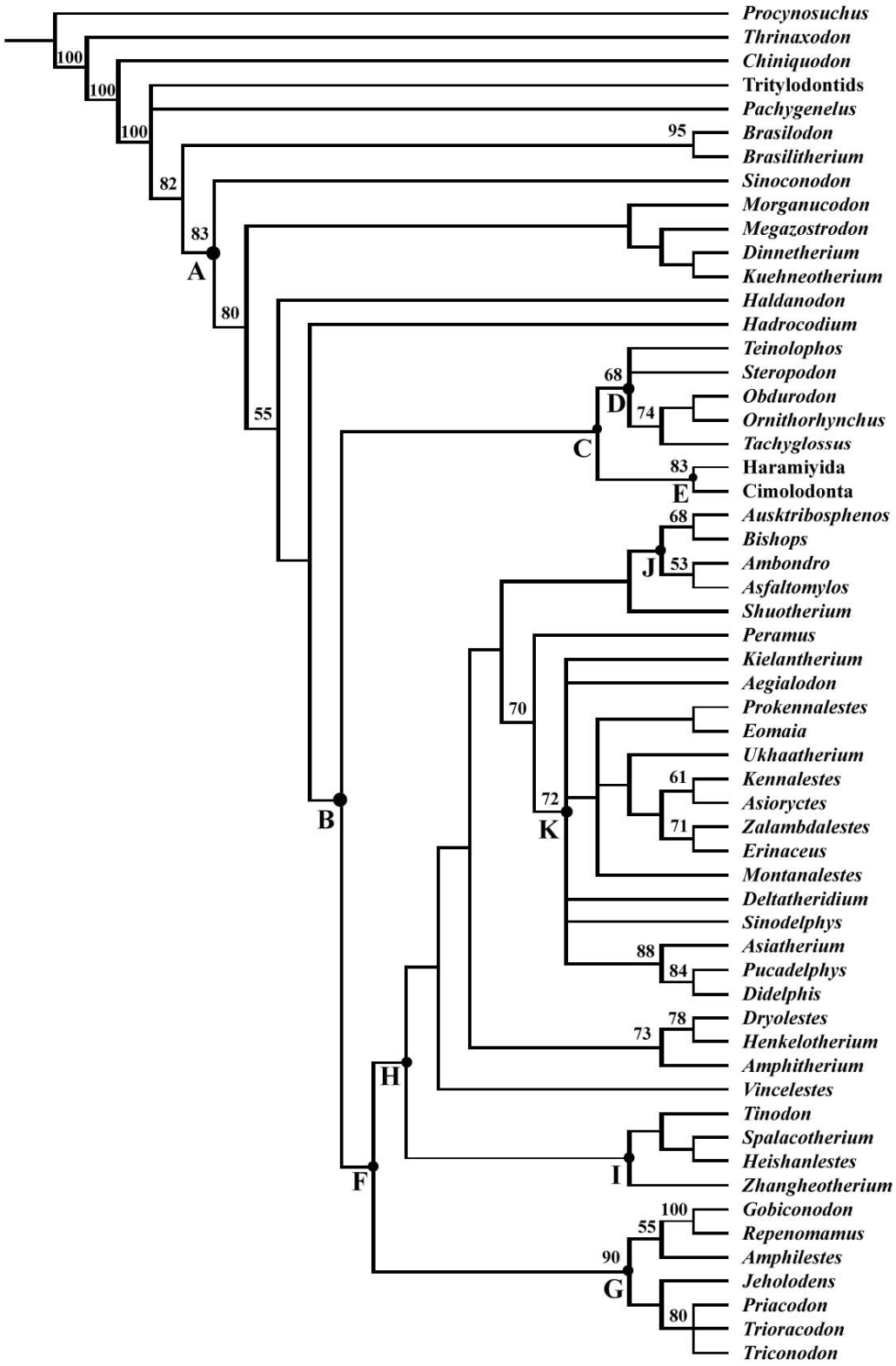
Procynosuchus
Thrinaxodon
Chiniquodon
Tritylodontids
Pachygenelus
Brasilodon
Brasilitherium
Sinoconodon
Morganucodon
Megazostrodon
Dinnetherium
Kuehneotherium
Haldanodon
Hadrocodium
Teinolophos
Steropodon
Obdurodon
Ornithorhynchus
Tachyglossus
Haramiyida
Cimolodonta
Ausktribosphenos
Bishops
Ambondro
Asfaltomylos
Shuotherium
Peramus
Kielantherium
Aegialodon
Prokennalestes
Eomaia
Ukhaatherium
Kennalestes
Asioryctes
Zalambdalestes
Erinaceus
Montanalestes
Deltatheridium
Sinodelphys
Asiatherium
Pucadelphys
Didelphis
Dryolestes
Henkelotherium
Amphitherium
Vincelestes
Tinodon
Spalacotherium
Heishanlestes
Zhangheotherium
Gobiconodon
Repenomamus
Amphilestes
Jeholodens
Priacodon
Trioracodon
Triconodon
A
B
C
D
E
F
G
H
I
J
K
100
100
100
82
83
80
55
68
74
83
68
53
70
72
61
71
88
84
78
73
100
55
90
80

Figure 4-1

The apomorphies of all internodes under ACCTRAN (accelerated transformation) are listed in appendix III. The result of this study is consistent with most previous phylogenetic analyses of Mesozoic mammals in regarding the monophyly of Mammalia, polyphyly of nontherian mammals and polyphyly of triconodonts. These conclusions were not explicitly reached in the pre-cladistic times.

(1) Mammals as a monophyletic clade of the synapsids.

Monophyly and polyphyly represent very different evolutionary scenarios. The monophyly vs. polyphyly of mammals had been debated in pre-cladistic era (Crompton and Jenkins, 1979; Miao, 1991). Simpson (1928) proposed that various groups of mammals evolved independently from cynodonts. Similar and slightly modified opinions can be found in some of his later publications (Simpson, 1929; 1959, 1960). In his viewpoint as an evolutionary taxonomist, mammalness represents an evolutionary grade and several groups of animals reached that grade during evolution (Simpson, 1959). Several later authors (Olson, 1959; Mills, 1971; Kermack *et al*., 1973) further proposed that mammals are at least diphyly and can be divided into nontherians (triconodonts, multituberculates, monotremes, and docodonts) and therians (symmetrodonts [including *Kuehneotherium*], pantotheres, eutherians, and metatherians) that evolved independently to a mammal grade from the cynodont or therapsid stocks. On the other hand, Crompton and Jenkins (1968), Hopson and Crompton (1969) and Parrington (1971) supported the close relationships of *Kuehneotherium* and morganucodontids (compared to their relationships to nonmammalian cynodonts) and the monophyly of mammals. But the issue was never settled in the pre-cladistic era. Crompton and Jenkins (1979) admitted that the evidence was insufficient to settle the question of monophyly vs. polyphyly of

mammals even though they preferred a monophyly of mammals. The monophyly vs. polyphyly debate probably roots from the methodological defect of the pre-cladistic evolutionary taxonomy, which is authority-biased and defined taxa with diagnostic features rather than based on phylogenetic tree. With the advance of phylogenetics (including cladistics) in recent decades, the relationships of mammalian groups and related cynodonts were depicted with cladograms based on morphological data. All studies (Sidor and Hopson, 1998; Hopson and Kitching, 2001; Bonaparte *et al*., 2003, 2005; Martinez *et al*., 2005; and references listed above) showed that mammals did form a monophyletic group within cynodonts and that origin of mammals most likely represents sequential events during the evolution of cynodonts.

The present study confirms that mammals (sinoconodontids, morganucodontids, docodonts; monotremes, haramiyids, multituberculates, eutriconodonts, and trechnotheres) form a monophyletic clade that is characterized with 21 unequivocal synapomorphies (185[0], 202[1], 211[2], 221[1], 235[2], 237[1], 240[1], 241[1], 242 [1], 246[1], 247[1], 261[1], 265[1], 268[1], 284[1], 286[1], 328[1], 333[0], 346[1], 347[2], and 391[1]). The cluster of all mammals with substantial osteological support is the basis for defining the taxon Mammalia (figure 4-1: node A).

(2) Paraphyly of non-therian mammals.

The taxonomic division of mammals into non-therian and therian lineages prevailed in 1960s and 1970s. Kermack (1967) established the division between non-therian and therian mammals based on the differences in their braincase structures. He proposed that triconodonts, docodonts, multituberculates, and monotremes together form a lineage of mammals and "have had a common ancestor at the reptilian level of

evolution" while therians represent a completely separate lineage. Kermack and Kielan-Jaworowska (1971) further discussed the interrelationships of non-therians based on the braincase structures and maintained division between non-therians and therians. Crompton and Jenkins (1979) provided the latest review of non-therian-therian division of mammals of pre-cladistic era. Although they proposed that differences in braincase structures of non-therians and therians did not necessarily indicate their separate originations from cynodonts, they clearly supported that non-therians (their Prototheria) and therians (Theria) represent two lineages of mammals (Crompton and Jenkins, 1979: fig 3-1).

The phylogenetic studies of Mesozoic mammals in the past two decades dismissed non-therians as a lineage of mammals. All cladograms of early mammals in the studies mentioned above showed that non-therian mammals never form a monophyletic clade; instead, they represent successive outgroups of therian mammals in one way or another. The simplest explanation for this is that the braincase structure in non-therian mammals represents the primitive condition of mammals, which does not indicate common ancestry.

In the present study, the non-therian mammals form a series of successive outgroups of trechnotheres; the latter is composed of all known mammals with triangular molariforms except kuehneotheriids (figure 4-1: node H).

(3) Polyphyly of triconodonts.

As mentioned above, triconodonts are Mesozoic mammals with triconodont dental structure, in which three major cusps on molariforms mesiodistally aligned (Jenkins and Crompton, 1979). Triconodonts have a conservative molar pattern among Mesozoic mammals and a long history (from late Triassic to late Cretaceous). In pre-cladistic time,

most students assigned triconodonts as an Order (Osborn, 1907; Simpson, 1928, 1929, 1959, 1971; Patterson and Olsen, 1961; Kermack, 1967; Hopson, 1970; Hopson and Crompton, 1969; Kermack and Kielan-Jaworowska, 1971; Kermack *et al*., 1973; 1981; Jenkins and Crompton, 1979) and regarded them as the basal stock of non-therians, from which other non-therian mammals evolved (Kermack, 1967; Kermack and Kielan-Jaworowska, 1971; Mills, 1971; Jenkins and Crompton, 1979).

Phylogenetic analyses of Mesozoic mammals (references listed on page XXX) indicated that triconodonts never formed a monophyletic clade, instead, they represent a series of stem groups of mammals. The triconodont pattern is a primitive dental model of mammals, and all other mammalian dental models probably evolved from it. This study reaches the same conclusion. Triconodonts are not a monophyletic clade; instead, they represent series of stem groups of mammals and outgroups of mammals with various other dental patterns.

Sinoconodontids form the sister group of all other mammals. The morganucodontids plus kuehneotheriids form a sister group of other mammals. *Hadrocodium* is closer to extant mammals (figure 4-1: node B) than docodonts. The eutriconodonts form a monophyletic group (figure 4-1: node G), which pairs with trechnotheres.

Nevertheless, there are still several issues that continue on debating in the phylogenetic study of Mesozoic mammals, which are mainly related to the inter-relationships among different lineages of mammals. The present study reveals several interesting relationships among various groups of mammals, which are not common in previous studies.

A. Relationships of monotremes and multituberculates

There is no doubt that monotremes and multituberculates are more derived than basal mammals, such as sinoconodontids and morganucodontids, and represent separate mammalian lineages with distinct dental, cranial and postcranial features. What has been debated is their relationships with each other and with other mammalian lineages, especially tribosphenic mammals (marsupials and placentals) . Rowe (1988) suggested that multituberculates have a closer relationship with Theria, and proposed a new mammalian taxon, Theriiformes, for them. Many later studies endorsed Rowe (1988) in advocating the close relationship between multituberculates and therians (Rougier *et al*., 1996a; Hu *et al*., 1997; Ji *et al*., 1999, 2002; Lou *et al*., 2001a and b, 2002, 2003; Wang Y.-q. *et al*., 2001; Rauhut *et al*., 2002; Woodburne, 2003; Woodburne *et al*, 2003; Luo and Wible, 2005; Li and Luo, 2006). The close relationships of monotremes and multituberculates to therians were reversed in Wible (1991), which employed Rowe's (1988) cranial dataset with substantial modifications. Based on basicranial characters, Wible and Hopson (1993) proposed a close relationship between monotremes and multituberculates. Meng and Wyss (1995) studied ear ossicles of a Tertiary multituberculate, *Lambdopsalis*, from China and also favored the affinity between monotremes and multituberculates. The present study echoes with Wible and Hopson (1993) and Meng and Wyss (1995) in identifying a sister-group relationship between monotremes and multituberculates (figure 4-1: node C). The cluster of the two clades is supported by 14 unequivocal synapomorphies (22[0], 125[1], 128[1], 147[1], 162[0], 176[1], 182[0], 200[1], 209[1], 210[2], 278[1], 281[1], 380[3], and 423[0]).

B. Monophyly of eutriconodonts

Eutriconodonts are composed of late Jurassic to late Cretaceous triconodonts (gobiconodontids, repenomamids; amphelestids, triconodontids, Jeholodens, etc.). Their phylogenetic relationships are have only been explored in a handful studies. Based on dental and lower jaw structures, Rougier *et al*. (2001) reached the conclusion that the taxa included as eutriconodonts did not form a clade and some of them are closer to symmetrodonts than to other triconodonts. A few other studies (Rowe, 1988; Ji *et al*., 1999) also recognized polyphyly of eutriconodonts. The monophyly of eutriconodonts was reached in Wang Y.-q. *et al*. (2001) and Luo *et al*. (2002, and also Kielan-Jaworowska *et al*., 2004), a notion that is endorsed by this study. Moreover, eutriconodonts form the sister group of trechnotheres. The synapomorphies supporting the eutriconodont clade include 8 unequivocal synapomorphies (37[1], 153[1], 268[1], 301[0], 349[3], 371[2], 387[1], and 391[1]).

Within eutriconodonts, repenomamids and gobiconodontids form a clade with 5 unequivocal synapomorphies (360[1], 366[0], 367[1], 369[1], and 380[3]), which further unites with *Amphilestes*. *Jeholodens* is the sister group of triconodontids. The cluster of repenomamids and gobiconodontids was also reached in a previous study (Wang Y.-q. *et al*., 2001). Kielan-Jaworowska *et al*. (2004: p241) abandoned the Family Repenomamidae and moved *Repenomamus* into Gobiconodontidae. The diagnostic features they provided for the latter family include “i1, the only lower incisor, is procumbent and enlarged”, “anterior molariform teeth replaced ontogenetically in a sequential fashion”, and “upper molariforms wide transversely, with well-developed labial and lingual cingula and characterized by increasing triangulation of principal cusps

from M1 to M5". These features are not present or unclear in *Repenomamus (*Meng *et al*., in press*)*.

C. Relationship of symmetrodonts

The symmetrodonts are Mesozoic mammals with cheek teeth that have three major cusps nearly symmetrically arranged in a reversed triangle pattern (Cifelli and Madsen, 1999). Simpson (1925) created the Order Symmetrodonta for then known symmetrodont species. Crompton and Jenkins (1968) added the family Kuehneotheriidae to Symmetrodonta based on the occlusal pattern shared between *Kuehneotherium* and symmetrodonts. However, in any of the cladistic analyses of Mesozoic mammals mentioned above, *Kuehneotherium* never joined other symmetrodonts to form a monophyletic clade. Several authors excluded Kuehneotheriidae from symmetrodonts based on results of phylogenetic analyses (McKenna, 1975; Prothero, 1981; McKenna and Bell, 1997). Prothero recognized the modified Symmetrodonta (including Tinodontidae, Amphidontidae and Spalacotheriidae) as a monophyletic clade, which was nonetheless rejected by Luo *et al*. (2002), Kielan-Jaworowska *et al*. (2004) and Li and Luo (2006).

This study recovers a monophyletic group of symmetrodonts (including *Tinodon*, *Zhangheotherium*, *Spalacotherium* and *Heishanlestes;* figure 4-1: node I), which forms the sister group of remaining trechnotheres included in the analysis. Supporting characters for the clade include 4 unequivocal synapomorphies (349[2], 376[1], 382[1], and 388[1]), but the consistency indices for these character and equivocal characters (13 in ACCTRAN reconstruction and 6 in DELTRAN reconstruction) are low. The grouping of symmetrodont taxa deserves further consideration.

D. Relationships of tribosphenic mammals and mammals with similar lower molariforms.

Tribosphenic mammals have cheek teeth in which the protocone on upper molariforms occludes into the talonid basin of lower molariforms in addition to the shearing between the trigon of the uppers and trigonid of the lowers (Bown and Kraus, 1979). For a long time, tribosphenic mammals were regarded as a monophyletic group originated in northern continents (Kielan-Jaworowska *et al*., 2004). Rich *et al*. (1997) reported the finding of *Ausktribosphenos nyktos*, first Mesozoic mammal from Gondwanan landmasses with lower molariforms with the trigonid and talonid basin. Flynn *et al*. (1999) reported another mammal, *Ambondro mahabo*, from the Jurassic of Madagascar that has the trigonid and talonid basin on lower molariforms. Rich *et al*. (2001) reported the third Mesozoic Gondwanan mammal with tribosphenic lower molariforms, *Bishops whitemorei*. All of these authors considered the mammals they found as tribosphenic mammals and further challenged the northern origin of tribosphenic mammals, but neither of them doubted the monophyly of tribosphenic mammals. While admitting the Gondwanan taxa as tribosphenic mammals, Luo *et al*. (2001, 2002) proposed that the southern continent tribosphenic mammals are closer to extant monotremes and *Shoutherium*, a enigmatic mammal from China and England, than to northern continent tribosphenic mammals. These authors argued for dual evolution of tribosphenic mammals. They erected a new taxon, Australosphenida, for these purported Gondwanan tribosphenic mammals, *Shoutherium* and monotremes, and its counterpart, Boreosphenida, for northern continent tribosphenic mammals, including metatherians and eutherians. Rauhut *et al*. (2002), in reporting the fourth Mesozoic Gondwanan mammal

with tribosphenic lower molariforms, *Asfalotomylos patagonicus*, followed Luo *et al*. in regarding the dual origins of tribosphenic mammals. Luo *et al*'s hypothesis is attractive in relating monotremes with mammals with tribosphenic lower teeth. But so far no other study supports the idea. Instead, the hypothesis was challenged by Rich *et al*. (2002), Woodburne (2003) and Woodburne *et al*. (2003). These authors indicated several coding errors in Luo *et al*'s (2001) original data matrix and insisted that southern continent tribosphenic mammals were indeed ingroups of eutherians, a view even more radical than that of Luo *et al*.

This study does not recover the close relationships between monotremes and Mesozoic Gondwanan tribosphenic mammals. Instead, the Gondwanan tribosphenic mammals and *Shoutherium* form a clade within trechnotheres and is closer to northern tribosphenic mammals than to the clade consisting of *Amphitherium* plus (*Henkelotherium* + *Dryolestes*). Because upper molariforms are unknown for these Gondwanan taxa, their tribosphenic status is yet to be confirmed. Martin and Rauhut (2005) also noticed that there is no wear facet within talonid basins on the teeth of these taxa and that the development of the protocone remains uncertain.

5. BODY MASS AND DIET

Mesozoic mammals are commonly portrayed as shrew- or rat-sized animals that were mainly insectivorous and probably nocturnal and lived in the shadow of dinosaurs (Bakker, 1971; Hopson 1973; Jerison 1973; Crompton *et al*., 1978; Lillegraven, 1979). Earliest mammals, i.e. kuehneotheriids and morganucodontids, in the late Triassic-early Jurassic, were small and considered to be nocturnal insectivores (Hopson 1973; Jerison 1973); the same is true of most later Mesozoic mammals (Lillegraven *et al*. 1979; Kielan-Jaworowska *et al*. 2004). The reason for the minuscule nature of Mesozoic mammals is uncertain (Lillegraven 1979), but it has often been hypothesized that diurnal reptilian carnivores and herbivores of various sizes, particularly dinosaurs, have dominated the land of Mesozoic and prevented mammals from invading those niches, so that mammals did not have the chance to 'experiment' with large body size (Crompton, 1980). Exploitation of niches may be related to many factors other than body size, such as key innovations that enable organisms to involve adoption of new foraging modes (Mitter *et al*. 1988; Hunter and Jernvall 1995) or new modes of reproduction (Slowinski and Guyer 1993) or to promote reproductive divergence (Vrba 1987). However, for small-sized mammals the number of niches is potentially greatest as known from living mammals (Gardezi and Silva, 1998) so that mammals may have a chance to survive as being small.

The discovery of *Repenomamus* changes the image of Mesozoic mammals illustrated above. An adult individual of *R. robustus* has the size of a Virginia opossum; and the adult of *R . giganticus* is at least 50% larger than that of *R. robustus* in skull length (Table 5-1). The head-body plus preserved tail length of *G. giganticu*s, IVPP V

14155, is more than 1 meter long; and the individual is probably just a young adult, which suggests that adults of the species could grow even larger. In addition, stomach content associated with a skeleton of *R. robustus* reveals remains of a juvenile *Psittacosaurus,* a ceratopsian dinosaur. These discoveries constitute the first substantial evidence that Mesozoic

Table 5-1 Measurements of *Repenomamus* and selected recent mammals (in mm)

Specimens / Measurements	*A*	B	C	D	E	F
Skull length	160	110	112	106*	44	119.5
Mandibular length	128	78			32	100.3
Trunk length	522			315	111	297
Head-body length	682			421	155	416.5
Skull length/head-body length	0.23			0.25	0.28	0.287
Scapular depth	81				22	65
Humeral length	83		64	60	28	70.6
Humeral midshaft circumference	40		31	28	6	23.5
Humeral midshaft diameter	13		10	9	2	7.5
Humeral circumference/length	0.49		0.48	0.47	0.21	0.33
Ulnar length	87	64	68	55	32	79
Radial length	65*	47	51	43	25	69.4
Forelimb length (radius + humerus)	148		113	103	53	140
Femoral length	95	69	69	67	36	86.6
Femoral midshaft circumference	39	27	27	26	8	21
Femoral midshaft diameter	12.5	9	9	8	3	7
Femoral circumference/length	0.42	0.39	0.39	0.38	0.22	0.24
Tibial length	73	54		48	38	86.2
Hindlimb length (tibia + femur)	168			115	74	172.8
Intermembral index	88%			90%	72%	81%
Mean limb length	158			109	64	156
Mean limb length/trunk length	0.30			0.35	0.58	0.52

* Estimated data.
A, *R. giganticus*, IVPP V 14155; B, *R. robustus*, IVPP V 12549; C, *R. robustus*, IVPP V 12728; D, *R. robustus*, IVPP V 13605; E, *Tupaia glis*, AMNH 215174; F, *Didelphis virginiana*, AMNH 146532

mammals had a much greater range of body size than previously known and show that some Mesozoic mammals were carnivorous and fed on small vertebrates including young dinosaurs.

5.1 BODY MASS ESTIMATION

Many empirical regression equations that express the exponential relationships between body mass and dimensions of skeletal elements have been generated based on data from various groups of extant mammals (Alexander *et al*., 1979; Damuth and MacFadden, 1990; Silva and Downing, 1995). Some of these equations have been used to estimate body masses of fossil mammals given that fossil mammals are most similar to extant mammals among extant vertebrates in body mass-body structure relationships (Gingerich, 1990; Damuth and MacFadden, 1990). Here two groups of equations, one from Alexander *et al.* (1979) and the other from Van Valkenburgh (1990), are employed to estimate the body mass of *Repenomamus.*

The specific equations derived from Alexander *et al.* (1979) are:

Log (body mass) = (Log femoral length – Log 63)/0.36

Log (body mass) = (Log humeral length – Log 51)/0.36

Log (body mass) = (Log femoral diameter – Log5.2)/0.36

Log (body mass) = (Log humeral diameter – Log4.9)/0.38

The specific equations used by Van Valkenburgh (1990) include:

Log (body mass) = 3.13 x Log (skull length) - 5.59

Log (body mass) = 2.88 x Log (head-body length) - 7.24

Table 5-2. *Repenomamus* body mass estimated from limb sizes

Measure in mm	Equation	L or D/ M V14155	L or D/ M V12549	L or D/ M V12728	L or D/ M V13605
femoral length	Log M=(Log L – Log 63)/0.36	95mm/ 3.13kg	69mm/ 1.29kg	69mm/ 1.29kg	67mm/ 1.19kg
humeral length	Log M=(Log L – Log 51)/0.36	83mm/ 3.87kg		64mm/ 1.87kg	60mm 1.57kg
Mean mass predicted from length data		**3.5kg**		**1.58kg**	**1.38kg**
femoral diameter	Log M=(Log D – Log5.2)/0.36	12.5mm/ 11.43kg	9mm/ 4.58kg	9mm/ 4.58kg	8mm/ 3.31kg
Humeral diameter	Log M=(Log D – Log4.9)/0.38	13mm/ 13.03kg		10mm/ 6.53kg	9mm/ 4.95
Mean mass predicted from diameter data		**12.23 kg**		**5.56kg**	**4.13kg**

The equations are converted from Alexander *et al.*, 1979. L = length; D = diameter; M = mass.

Table 5-3 Log (SKL) and Log (HBL) values of *Repenomamus* and selected carnivores

	R. giganticus V14155	*R. robustus* V13605	*Canis lupus*	*Ursus americanus*	*Mustela vison*	*Hyaena brunnea*	*Felis serval*
Log (HBL)	2.8338	2.6243	3.122	3.228	2.568	3.023	2.919
Log (SKL)	2.2041	2.0253	2.318	2.328	1.735	2.342	2.021
SKL/HBL	0.23	0.25	0.16	0.15	0.15	0.20	0.13

V14155: Head & Body length (HBL) =682 mm; Skull length (SKL) = 160 mm

V13605: Head & Body length (HBL) =421mm; Skull length (SKL) = 106 mm

Log (HBL, head-body length) and Log (SKL, skull length) values of carnivores are from Van Valkenburgh, 1990: Table 10.1.

Table 5-4. Estimated body mass of *Repenomamus* from HBL and SKL

Length in mm	Slope a	Intercept b	r^2	%SEE	%PE	Mass in kg V14155	Mass in kg V13605
HBL	2.88	-7.24	.92	53	36	**8.34**	**2.08**
SKL	3.13	-5.59	.90	66	47	**20.37**	**5.61**
Mean value of two estimates						**14.36**	**3.85**

The equations are from Van Valkenburgh, 1990.

r^2, the square of the correlation coefficient; %SEE, percent standard error of the estimate; %PE, mean percent prediction error.

V14155: Head & Body length (HBL) =682 mm; Skull length (SKL) = 160 mm

V13605: Head & Body length (HBL) =421mm; Skull length (SKL) = 106 mm

Table 5-5 Body mass of *Repenomamus* and some extant mammals with similar body length

taxon	Head-Body length (mm)	Body mass (weight) (kg)
***R. giganticus* V14155**	**682**	**12-14 (estimated)**
Tasmanian devil (*Sarcophilus*)	525-800	5.5-11.8
two-toed sloth (*Cloloepus*)	540-740	4.0-8.5
Tamanduas (*Tamandua*)	470-770	2-7
Crab-eating fox (*Cerdocyon*)	600-700	5-8
Small-eared dog (*Atelocynus*)	700-1000	9-10
Tayra (*Eira*)	560-680	4-5
Chinese desert cat (*Felis bieti*)	680-840	6.5-9.5
***R. robustus* (V13605)**	**421**	**4-6 (estimated)**
Mumming (*Lagostrophus*)	400-460	1.3-3.0
Rock possum (*Petropseudes*)	325-425	1.3-2.0
Greater bushbaby (*Otolemur*)	230-465	0.6-2.0
Ring-tailed lemur (*Lemur*)	385-455	2.3-3.5
Swift fox (*Vulpes velox*)	375-525	1.8-3.0
Stink badgers (*Mydaus*)	370-510	1.4-3.6

Body mass and length data of extant taxa are from Nowak, 1999.

Measurements and estimated body masses of *Repenomamus,* in comparison with those of a few selected mammals, are listed in tables 5-1 to 5-5. The inferred body masses using limb bone lengths, 3.5 kg for *R. giganticus* and 1.38-1.58 kg for *R. robustus*, are apparently underestimated (Table 5-2). This is because the limbs of *Repenomamus* are proportionally significantly shorter than those of generalized therians, such as *Didelphis* and *Tupaia* (see table 5-1). The estimated values using limb diameter, 12 kg for *R. giganticus* and 4.13-5.56 kg for *R. robustus*, are probably more reliable (Table 5-2).

Body masses derived from skull length are 20.37 kg and 5.61 kg for *R. giganticus* and *R. robustus*, respectively, whereas the values derived from head-body length are 8.34 and 2.08 kg for the two species (Tables 5-3 and 5-4). The skull of *Repenomamus* is proportionally larger than those of extant carnivores, as indicated by greater ratio of skull length to head-body length (Table 5-3). Van Valkenburgh (1990) noted that, for carnivores that have relatively large head, skull length overestimates mass and that head-body length tends to underestimate mass. This is probably also true for the estimated masses of *Repenomamus.* Van Valkenburgh (1990) chose to use the average of the two, which is followed in our study. The averaged masses for *R. giganticus* and *R. robustus* are 14.36 and 3.85 kg, respectively (Table 5-4). These figures are similar to those derived from the long bone diameters. Taking all the estimates into account, the body masses are 12-14 kg for *R. giganticus* and 4-6 kg for *R. robustus*.

Given these estimated body masses, it appears that species of *Repenomamus* are relatively heavier than those of extant therians that have similar body length (Table 5-5). This is consistent with the body structure of *Repenomamus* that is characterized by relatively long trunk and short, robust limbs.

5.2 DIET AND STOMACH CONTENTS

For fossil mammals, the diet is commonly inferred from the craniodental structures and, in rare case, from remains of feces or stomach contents. Many superb specimens of *Repenomamus*, one of which is associated with stomach content. These specimens provides us a good opportunity to study the dietary of the animal.

The dentition of *Repenomamus* is suitable for meat-eating, although invertebrates and vegetable items could also be parts of its diet, as in the case of some extant carnivores (Carbone *et al*., 1999). The large and pointed incisors and similarly shaped canines and premolariforms form an apparatus for catching, holding and ripping prey (figure 5-1). This apparatus is powered by strong jaw musculature, as evidenced by the robust dentary and zygoma, large temporal fossa, and deep masseteric fossa. The molariform teeth in the back of the dentition of *Repenomamus* are small with blunt crowns; they probably played a minor role in food processing. Large pointed anterior teeth followed by small posterior teeth characterize many carnivorous non-mammalian synapsids (Van Valkenburgh and Jenkins, 2002).

Figure 5-1. A1-2**,** Lateral view of the skull and associated lower jaw of *Repenomamus giganticus* (holotype, IVPP V14155); B**,** ventral view of right upper dentition of *R. giganticus*, V 14155; C**,** medial view of the right mandible of *R. giganticus,* V 14155. The straight line indicates the skull length of *R. robustus*. cp, coronoid process; mc, mandibular condyle; mf, masseteric fossa; oc, occipital condyle; pms, premaxilla-maxillary suture;

sy, symphysis; zm, zygomatic arch. The upper incisors, canine, premolariforms and molariforms are denoted as I1-I3, C, P1-2 and M1-4; the corresponding lower teeth are denoted as i1-2, c, p1-2, and m1-5.

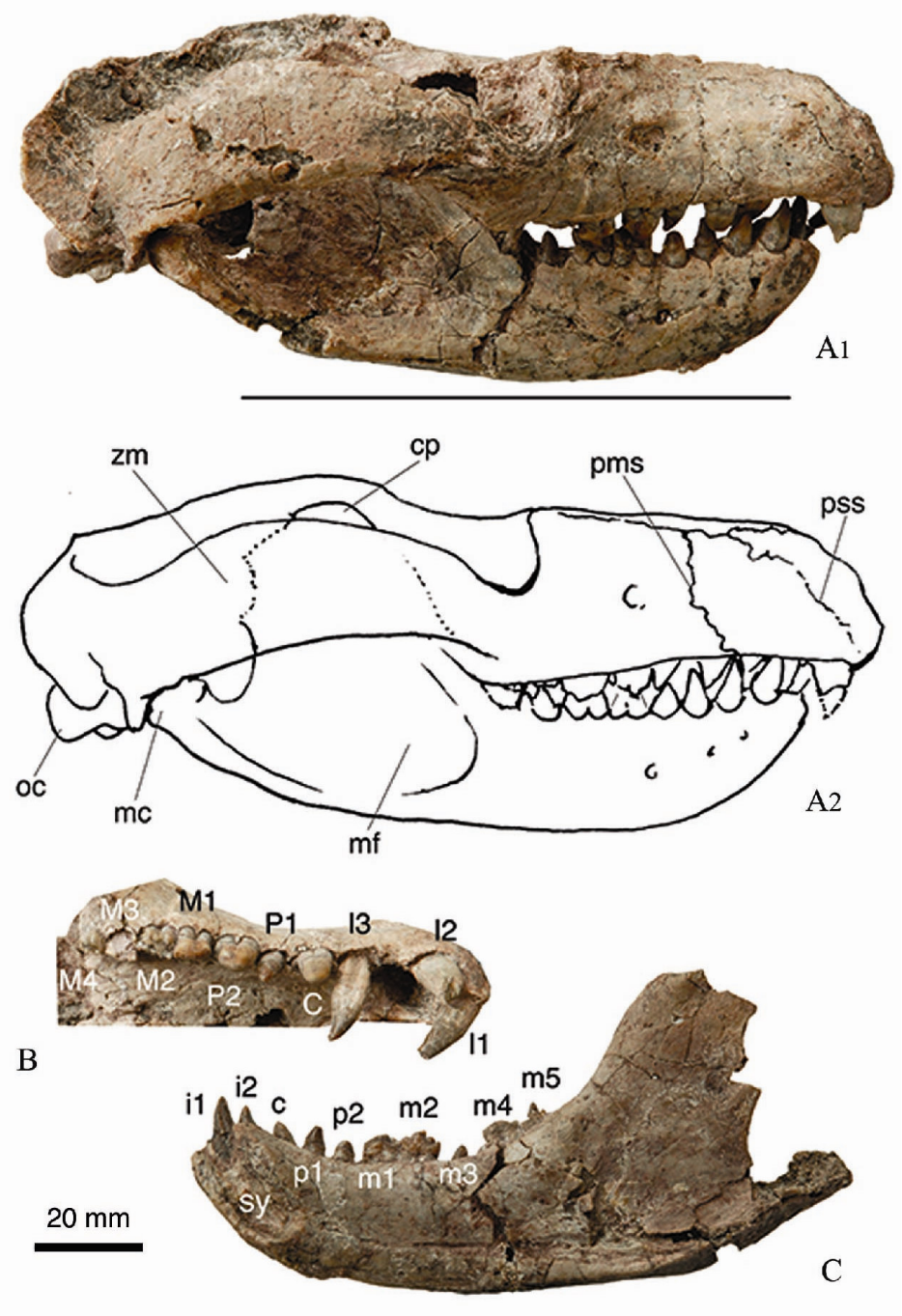

Figure 5-1

In addition to craniodental morphology, the evidence of the stomach content preserved in an individual of *R. robustus* (V 13605) also indicates carnivory. V 13605 is a skeleton of adult *R. robustus*. During preparation a patch of small bones was revealed within the ribcage of the mammal, on the ventral sides of the posterior left thoracic ribs and vertebrae (figures 2-4 and 3-9: enclosed bony mass). The patch of small bones are broken, disarticulated, and displaced (figure 5-2), in contrast to the preservation of the *R. robustus* skeleton that is basically in its anatomical relation. Although fragmentary, the small bones are packed in a restricted area, where the stomach is positioned in extant mammals. These conditions indicate that they are most likely the remains of the stomach contents of the mammal.

The remains of stomach contents are identified as belonging to a juvenile *Psittacosaurus.* The serrated teeth, long limb bones and phalanges within the stomach content (figures 5-2 and 5-3) are similar to those of juvenile individuals of *Psittacosaurus* from Mongolia (Coombs, 1982) and from Lujiatun locality. There are at least seven teeth on each quadrant (figure 5-3). The lower teeth are worn on buccal side (1-7 in figure 5-3) and on lingual side of each tooth are three ridges (2, 3 in figure 5-3). The two well-preserved upper teeth have a primary ridge with two small ridges anterior and posterior to it, respectively (figure 5-3: 6' and 7'). These are diagnostic feature of the genus (Averianov *et al*., 2003; Brinkman *et al*., 2001). The teeth illustrated are closely spaced,

---

Figure 5-2. Juvenile *Psittacosaurus* skeleton preserved within the ribcage of V13605. A1 outlines the position of the bony elements, identified elements are marked in different colors. Measurements (length): humerus, 21mm; radius, 18mm; ulna, 19mm; tibia, 36mm; and fibula, 35mm.

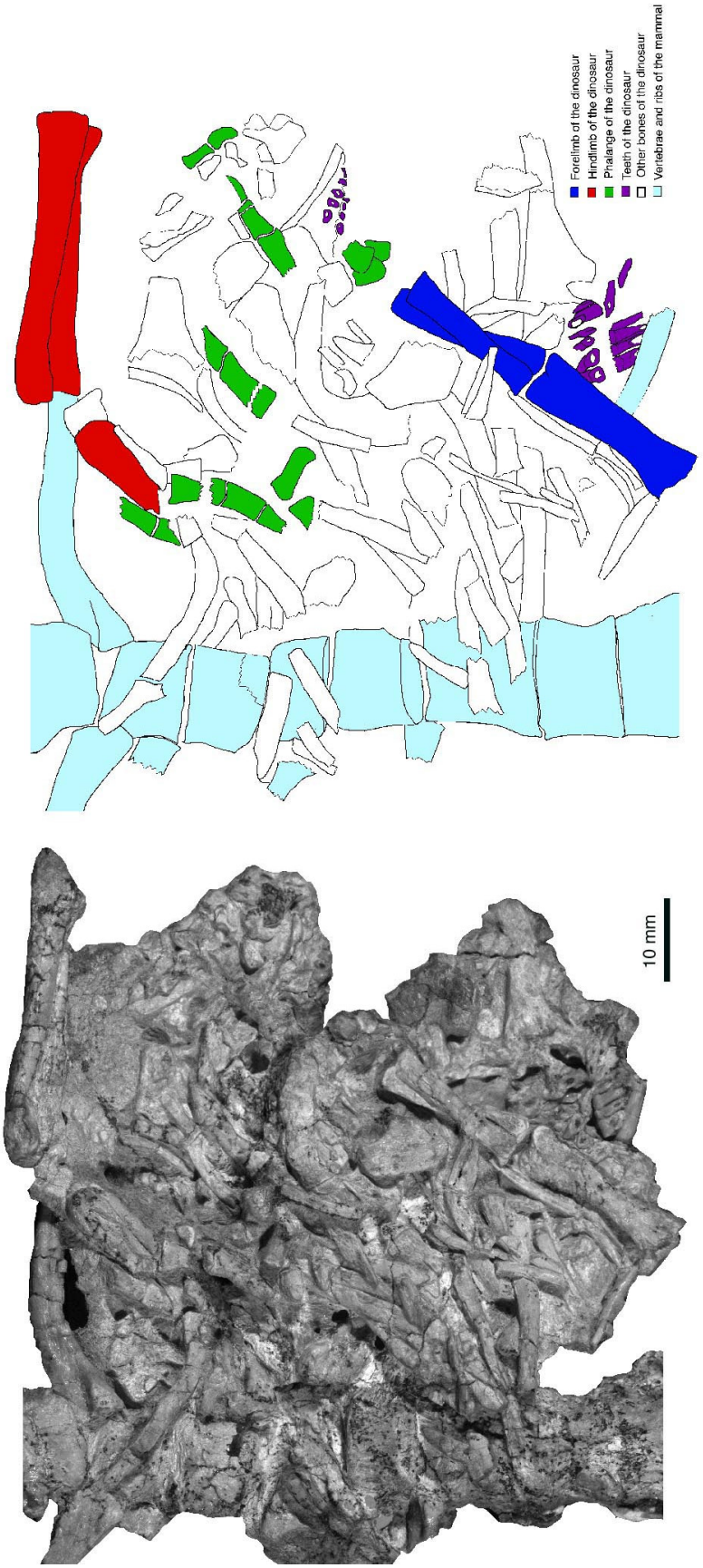
Forelimb of the dinosaur
Hindlimb of the dinosaur
Phalange of the dinosaur
Teeth of the dinosaur
Other bones of the dinosaur
Vertebrae and ribs of the mammal
10 mm

Figure 5-2

but it is typical of dentition of *Psittacosaurus* found in Lujiatun locality. Numerous skulls and skeletons of *Psittacosaurus* of different ontogenetic stages have been collected from the locality, some are illustrated in Figure 5-4 for comparison. The teeth of these young dinosaurs are identical and the limb proportions of the skeletons are similar. Judging from sizes of teeth and long bones, the swallowed juvenile has similar size to those shown in figure 5-4A and B but smaller than the individual illustrated in figure 5-4 C; its head-body length is estimated 140 mm (skull about 40 mm; trunk about 100 mm).

Figure 5-3. Teeth of the juvenile *Psittacosaurus:* A, view from ventral side of the *Repenomamus* skeleton; B, view from the dorsal side of the *Repenomamus* skeleton.

1-7, lower teeth; 1'-7', upper teeth. Precise number of the teeth for the individual is unknown. Tooth lengths: lower tooth 1 --2.1mm; lower tooth 2 – 2.1mm; lower tooth 3-- 2.2mm; upper tooth 6 – 2.4mm; upper tooth 7 – 2.8 mm.

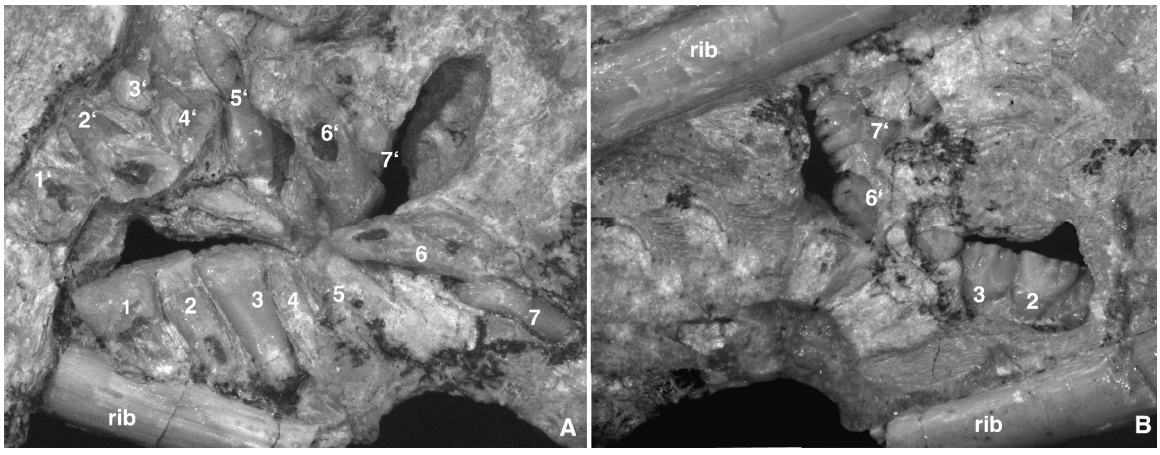

Figure 5-3

The head-body length of the eaten juvenile *Psittacosaurus* is about one third of the head-body length of the mammal. Most of teeth on each quadrant jaw were worn. These demonstrate that the *Psittacosaurus* skeleton is not from an embryo. A few long bones are preserved in articulation (figure 5-2), suggesting that the juvenile *Psittacosaurus* was dismembered and swallowed in as chunks. Although mammals are considered as definitive chewers within amniotes (Reilly *et al*., 2001), the dental morphology and large pieces of prey in the stomach content of *Repenomamus* suggest that chewing as a derived feature in mammals was probably not achieved in *Repenomamus*.

It is not easy to assess whether *Repenomamus* is a predator or scavenger. Scavengers are relatively rare among mammals; among extant carnivorous mammals, only two hyenas are habitual scavengers (Nowak, 1999; Van Valkenburgh *et al*., 2004). Compared to their hunting cousins, these hyenas have smaller second upper incisor and less jaw muscle leverage, which probably reflect their inability to capture and handle live preys. In contrast, the enlarged incisors and strong jaw muscles of *Repenomamus* are well shaped to catch preys, favoring a predator over a scavenger.

Figure 5-4. *Psittacosaurus* specimens from Lujiatun where *Repenomamus* material was collected. All are uncatalogued specimens deposited in Institute of Vertebrate Paleontology and Paleoanthropology (IVPP), Chinese Academy of Sciences, Beijing, China. A, Lateral view of skull of a juvenile. B, skull of a juvenile *Psittacosaurus* with partial postcranial elements attached. C, skeleton of a juvenile *Psittacosaurus*, long limb bone lengths: humerus – 32 mm; ulna and radius – 28 mm; femur – 52 mm; preserved vertebral column is about 90 mm long. Scale bar in C is 30 mm.

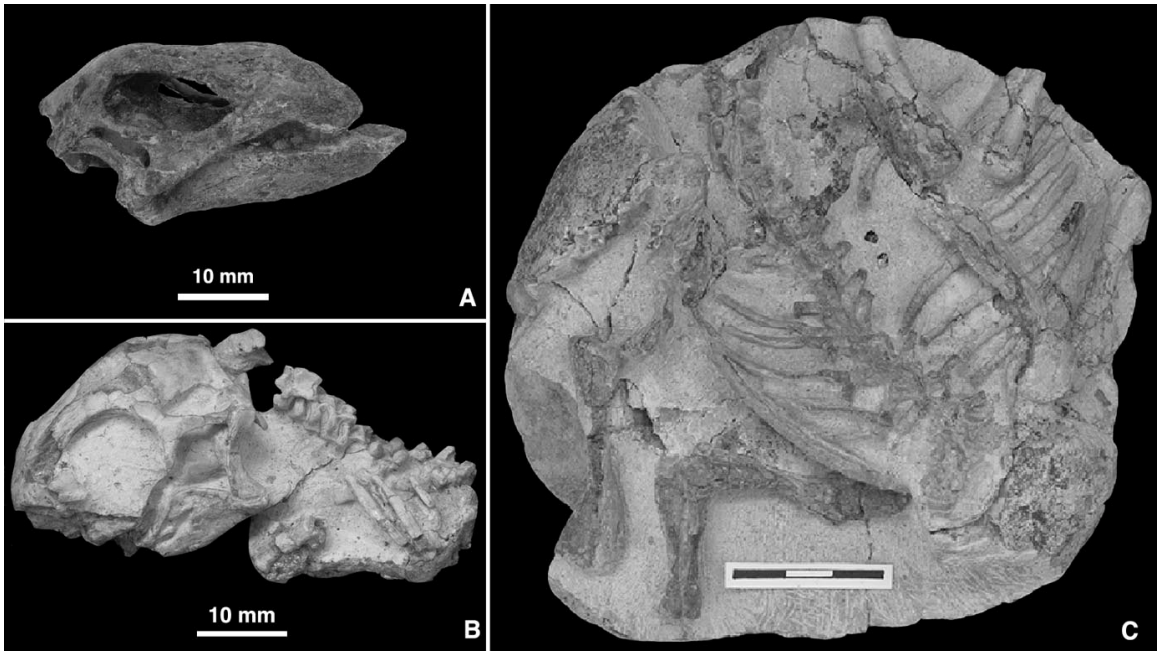

Figure 5-4

For fossil mammals, body size is one of the most important factors influencing life strategy (Lillegraven *et al*., 1979). Early mammals or their close relatives, such as morganocodontids and kuehneotheriids in the late Triassic-early Jurassic, were small and considered to be nocturnal insectivores)Hopson, 1973; Jerrison, 1973); the same is true of most later Mesozoic mammals (Lillegraven *et al*., 1979). The reason for the miniscule nature of Mesozoic mammals is uncertain (Lillegraven, 1979), but it has often been hypothesized that well-established fauna of large, medium, and small and presumably diurnal reptilian carnivores and herbivores, particularly dinosaurs, have prevented mammals from invading those niches, so that mammals did not have the chance to 'experiment' with large body size (Crompton, 1980). *Repenomamus* significantly expand the upper limit of body size of Mesozoic mammals and are actually larger than several small dinosaurs, particularly carnivorous dromaeosaurid dinosaurs, from the same fauna (Xu and Wang, 2004). Larger animals can live longer and move faster; they also need

more food supply and broader home range (Eisenberg, 1990). Judging from their body sizes, *R. giganticus* could feed on larger preys and forage a wider area for food. These large Mesozoic mammals have probably played the ecological role as carnivores that competed with small dinosaurs for food and territory.

6. HYOID AND LARYNX

The vertebrate hyoid and larynx form the hyobranchial apparatus, which is part of the feeding system and respiratory system. The framework of the hyobranchial apparatus belongs to the visceral skeleton (or splanchnocranium, Walker and Liem, 1994). In the majority of extant mammals the framework of the hyoid apparatus and larynx are cartilages. Even if they are ossified, the bones are normal tiny elements embedded in soft tissues and are easily ignored; only the dorsal part of the hyoid apparatus, especially the tympanohyal, is fused to the basicranium and easily recognized. This is probably also the case for fossil mammals, which explains why the fossil record of these elements is so rare. Except the tympanohyal, only a few taxa among Mesozoic mammals have hyoid elements preserved (Kielan-Jaworowska and Gambaryan, 1994; Hu *et al*., 1997: an unmarked bone in figure 1 between the left and right petrosal on the surface of basicranium is the ossified basihyal). So far, no fossilized larynx has been reported from extinct mammals.

In one specimen of *Repenomamus robustus*, IVPP V 12728, there are some tiny elements preserved on the ventral side of the cervical vertebrae (figure 6-1). The elements are identified as ossified hyoid and laryngeal elements, which represent the first fossil record of the hyoid (except the tympanohyal) in triconodonts and first fossil record of the larynx in mammals.

6.1 MORPHOLOGY

The tympanohyal of *Repenomamus* is fused to basicranium and preserved in

several specimens (Wang Y.-q. *et al*., 2001). The element is described elsewhere (Meng *et al*., in preparation) and not further discussed in this study. Besides that, V 12728 preserved three more elements of the hyoid apparatus (figure 6-1). The basihyal is preserved on the ventral surface of C3, next to the junction of the right transverse process and the vertebral body (figure 6-1: Bh). The bone is a curving and symmetrical bony bar, similar to that found in the specimen of *Zhangheotherium* (Hu *et al*., 1997: figure 1). A stout prismy bone is preserved ventrolateral to C2 and C3 on the right side (figure 6-1: Th). It is identified as a thyrohyal. One of its ends is smooth, and probably connected with the superior process of the first thyroid arch through ligaments. An asymmetrical bony rod is preserved near the vertebral column is separated during the preparation (figure 6-1: F). The bone is rounded in cross section, and probably represents an ossified element of the upper bony/cartilaginous chain of the hyoid.

Figure 6-1. Hyoid and laryngeal elements of *Repenomamus robustus*, IVPP V 12728: A and A1, Ventral view of the axis, third and fourth cervical vertebrae and associated hyoid and laryngeal elements; B and C, Medial and lateral view of left caudal portion of first arch of the thyroid; D and E, lateral and medial view of right arytenoid; F, an isolated hyoid element. Atl, left arytenoid; Bh, basihyal; C2, axis; C3, third cervical vertebra; C4, fourth cervical vertebra; T1r, right caudal portion of first arch of the thyroid; T2r, right caudal portion of second arch of the thyroid; Th thyrohyal; 1, superior process; 2, dorsal process; 3, ventral process; 4, muscular process; 5, apex; 6, vocal process; 7, muscular process; 8, internal process; 9, facet for cricoid.

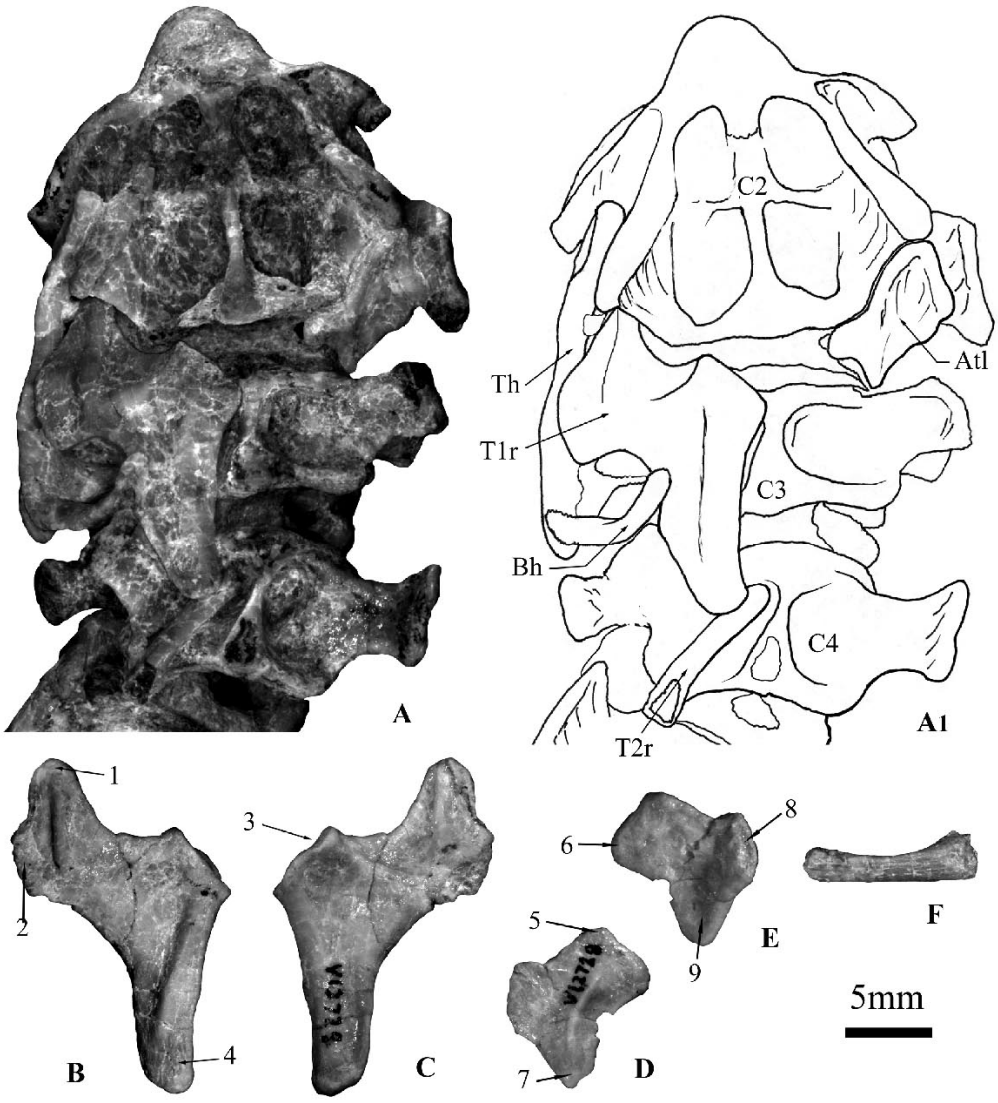

Figure 6-1

The framework of the mammalian larynx includes the epiglottic, thyroid, cricoid, and arytenoid elements (Negus, 1929; Schneider, 1964). IVPP V 12728 preserved the thyroid and arytenoid elements. The thyroid has two arches. Both the left and right caudal portions of the first arch are preserved, the right one on the ventral surface of C3 and C4 (figure 6-1: T1r), and the left one nearby (figure 6-1: B and C). The ossified right caudal portion of the second arch is preserved on the ventral surface of C4 (figure 6-1: T2r).

Both the left and right arytenoid elements are preserved, the left one on the ventral surface of C2 (figure 6-1: Atl), and the right one nearby (figure 6-1: D and E). There is no remain of the epiglottic and cricoid elements preserved. The epiglottic element is probably a cartilage as that in extant mammals. Therefore, it is hardly preserved as fossil. The cricoid is either cartilaginous or ossified, but not preserved in this specimen.

The caudal portion of the first arch of the thyroid is irregular in shape. The bony piece has four processes and three ridges connecting them. The superior process is short (figure 6-1: 1). The dorsal process is low and broad (figure 6-1: 2). The ventral process is stout and broad, contacting the more medial portion of the arch, which is cartilaginous and not preserved (figure 6-1: 3). The muscular process is long (figure 6-1: 4). The ossified right caudal portion of the second arch of is slender and rod-like (figure 6-1: Tr2).

The arytenoid is a small element (figure 6-1: Atl, D and E). The apex is blunt (figure 6-1: 5). The vocal process is short (figure 6-1: 6). The muscular process is slightly elongated (figure 6-1: 7). The internal process of the bone bears an articular facet(figure 6-1: 8), which probably articulates with an interarytenoid cartilage. The concave facet near the tip of muscular process (figure 6-1: 9) is probably for contact with the cricoid.

The identification of the laryngeal and hyoid elements is mainly based on their morphology. But the locations they are preserved is also useful clue. The laryngeal elements are preserved on or near the ventral side of axis and third and fourth cervical vertebrae (figure 6-1: A and A1), which is very close to the original location of the larynx observed in extant mammals (Harrison, 1995).

6.2 EVOLUTIONAY AND FUNCTIONAL IMPLICATIONS

The thyroid of *Repenomamus* is more similar to that of monotremes than to any other extant mammals. In extant mammals, only monotremes have the thyroid with two arches connected by a central copula (Symington, 1900; Schneider, 1964). Ontogenetically, the arches of monotreme thyroid are derived from fourth and fifth visceral arches, which are further fused in marsupial and placental thyroid (Goodrich, 1930). The thyroid of *Repenomamus* probably has the same constitution as that of monotremes, but only the ossified caudal portions of the arches are preserved as fossil (figure 6-2). This similarity between monotremes and *Repenomamus* probably represents a primitive condition of mammals, as arches of the visceral skeleton of vertebrates are originally separated (Walker and Liem, 1994). The larynx of *Repenomamus* is further similar to that of monotremes in that its two arytenoids connect to each other through an interarytenoid element, and the cricoarytenoid articulation is simple. Therefore, the mobility of the arytenoid is probably quite limited. This condition is also found in many marsupials (Symington, 1899; Negus, 1929; Schneider, 1964). The larynx of R*epenomamus*, like that of marsupials and placentals, differs from that of monotremes in the independence of the thyroid from the hyoid, while in monotremes the thyroid is fused to the hyoid (Negus, 1929). Given that the fourth and fifth visceral arches (which develop into the thyroid in mammals) are continuous with the hyoid in other tetrapods, the feature shared by *Repenomamus*, marsupials and placentals probably represents a derived condition evolved in the common ancestor of these taxa. Figure 6-2 is a simplified phylogeny of four taxa derived from two hyoid/larynx characters, which is consistent with the high-level phylogeny of mammals derived from 435 skeletal characters.

Figure 6-2. Reconstruction of the laryngeal and hyoid apparatus of *Repenomamus* and its phylogenetic relationships with extant mammals. Bh, basihyal; Cc, cricoid; Ch, ceratohyal; Th, thyrohyal; Tr, thyroid; T1, the first arch of thyroid; T2, second arch of thyroid. The parts in light shade are not preserved. *Repenomamus* shares with Marsupialia + Placentalia the independence of the thyroid from the hyoid (node A); Marsupialia and Placentalia further share the integration of the thyroid arches (Node B). This simplified cladogram is consistent with the phylogeny of Mesozoic mammals derived from 435 skeletal characters (figure 4-1).

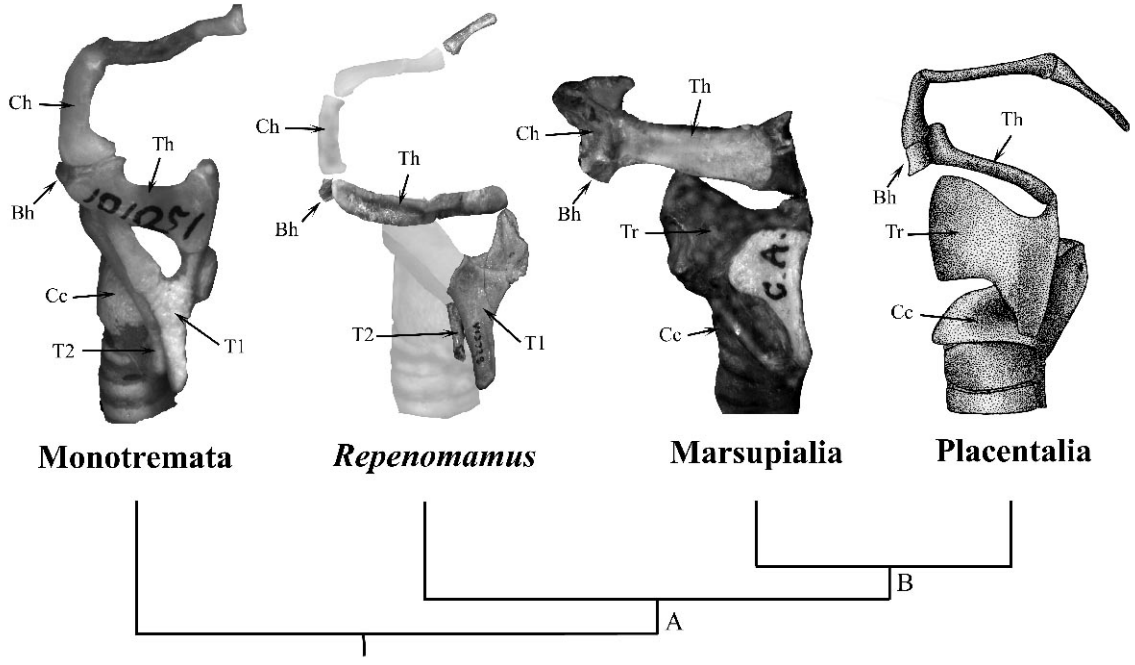

Figure 6-2

The primary function of the larynx is to protect the lower airway from intrusion of water and other foreign matter by shutting the glottis, the opening of the low respiratory

tract (Harrison, 1995). The thyroid element and the epiglottic cartilage are unique to mammalian larynx. In vertebrates other than mammals, the thyroid is never developed and the glottis lies on the bottom (ventral side) of the digestive tract near the root of tongue (Negus, 1929). The presence of the thyroid in mammalian type of larynx separates the glottis from the root of the tongue. If the epiglottic cartilage did not develop, there would be an extra space in front of the glottis and food bolus and water would easily accumulate there and threaten the life of the animal in every respiratory circle. Therefore, the presence of the thyroid in *Repenomamus* necessitates the simultaneous development of the epiglottic cartilage in the taxon. Two elements probably co-evolved during the mammalian evolution. The thyroid provides a supporting base for the epiglottis (the epiglottic cartilage and associated soft tissue), which is probably the main reason for its appearance in the mammalian history. The high-level phylogeny of mammals (figures 4-1 and 6-2) also favors the presence of the epiglottic cartilage in *Repenomamus*.

The development of the thyroid and epiglottic elements in *Repenomamus* suggests that the animal has a similar mechanism to control the respiration and deglutition as that of extant mammals. No matter what is its initial function, the epiglottis can approximate the internaries and shut off the oral cavity from the respiratory pathway during food processing, minimizing the interface of mastication to respiration and allowing continuing respiration as much as possibly. The presence of this type of larynx in early Cretaceous *Repenomamus* and all extant mammals suggests its evolution deep in the mammalian history, which has profound evolutionary implications.

Extant mammals and birds are only endotherms among extant terrestrial vertebrates (Hillenius and Ruben, 2004). Endothermy requires high levels of oxygen

consumption and elevated rates of lung ventilation (Ruben *et al*., 2003), the rates even higher in mammals due to their low-efficiency alveolar lungs in respiration compared to the parabronchial lung/air sac system of birds (Hillenius, 1992; Hillenius and Ruben, 2004). Therefore, mammals require particularly continuous respiration to survive (except that some aquatic mammals secondarily evolve the ability to hold breathe for a prolonged period). On the other hand, endothermy also requires large amount of nutrients through frequent food intaking. The mammalian type of larynx allows the animal to perform both functions simultaneously. It has been suggested that all mammals, including those of late Triassic and early Jurassic, and even some derived nonmammalian therapsids, are endothermic judged by the presence of the maxillioturbinate in the nasal cavity (Hillenius, 1992, 1994; Hillenius and Ruben, 2004). But it is unclear whether the mammalian type of larynx predated the endothermy or co-evolved with the latter. Nevertheless, it is unlikely that the mammalian type of larynx developed later than the endothermic condition as that seen in extant mammals.

All extant mammals suckle their neonates, which is a unique mammalian feature (Pough *et al*., 1999). Mammalian neonates rely on frequent and prolonged milk sucking to get nutrient. Meanwhile, the neonates also have high demand of oxygen consumption(per unit of body weight) and, therefore, high rates of breathe (Mortola, 1984), which demands minimum interruption of the respiratory airflow. Both functions are essential for survival of the neonates. The mammalian type of larynx provides a seal between the epiglottis and the back of the soft palate and also allows milk to pass around the larynx; therefore the neonates can suckle and breathe at the same time (Pough *et al*., 1999). The mammalian type of larynx is prerequisite for simultaneous lactation and

oxygen-intake. Its presence in *Repenomamus* suggests that the animal and its relatives (other eutriconodonts) are capable of suckling their neonates as extant mammals. It has been argued that the origin of lactation probably correlated with delayed tooth replacement and determined growth pattern, which evolved in mammals, including morganucodontids (Kielan-Jaworowska *et al*., 2004: p 148 and references therein). If this is the case, the mammalian type of larynx must have evolved in the common ancestor of morganucodontids and later mammals at least in the late Triassic or early Jurassic.

By allowing continuous airflow in/out the lung, the mammalian type of larynx enhances the respiratory ability in low-oxygen environments, which is probably an external factor inducing the origin of this kind of larynx. After end-Permian mass extinction, the atmospheric oxygen level dropped dramatically (Falkowski *et al*., 2005). It is unclear whether cynodont predecessors of mammals, who lived in the Triassic and Jurassic, have evolved mammalian type of larynx. It has been suggested that nonmammalian cynodonts did not evolve lactation (Kielan-Jaworowska *et al*., 2004: p 150). If the mammalian type of larynx did originate in nonmammalian cynodonts , it would be mainly for maintaining continuous oxygen-intake in low-oxygen environments and preadapting for the lactation.

Appendix I:

CHARACTER LIST

POSTCRANIAL CHARACTERS (176 characters)

VERTEBRAL COLUMN AS WHOLE

1. **Vertebral centra: (0) amphicoelous; (1) platycoelous** (Rowe, 1988: Ch 108; Sidor and Hopson, 1998: Ch 123; Hopson and Kitching, 2001: Ch 101).

2. **Neural arches synostosed with the centrum: (0) absent; (1) present**.

ATLAS AND AXIS

3. **The facet for the proatlas on the atlas: (0) the facet is present at the neural arch of the atlas; (1) the neural arch of the atlas bears no facet for the proatlas** (modified from Rowe, 1988: Ch 92; Hu *et al*., 1997: Ch 1; Ji *et al*., 1999: Ch 1; Luo *et al*., 2002: Ch 1**19**).

4. **Fusion of the atlantal intercentrum with neural arch in adults: (0) unfused; (1) fused** (modified from Rowe, 1988: Ch 93; and Hu *et al*., 1998: Ch 2; Luo *et al*., 2002: Ch 120).

5. **The articular facet for occipital condyle on the atlantal intercentrum: (0) present; (1) absent.**

6. **Fusion of two halves of the atlantal neural arch in adult: (0) not fused; (1) fused**. Jenkins (1971: p17) stated that two halves of the atlantal neural are not fused, even not contact, in some nonmammalian cynodonts.

7. **Anteroposterior length of the neural arch of the atlas: (0) long; (1) short.**

8. **Atlas rib in adult: (0) present; (1) absent** (Rowe 1988: Ch 9; Hu *et al*., 1997: Ch 3; Luo *et al*., 2002: Ch 121).

9. **Development of atlantal transverse process (including the rib): (0) more vertically than transversely oriented, narrow and not expanded; (1) more transversely than vertically oriented, wing-like and anteroposteriorly expanded.**

10. **Posterior extension of the atlas transverse process or rib: (0) beyond the caudal facets for axis; (1) not beyond the caudal facets** (modified from Horovitz and Sánchez-Villagra, 2003: Ch 4).

11. **Prezygapophysis on axis: (0) present; (1) absent**.

12. **Enlargement of the second intervertebral foramen: (0) slightly; (1) moderately; (2) greatly.**

13. **Atlantal and axial centra: (0) sutured; (1) fused with no suture**.

14. **Shape of axis body (atlantal and axial centra): (0) more or less round in cross section; (1) dorsoventrally flattened.**

15. **Development of dens: (0) as anterior extension of the atlas centrum, without constriction at the base; (1) as small protuberance from the atlas centrum, with constriction at the base; (2) tongue-like or tooth-like and with constriction at its base** (modified from Sidor and Hopson, 1998: Ch 128).

16. **Axis intercentrum: (0) suturing to axis centrum; (1) fused with axis centrum** (modified from Sidor and Hopson, 1998: Ch 126).

17. **Anterior articular facets of axis: (0) extended ventrally to atlantal centrum; (1) posterolateral to the dens and not linked to each other** (modified from Horovitz and Sánchez-Villagra, 2003: Ch 12).

18. **Rib of axis in adults: (0) present; (1) absent** (Hu *et al*., 1997: Ch 5; Luo *et al*., 2002: Ch 124; Horovitz and Sánchez-Villagra, 2003: Chs 9, 13).

19. **Lateroventral lamella of the axial body: (0) absent; (1) present.**

20. **Anapophysis of the axis: (0) absent; (1) present**.

21. **Anterior extension of the axial spinous process relative to anterior articular facets: (0) not extended, the spinous process mainly posterodorsal to the facets; (1) extended and the process over the facets.**

22. **Posterior extension of the axial spinous process: (0) not extended beyond the centrum; (1) beyond the centrum** (modified from Horovitz and Sánchez-Villagra, 2003: Ch 10).

POST-AXIAL CERVICAL VERTEBRAE

23. **Postaxial cervical rib in adults: (0) present; (1) absent** (Rowe, 1988: Ch 101; Hu *et al*., 1997 Ch 6; Luo *et al*., 2002: Ch 125).

24. **Attachment of the head of the postaxial ribs: (0) margins of the vertebral centra; (1) ventral lamellae**.

25. **Articulation of postaxial cervical rib with the vertebral body: (0) mobile articulation; (1) immobile.**

26. **Shape of bodies of postaxial cervicals: (0) circular in cross section; (1) dorsoventral flattened.**

27. **Lateroventral lamellae of postaxial cervical vertebrae (0) absent; (1) present.**

28. **Midventral keel on the body of postaxial cervicals: (0) the ventral surface is gently round without distinct midventral keel and lateral concavities; (1) prominent midventral keel and associated lateral concavities present on the ventral surface of the centra.**

29. **Length of the neural lamina relative to the centrum in postaxial cervicals: (0) not shortening; (1) shortening, narrow and thin.**

30. **Development of cervical spinous process: (0) large, with the height equal or larger than the length of vertebral body; (1) reduced with the height less than the length of the vertebral body**.

31. **Prezygapophyses and postzygapophyses of postaxial cervicals: (0) as distinct processes on neural laminae; (1) reduced to be facets on laminae** (Modified from Horovitz and Sánchez-Villagra, 2003: Ch 22).

32. **Vertebral anapophysis in cervicals: (0) absent; (1) present** (modified from Sidor and Hopson, 1998: Ch 124).

33. **Number of cervical vertebrae: (0) more than seven; (1) seven.**

34. **Postaxial intercentra of cervical vertebrae in adults: (0) sutured with centra; (1) fused with centra**.

THORACIC VERTEBRAE

35. **Transition from cervical to thoracic vertebrae: (0) gradual; (1) distinct**.

36. **Transition from the cervical to thoracic ribs: (0) gradual; (1) distinct.**

37. **Number of thoracic vertebrae: (0) 15 or less; (1) 16 or more** (modified from Luo *et al*., 2002: Ch 126).

38. **Shape of the thoracic vertebral body: (0) roughly circular or oval in cross section; (1) strongly dorsoventrally flattened.**.

39. **Development of spinous processes of thoracics: (0) well developed; (1) reduced.**

40. **Vertebral anapophysis in thoracics: (0) absent; (1) present** (modified from Sidor and Hopson, 1998: Ch 124).

41. **T1 transverse process: (0) present; (1) absent.** (modified from Horovitz and Sánchez-Villagra, 2003: Ch 24).

42. **Intervertebral foramen in thoracic region: (0) intervertebral; (1) enclosed by the caudal edge of the neural arches**. (Modified from Horovitz and Sánchez-Villagra, 2003: Ch 28).

THORACIC RIBS

43. **Thoracic ribs: (0) at least anterior ribs double-headed with capitulum and tuberculum separated; (1) single-headed with capitulum and tuberculum not separated.**

44. **Sternal ribs of the thoracic ribs: (0) cartilage; (1) ossified. (Modified from Horovitz and Sánchez-Villagra, 2003: Ch 34).**

45. **Anterior Thoracic ribs' (true ribs) articulation with sternum: (0) with single sternebra (1) with two sternebrae** (modified from Horovitz and Sánchez-Villagra, 2003: Ch 35).

LUMBAR VERTEBRAE

46. **Demarcation between thoracic and lumbar series based on rib morphology: (0) gradually; (1) distinct.**

47. **Lumbar ribs: (0) present and sutured with transverse process; (1) synostosed to transverse process without suture.** (Modified from Luo *et al*., 2002: Ch 127).

48. **Lumbar rib articulation with the vertebra: (0) with an intervertebral capitular articulation; (1) no intervertebral articulation.**

49. **Zygapophyseal articulation in lumbar region: (0) nearly horizontal; (1) more vertical than horizontal.**

SACRAL VERTEBRAE

50. **Number of sacral vertebrae: (0) five or more; (1) four; (2) three or less**.

51. **Development of sacrum: (0) sacral vertebrae articulated; (1) sutured or synostosed.**

52. **Sacral rib development: (0) not fused with vertebral body; (1) fused (modified from Sidor and Hopson, 1998: Ch 125).**

CAUDAL VERTEBRAE

53. **Caudal ribs: (0) present in at least some anterior caudals; (1) absent.**

STERNAL STRUCTURE, INTERCLAVICLE

54. **Interclavicle as separate element in adults: (0) present; (1) absent.** (Rowe, 1988: Ch 110 and 113; Hu *et al*., 1997: Ch 8; Luo *et al*., 2002: Ch 128; Horovitz and Sánchez-Villagra, 2003: Ch 39).

55. **Anterior part (articulating with clavicle) of the sternal manubrium/interclavicle): (0) with short and narrow lateral process; (1) as broad and expanded plate; (2) with extra elongated lateral process.**

56. **Articulation between the interclavicle and sternal manubrium (0) posterior edge of the interclavicle contacts the anterior edge of the sternal manubrium; (1) posterior process of the interclavicle overlaps ventral side of the sternal manubrium.** (Modified from Luo *et al*., 2002: Ch 129).

57. **Posterior portion of the interclavicle: (0) much longer than anterior portion (clavicle articulation); (1) equal to anterior portion or less than anterior portion in length** (modified from Sidor and Hopson, 1998: Ch 140).

58. **Interclavicle posterior process shape: (0) uniformly broad; (1) paddle-like; (2) narrow (Sidor and Hopson, 1998: Ch 141).**

59. **Anterior median process of sternal apparatus: (0) present; (1) absent** (Modified from Luo *et al*., 2002 Ch 130).

60. **Size of the anterior-most sternal element relative to the sternebrae in the sternal apparatus in adults: (0) large; (1) small** (Hu *et al*., 1997: Ch 15; Luo *et al*., 2002: Ch 140).

SHOULDER GIRDLE

61. **Scapular blade: (0) narrow and high, dorsal part not distinctly expanded compared with ventral part of the blade; (1) dorsal part distinctly expanded.**

62. **Lateral surface of the scapular blade: (0) gently flat anteroposteriorly; (1) forming distinct supracoracoideus fossa or infraspinous fossa.**

63. **Scapular blade: (0) laterally bowed; (1) not bowed and flat in dorsoventral direction.**

64. **Twist of the scapular blade: (0) twist; (0) not twist.**

65. **Acromial process of the scapula: (0) absent; (1) weakly developed as short process above the glenoid; (2) as a long hook-like process extending ventrally beyond the glenoid process**. (Modified from Rowe, 1988 Ch 115; Hu *et al*., 1997: Ch 11; Sidor and Hopson, 1998: Ch 134; Hopson and Kitching, 2001: Ch 85; Luo *et al*., 2002: Ch 135; Horovitz and Sánchez-Villagra, 2003: Ch 37).

66. **The neck of the scapula: (0) not developed; (1) as short constriction below the acromial process; (2) moderate or elongated constriction between the acromial process and glenoid** (modified from Sidor and Hopson, 1998: Ch 135 and 136; Hopson and Kitching, 2001: Ch 86 and 87; Bonaparte *et al*., 2003: Ch 41).

67. **Development of supraspinous fossa: (0) absent; (1) incipiently developed; (2) weakly developed; (3) fully developed** (Modified from Rowe, 1988: Ch 114; Hu *et al*., 1997: Ch 10; Luo *et al*., 2002: Ch 134).

68. **Development of the scapular spine: (0) absent; (1) low bony ridge; (2) high bony plate.**

69. **Development of the Procoracoid: (0) present as a separated element in adult, contact with scapula greater than coracoid; (1) present, contact with scapula less than coracoid; (2) present, no contact with scapula; (3) absent in adult as individual element**. (Modified from Rowe, 1988: Ch 117; Hu *et al*., 1997: Ch 12; Sidor and Hopson, 1998: Ch 138; Hopson and Kitching, 2001: Ch 89; Luo *et al*., 2002: Ch 137; Bonaparte *et al*., 2003: Ch 43).

70. **Procoracoid participating in the glenoid: (0) present; (0) absent**. (Sidor and Hopson, 1998: Ch 137; Hopson and Kitching, 2001: Ch 88; Bonaparte *et al*., 2003: Ch 42).

71. **Procoracoid foramen: (0) present; (1) absent (Luo *et al*., 2002: Ch 13).**

72. **Morphology of the coracoid: (0) as a large bone with a posterior process; (1) as a large coracoid process of the scapulocoracoid, well contributing to the glenoid fossa and without posterior process; (2) as a small hook-like coracoid process, barely or not contributing to the glenoid**. (Modified from Rowe, 1988: Ch 118; Hu *et al*., 1997: Ch 13; Luo *et al*., 2002: Ch 139; Horovitz and Sánchez-Villagra, 2003: Ch 36).

73. **Articulation of coracoid with the sternal apparatus (including interclavicle): (0) not articulating; (1) articulation.**

74. **Orientation of scapular portion of the glenoid relative to the plane of scapula: (0) facing posterolaterally and ventrally; (1) facing**

ventroposteriorly or facing ventrally; (2) facing laterally (modified from Hu *et al*., 1997: Ch16; Sidor and Hopson, 1998: Ch 131).

75. **Contour of the scapular surface of the glenoid: (0) lateromedially convex and dorsomedially concave; (1) gently flat with out lip convex; (2) concave** (Modified from Hu *et al*. 1997: Ch 17 and Luo *et al*., 2002: Ch 142).

76. **Contour of coracoid surface of the glenoid: (0) gently convex or saddle-shaped (lateromedially convex and dorsomedially concave); (1) concave** (Modified from Hu *et al*. 1997: Ch 17 and Luo *et al*., 2002: Ch 142).

77. **Medial surface of the scapula (in anteroposterior direction): (0) slightly convex; (1) distinctly convex; (2) flat** (Modified from Hu *et al*. 1997: Ch 18; Luo *et al*., 2002: Ch 143).

78. **Morphology of the clavicle: (0) medial end expanded in to a plate; (1) the medial end not expanded and the whole bone rod-like.**

79. **Mobility of clavicle-sternal apparatus joint: (0) immobile; (1) mobile** (Hu *et al*., 1997: Ch 9; Luo *et al*., 2002: Ch 131).

FORELIMB

HUMERUS

80. **Humeral head: (0) elongate oval; (1) subspherical and weakly inflected dorsally; (2) nearly spherical and strongly inflected dorsally** (modified from Rowe, 1988: Ch 120; Hu *et al*., 1997: Ch 19; Sidor and

Hopson, 1998: Ch 144; Luo *et al*., 2002: Ch 144; Horovitz and Sánchez-Villagra, 2003: Ch 55).

81. **The development of greater and lesser tubercles: (0) no actual tuberosities visible; (1) distinct tuberosities.**

82. **Intertubercular groove: (0) broad; (1) narrow** (Modified from Rowe, 1988: Chs 121, 122, and 123; Hu *et al*., 1997: Ch 20; Luo *et al*., 2002: 145).

83. **Size of lesser tubercle of humerus relative to the greater tubercle: (0) wider than the greater tuberosity; (1) narrower** (Hu *et al*., 1997: Ch 21; Luo *et al*., 2002: Ch 146):.

84. **The orientation of the greater tubercle and deltopectoral crest: (0) extending lateroventrally from the humeral head and shaft; (1) reflected anteromedially from the anterolateral corner of the humeral head and shaft.**

85. **Distal extension of the deltopectoral crest on humeral shaft: (0) reaching the midpoint of the humeral shaft or beyond; (1) not reaching the midpoint of the humeral shaft** (Modified from Hu *et al*., 1997: Ch 23; Sidor and Hopson, 1998: Ch 146; Luo *et al*., 2002: Ch 1148; Horovitz and Sánchez-Villagra, 2003: Ch 50).

86. **Width of the deltopectoral crest: (0) broad, about one third width of the proximal shaft of the humerus or broader; (1) narrow, much less than one third width of the proximal shaft of the humerus.**

87. **The dorsal flexure of the proximal half of the humeral shaft: (0) distinct; (1) not distinct** (See Jenkins, 1971: p113).

88. **The tuberosity distal to the lesser tubercle, on the medial aspect of the humeral shaft, for the teres major muscle: (0) prominent; (1) weak or absent.**

89. **Torsion between the proximal and distal ends of humerus: (0) strong (>= 30°); (1) moderate 15°-30°); (2) weak (< 15°)**. (Hu *et al*., 1997: Ch 22; Luo *et al*., 2002: Ch 147).

90. **Relative breadth of the distal humerus: (0) broad; (1) moderate; (2) slender; (3) extremely broad.**

91. **Humero-ulnar articulation of the distal humerus: (0) condylar; (1) trochlea with vestigial condyle; (2) trochlea** (modified from Rowe, 1988: Ch 126; Hu *et al*., 1997: Ch 24; Sidor and Hopson, 1998: Ch 147; Luo *et al*., 2002: Ch 149; Horovitz and Sánchez-Villagra, 2003: Ch 51).

92. **The radial condyle (capitulum) of the humerus: (0) bulbous; (1) spindly** (Modified from Luo *et al*., 2002: Ch 150 and Horovitz and Sánchez-Villagra, 2003: Ch 45).

93. **The separation vs. conjoining of ulnar and radial articulations on humerus: (0) separation; (1) conjoining.**

94. **The ectepicondylar foramen on humerus: (0) present; (1) absent** (Sidor and Hopson, 1998: Ch 143; Hopson and Kitching, 2001: Ch 90; Bonaparte *et al*., 2003: Ch 44).

95. **The entepicondylar foramen on humerus: (0) present; (1) absent** (Modified from Horovitz and Sánchez-Villagra, 2003: Ch).

96. **Epicondyles of the humerus (0) robust; (1) weak** (Rowe, 1988: Ch 124; Hu *et al*., 1997: Ch 25; Luo *et al*., 2002: Ch151; Horovitz and Sánchez-Villagra, 2003: Ch 53).

97. **Entepicondyle of the humerus: (0) much less than one-half width of the distal humerus; (1) about one half of the distal humerus width.**

98. **Ectepicondoid crest (supinator crest): (0) well developed with proximal extremity confluent with the humeral shaft; (1) well developed with marked notch separating the crest from the shaft (2) weak or absent.** (Modified from Luo *et al*., 2002: Ch 152; Horovitz and Sánchez-Villagra, 2003: Ch 48).

99. **Olecranon fossa: (0)shallow fossa; (1) deep fossa; (2) perforated** (Modified from Horovitz and Sánchez-Villagra, 2003: Ch 47).

FOREARM

100. **Olecranon process of the ulna: (0) absent or unossified; (1) present or ossified** (Modified from: Sidor and Hopson, 1998: Ch 149; Hopson and Kitching, 2001: Ch 91; Bonaparte *et al*., 2003: Ch 45).

101. **The coronoid process of the ulna: 0: absent or weakly developed; 1: prominent.** (Modified from Horovitz and Sánchez-Villagra, 2003: Ch 59).

102. **Ulnar flange: (0) high and prominent; (1) low and weak.**

103. **Radial tuberosity for m. biceps brachii: (0) indistinct or a swelling on a low ridge; (1) tuberosity distal to ulnar facet.**

104. **Styloid process of the ulna: (0) weak or absent; (1) prominent.**

MANUS

105. **The size of the scaphoid: (1) smaller than triquetrum; (1) larger than triquetrum.**

106. **The proximal articular surface of the scaphoid: (0) mainly on the dorsal aspect of the bone; (1) extending medially.**

107. **Morphology of the triquetrum: (0) roughly rectangular; (1) roughly triangular.**

108. **Distomedial process of the scaphoid: (0) absent; (1) present (Modified from Luo *et al*., 2002: Ch 154).**

109. **Distal carpal V: (0) present; (1) fused with carpal IV to form hamate or absent** (Modified from Sidor and Hopson, 1998: Ch 151).

110. **Size of the triquetrum vs. hamate: (0) triquetrum larger; (1) subequal; (2) hamate larger** (Modified from Luo *et al*., 2003: Ch 192; Luo and Wible, 2005: Ch 209).

111. **Size ration between trapezium and trapezoid: (0) trapezium larger; (1) subequal; (2) trapezoid larger** (modified from Luo *et al*., 2003: Ch 193; Luo and Wible, 2005: Ch 210).

112. **Development of centrale (Centralia) in carpus: (0) two; (1) one centrale; (2) no separated centrale present.**

113. **Phalanx number of manual digit III: (0) four; (1) three** (Hopson and Kitching, 2001: Ch 92; Modified from Sidor and Hopson, 1998: Ch 152).

114. **Phalanx number of manual digit IV: (0) four; (1) three** (Hopson and Kitching, 2001: Ch 93; Modified from Sidor and Hopson, 1998: Ch 153).

115. **Ration of the length of metacarpal II to that of metacarpal IV: (0) Mc II much shorter than Mc IV (ratio < 0.8); (1) roughly equal in length (ratio > 0.8).**

116. **Length of metacarpal III: (0) Mc III shorter than Mc IV; (1) longer than Mc IV or roughly equal in length.**

PELVIC GIRDLE

117. **Development of the posterior process of the ilium (measured by its length relative to the diameter of the acetabulum, Hopson and Kitching, 2001: Ch 95): (0) well-development (> 0.5 time of the acetabular diameter); (1) weak or absent (<= 0.5 time of the acetabular diameter)**. (Modified from Sidor and Hopson, 1998: Ch 156; Hopson and Kitching, 2001: Ch 95; Bonaparte *et al*., 2003: Ch 47; Luo *et al*., 2003: Ch 196; Luo and Wible, 2005: Ch 213).

118. **Relative length of the anterior process of ilium anterior to the acetabulum (relative to the diameter of the acetabulum): (0) less than 1.0; (1) 1.0-1.5; (2) greater than 1.5** (Hopson and Kitching, 2001: Ch 94).

119. **Orientation of the acetabular facet of the ilium: (0) facing lateroventrally; (1) facing posteriorly or posteroventrally.**

120. **Dorsal profile of the ilium: (0) strongly convex; (1) flat to concave** (Hopson and Kitching, 2001: Ch 96)..

121. **Longitudinal ridge on the lateral aspect of the ilium: (0) absent; (1) present.**

122. **Anterior extension of the pubis: (0) anterior process beyond the acetabulum; (1) ventral or posteroventral to acetabulum, no anterior process.**

123. **Total length (or anteroposterior width) of the pubis relative to acetabular diameter: (0) much greater than 1; (1) subequal or less than 1** (Modified from Sidor and Hopson, 1998: Ch 161; Hopson and Kitching, 2001: Ch 97).

124. **The acetabular facet of the pubis: (0) facing posterodorsally; (1) facing dorsally.**

125. **Development of the ischial tuberosity: (0) rounded tuberosity, thicker than the ischial blade; (1) hypertrophied protuberance projecting posterodorsally.**

126. **Development of the ischiatic spine: (0) absent or indistinct; (1) present** (Modified from Luo *et al*., 2003: Ch 200).

127. **Development of the iliopubic eminence: (0) small, low and rounded eminence; (1) hypertrophied broad process** (Modified from Horovitz and Sánchez-Villagra, 2003: Ch 73).

128. **Fusion of the ilium, ischium and pubis in adult: (0) unfused; (1) fused** (Modified from Ji *et al*., 1999: Ch 36; Luo *et al*., 2002: Ch 157; Luo *et al*., 2003: Ch 198; Luo and Wible, 2005: Ch 215).

129. **Epipubic bone: (0) absent; (1) present** (Horovitz and Sánchez-Villagra, 2003: Ch 76; (Luo *et al*., 2003: Ch 201; Luo and Wible, 2005: Ch 218).

130. **Acetabulum position relative to auricle facet: (0) ventral; (1) posteroventral** (Modified from Sidor and Hopson, 1998: Ch 165).

131. **Acetabular dorsal emargination between ilium and ischium: open; (1) closed.** (Modified from Rowe, 1988: Ch 134; Hu *et al*., 1997: Ch 27; Luo *et al*., 2002: Ch 156; Luo *et al*., 2003: Ch 197; Luo and Wible, 2005: Ch 214).

132. **Development of the acetabular notch: (0) between iliac and ischial parts of the acetabulum; (1) between the acetabular surface and the pubic process of the ischium; (2) absent** (Modified from Horovitz and Sánchez-Villagra, 2003: Ch 75).

133. **Obturator foramen position relative to the acetabulum: (0) ventral; (1) posteroventral.**

134. **Size of the obturator foramen: (0) smaller than that of the acetabulum; (1) larger than or equal to that of the acetabulum** (Rowe, 1988: Ch 139; Hu *et al*., 1997: Ch 28; modified in Horovitz and Sánchez-Villagra, 2003: Ch 72).

HINDLIMB

FEMUR

135. **Morphology of the Femoral shaft: (0) proximal portion turns dorsomedially; (1) roughly straight.**

136. **Femoral head: (0) oval; (1) nearly spherical** (Modified from Sidor and Hopson, 1998: Ch 168).

137. **Development of the neck below the femoral head: (0) absent, no constriction below the head; (1) incipient neck indicated by faint constriction; (2) well defined neck, well constricted** (Modified from Rowe, 1988: Ch 141, 142; Hu *et al*., 1997: Ch 29; Sidor and Hopson, 1998: Ch 172; Hopson and Kitching, 2001: Ch 98; Luo *et al*., 2002: Ch 159; Bonaparte *et al*., 2003: Ch 49).

138. **Separation between the greater trochanter and the femoral head: (0) greater trochanter and head confluent; (1) a distinct notch separating two structures** (Sidor and Hopson, 1998: Ch 172; Hopson and Kitching, 2001: Ch 98; Bonaparte *et al*., 2003: Ch 49).

139. **Ridge connecting the greater trochanter and the femoral head: (0) present; (1) absent** (Hopson and Kitching, 2001: Ch 99).

140. **Orientation of the greater trochanter: (0) directed proximolaterally; (1) directly proximally** (Modified from Rowe, 1988: Ch 143; Hu *et al*., Ch 30; Luo *et al*., 2002: Ch 161).

141. **Dorsal reflection of the greater trochanter: (0) present; (1) absent.**

142. **Development of Trochanteric fossa: (0) large, shallow and rounded fossa; (1) small, deep and irregular fossa.**

143. **Position of the lesser trochanter: (0) on the ventral surface of the femoral shaft; (1) on the ventromedial aspect of the femoral shaft; (2) on the medial aspect of the femoral shaft** (Modified from Rowe, 1988:

Ch 144; Hu *et al*., 1997 Ch 31; Sidor and Hopson, 1998: Ch 174; Hopson and Kitching, 2001: Ch 100; Luo *et al*., 2002: Ch 162; Bonaparte *et al*., 2003: Ch 50).

144. **Size and shaper of the less trochanter: (0) elongate bony wing extending more than 1/3 of the femoral length; (1) triangular bony wing about 1/4 to 1/5 of the femoral length; (2) triangular bony wing less than 1/6 of the femoral length; (3) nearly rounded eminence** (Modified from Rowe, 1988: Ch 144; Hu *et al*., 1997 Ch 32; Luo *et al*., 2002: Ch 163).

145. **Shape of femur at cross section: (0) rounded or rectangular; (1) dorsoventrally compressed.**

146. **Patellar facet the femur: (0) flat, no groove; (1) shallow groove; (2) deep groove with lateral and medial ridges.** (Modified from Rowe, 1988: Ch 145; Hu *et al*., 1997: Ch 33; Luo *et al*., 2002: Ch 164).

147. **Patella: (0) absent; (1) present.**

148. **Development of intercondylar fossa of the femur: (0) indistinct; (1) distinct.**

LOWER HINDLIMB

149. **Dimension of tibia at Cross section: (0) anteroposterior flattening; (1) not flattening anteroposteriorly.**

150. **Lateral margin of the tibia: (0) markedly concave along the entire length; (1) concave at the proximal 1/3 of the shaft; (2) concave near the proximal end.**

151. **Proximolateral process of the tibia: (0) distinct laterally projecting process; (1) indistinct; (2) hook-like process**. (Modified from Luo *et al*., 2002: Ch 165).

152. **Tibial tuberosity and cnemial crest: (0) indistinct; (1) distinct.**

153. **Articulation between femur and fibula: 0: present; 1: absent.** (Modified from Luo *et al*., 2002: Ch 167; Horovitz and Sánchez-Villagra, 2003: Ch 84).

154. **Proximal head of the fibula: (0) not extending beyond the knee joint; (1) well beyond the knee joint.** (Modified from Horovitz and Sánchez-Villagra, 2003: Ch 85).

155. **Tibial medial malleolus (0) indistinct; (1) distinct** (Modified from Hu *et al*., 1997: Ch 34; Luo *et al*., 2002: Ch 166; Horovitz and Sánchez-Villagra, 2003: Ch 88).

156. **Fibular external malleolus (0) absent or indistinct; (1) distinct** (Modified from Hu *et al*., 1997: Ch 34; Luo *et al*., 2002: Ch 168).

PES

157. **Calcaneofibular articulation: (0) well-developed; (1) reduced or absent** (Modified from Hu *et al*., 1997: Ch 35; Horovitz, 2000: Ch 4; Luo *et al*., 2002: Ch 169; Horovitz and Sánchez-Villagra, 2003: Ch 125).

158. **Astragalofibular facet of astragalus: (0) separated from lateral astragalotibial facet by a nonarticular groove; (1) continuous with lateral astragalotibial facet without distinct angle; (2) forming an obtuse angle with lateral astragalotibial facet; (3) forming a right**

angle with lateral astragalotibial facet (Modified from Horovitz, 2000: Ch 14; Horovitz and Sánchez-Villagra, 2003: Ch 99).

159. **Astragalotibial facet(s) of astragalus: (0) lateral and medial facets continuous; (1) a ridge separating lateral and medial facets.** (Horovitz and Sánchez-Villagra, 2003: Ch 107).

160. **Lateral astragalotibial facet of the astragalus: (1) gently flat or slightly convex; (1) as trochlea** (Luo *et al*., 2002: Ch 173; Horovitz, 2000: Ch 14).

161. **Astragalar neck: (0) absent; (1) present** (Modified from Ji *et al*., 1999: Ch 46; Horovitz, 2000: Ch 12, 16; Luo *et al*., 2002: Ch 172; Horovitz and Sánchez-Villagra, 2003: Ch 100).

162. **Astragalar head: (0) absent; (1) present as the narrowed distal extremity; (2) present as expanded distal extremity** (Modified from Horovitz, 2000: Ch 13).

163. **Astragalonavicular facet extension on medial side of the bone: (0) absent; (1) present** (Modified from Horovitz and Sánchez-Villagra, 2003: Ch 95).

164. **Astragalonavicular facet extension on ventromedial area of the bone: (0) absent; (1) present** (Modified from Horovitz and Sánchez-Villagra, 2003: Ch 96).

165. **Superposition (overlapping) of the astragalus over the calcaneus: (0) slight overlapping; (1) partially superposition; (2) well-developed; (3) absent** (Modified from Hu *et al*., 1997 Ch 36; Luo *et al*., 2002: Ch 170).

166. **Development of sustentaculum tali of the calcaneus: (0) blunt protuberance; (0) acute process; (2) absent** (Modified from Horovitz and Sánchez-Villagra, 2003: Ch 111).

167. **Orientation of the sustentacular facet of the calcaneus: (0) nearly vertical (medial or anteromedial); (0) oblique (dorsomedial); (2) nearly dorsal** (Modified from Horovitz, 2000: Ch 1; Luo *et al*., 2002: Ch 171; Horovitz and Sánchez-Villagra, 2003: Ch 118).

168. **Calcaneal tuber (0) with tip ventromedially pointed; (1) with a terminal swelling dorsally pointed** (Modified from Rowe, 1988: Ch 151; Hu *et al*., 1997: Ch 37; Sidor and Hopson, 1998: Ch 175; Horovitz, 2000: Ch 3; Luo *et al*., 2002: Ch 174).

169. **Calcaneus body cross-section at level of calcaneoastragalar facet: (0) dorsoventrally depressed; (1) mediolaterally compressed** (Horovitz, 2000: Ch 2).

170. **Peroneal process of the calcaneus: (0) as broad and laterally directed shelf; (1) as anteriorly positioned process with shallow or no groove at the base; (2) as anteriorly positioned process with deep groove at the base** (Modified from Hu *et al*. 1997: Ch 38; Horovitz, 2000: Ch 10; Luo *et al*., 2002: Ch 175; Horovitz and Sánchez-Villagra, 2003: Ch 115 and 116).

171. **Calcaneocuboid facet of the calcaneus: (0) facing distoventrally and medially; (1) facing distomedially; (2) facing distally** (Modified from Horovitz, 2000: Ch 8; Luo *et al*., 2002: Ch 176).

172. **Approximation between the Metatarsal V and the peroneal process of the calcaneus: (0) absent; (1) present.**

173. **Orientation of calcaneus relative to the long axis of the foot: (0) nearly aligned; (1) calcaneus transversely oriented** (Modified from Luo *et al*., 2002: Ch 179).

174. **Phalangeal number of pedal digital IV: (0) four; (1) three** (modified from Sidor and Hopson, 1998: Ch 179).

OTHER POSTCRANIAL FEATURES

175. **Sesamoid bones in flexor tendons: (0) absent; (1) present, single; (2) present, paired** (modified from Rowe, 1988: Ch 158; Hu *et al*., 1997: Ch 39; Luo *et al*., 20002: Ch 180).

176. **External pedal (tarsal) spur: (0) absent; (1) present** (Hu *et al*., 1997 Ch 40; Luo *et al*., 2002: Ch 181).

CRANIAL CHARACTERS (151 characters)

FACIAL PORTION

177. **Development of the internarial process of the premaxilla between the external nares: (0) present and separating the external nares; (1) absent and external nares confluent** (Kemp, 1983: p 364; Sues, 1985: p 207; modified from Luo *et al*., 2002: Ch 260).

178. **Development of the septomaxilla: (0) present with intranarial process; (1) present without intranarial process; (2) absent** (Modified from Rougier *et al*., 1998: Ch 78; Sidor and Hopson, 1998: Ch 6; Wang *et al*.,

2001: Ch 1; Wible *et al*., 2001: Ch 78; Luo *et al*., 2002: Ch 259; Horovitz and Sánchez-Villagra, 2003: Ch 201; Luo and Wible, 2005: Ch 404).

179. **Facial process of the premaxilla (0) not contacting the nasal; (1) contacting the nasal** (Wible, *et al*., 2001: Ch 80; Luo *et al*., 2002: Ch 261).

180. **Shape of nasals: 0 posteriorly expanded; 1: not posteriorly expanded** (Horovitz and Sánchez-Villagra, 2003: Ch 200).

181. **Prefrontal: (0) present; (1) absent** (Sidor and Hopson, 1998: Ch 9; Hopson and Kitching, 2001: Ch 3; Bonaparte *et al*., 2003: Ch 22).

182. **Naso-frontal contact: (0) medial process of frontals wedged between nasals; (1) anterolateral projection of frontal contacting nasals medially; (2) no distinct wedging between nasals and frontals** (modified from Wible *et al*., 2001: Ch 84; Bonaparte *et al*., 2003: Ch 20).

183. **Nasolacrimal contact vs. maxillofrontal contact: (0) nasolacrimal contact; (1) maxillofrontal contact** (modified from Wible *et al*., 2001: Ch 86; Horovitz and Sánchez-Villagra, 2003: Ch 183).

184. **Exist (s) of infraorbital canal on maxilla: (0) two or more; (1) single** (Modified from Wible *et al*., 2001: Ch 82; Luo and Wible, 2005: Ch 375).

185. **Nasal foramina: (0) present; (1) absent** (Wible *et al*., 2001: Ch 85; Luo *et al*., 2002: Ch 258).

186. **Facial process of the lacrimal: (0) large triangular; (1) small crescentic; (2) absent (Luo *et al*., 2002: Ch 246).**

187. **Lacrimal foramen number: (0) double; (1) single** (Wible *et al*., 2001: Ch 89).

188. **Location of lacrimal foramen (0) on the edge of the orbit or on face; (1) within orbit** (Modified from Wible *et al*., 2001: Ch 88).

189. **Relative length of the face (preorbital length relative to postorbital length): (0) two-thirds or more; (1) less than two-thirds** (modified from Wible *et al*., 2001: Ch 90).

PALATE

190. **Incisive foramen: (0) absent; (1) present** (Sidor and Hopson, 1998: Ch 5).

191. **Posterior edge of the incisive foramen: (0) formed by maxilla; (1) formed by premaxilla** (Modified from Sidor and Hopson, 1998: Ch 4; Hopson and Kitching, 2001: Ch 1; Bonaparte *et al*., 2003: Ch 21).

192. **Palatal process of the premaxilla: (0) not reaching the canine alveolus; (1) reaching the canine alveolus** (Horovitz and Sánchez-Villagra, 2003: Ch 203).

193. **Ventral surface of the vomer: (0) broad plate; (1) narrow keel** (Modified from Sidor and Hopson, 1998: Ch 24; Hopson and Kitching, 2001: Ch 8).

194. **Secondary palatal plate on maxilla: (0) not reaching the midline; (1) reaching the midline** (Modified from Sidor and Hopson, 1998: Ch 31; Hopson and Kitching, 2001: Ch 12).

195. **Secondary palatal plate on palatine: (0) not reaching the midline; (1) reaching the midline** (Modified from Sidor and Hopson, 1998: Ch 33; Hopson and Kitching, 2001: Ch 13).

196. **Length of secondary palate relative to tooth row: (0) shorter; (1) about equal; (2) longer** (Sidor and Hopson, 1998: Ch 34; Hopson and Kitching, 2001: Ch 14; Wang *et al*., 2001: Ch 7; Luo *et al*., 2002: Ch 237; Bonaparte *et al*., 2003: Ch 26).

197. **Posterior extension of the secondary palate relative to the anterior border of the orbit: (0) anterior to the orbit; (1) posterior to the anterior border of the orbit** (Modified from Hopson and Kitching, 2001: Ch 15).

198. **Minor palatine foramen: (0) absent; (1) present** (modified from Wible *et al*., 2001: Ch 97; Horovitz and Sánchez-Villagra, 2003: Ch 204; Luo and Wible, 2005: 371).

199. **Postpalatine torus: (0) absent; (1) present** (Wible *et al*., 2001: Ch 95; Luo and Wible, 2005: Ch 367).

ORBIT AND SIDE WALL OF BRAINCASE

200. **Jugal: (0) contact the lacrimal and facial process of the maxilla; (1) not contacting the lacrimal;** (Modified from Wang *et al*., 2001: Ch 2; Luo *et al*., 2002: Ch 249; Luo and Wible, 2005: Ch 392).

201. **Maxillary-jugal contact on lateral side: (0) bifurcated; (1) not bifurcated** (Wible *et al*., 2001: Ch 91).

202. **Glenoid process of jugal: (0) absent; (1) present** (modified from Wible *et al*., 2001: Ch 116; Luo and Wible, 2005: Ch 393).

203. **Zygomatic arch: (0) stout, (1) delicate** (Modified from Wible *et al*., 2001: Ch 92; Hopson and Kitching, 2001: Ch 18; Luo *et al*., 2002: Ch 250).

204. **Dorsal extension of the zygomatic arch: (0) below middle of orbit; (1) above middle of the orbit** (Hopson and Kitching, 2001: Ch 19).

205. **Palatine participating in the subtemporal margin of the orbit: (0) excluded; (1) participating** (Luo *et al*., 1994; Kielan-Jaworowska *et al*., 2004: p 115).

206. **Postorbital: (0) present; (1) absent** (Sidor and Hopson, 1998: Ch 12; Hopson and Kitching, 2001: Ch 5; Bonaparte *et al*., 2003: Ch 23).

207. **Postorbital bar: (0) present; (1) absent** (Sidor and Hopson, 1998: Ch 17; Bonaparte *et al*., 2003: Ch 40).

208. **Frontal-palatine contact in orbit: (0) absent; (1) present** (Sidor and Hopson, 1998: Ch 53; Hopson and Kitching, 2001: Ch 23; Bonaparte *et al*., 2003: Ch 29).

209. **Alisphenoid-parietal contact: (0) present; (1) absent** (Modified from Wang *et al*., 2001: Ch 3; Luo *et al*., 2002: Ch 244; Horovitz and Sánchez-Villagra, 2003: Ch 176).

210. **Alisphenoid-frontal contact: (0) anterodorsal corner of the alisphenoid contact posteroventral corner of the frontal; (1) half of dorsal edge of the alisphenoid contacting the frontal; (2) no contact** (modified from Luo *et al*., 248).

211. **Development of the orbitosphenoid: (0) no ossified orbitosphenoid developed, and a large orbital vacuity present; (1) a small ossified orbitosphenoid and a sizable orbital vacuity present; (2) orbitosphenoid closing the orbital vacuity** (modified from Wang *et al*., 2001: Ch2; Luo *et al*., 2002: Ch 243; Luo and Wible, 2005: Ch 387).

212. **Optic foramen as individual foramen: (0) absent; (1) present** (Wible *et al*., 2001: Ch 102; Luo and Wible, 2005: Ch 388).

213. **Anterior lamina of the petrosal vs. squama of squamosal: (0) anterior lamina large and forming the lateral braincase wall, squama absent; (1) both anterior lamina and squama present; (2) anterior lamina vestigial or absent, squama present** (modified from Hu *et al*., 1997 Ch 41; Wible *et al*., 2001: Chs 108, 113; Wang *et al*., 2001: Ch 4; Luo *et al*., 2002: Ch 183; Luo and Wible, 2005: Chs 278, 320).

214. **Exit for maxillary branch of trigeminal nerve: (0) between the anterior lamina and alisphenoid; (1) within anterior lamina; (2) within the alisphenoid; (3) anterior to alisphenoid** (Modified from Sidor and Hopson, 1998: Ch 57; Hopson and Kitching, 2001: Ch 28; Wang *et al*., 2001: Ch 5; Wible *et al*., 2001: Ch 110; Bonaparte *et al*., 2003: Ch 33; Luo and Wible, 2005: Ch 389).

215. **Exit for mandibular branch of trigeminal nerve: (0) between the anterior lamina and alisphenoid; (1) within anterior lamina; (2) within the alisphenoid; (3) between alisphenoid and squamosal** (Modified from Sidor and Hopson, 1998: Ch 57; Hopson and Kitching,

2001: Ch 28; Wang *et al*., 2001: Ch 5; Wible *et al*., 2001: Ch 110; Bonaparte *et al*., 2003: Ch 33; Luo and Wible, 2005: Ch 389).

216. **Orbitotemporal groove/canal: (0) orbitotemporal groove present on lateral side of braincase; (1) intramural or endocranial, with posterior opening of orbitotemporal canal present; (2) absent** (See Rougier *et al*., 1992 for detailed discussion; modified from Wible *et al*., 1995: Ch 43; Rougier *et al*., 1996a, b: 50; Wible *et al*., 2001: Ch 103; Luo and Wible 2005: Ch 390).

BASICRANIUM

PTERYGOID-BASISPHENOID REGION

217. **Ectopterygoid: (0) present; (1) absent** (Modified from Sidor and Hopson, 1998: Ch 27; Hopson and Kitching, 2001: Ch 9).

218. **Interpterygoid vacuity in adults: (0) present; (1) closed** (Sidor and Hopson, 1998: Ch 28; Hopson and Kitching, 2001: Ch 10; Bonaparte *et al*., 2003: Ch 25).

219. **Pterygopalatine crests: (0) present; (1) absent** (Wang *et al*., 2001: Ch 9; Wible *et al*., 2001: Ch 100; Luo *et al*., 2002: Ch 239).

220. **Pterygoid contact on midline: (0) contact; (1) separate** (Wible *et al*., 2001: Ch 99).

221. **Lateral flange of the pterygoid: (0) massive and lateroventrally projecting flange; (1) small, posteroventrally directed process; (2) reduced or absent** (Modified from Luo *et al*., 2002: Ch 240).

222. **Ectopterygoid process of alisphenoid: (0) absent, (1) present** (Wible *et al*., 2001: Ch 101; Luo and Wible, 2005: Ch 339).

223. **Pterygoid constriction of the basicranium (0) distinct; (1) not distinct** (modified from Wang *et al*., 2001: Ch 10; Luo *et al*., 2002: Ch 241).

EAR AND NEIGHBORING REGIONS

224. **Suspension of the quadrate (incus) on the basicranium: (0) primarily squamosal with quadrate notch on squamosal; (1) both squamosal and petrosal; (2) primarily petrosal with fossa incudis** (modified from Hu *et al*., 1997 Ch 42; Sidor and Hopson, 1998: Ch 58; Hopson and Kitching, 2001: Ch 29, 31; Wang *et al*., 2001: Ch 14; Luo *et al*., 2002: Ch 234; Luo and Wible, 2005: Ch 356).

225. **Development of a glenoid fossa for a condyle of the dentary: (0) absent; (1) as medially facing facet; (1) as ventrally facing fossa** (Modified from Wang *et al*., 2001: Ch 17; Luo *et al*., 2002: Ch 187; Luo and Wible, 2005: Ch 26).

226. **Shape of the glenoid fossa: (0) concave fossa, open anteriorly; (1) troughlike fossa, mediolaterally oriented** (modified from Wible *et al*., 2001: Ch 115).

227. **Postglenoid process: (0) indistinct; (1) distinct** (Wible *et al*., 2001: Ch 118; Luo *et al*., 2002: Ch 188; Horovitz and Sánchez-Villagra, 2003: Ch 187).

228. **External auditory meatus on squamosal: (0) as sulcus on the posterolateral surface of the squamosal; (1) indistinct; (2) as**

postglenoid depression of the squamosal (modified from Hu *et al*., 1997: Ch 43; Sidor and Hopson, 1998: Ch 52; Wang *et al*., 2001: Ch 15; Hopson and Kitching, 2001: Ch 22; Luo *et al*., 2002: Ch 185; Bonaparte *et al*., 2003: Ch 28).

229. **Postglenoid foramen: (0) absent; (1) behind the postglenoid process; (2) medial or anteromedial to the postglenoid process** (Modified from Wible *et al*., 2001: Ch 120; Luo *et al*., 2002: Ch 189; Horovitz and Sánchez-Villagra, 2003: Ch 190, 191).

230. **Development of the petrosal: (0) prootic and ophistotic sutured; (1) prootic and ophistotic fused** (Rowe, 1988: Ch 51; Bonarparte *et al*., 2005: Ch 56).

231. **Petrosal promontorium: (0) absent; (1) present, narrow and elongate; (2) present, oval or globular** (modified from Rowe, 1988: Ch 52; Wible, 1991: Ch 6; Wible and Hopson, 1993: Ch 28; Hu *et al*., 1997: Ch 45; Wang *et al*., 2001: Ch 19, 20; Luo *et al*., 2002: Ch 193; Horovitz and Sánchez-Villagra, 2003: Ch 214; Luo and Wible, 2005: Ch 297).

232. **Cochlea: (0) short recess or canal, uncoiled; (1) elongate canal and not coiled; (2) elongate canal and partly coiled; (3) coiled at least 360 degree** (Rowe, 1988: Ch 59; Wible, 1991: Ch19; Wible and Hopson, 1993: Ch 15; Wible *et al*., 1995: Ch 9; Rougier *et al*., 1996a: Ch 6; Rougier *et al*., 1996b: Ch 6; Hu *et al*., 1997 Ch 46; Wang *et al*., 2001: Ch 21; Luo *et al*., 2002: Ch 194; Horovitz and Sánchez-Villagra, 2003: Ch 222; Luo and Wible, 2005: Ch 298).

233. **Crista interfenestralis: (0) horizontally extended to base of the paroccipital process; (1) vertical, delimiting the back of the promontorium; (2) connecting with caudal tympanic process** (Modified from Rougier *et al*., 1996a, b: Ch 15; Hu *et al*., 1997: Ch 47; Wang *et al*., 2001: Ch 22; Wible *et al*., 2001: Ch 133; Luo *et al*., 2002: Ch 198; Luo and Wible, 2005: Ch 303).

234. **Osseous spiral laminae within the cochlea: (0) absent; (1) present** (see Meng and Fox, 1995a, b for discussion; modified from Wible *et al*., 1995: Ch 10; Rougier *et al*., 1996 a, b: Ch 7; Wang *et al*., 2001: Ch 23; Luo *et al*., 2002: Chs 196, 197; Luo and Wible, 2005: Ch 301, 302).

235. **Separation of the fenestra cochleae from the jugular foramen (0) confluent; (1) partially separated by fingerlike projection from posterolateral wall of jugular foramen; (2) completely separate** (modified from Hopson and Kitching, 2001: Ch 42; Wang *et al*., 2001: Ch 43; Luo *et al*., 2002: Ch224; Bonaparte *et al*., 2003: Ch 39).

236. **Jugular fossa (common depression for the fenestra cochleae and the jugular foramen): (0) present; (1) absent** (Rougier *et al*., 1996 a, b: Ch 13; Wang *et al*., 2001: Ch 44).

237. **Development of the osseous sulcus/canal for the perilymphatic duct: (0) absent; (1) open sulcus or partially enclosed canal; (2) enclosed canal** (modified from Wible and Hopson, 1993; Rougier *et al*., 1996a; Wang *et al*., 2001: Ch 45; Luo *et al*., 2002: Ch 225).

238. **Hypoglossal foramen: (0) separated from jugular foramen; (1) confluent with jugular foramen** (modified from Rougier *et al*., 1996: Ch 51; Wang *et al*., 2001: Ch 55; Luo *et al*., 2002: Ch 227; Horovitz and Sánchez-Villagra, 2003: Ch 205). Only in monotremes the hypoglossal foramen is confluent with the jugular foramen.

239. **Separate foramina for vestibular and cochlear nerves: (0) absent; (1) present** (Wible and Hopson, 1993: Ch 12; Wible *et al*., 1995: Ch 35; Sidor and Hopson, 1998: Ch 71; Hopson and Kitching, 2001: Ch 36; Bonaparte *et al*., 2003: Ch 36).

240. **Development of an osseous floor beneath the geniculate ganglion: (0) absent; (1) present** (Modified from Wible and Hopson, 1993: Ch 5; Wible *et al*., 1995: Ch 24; Rougier *et al*., 1996a, b: Ch 35; Wang *et al*., 2001: Ch 27; Luo *et al*., 2002: Ch 203).

241. **Hiatus Fallopii: (0) absent; (1) on the tympanic surface of the petrosal; (2) at the anterior edge of the petrosal** (Wang *et al*., 2001: Ch 28; Wible *et al*., 2001: Ch 123; Luo and Wible, 2005: Ch 314).

242. **Lateral flange of the petrosal: (0) laterally or lateroventrally directed shelf; (1) ventrally directed ridge; (2) ventromedially extended shelf, contacting or overlapping the promontorium; (3) vestigial or absent** (modified from Wible *et al*., 1995: Ch 30; Rougier *et al*., 1996a, b: Ch 29; Hopson and Kitching, 2001: Ch 34; Wang *et al*., 2001: Ch 34; Wible *et al*., 2001: Ch 126; Luo *et al*., 2002: Ch 207; Luo and Wible, 2005: Ch 321).

243. **Quadrate ramus of the pterygoid: (0) present; (1) absent** (Wible, 1991: Ch 47; Sidor and Hopson, 1998: Ch 63; Hopson and Kitching, 2001: Ch 30; Bonaparte *et al*., 2003: Ch 34).

244. **Quadrate ramus of the alisphenoid: (0) well-developed; (1) vestigial or absent** (Wible 1991: Ch 46; Wible and Hopson, 1993: Ch 32; Rougier *et al*., 1996a, b: Ch 37; Wang *et al*., 2001: Ch 52; Luo *et al*., 2002: Ch206; Luo and Wible, 2005: Ch 318).

245. **Tympanic process of the alisphenoid: (0) absent; (1) present** (Wible *et al*., 2001: Ch 121; Luo *et al*., 2002: Ch 222; Luo and Wible, 2005: Ch 340).

246. **Lateral trough: (0) absent; (1) present** (Wible *et al*., 1995: Ch 25; Rougier *et al*., 1996a, b: Ch 34; Wang *et al*., 2001: Ch 26; Luo *et al*., 2002: Ch 202; Luo and Wible, 2005: Ch 311).

247. **Cavum epiptericum: (0) no floor; (1) only partially floored by lateral trough; (2) completely floored, by lateral trough; (3) floored by alisphenoid and petrosal; (4) with a narrow piriform fenestra on floor** (Modified from Rowe, 1988: Ch 49; Wible, 1991: Ch 54; Wible and Hopson, 1993: Ch 6; Wible *et al*., 1995: Ch 23; Rougier *et al*., 1996: Ch 35; Wang *et al*., 2001: Ch 51; Wible *et al*., 2001: Ch 109; Luo *et al*., 2002: Ch 204; Luo and Wible, 2005: Ch 312).

248. **Ossified base of the pila antotica: (0) present; (1) absent** (Rowe, 1988: Ch 43; Wible, 1991: Ch 4; Wible and Hopson, 1993: Ch 14; Wible *et al*., 1995: Ch 37; Luo *et al*., 2002: Ch 247; Luo and Wible, 2005: Ch 386).

249. **The crista parotica: (0) indistinct; (1) as bulbous process; (2) as crest** (Modified from Wang *et al*., 2001: Ch32; Luo *et al*., 2002: Ch 215; Luo and Wible, 2005: Ch 329).

250. **Paroccipital posterior ridge bounding middle ear: (0) absent; (1) present** (Sidor and Hopson, 1998: Ch 74).

251. **Epitympanic recess: (0) absent; (1) present** (Rougier *et al*., 1996a, b: Ch 25; Hu *et al*., 1997: Ch 50; Wang *et al*., 2001: Ch 46; Luo *et al*., 2002: Ch 216; Luo and Wible, 2005: Ch 330).

252. **Epitympanic recess flanked laterally by squamosal: (0) absent; (1) present** (Modified from Hu *et al*., 1997: Ch 51; Wible *et al*., 2001: Ch 138; Wang *et al*., 2001: Ch 48). This character is only applicable to taxa with epitympanic recess developed.

253. **Hypotympanic recess of the middle ear: (0) absent; (1) present** (Modified from Wible *et al*., 2001: Ch 140; Luo *et al*., 2002: Ch 223).

254. **Relationship of the lateral flange to the paroccipital region: (0) separated; (1) continuous** (modified from Rougier *et al*., 1996a: Ch 30; Wang *et al*., 2001: Ch 36; Luo *et al*., 2002: Ch 210; Luo and Wible, 2005: Ch 324).

255. **Ventral projection of the paroccipital process of the petrosal beyond surrounding structures: (0) indistinct; (1) distinct** (Wible, 1991: Ch 57; Wible and Hopson, 1993: Ch 25; Wible *et al*., 1995; Rougier *et al*., 1996: Ch 17; Wang *et al*., 2001: Ch 41; Wible *et al*., 2001: Ch 131; Luo *et al*., 2002: Ch 214; Luo and Wible, 2005: Ch 328).

256. **Tympanohyal: (0) not fused to petrosal; (1) fused to petrosal** (Modified from Rowe, 1988: Ch 63; Wible, 1991: Ch 31; Wible *et al*., 1995: Ch 16; Rougier *et al*., 1996: Ch 21; Luo and Wible, 2005: Ch 331).

257. **Tympanohyal contact with the promontorium: (0) not contact; (1) contact** (Rougier *et al*., 1996a, b: Ch 22; Luo and Wible, 2005: Ch 331).

258. **Fossa for stapedius muscle: (0) absent; (1) present** (modified from Rowe, 1988: Ch 55; Wible, 1991: Ch 56; Wible and Hopson, 1993: Ch 35; Wible *et al*, 1995: Ch 14; Rougier *et al*., 1996a, b: Ch 16; Wang *et al*., 2001: Ch 42; Luo *et al*., 2002: Ch 226).

259. **Post-promontorial tympanic recess: (0) absent; (1) present** (modified from Wible and Hopson, 1993: Ch 27; Rougier *et al*., 1996: Ch 19; Wang *et al*., 2001: Ch 30; Luo *et al*., 2002: Ch 199; Luo and Wible, 2005: Ch 304).

260. **Caudal tympanic process of the petrosal: (0) absent; (1) present as a tall ridge; (2) present as a notched ridge** (Modified from Wible and Hopson, 1993: Ch 26; Wible *et al*., 1995: Ch 12; Rougier *et al*., 1996a, b: Ch 18; Hu *et al*., 1997 Ch 49; Wang *et al*., 2001: Ch 31; Wible *et al*., 2001: Ch 132; Luo *et al*., 2002: Ch 200; Luo and Wible, 2005: Ch 306).

261. **Development of the para/basisphenoid wing: (0) present; (1) absent** (Modified from Rougier *et al*., 1996a, b: Ch2; Wang *et al*., 2001: Ch 53; Luo *et al*., 2002: Ch 190; Luo and Wible, 2005: Ch 292).

262. **Basioccipital Overlapping the petrosal pars cochlearis: (0) present, overlapping petrosal pars cochlearis and reach the fenestra vestibuli;**

(1) (0) present, overlapping petrosal pars cochlearis and not reach the fenestra vestibuli (2) absent, petrosal pars cochlearis exposed (Modified from Wang *et al*., 2001: Ch 54; Luo *et al*., 2002: Ch 191; Luo and Wible, 2005: Ch 292).

263. **Ventrally exposed epitympanic wing medial to the promontorium (the pars cochlearis): (0) absent; (1) present** (Modified from Wible *et al*., 2001: Ch 122; Wang *et al*, 2001: Ch 47; Luo and Wible, 2005: Ch 338).

264. **Medial process of squamosal in tympanic cavity: (0) absent; (1) present** (Wible *et al*., 2001: Ch 141; Luo *et al*., 2002: Ch 218; Luo and Wible 2005: Ch 333).

265. **Thickened rim of the fenestra vestibuli: (0) present; (1) absent** (Rougier *et al*., 1996a, b: Ch 10; Luo and Wible, 2005: Ch 294).

266. **Bony sulcus/canal for the stapedial artery on the petrosal: (0) absent; (1) present** (Wible *et al*., 2001: Ch 147; Wang *et al*., 2001: Ch 49; Luo *et al*., 2002: Ch 219; Horovitz and Sánchez-Villagra, 2003: Ch 221; Luo and Wible, 2005: Ch 334).

267. **Transpromontorial sulcus for the internal carotid artery: (0) absent; (1) present** (Wible *et al*., 2001: Ch 146; Wang *et al*., 2001: Ch 50; Luo *et al*., 2002: Ch 220; Luo and Wible, 2005: Ch 335).

268. **Foramen for the ramus superior of the stapedial artery (pterygoparoccipital foramen): (0) large fenestra penetrating the petrosal (or between lateral edge of the prootic and ophistotic, squamosal or quadrate may enclose the foramen laterally); (1) open**

notch on the lateral flange of the petrosal; (2) small foramen with petrosal or between petrosal and squamosal; (3) absent (modified from Hu *et al*., 1997 Ch 52; Wang *et al*., 2001: Ch37; Wible *et al*., 2001: CH 154; Luo *et al*., 2002: Ch 211; Luo and Wible, 2005: Ch 325).

269. **Position of the pterygoparoccipital foramen relative to the fenestra vestibuli: (0) Posterior or lateral to the fenestra vestibuli; (1) anterior to the fenestra vestibuli** (Wible *et al*., 1995: Ch 19; Rougier *et al*., 1996 a, b: Ch 28; Wang *et al*., 2001: Ch 38; Luo and Wible, 2005: Ch 326).

270. **Lateral flange vascular groove: (0) present; (1) absent** (Modified from Sidor and Hopson, 1998: Ch 56).

271. **The ascending canal: (0) as extracranial sulcus; (1) intramural or intracranial; (2) absent** (Modified from Wible *et al*., 1995: Ch 41; Rougier *et al*., 1996a, b: Ch 48; Wang *et al*., 2001: Ch57; Wible *et al*., 2001: Ch 152).

272. **The prootic canal: (0) absent; (1) present with a distinct tympanic aperture/apertures; (2) present with the tympanic aperture confluent with the pterygoparoccipital foramen** (modified from Rowe, 1988: Ch 50; Wible, 1991: Ch 28; Wible and Hopson, 1993: Chs 18, 20; Wible *et al*., 1995: Chs 20, 22; Rougier *et al*., 1996: Ch 27; Wang *et al*., 2001: Ch 25; Wible *et al*., 2001: 124; Luo *et al*., 2002: Ch 201; Horovitz and Sánchez-Villagra, 2003: Ch 217; Luo and Wible, 2005: Ch 309).

273. **Notch separating lambdoidal crest (edge) from zygomatic arch: (0) absent; (1) present** (Hopson and Kitching, 2001: Ch 43).

EAR OSSICLES

274. **Stapedial process (crus longum) of the quadrate (incus): (0) absent; (1) present as short process; (1) present as long process** (modified from Sidor and Hopson, 1998: Ch 60; Luo *et al*., 2002: 231).

275. **Dorsal plate (crus brevis) of the quadrate (incus): (0) as large and broad plate bigger than the trochlea (or head); (1) as reduced short process** (modified from Luo *et al*., 2002: Ch 232; Luo and Wible, 2005: Ch 354).

276. **Shape of the quadrate (incus): (0) complex with dorsal plate and/or stapedial process twisted with the trochlea; (1) simple with head and crura brevis and longum roughly in same plane (2) flat** (Meng and Wyss, 1995; modified from Rougier *et al*., 1996: Ch 55; Luo and Wible, 2005: Ch 352).

277. **Dorsal process of the stapes: (0) present; (1) absent** (modified from Sidor and Hopson, 1998: Ch 78).

278. **Stapedial foramen: (0) well developed; (1) vestigial or absent** (modified from Rougier *et al*., 1996b: Ch 54).

279. **Prearticular and articular: (0) not fused; (1) at least partially fused** (Sidor, 2003: Ch 48).

280. **Quadroarticular (incudomallear) articulation: (0) quadrate head (convex)-articular trough; (1) roughly saddle-shaped; (2) gently flat** (Meng and Wyss, 1995; modified from Rougier *et al*., 1996b: Ch 58;

Sidor and Hopson, 1998: Ch 101; Luo *et al*., 2002: Ch 228; Sidor, 2003: Ch 53; Luo and Wible, 2005: Ch 350).

281. **Relative position of quadrate (incus) and articular (malleus): (0) quadrate posterodorsal or posterior to the articular; (1) quadrate dorsal to the articular** (Meng and Wyss, 1995; Rougier *et al*., 1996b: Ch 56; Luo *et al*., 2002: Ch 229; Luo and Wible, 2005: Ch 351).

ROOF OF BRAINCASE

282. **Anterior extension of the frontal: (0) posterior to the anterior border of the orbit; (1) anterior to the orbit but posterior to anterior tip of the lacrimal; (2) anterior to lacrimal.**

283. **Parietal foramen: (0) present; (1) absent** (Sidor and Hopson, 1998: Ch 20; Hopson and Kitching, 2001: Ch 7; Bonaparte *et al*., 2003: Ch 24).

284. **The interparietal: (0) present; (1) absent** (Rowe, 1988: Ch 21; Luo *et al*., 2002: Ch 265).

285. **The sagittal crest: (0) high; (1) low; (2) absent** (Luo *et al*., 2002: Ch 254).

286. **Lateral expansion of the braincase at parietal region: (0) narrow, much alisphenoid and petrosal visible in dorsal view; (1) slightly expanded, only lateral edge of alisphenoid and petrosal visible in dorsal view; (2) moderate expanded, alisphenoid and petrosal not visible in dorsal view, but parietal region not wider than lambdoidal region; (3) well expanded, parietal region wider than lambdoidal**

region (modified from Luo *et al*., 2002: Ch 264; Luo and Wible, 2005: Ch 414).

OCCIPITAL REGION

287. **Tabular: (0) present; (1) absent** (modified from Sidor and Hopson, 1998: Ch 54; Hopson and Kitching, 2001: Ch 24; Luo *et al*., 2002: Ch 255; Luo and Wible, 2005: Ch 400).

288. **The posterior opening of the posttemporal canal: (0) large; (1) small; (2) absent** (Wible *et al*., 2001: Ch 144; Wang *et al*., 2001: Ch 56; Luo *et al*., 2002: Ch 251; Luo and Wible, 2005: Ch 397).

289. **Development of occipital condyle: (0) kidney-shaped and incipiently bicondylic; (1) bicondylic and two condyles clearly separate.**

290. **Position of the occipital condyles relative to the foramen magnum: (0) at the ventrolateral corners of the foramen; (1) lateral to the foramen**.

291. **The lambdoidal crest: (0) well developed; (1) weak or absent** (modified from Luo *et al*., 2002: Ch 253).

292. **Orientation foramen magnum: (0) facing posteriorly; (1) facing posteroventrally**.

LARYNX CHARACTERS

293. **Fusion of the thyroid to hyoid: (0) present; (1) absent.**

294. **Thyroid: (0) with two arches connected by a central copula; (1) arches and copula fused.**

LOWER JAW

295. **Mandibular symphysis: (0) dentary and splenial; (1) dentary only** (Sidor, 2003: Ch 25).

296. **The location of the most posterior mental foramen: (0) anterior half of postcanine region (or premolariform region); (1) posterior half of postcanine region** (or molariform) (modified from Wible *et al*., 2001: Ch 77; Luo and Wible, 2005: Ch 25).

297. **The craniomandibular joint: (0) quadrate-articular; (1) double joint; (2) dentary condyle-squamosal glenoid** (modified from Wang *et al*., 2001: Ch 74; Sidor, 2003: Ch 66; Bonaparte *et al*., 2003: Ch 19).

298. **Articular process (peduncle) of the dentary: (0) absent; (1) present** (Sidor and Hopson, 1998: Ch 87; Sidor, 2003: Ch 18).

299. **Morphology of articular facet of the dentary condyle: (0) as a lateral bulge; (1) flat fact; (2) convex** (modified from Luo *et al*., 2002: Ch 22; Luo and Wible, 2005: Ch 27).

300. **Posteroventral margin of the dentary below the articular process (or posterior corner of the bone if the articular process absent): (0) concave; (1) convex; (2) straight and oblique; (3) straight and nearly vertical** (Modified from Luo *et al*., 2002: Ch 21; Luo and Wible, 2005: Ch 28, 29).

301. **Position of the craniomandibular joint relative to the level of the lower postcanine alveoli: (0) below the alveolar level; (1) about the same level; (2) above the alveolar level** (Modified from Wang *et al*.,

2001: Ch 76; Luo *et al*., 2002: Ch 24; Sidor, 2003: Ch 52; Luo and Wible, 2005: Ch 31).

302. **Postdentary trough of the dentary: (0) broad facets for postdentary bones; concave trough behind the mandibular foramen; (2) absent** (Allin, 1975; modified from Wang *et al*., 2001: Ch 60; Luo *et al*., 2002: Ch 1; Luo and Wible, 2005: Ch 1).

303. **Medial ridge overhang the postdentary trough: (0) absent; (1) present** (modified from Wang *et al*., 2001: Ch 60; Luo *et al*., 2002: Ch 3; Luo and Wible, 2005: Ch 3).

304. **Postdentary bones (articular, prearticular, angular, and surangular) location: (0) contact dentary broadly and well exposed laterally; (1) largely within the postdentary trough; (2) detached from dentary** (Modified from Wang *et al*., 2001: Ch 62; Sidor, 2003: Ch 67).

305. **Size of the postdentary unit (articular, prearticular, angular, and surangular): (0) broad plate, with the height larger than the depth of the horizontal ramus of the dentary (1) rod-like elongate bony bar, with the height much smaller than the depth of the horizontal ramus of the dentary; (2) tiny ring-like complex** (Allin, 1975; Modified from Sidor and Hopson, 1998: Ch 88; Hopson and Kitching, 2001: Ch 49).

306. **Reflected lamina of angular: (0) broad, plate-like; (1) slender, hook-like** (Allin, 1975; Modified from Hopson and Kitching, 2001: Ch 52).

307. **Surangular: (0) distinct element; (1) partially fused with other postdentary bone but still recognizable; (2) lost or fused with other**

element, not recognizable in adult (modified from Sidor and Hopson, 1998: Ch 100; Luo *et al*., 2002: Ch 15; Sidor, 2003: Chs 41, 42).

308. **Lateral exposition of the surangular: (0) present; (1) absent** (Sidor 2003: Chs 45, 47).

309. **Splenial: (0) present in adult; (1) absent in adult** (Wang *et al*., 2001: Ch 72; Luo *et al*., 2002: Ch 14; Sidor, 2003: Ch 23; Luo and Wible, 2005: Ch 15).

310. **Coronoid in adults: (0) present; (1) absent** (modified from Rowe, 1988: Ch 72; Wible, 1991: Ch 86; Hu *et al*., 1997: Ch 55; Wang *et al*., 2001: Ch 67; Luo *et al*., 2002: Ch 11; Luo and Wible, 2005: Ch 11).

311. **Development of the coronoid process of the dentary: (0) present, small and below mid of the orbit; (1) large and above the middle of orbit; (2) vestigial** (modified from Sidor and Hopson, 1998: Ch 86; Hopson and Kitching, 2001: Ch 47; Sidor, 2003: Ch 13; Luo and Wible, 2005: Ch 33).

312. **Orientation of the anterior edge of the coronoid process: (0) strongly tilting posteriorly (with coronoid angle more than 135 degree); (1) moderately tilting posteriorly (with coronoid angle no more than 135 degree); (2) nearly vertical oriented** (modified from Luo *et al*., 2002: Ch 25; Luo and Wible, 2005: Ch 32).

313. **Meckelian groove in adults: (0) as anterior extension of the postdentary trough (or facet for postdentary unit); (1) Well-developed groove anteroventral to the mandibular foramen; (2) vestigial groove (thread-like); (3) absent** (Modified from Rowe, 1988: Ch 69; Wible,

1991: Ch 83; Hu *et al*., 1997 Ch 53; Wang *et al*., 2001: Ch 61; Luo *et al*., 2002: Ch 5; Luo and Wible, 2005: Ch 4).

314. **Ossified Meckel's cartilage: (0) no ossified Meckel's cartilage in wide Meckelian groove; (1) ossified Meckel's cartilage lodged in the meckelian groove in adult; (2) Meckel's cartilage absorbed into the dentary or persisted as a ligament** (Wang *et al*., 2001: Ch 63).

315. **Angular process: (0) absent; (1) weakly developed; (2) well developed** (Rowe, 1988: Ch 70; Wible, 1991: Ch 84; Hu *et al*., 1997: Ch 54; Wang *et al*., 2001: Chs 64, 65; Luo *et al*., 2002: Ch 8; Luo and Wible, 2005: Ch 7).

316. **Orientation of the angular process of the dentary: (0) pointed posteriorly or posteroventrally; (1) medially inflected; (2) as mediolaterally expanded plate** (Modified from Wang *et al*., 2001: Ch 66; Luo *et al*., 2002: Ch 8; Horovitz and Sánchez-Villagra, 2003: Ch 178; Luo and Wible, 2005: Ch 7).

317. **Anteroposterior position of the angular process: (0) anteriorly positioned, far anterior than the articular process, and under the coronoid process; (1) posteriorly positioned, near the articular process, posterior than the coronoid process** (Modified from Luo *et al*., 2002: Ch 9; Luo and Wible, 2005: Ch 8). .

318. **Position of the angular process in vertical direction: (0) low at the posteroventral corner of the dentary and the ventrally margin of the dentary roughly straight; (1) elevated well elevated and the ventral**

margin of the dentary strongly convex. (Modified from Luo *et al*., 2002: Ch 10; Luo and Wible, 2005: Ch 9).

319. **Mandibular foramen: (0) absent or at the junction of postdentary trough (or surface) and the meckelian groove; (1) within the pterygoid fossa; (2) not associated with meckelian groove or pterygoid fossa** (modified from Hu *et al*., 1997: Ch 56; Wang *et al*., 2001: Ch 68; Luo *et al*., 2002: Ch 12; Luo and Wible, 2005: Ch 12).

320. **Development of a pterygoid fossa on the medial side of the mandible: (0) absent; (1) present**(Modified from Wang *et al*., 2001: Ch 69; Luo *et al*., 2002: Ch 16; Luo and Wible, 2005: Ch 18).

321. **Pterygoid ridge below the pterygoid fossa: (0) absent; (1) medially directed shelf; (2) prominent crest; (3) elevated crest** (modified from Wang *et al*., 2001: Ch 70; Luo *et al*., 2002: Ch 17; Luo and Wible, 2005: Ch 19).

322. **Masseteric fossa: (0) high on coronoid region; (1) extends to lower portion of the dentary (2) extending to lower border of the dentary**(Sidor and Hopson, 1998: Ch 83; Hopson and Kitching, 2001: Ch 45; Wang *et al*., 2001: Ch 71).

323. **The ventral border of the masseteric fossa: (0) no distinct edge; (1) with thick ridge; (2) with laterally flared shelf** (modified from Luo *et al*., 2002: Ch 18; Luo and Wible, 2005: Ch 20).

324. **Anterior edge of the masseteric fossa: (0) low border; (1) laterally flared crest** (Modified from Luo *et al*., 2002: Ch 19; Luo and Wible, 2005: Ch 21).

325. **Anterior extremity of the masseteric fossa: (0) posteroventral to the last tooth, reaching the horizontal ramus; (1) below the last premolariform; (2) posteriorly shifted and having distance from the horizontal ramus.**(Luo *et al*., 2002: Ch 20; Luo and Wible, 2005: Ch 22).

326. **Reduction of the dentary: (0) not reduced; (1) reduced.**

327. **Dental groove for tooth replacement: (0) present; (1) absent** (Kemp, 1979: p 81 and fig. 4; modified from Wang *et al*., 2001: Ch 78; Luo *et al*., 2002: Ch 7).

DENTITION (108 CHARACTERS)

328. **Tooth implantation: (0) subthecodont; (1) thecodont** (Sidor and Hopson, 1998: Ch 121; Sidor, 2003: Ch 80).

329. **Posteriormost dentary tooth: (0) align with the coronoid process; (1) medial to the coronoid process** (modified from Luo *et al*., 2002: Ch 26; Sidor, 2003: Ch 77; Luo and Wible, 2005: Ch 34).

330. **Axis of Posterior maxillary tooth row: (0) lateral to subtemporal fossa; (1) toward center of fossa; (2) toward medial area of subtemporal fossa** (Hopson and Kitching, 2001: Ch 78; Bonaparte *et al*., 2003: Ch 13).

331. **Mode of occlusion: (0) bilateral and primarily orthal; (1) bilateral with strong longitudinal component; (2) unilateral with some medial component; (3) unilateral with strong medial component** (modified

from Hu *et al*., 1997: Chs 57 58; Wang *et al*., 2001: Chs 79 80; Luo *et al*., 2002: Chs 274 275; Bonaparte *et al*., 2003: Ch 1; Sidor, 2003: Ch 68; Luo and Wible, 2005: Ch 35).

INCISORS

332. **Number of upper incisors: (0) five; (1) four; (2) three; (3) two; (4) one; (5) zero** (modified from Sidor and Hopson, 1998: Ch 102; Hopson and Kitching, 2001: Ch 53; Bonaparte *et al*., 2003: Ch 3; Horovitz and Sánchez-Villagra, 2003: Ch 150; Luo and Wible, 2005: Ch 136).

333. **Number of lower incisors: (0) four; (1) three; (2) two; (3) one; (4) zero** (modified from Sidor and Hopson, 1998: Ch 103; Hopson and Kitching, 2001: Ch 54; Wang *et al*., 2001: Ch 82; Luo *et al*., 2002: Ch 105; Sidor, 2003: Ch 75; Bonaparte *et al*., 2003: Ch 4; Horovitz and Sánchez-Villagra, 2003: Ch 151; Luo and Wible, 2005: Ch 135).

334. **Size of upper incisor(s): (0) all incisors small; (1) I2 larger than neighboring teeth; (2) all incisors similarly stout** (modified from Sidor and Hopson, 1998: Ch 109; Hopson and Kitching, 2001: Ch 56; Bonaparte *et al*., 2003: Ch 5).

335. **Position of upper incisors: (0) all marginal; (1) posterior teeth medially positioned on the palate** (Wang *et al*., 2001: Ch 84).

336. **Size of lower incisors: (0) all small and even in size; (1) mesial incisor slightly to moderately larger than lateral ones; (2) mesial incisor very large and procumbent** (modified from Wang *et al*., 2001: Ch 83; Luo *et al*., 2002: Ch 115; Bonaparte *et al*., 2003: Ch 6).

337. **Diastema behind the upper incisors: (0) indistinct; (1) distinct.**

338. **Diastema behind the lower incisors: (0) indistinct; (1) distinct** (modified from Wang *et al*., 2001: Ch 2001: Ch 86; Luo *et al*., 2002: Ch 117).

CANINES

339. **Upper canine: (0) larger than neighboring teeth; (1) reduced, similar to neighboring teeth in size; (2) absent** (modified from: Hopson and Kitching, 2001: Ch 57; Luo *et al*., 2002: Ch 106; Horovitz and Sánchez-Villagra, 2003: Ch 170; Luo and Wible, 2005: Ch 141).

340. **Roots of upper canine: (0) single; (1) double** (Wible *et al*., 2001: Ch 10; Luo and Wible, 2005: Ch 142).

341. **Diastema behind upper canine: (0) indistinct; (1) distinct.**

342. **Precanine maxillary teeth: (0) present; (1) absent** (Sidor and Hopson, 1998: Ch 110).

343. **Lower canine: (0) larger than neighboring teeth; (1) reduced, similar to neighboring teeth in size; (2) absent** (modified from: Hopson and Kitching, 2001: Ch 58; Wang *et al*., 2001: Ch 85; Luo *et al*., 2002: Ch 107; Horovitz and Sánchez-Villagra, 2003: Ch 169; Sidor, 2003: Ch 76; Luo and Wible, 2005: Ch 143).

344. **Roots of lower canine: (0) single; (1) double** (Wible, *et al*., 2001: Ch 44; Luo and Wible, 2005: Ch 144).

345. **Diastema behind lower canine: (0) indistinct; (1) distinct** (modified from Wang *et al*., 2001: Ch 86).

POSTCANINES

346. **Postcanines differentiated into distinct premolariform and molariform regions: (0) absent; (1) present** (modified from Rowe, 1988: Ch 87; Hu *et al*., 1997: Ch 59; Wang *et al*., 2001: Ch 87).

347. **Root division of upper postcanine: (0) single-root; (1) incipient bifurcation; (2) at least posterior teeth double-rooted; (3) multiple-rooted** (modified from Rowe, 1988: Ch 88; Hu *et al*., 1997: Ch 60; Sidor and Hopson, 1998: Ch 117; Wang *et al*., 2001: Ch 88; Luo *et al*., 2002: Ch 111; Bonaparte *et al*., 2003: Ch 8; Sidor, 2003: Ch 79).

348. **Root division of lower postcanine: (0) single-root; (1) incipient bifurcation; (2) at least posterior teeth double-rooted; (3) multiple-rooted** (modified from Rowe, 1988: Ch 88; Hu *et al*., 1997: Ch 60; Sidor and Hopson, 1998: Ch 117; Wang *et al*., 2001: Ch 88; Luo *et al*., 2002: Ch 111; Bonaparte *et al*., 2003: Ch 8; Sidor, 2003: Ch 79).

349. **Number of total lower postcanine teeth: (0) ten or more; (1) nine; (2) eight; (3) seven; (4) six; (5) five to one; (6) absent** (modified from Luo and Wible, 2005: Ch 149).

350. **Buccal cingulum of upper postcanines: (0) absent; (1) present at least in some teeth** (modified from Rowe, 1988: Ch 85; Hopson and Kitching, 2001: Ch 6; Luo *et al*., 2002: Ch 76; Bonaparte *et al*., 2003: Ch 9).

351. **Arrangement of main tooth cusps on postcanines: (0) one main cusp; (1) several main cusps anteroposteriorly aligned or in triangular pattern; (2) multiple small cusps in two or more rows** (modified from

Rowe, 1988: Ch 90; Hu *et al*., 1997: Ch 61; Hopson and Kitching, 2001: Ch 63; Wang *et al*., 2001: Ch 89).

352. **Development of cusp B on upper postcanines: (0) absent; (1) present as accessory cusp beyond the cingulum; (2) as crown cusp.**

353. **Development of cusp C (metacone) on upper postcanines: (0) absent; (1) present as accessory cusp beyond the cingulum; (2) as crown cusp.**

354. **Development of cusp b (paraconid) on lower postcanines: (0) absent; (1) present as accessory cusp above the cingulid; (2) as crown cusp.**

355. **Development of cusp c (metaconid) on lower postcanines: (0) absent; (1) present as accessory cusp above the cingulid; (2) as crown cusp.**

356. **Development of cusp d or heel (talonid) on lower postcanines: (0) absent; (1) present at least on middle postcanines.**

357. **The size of ultimate lower postcanine relative to penultimate tooth: (0) smaller; (1) subequal or larger** (modified from Wible *et al*., 2001: Ch 61; Luo *et al*., 2002: Ch 59; Luo and Wible, 2005: Ch 73).

PREMOLARIFORMS

Characters in this section are only applicable for those with premolariform/molariform differentiation.

358. **Number of lower premolariforms: (0) five or more; (1) four; (2) three; (3) two or fewer** (Wang *et al*., 2001: Ch 90; Wible *et al*., 2001: 1; Luo *et al*., 2002: Ch 108; Luo and Wible, 2005: Ch 146).

359. **Number of upper premolariforms: (0) five or more; (1) four; (2) three; (3) two or fewer** (Modified from Wible *et al*., 2001: Ch 1; Luo and Wible, 2005: Ch 145).

360. **Size change within lower premolariform series: (0) size increasing posteriorly; (1) size decreasing posteriorly** (Wang *et al*., 2001: Ch 92).

361. **Anteriormost upper premolariform (or anteriormost cheek tooth): (0) single root; (1) double roots (2) multiple** (modified from Wang *et al*., 2001: Ch 91).

362. **Diastema behind the anteriormost upper premolariform (or anteriormost cheek tooth): (0) absent; (1) present** (Luo *et al*., 2002: Ch 109; Luo and Wible, 2005: Ch 43).

363. **Roots of the ultimate upper premolariform: (0) double roots; (1) three roots.**

364. **Crown of the ultimate upper premolariform: (0) with buccal main cusps and no protocone; (1) triangular with a protocone; (2) multiple small cusps.**

365. **Metacone of the ultimate upper premolariform: (0) absent; (1) present** (Luo and Wible, 2005: Ch 39).

366. **Roots of anteriormost lower premolariform (anteriormost lower postcanine): (0) single root; (1) double roots** (modified from Wang *et al*., 2001: Ch 91).

367. **Roots of ultimate lower premolariform: (0) double roots; (1) single root** (modified from Wang *et al*., 2001: Ch 91).

368. **Crown of the ultimate lower premolariform: (0) with principal cusps anteroposteriorly aligned; (1) with principal cusps arranged in a triangle; (2) forming a compressed blade with multiple small cupids** (modified from Wang *et al*., 2001: Ch 93; Luo *et al*., 2002: Chs 29, 31).

369. **The cusp b of the ultimate lower premolariform: (0) present; (1) absent** (modified from Luo *et al*., 2002: Ch 28).

370. **The cusp c of the ultimate lower premolariform: (0) present; (1) absent.**

371. **The heel of the ultimate lower premolariform: (0) as cingular cusped d; (1) as a talonid; (2) absent** (modified from Luo *et al*., 2002: Ch 30).

372. **Posterior cingulid of the ultimate lower premolariform: (0) absent; (1) present.** (Modified from Luo *et al*., 2002: Ch 30).

373. **Buccal cingulid of the ultimate lower premolariform: (0) absent; (1) present.** (modified from Luo *et al*., 2002: Ch 32).

374. **Lingual cingulid of the ultimate lower premolariform: (0) absent; (1) present.** (modified from Luo *et al*., 2002: Ch 33).

MOLARIFORMS

375. **Number of lower molariforms: (0) five or more; (1) four; (2) three; (3) two; (1) absent** (modified from Wang *et al*., 2001: Ch 94; Wible *et al*., 2001: Ch 4; Luo *et al*., 2002: Ch 110; Horovitz and Sánchez-Villagra, 2003: Ch 152; Luo and Wible, 2005: Ch 147).

376. **Number of upper molariforms: (0) at least as many as lower ones; (1) one less than lower ones; (2) absent.**

Upper molariforms

377. **Transverse widening of upper molariforms relative to lower molariforms (or posterior cheek teeth): (0) upper teeth not wider; (1) upper teeth about one third wider than the lowers; (2) upper teeth much wider than the lowers (> 1/3)** (modified from Wang *et al*., 2001: Ch 97).

378. **Transverse widening of upper molariforms (or posterior cheek teeth) at the level of cusp C relative to cusp A: (0) absent; (1) present** (Wang *et al*., 2001: Ch 98).

379. **Roots of upper molariforms (or posterior cheek teeth): (0) one root; (1) two roots; (2) three roots; (3) multiple roots.**

380. **Crown shape of upper molariforms (or posterior cheek teeth): (0) roughly conical; (1) roughly oval; (2) wide and roughly triangular; (3) roughly rectangular** (modified from Wible *et al*., 2001: Chs 15, 16; Luo *et al*., 2002: Ch 88; Luo and Wible, 2005: Ch 121).

381. **The astylar shelf of upper molariforms (or posterior cheek teeth): (0) absent; (1) present** (Hu *et al*., 1997: Ch 62; Wang *et al*., 2001: Ch 106; Luo *et al*., 2002: Ch 75; Lu and Wible, 2005: Ch 92).

382. **The ectoflexus on the upper molariforms (or posterior cheek teeth): (0) absent; (1) present** (modified from Wible *et al*., 2001: Ch 19; Luo *et al*., 2002: Ch 75; Luo and Wible, 2005: Ch 93).

383. **Protocone of the upper molariforms (or posterior cheek teeth): (0) absent; (1) present, much lower than paracone; (2) present,**

approaching paracone in height (modified from Hu *et al*., 1997: Ch 64; Wible *et al*., 2001: Chs 36, 38; Wang *et al*., 2001: Ch 110; Luo *et al*., 2002: Ch 77; Luo and Wible, 2005: Chs 96, 99).

384. **Cusp B of the upper molariforms: (0) anterior to the cusp A (paracone); (1) anterolateral or lateral to the cusp A.**

385. **Stylocone (stylar cusp B) of the upper molariforms(or posterior cheek teeth): (0) absent; (1) present** (modified from Wible *et al*., 2001: Ch 22; Luo and Wible, 2005: Ch 111).

386. **Parastyle of upper molariforms (or posterior cheek teeth): (0) absent; (1) present** (Wible *et al*., 2001: Ch 21; Luo and Wible, 2005: Ch 109).

387. **Development of an internal cingulum on upper molariforms(or posterior cheek teeth): (0) continuous cingulum with many small cuspules; (1) discontinuous cingulum with distinct anterior and posterior cuspules; (2) vestigial or absent** (Wang *et al*., 2001: Ch 107).

388. **Cusp C (metacone) of the upper molariforms: (0) posterior to the paracone; (1) posterolateral to the paracone** (modified from Wible *et al*., 2001: Ch 28; Luo and Wible, 2005: Ch 101).

389. **Height of cusp C: (0) lower than cusp A; (1) subequal to cusp A** (modified from Wible *et al*., 2001: Ch 27; Luo *et al*., 2002: Ch 81; Luo and Wible, 2005: Ch 100).

390. **Bases of cusp A and C: (0) adjoined; (1) separated** (Wible *et al*., 2001: Ch 30; Luo and Wible, 2005: Ch 102).

391. **Cusp D (metastyle): (0) posterior to cusp C; (1) posterolateral to cusp C; (2) absent** (modified from Wible *et al*., 2001: Ch 18; Luo *et al*., 2002: Ch 83; Luo and Wible, 2005: Ch 114).

392. **Stylar cusp C: (0) absent; (1) present** (Wible *et al*., 2001: Ch 23; Luo and Wible, 2005: Ch 112).

393. **Stylar cusp D: (0) absent; (1) present** (Wible *et al*., 2001: Ch 24; Luo and Wible, 2005: Ch 113).

394. **The paraconule and metaconule on the upper molariforms: (0) absent; (1) present** (Wible *et al*., 2001: Ch 35; Luo *et al*., 2002: Ch 80; Horovitz and Sánchez-Villagra, 2003: Ch 157; Luo and Wible, 2005: Ch 105).

Lower molariforms

395. **Transverse compression of lower molariforms relative to the dentary: (0) not compressed (the widths of molariforms being more than half of the width of the dentary); (1) compressed (the width of the tooth being half or less than half of the width of the dentary)** (Wang *et al*., 2001: Ch 96).

396. **Cusp b on middle lower molariforms: (0) smaller and lower than cusp a; (1) subequal to cusp a** (modified from Wang *et al*., 2001: Ch 100).

397. **Cusp c on middle lower molariforms: (0) smaller and lower than cusp a; (1) subequal to cusp a** (modified from Wang *et al*., 2001: Ch 100; Luo *et al*., 2002: Ch 44; Luo and Wible, 2005: Ch 61).

398. **Relative size of cusp b to cusp c: (0) b smaller than c; (1) subequal; (2) b larger than c** (modified from Wible *et al*., 2001: Ch 60; Luo *et al*., 2002: Ch 45; Luo and Wible, 2005: Ch 62).

399. **Development of cusp e of the lower molariforms (or posterior lower cheek teeth): (0) present; (1) absent** (Wang *et al*., 2001: Ch 101; Luo *et al*., 2002: Ch 53; Bonaparte *et al*., 2003: Ch 11; Luo and Wible, 2005: Ch 67).

400. **Cusp f of the middle lower molariforms (or posterior lower cheek teeth): (0) absent; (1) present** (Wang *et al*., 2001: Ch 102; Luo *et al*., 2002: Ch 54; Luo and Wible, 2005: Ch 68).

401. **Interlocking of lower molariforms (or posterior lower cheek teeth): (0) absent; (1) posterior extremity of anteriorly tooth lodged between cusp b and e; (2) posterior extremity of anteriorly tooth lodged between cusp e and f; (3) posterior extremity of anteriorly tooth lodged in vertical sulcus on the anterior wall of the posterior tooth** (Wang *et al*., 2001: Ch 99; Luo *et al*., 2002: Ch 58; Bonaparte *et al*., 2003: Ch 14; Luo and Wible, 2005: Ch 72).

402. **Anterior cingulid of the lower molariforms (or posterior lower cheek teeth): (0) absent; (1) present and interrupted by the contacting with previous tooth; (2) present and continuous midiolaterally** (modified from Wang *et al*., 2001: Ch 104; Luo *et al*., 2002: Ch 55; Luo and Wible, 2005: Ch 69).

403. **Anterior cingulid around the anterolingual corner of the trigonid (or cusp a, b and c) on lower molariforms (or posterior lower cheek teeth): (0) absent; (1) present** (modified from Luo *et al*., 2002: Ch 56; Luo and Wible, 2005: Ch 70).

404. **Lingual cingulid below the trigonid (or cusp a, b, c) of lower molariforms (or posterior lower cheek teeth): vestigial or absent; (1) well developed but discontinuous; (2) distinct and continuous** (modified from Wang *et al*., 2001: Ch 103; Luo *et al*., 2002: Ch 52).

405. **Buccal cingulid of the lower molariforms (or posterior lower cheek teeth)below the cusp a: (0) absent; (1) present.**

406. **Posterior cingulid posterior to trigonid (or cusp a, b and c): (0) absent; (1) present, extending buccally from the cusp d** (modified from Luo *et al*., 2002: Ch 57; Luo and Wible *et al*., 2005: Ch 71).

407. **Postcingulid posterior to the talonid: (0) absent; (1) present, about half width of the talonid; (2) present along the whole width of the talonid.** (modified from Luo *et al*., 2002: Ch 57; Luo and Wible *et al*., 2005: Ch 71). The character is only applicable for taxa with talonid.

408. **Orientation of the paracristid (a crest between cusps a and b) relative to the long axis of the lower molariforms: (0) longitudinal; (1) oblique** (modified from Wang *et al*., 2001: Ch 108; Luo *et al*., 2002: Chs 60, 61; Luo and Wible, 2005: Chs 74, 75).

409. **Orientation of the protocristid (a crest between cusps a and c) relative to the long axis of the lower molariforms: (0) longitudinal; (1) oblique**

(2) nearly transverse (modified from Hu *et al*., 1997: Ch 63; Wang *et al*., 2001: Ch 109).

410. **Angle of the trigonid (between paracristid and protocristid) on middle lower molariforms: (0) obtuse angle; (1) acute angle with cusp b and c not appressed; (2) acute angle with cusp b and c appressed** (modified from Wible *et al*., 2001: Ch 48; Luo *et al*., 2002: Ch 38; Luo and Wible, 2005: Ch 76). The character only applicable for taxa with trigonid on lower molariforms.

411. **Angle of the trigonid (between paracristid and protocristid) on first lower molariforms: (0) 180 degree; (1) obtuse angle; (2) acute angle** (modified from Luo *et al*., 2002: Ch 39).

412. **The heel of the lower molariforms (or posterior lower cheek teeth): (0) absent; (1) as cingular cusp d posterior to cusp c; (2) as posterolingual cingular cusp; (2) as single-cuspidated talonid heel; (4) as multicuspidated basin** (modified from Hu *et al*., 1997 Ch 65; Wang *et al*., 2001: Ch 111; Wible *et al*., 2001: Ch 49; Luo *et al*., 2002: Chs 65, 66; Luo and Wible, 2005: Chs 81, 82).

413. **Anteroposterior position of hypoconulid relative to hypoconid: (0) posterior to hypoconid; (1) about the same level** (modified from Wang *et al*., 2001: Ch 112; Wible *et al*., 2001: Ch 52; Luo *et al*., 2002: Ch 67, 68; Luo and Wible, 2005: Ch 84). The character is only applicable to taxa with mluticuspidated talonid developed.

414. **Mediolateral position of hypoconulid on talonid: (0) at median position; (1) at more lingual position** (modified from Wang *et al*., 2001: Ch 112; Wible *et al*., 2001: Ch 52; Luo *et al*., 2002: Ch 67; Luo and Wible, 2005: Ch 83). The character is only applicable to taxa with mluticuspidated talonid developed.

415. **Development of the entoconid on talonid basin: (0) absent; (1) present and lower than hypoconulid; (2) present and as high as hypoconulid** (modified from Wible *et al*., 2001: Ch 54; Luo *et al*., 2002: Chs 70, 71; Luo and Wible, 2005: Chs 87, 88). The character is only applicable to taxa with mluticuspidated talonid developed.

416. **Width of talonid (or heel) relative to trigonid on lower molariforms: (0) narrower; (1) subequal or wider** (mofified from Luoe t al., 2002: Ch 63; Horovitz and Sánchez-Villagra, 2003: Ch 158; Luo and Wible, 2005: Ch 79). The character is only applicable to taxa with mluticuspidated talonid developed.

417. **Shape of the talonid in middle lower molariforms: (0) longer than wider; (1) wide as long; (2) wider than long** (modified from Luo *et al*., 2002: Ch 73; Luo and Wible, 2005: Ch 90). The character is only applicable to taxa with mluticuspidated talonid developed.

418. **The cristid obliqua on talonid of middle lower molariforms: (0) absent; (1) extended toward metaconid; (2) extended toward notch on protocristid; (3) extended toward protoconid; (4) extended mesolingually toward the notch between metaconid and hypoconulid**

(modified from Wible *et al*., 2001: Ch 51; Luo *et al*., 2002: Ch 47; Horovitz and Sánchez-Villagra, 2003: Ch 160; Luo and Wible, 2005: Ch 64). This character is only applicable to taxa with talonid (with single or multiple cusps) on lower molariforms.

419. **Hypoflexid (the labial embayment between trigonid part and the talonid) between trigonid and talonid on middle lower molariforms: (0) absent; (1) shallow, less than 50 percent of talonid width); (2) deep, more than 50 percent of the talonid width but not reach the medial edge of the tooth; (3) well separating the talonid from the trigonid** (modified from Luo *et al*., 2002: Ch 64; Luo and Wible, 2005: Ch 80). This character is only applicable to taxa with talonid (with single or multiple cusps) on lower molariforms.

420. **Height difference between trigonid and posterior heel or talonid on lower molariforms: (0) posterior heel (talonid) at cingulid level; (1) posterior heel above the cingulid level but much lower than trigonid (no more than half height of the trigonid); (2) talonid more than half height of the trigonid** (modified from Luo *et al*., 2002: Ch 74; Luo and Wible, 2005: Ch 91).

TOOTH FUNCTION AND WEAR FACETS

421. **Occlusion pattern between upper and lower postcanine: (0) tooth-to-tooth occlusion; (1) interdigitated occlusion** (Kemp, 1982: p 219). Kemp (1982: p 219) indicated that in *Procynosuchus* a pair of opposing upper and lower postcanines piece the food when jaws occlude. In more

derived cynodonts, including Thrinaxodon, the occlusion between upper and lower postcanines is interdigitated, in which an upper tooth acts between two adjacent lowers. This pattern occurs in later cynodonts although precise opposition between cusps may not necessarily occur.

422. **Precise opposition between middle or posterior upper and lower postcanine: (0) lack consistent occlusion relationship; (1) cusp a between cusps A and B of upper tooth; (2) cusp a in the embrasure of two adjacent upper teeth; (3) occlusion between multiple rows of cusps** (modified from Wang *et al*., 2001: Ch 105; Luo *et al*., 2002: Chs 42, 43).

423. **Cutting edge and matching surfaces between occluding upper and lower postcanines: (0) absent; (1) developed by wearing the crown; (2) present upon eruption** (modified from Hopson and Kitching, 2001: Ch 66; Luo *et al*., 2002: Ch 93; Bonaparte *et al*., 2003: Chs 15, 16; Luo and Wible, 2005: 123).

424. **Location of major wear facets: (0) absent; (1) lingual side of main cusp on uppers and buccal side of main cusp on lowers; (2) between rows of multiple cusps.**

425. **Development of wear facets 1 and 2 on lower molariforms: (0) absent; (1) present** (modified from Luo *et al*., 2002: Chs 94, 96; Luo and Wible, 2005: Ch 126).

426. **The prevallum/postvallid shearing (double-scissor shearing) between molariforms: (0) absent; (1) present** (modified from Luo *et al*., 2005: Ch 95; Luo and Wible, 2005: Ch 125).

427. **Development of wear facets at the edges the talonid (or posterior heel): (0) wear facets (3 and 4) on flanks of talonid; (1) apical wear on the rim of talonid and tips of hypoconid and hypoconulid** (modified from Luo *et al*., 2002: Ch 98; Luo and Wible, 2005: Ch 128).

428. **Protocone-talonid basin contact on lower molariforms: (0) absent; (1) present** (modified from Hu *et al*., 1997: Ch 66; Luo *et al*., 2001a: Ch 101; Luo and Wible, 2005: Ch 133).

TOOTH REPLACEMENT

429. **Replacement of incisors and canines: (0) alternate and multiple; (1) diphyodont or no replacement** (Wang *et al*., 2001: Ch 81; Luo *et al*., 2002: Ch 112).

430. **Replacement of postcanines: (0) alternate and multiple; (1) single replacement without premolar/molar differentiation; (2) only premolars replaced; (3) only last premolar replaced (marsupial pattern); (4) no replacement** (modified from Sidor and Hopson, 1998: Chs 120, 122; Hopson and Kitching, 2001: Ch 81; Wang *et al*., 2001: Ch 95; Luo *et al*., 2002: Chs 113, 114; Bonaparte *et al*., 2003: Ch 7; Horovitz and Sánchez-Villagra, 2003: Ch 175; Luo and Wible, 2005: Ch 158).

ENAMEL CHARACTERS

431. **Sheath: (0) absent; (1) arc-shaped; (2) fully enclosed** (Wood and Rougier, 2005: Ch b).

432. **Prism seam: (0) present; (1) absent** (Wood and Rougier, 2005: Ch c).

433. **Prism packing: (0) hexagonal; (1) erratic; (2) stacked in rows** (Wood and Rougier, 2005: Ch d).

434. **Interprismatic matrix: (0) on all sides, widely separates prisms; (1) distinct inter-row sheets; (2) prisms "shoulder to shoulder," IPM therefore not abundant** (Wood and Rougier, 2005: Ch e).

435. **Thick outer AP layer: (0) present; (1) absent** (Wood and Rougier, 2005: Ch g).

Appendix II

DATA MATRIX

57 taxa 435 characters

Procynosuchus (79.5%)

0000?00000 0000000000 0100000000 0000000000 0000?00101
00?0??00?? 0000000000 0000000000 0000000?00 0000000000
0???0?0000 0000000000 0000000000 0000000000 0000000100
000000???? ?????????? ?????00000 0000000100 ?000000000
0000000000 0000000000 00000????? 0000000000 0000000000
0?00000000 0000000000 0000000000 0000000000 00??0000?0
0000000000 00000???00 0000000000 0000000000 0000000000
0000000??? 00???0???? ???????0?00 000?000??? 00000???00
000200???? ?0????????? 0000?0??00 ?????

Thrinaxodon (85%)

0100000000 0100100001 0100000000 0110100001 0000?10010
00000?000? 0100000000 0000101000 0000000100 0000000000
0000000000 0000000100 0010000000 000?000000 0010000100
0000000??? ?????????? ?????00000 0200000101 0011100000
0000000000 0000000100 00000??0?0 0000000000 0000000000
0?00000000 0000000000 0000000000 0000000010 01??0000?0
1000000000 10000???00 0100000000 0110000000 01000000G0
0111110??? 00???0???? ???????0001 0000001000 0000100010
000200?00? ?1?????000 1000?0??00 ?????

Chiniquodon (67%)

01???????? ?????????? ??0?0000?0 0??1???00? ?00??????0
00?00?010? 010?110001 0000101000 0000000100 0001000000
0000?????? ??11??0201 ??????0?0?0 ??0?000100 001000?0??
?????????? ?????????? ???1??0000 0200101001 1011101000
0000000002 100000A100 00000??0?0 0?0000??00 0010000?01
0?00000000 000000000? 00100???10 0010000010 01??0?01?0
211111010? 1100200000 011000?000 0110000000 0000000010
0010100??? 00???0???? ???????0001 000?002000 00001?0000
000000??0? ?0???????? 1000?0???0 ?????

tritylodontids (84%)

1110001001 ?10121001? ??01111101 001111?001 000???011A
0010000010 1101111001 0000101101 1000001000 0001000011
00001?0010 021?111211 1111000011 0111011100 0010000011
0100000000 0100000000 0???000000 1B0010A1A1 1?11101110
0001111100 2100011100 00010??0?1 0000000010 0010000011
0?00100100 0100000001 001100?010 001?000010 01??0001?0
211111110A 1200200000 0100101112 1GC102112? ?12??03230

2000000??? 20???1???? ??????1?33 000?002??? 00000??00
00?000???? ?????????? 1302?0??14 00?0?

Pachygenelus (60%)
1????????? ?????????? ?????????? ?????????? ??????????
???00?0?0? 0101121011 0000101111 00?0001?00 0001000?1
?????????? ????1112?1 ??1??????? ???????10? ??2????????
?????????? ?????????? ??????0110 1?00101001 1011111110
1010011100 A000011001 00001?0101 0?0?000?10 0010000001
0?00000000 0100000000 001000?010 0A1?100?10 ????0?1100
201111110? 11?02000?0 0100000012 2321011000 1100101131
0110211??? 00???0???? ??????0?01 0000000000 00001?0?00
000200??0? ?1?????000 101100???0 10001

Brasilodon (44%)
?????????? ?????????? ?????????? ?????????? ??????????
?????????? ?????????? ?????????? ?????????? ??????????
?????????? ?????????? ?????????? ?????????? ??????????
?????????? ?????????? ?????????0 110010??0? ?111121??0
1010111102 1001111000 0?1?1?0100 0?0?0000?0 0001000?11
0?00?0?100 010?000001 01?100???0 0110100010 0???1?A1?0
11?111?1?? 1000100000 0110000001 2?1??10000 11001011B0
1222210??? 00???0???? ??????0013 0000002000 0000000110
101000?00? ?1?????00 101100???A ?????

Brasilitherium (43%)
?????????? ?????????? ?????????? ?????????? ??????????
?????????? ?????????? ?????????? ?????????? ??????????
?????????? ?????????? ?????????? ?????????? ??????????
?????????? ?????????? ???????A0? 1?0010100? ???1121?1?
?010111?00 1000111000 00111?0101 1?0?1000?0 0001000??1
0?00?0?100 ?B0?000001 01?100???0 0?1?1???10 0???1?11?0
11111?1100 1000100000 0110000001 2110010010 0010001120
1221211??? 00???0???? ??????0013 0000002000 0000000010
101000?00? ?1?????00 101100???0 ?????

Sinoconodon (64%)
???0???0?? ?????????? ??0??????? ?????????? ??????????
???0?0??10 ?1??1?10A? 00????1?01 100000??0? 000??0????
???0?????? ?????????? ?????????? ????111100 001100?0??
?????????? ?????????? ??????0100 1200001101 0111121110
0110111100 2001111101 1011100100 1000210?1 1110011011
0?00000100 1100100101 0?110??01? 0011010010 01??101110
21111????0 1000200000 010000?101 2000000000 1100112240
1222210330 0000100000 2000100011 0000002000 1000000010
000000?000 01?????00 101100?001 10100

Morganucodon (89%)
11101?1011 1201210012 ??01111111 011111?001 0000???112
11100?020? ?1?1121011 0000101112 1000101001 0001000011
0100?????? ??????1211 1?1100?0?1 0111011100 0011010112
0100??0000 0100000000 000???0100 ?100000101 0011121110
01?0111100 2001111100 1011200100 1100201011 1110011021
0?00100100 1200100101 0111001010 0111111010 01??101110
2111111100 1000200000 0100000101 2100000000 0100112221
1222210000 0000100000 0001EA0011 0000000000 1000000010
111200?000 01??????00 111100?012 10100

Megazostrodon (73%)
111?1?1011 1201210012 ??01111111 011111?001 0000???11?
??1??????? ?1?1121011 00?0101??1 1000101001 0001000011
0100?????? ??????1211 1?1100?0?1 0111011100 0011010112
0100000??? ????0??000 000100???? ??00?0010? ???11??1??
?????11?00 2?0?1??1?? 101220?100 ?100201012 11?0011?21
0?001??100 1200100101 ?1???????? 0???1???1? ????101110
211111?1?0 110?200000 0100000102 210000?0?0 0100012201
1222210000 0000100000 0000000011 0000000000 1000000010
111220?000 01??????00 121100?0?? 10001

Dinnetherium (37%)
?????????? ?????????? ?????????? ?????????? ??????????
?????????? ?????????? ?????????? ?????????? ??????????
?????????? ?????????? ?????????? ?????????? ??????????
?????????? ?????????? ?????????? ?????0???? ??????????
?????????? ????1????? ???1200100 110?2010?1 11??011?21
0?00100100 1200100101 ?1???????? ???1????1? ????101120
211????1?0 100?2000?0 0100001102 2?0001?0?0 0100012211
1222101?0 ??00100000 0000000011 0000000000 1000000011
211200?000 01??????00 111100?0?? 10100

Haldanodon (67%)
?????????? ?????????? ?????????? ?????????? ??????????
?????????? 111112103? 1000101??1 100?001003 000?001001
0100?????? ??????1211 1??????0?1 ????011100 0020010112
01??0????? ?????????? ??????0100 1200000101 0011121100
1100111?00 20000?111? 2012200200 1100201011 111?01??21
0?0?110100 1200100??? ?11???1010 0010121011 01??101120
2111112100 1100200000 0110001101 1000000001 0101012221
1022010220 0000010001 0011001022 000?002000 100000??10
021200?0?? ?1??????00 120100?012 00??0

Kuehneotherium (20%)
?????????? ?????????? ?????????? ?????????? ??????????
?????????? ?????????? ?????????? ?????????? ??????????

?????????? ?????????? ?????????? ?????????? ??????????
?????????? ?????????? ?????????? ?????????? ??????????
?????????? ?????????? ?????????? ?????????? ??????????
?????????? ?????????? ?????????? ?????????? ????1?1110
111????1?0 100?0???00 0100000110? 1????????? ?????12201
1222210??0 ?????000?? ????0?0012 1001110100 2000000211
2112002111 ?1??????00 121111?0?2 00???

Hadrocodium (46%)
?????????? ?????????? ?????????? ?????????? ??????????
?????????? ?????????? ?????????? ?????????? ??????????
?????????? ?????????? ?????????? ?????????? ??????????
?????????? ?????????? ???????100 1?001?111? ?111121100
0?10?????0 2?0???1110 2012100200 2?00201011 1111011121
1001000100 1200100201 111??????? ??1?23101? 11??1021?0
2202??21?? 11?2200020 0100001101 1000010000 110011225?
1222210330 0100010001 00??300?11 000000?000 1000000110
0????0?000 01??????00 121100?0?? ?????

Teinolophos (15%)
?????????? ?????????? ?????????? ?????????? ??????????
?????????? ?????????? ?????????? ?????????? ??????????
?????????? ?????????? ?????????? ?????????? ??????????
?????????? ?????????? ?????????? ?????????? ??????????
?????????? ?????????? ?????????? ?????????? ??????????
?????????? ?????????? ?????????? ?????????? ????1?2122
211????1?1 110?220100 ?22100110? 0????????? ????????2??
1??221???? ?????????? ?????????? ?????????? ????001010
02010?0123 ?411012432 1201?010?? ?????

Steropodon (12%)
?????????? ?????????? ?????????? ?????????? ??????????
?????????? ?????????? ?????????? ?????????? ??????????
?????????? ?????????? ?????????? ?????????? ??????????
?????????? ?????????? ?????????? ?????????? ??????????
?????????? ?????????? ?????????? ?????????? ??????????
?????????? ?????????? ?????????? ?????????? ????1?????
?202???11? ??22??????? ?????0110? 0????????? ??2?????2??
1??2210??? ?????????? ?????????? ?????????? ????001010
02111?2123 ?411012432 1201?010?? ?????

Obdurodon (45%)
?????????? ?????????? ?????????? ?????????? ??????????
?????????? ?????????? ?????????? ?????????? ??????????
?????????? ?????????? ?????????? ?????????? ??????????
?????????? ?????????? ??????1101 101012??01 0?11121001
?011111?12 20031?1110 2012200101 1?0?001111 ?111011121

0?011??000 1200100201 120??????? ??11113101? 11??1021??
?202???1?1 2122110111 1221211101 054??????2? ???2?13351
1022210330 10100????? ????300033 0?????0011 2000000110
02011?2123 2411012432 120??010?? 2121?

Tachyglossus (74%)
11111?1110 1211210010 001??11?11 1011111110 1111010 1?2
1110200110 1111120021 1012100101 0000000003 001?001001
01?0100010 1?11001211 1111101111 1210011100 10201?1112
0001100100 0001320000 0111111101 1010121001 0?11121001
?011111?12 2003111110 2012200100 1200001111 1111011121
0?01111000 1200100201 1102121112 1?11131011 1100102121
2202212111 2132110120 1?00211??? 054??????2? ???2?????6?
???????33? ?????????? ????4????? ?????????? ??????????
?????????? ?????????? ????????0?? ?????

Ornithorhynchus (81%)
11111?1110 1211210010 001??11?11 1011111110 1111010 1?2
1110200110 1111120021 1012100101 0000000003 001?001001
01?0100010 1?11001211 1111101111 1210011100 10201?1112
0001100010 0000320000 0111111101 1010121001 0?111?1001
?011111?12 20031?1110 2012200100 1200201111 1111011121
0?01111000 1200100201 1202121112 1011131011 1100102121
2202212111 2132110111 1221211101 054??????2? ??????3351
102221033? ?????????? ????300?33 0?????0??? ????0????0
02????2??? 24???????? ??0????0?? 011??

Haramiyida (15%)
?????????? ?????????? ?????????? ?????????? ??????????
?????????? ?????????? ?????????? ?????????? ??????????
?????????? ?????????? ?????????? ?????????? ??????????
?????????? ?????????? ?????????? ?????????? ??????????
?????????? ?????????? ?????????? ?????????? ??????????
?????????? ?????????? ?????????? ?????????? ?????0?1??
?1?????1?? ?1???????0 ?200001117 1?0001112? ????12230
2????00110 ?0020002?? ????201?13 ??0???2??? ????0???00
00000????? ?0???????0? 130200?0?? 00???

Cimolodonta (80%)
11101?1011 12112?1010 0001111111 001111000? 0000?11111
1110101010 0111122213? 1101211112 1001A110A1 000?000011
1111?????? ??????1211 1111100111 0111112111 1103021112
2?10110210 0000110112 1001211210 1001001101 0?11101111
?01?111012 2003121107 201220?20? 111?201011 2211???0??
?????10101 12001AA201 111212?112 1211221010 01??102123
2202212111 01320???11 1200101112 1331121127 ???2?12250
2????003F0 00020002?? ????301?13 ??0???2??? ????0???00

00000????? ?0???????0? 1302002012 1100?

Ausktribosphenos (17%)
?????????? ?????????? ?????????? ?????????? ??????????
?????????? ?????????? ?????????? ?????????? ??????????
?????????? ?????????? ?????????? ?????????? ??????????
?????????? ?????????? ?????????? ?????????? ??????????
?????????? ?????????? ?????????? ?????????? ??????????
?????????? ?????????? ?????????? ?????????? ????1021??
?10????110 111?221100 ?20000110? 2?????????? ?????1?2??
1??2210??0 ??????0100 21112????? ?????????? ????000010
02110?0122 2411212312 1?21111??? ?????

Bishops (18%)
?????????? ?????????? ?????????? ?????????? ??????????
?????????? ?????????? ?????????? ?????????? ??????????
?????????? ?????????? ?????????? ?????????? ??????????
?????????? ?????????? ?????????? ?????????? ??????????
?????????? ?????????? ?????????? ?????????? ??????????
?????????? ?????????? ?????????? ?????????? ????102112
2202???111 1122221120 ?21000110? 2?????????? ?????1?2A?
1??2100?0 ??????0100 21012????? ?????????? ????000010
02010?0122 2411212312 1?21??1??? ?????

Ambondro (11%)
?????????? ?????????? ?????????? ?????????? ??????????
?????????? ?????????? ?????????? ?????????? ??????????
?????????? ?????????? ?????????? ?????????? ??????????
?????????? ?????????? ?????????? ?????????? ??????????
?????????? ?????????? ?????????? ?????????? ??????????
?????????? ?????????? ?????????? ?????????? ??????????
????????1?? ?????????? ?????011?? 2?????????? ????????2??
1??221???? ??????0100 00012????? ?????????? ????000?11
21110?0112 1400101111 1?11??1??? ?????

Asfaltomylos (14%)
?????????? ?????????? ?????????? ?????????? ??????????
?????????? ?????????? ?????????? ?????????? ??????????
?????????? ?????????? ?????????? ?????????? ??????????
?????????? ?????????? ?????????? ?????????? ??????????
?????????? ?????????? ?????????? ?????????? ??????????
?????????? ?????????? ?????????? ?????????? ????10?1?2
211????1?0 11??221000 ?20000110? 2?????????? ?????1?2??
1??221???0 ??????0??? ????2????? ?????????? ????000?10
01010?0112 1400000311 1?11??1??? ?????

Shuotherium (18%)

?????????? ?????????? ?????????? ?????????? ??????????
?????????? ?????????? ?????????? ?????????? ??????????
?????????? ?????????? ?????????? ?????????? ??????????
?????????? ?????????? ?????????? ?????????? ??????????
?????????? ?????????? ?????????? ?????????? ??????????
?????????? ?????????? ?????????? ?????????? ????10?1?0
?11????1?? ??0?0???00 12??00110? 2????????? ?????1?2?1
1022210??0 ??????0000 00011?10?2 112???2000 2000000110
0212002112 21??????00 121111?0?? ?????

Gobiconodon (74%)
111??????? ?????????? ?????????? ???111?001 0000?10112
1110?????? 111122323? 11?12????1 10?1001001 1001000011
1100?????? ??????1211 1111000?1 0111011100 ?01101?112
011000???? ?????10000 0?????1?10? 1?01?01001 ???1121110
0000111?0? 21011?1100 1012200200 110020?0?1 111?012021
0?00110100 1200100101 011??????? ??11011010 01??102121
0202???110 11110???11 2220001101 2332010010 01100122D1
1222210121 0000101010 2000011113 0000001000 1000100111
200000?000 01??????00 121110?0?1 10100

Repenomamus (91%)
1110111111 1211211010 1101111100 0011111001 0000110111
1110111210 111122323? 1101212111 1001001011 1001000011
1100?????? 0???111211 1111000011 0111011100 1011010112
01?0000100 0100110000 0001101100 1201100001 0111121110
0000111100 2001111100 1012200200 1100201011 1110012?21
0?00110100 1200100101 011??????? ?011011010 0110102121
0202???111 11110???11 2220001101 2222010010 0110012231
12222102D1 0000101010 2000101113 0000001000 1000100111
200000?000 01??????00 121110?001 ?????

Jeholodens (61%)
11?0???0?? 1?0????0?? ??011????? 0?1111100? ?000110112
1?10?1??00 111122323? 1101212111 ????00??0? 10???10??1
?1?0001010 0211111211 1111000011 0???0?11?0 ?????10??2
0?10000?0 0100?10000 ?00100?10? ???110??0? ???11????1
0010111??? ??0??????? ????200200 11?0?????? ???????0??
?????????? 1?0?1????? ?1???????? ??11121??? ?1??1?2121
?202???11? 111?0???11 222000110? 2100000010 0110012241
1222210330 0000100000 200010???1 000000?000 1000100110
300000?000 01??????00 111100?0?? ?????

Amphilestes (18%)
?????????? ?????????? ?????????? ?????????? ??????????
?????????? ?????????? ?????????? ?????????? ??????????
?????????? ?????????? ?????????? ?????????? ??????????

?????????? ?????????? ?????????? ?????????? ??????????
?????????? ?????????? ?????????? ?????????? ??????????
?????????? ?????????? ?????????? ?????????? ??????2121
0202???111 111?0???11 222000110? 2????????? ?????1222?
1??2210??0 ?????10000 20000????1 00???????? ????100111
200200?000 01??????00 121110?0?? ?????

Priacodon (37%)
?????????? ?????????? ?????????? ?????????? ??????????
?????????? ?????????? ?????????? ????0????? 100??10???
?????????? ?????????? ?????????? ?????????? ??????????
?????????? ?????????? ?????????? ???0????1? ???11???1?
?????????? ?????????? ?0?2?????1 110?20?011 ?1????1??21
0??????100 12??100101 ?1???????? ????????0?? ????102121
0202???111 111?0???11 222000110? 2320000000 0100012231
1222210210 1000110010 2001100111 0000001000 1000111110
300200?000 01??????00 111100?0?? 10100

Trioracodon (30%)
?????????? ?????????? ?????????? ?????????? ??????????
?????????? ?????????? ?????????? ?????????? ??????????
?????????? ?????????? ?????????? ?????????? ??????????
?????????? ?????????? ?????????? ?????????? ??????????
?????????? ?????????? ?????????? ????20??1? ?????1????
0????101?? 12??100??? ?1???????? ????????0?? ????102121
0202???111 111?0???11 222000110? 2??2?0?001 0100012231
1222210210 1000110000 0001200?11 0000001000 1000111110
300200?000 01??????00 111100?01? ?????

Triconodon (22%)
?????????? ?????????? ?????????? ?????????? ??????????
?????????? ?????????? ?????????? ?????????? ??????????
?????????? ?????????? ?????????? ?????????? ??????????
?????????? ?????????? ?????????? ?????????? ??????????
?????????? ?????????? ???2?????? ?????????? ??????????
?????????? ?????????? ?????????? ?????????? ????102121
0202???111 11??0???11 222000110? 2????????? ??01012221
1222101?0 ??00?100?? ????1?0??1 0000001000 1000111110
300200?000 01??????00 111100?0?? ?????

Tinodon (22%)
?????????? ?????????? ?????????? ?????????? ??????????
?????????? ?????????? ?????????? ?????????? ??????????
?????????? ?????????? ?????????? ?????????? ??????????
?????????? ?????????? ?????????? ?????????? ??????????
?????????? ?????????? ?????????? ?????????? ??????????
?????????? ?????????? ?????????? ?????????? ????1?2121

?202???110 121?0???11 22??00110? 2?????????? ??11012221
1222102?0 ?????10000 20011?0012 1101110100 2000000211
200200?111 12??????00 121111?0?? ?????

Zhangheotherium (84%)
111??1111? 1211211101? ??01111??? 0?11110?0? 0000?111?1
1110111210 111122323? 1101212112 1111011112 1001010211
1100001011 0111111211 1111000011 111?112111 1111020112
1100000000 0100111101 2001211100 1200101001 0111111?10
0010111?00 2?????1100 ?012200200 111?20???1 ?11?01??21
1101110111 1200100201 ?1???????? ?01?22??1? ????102121
2202???110 101?0???11 2220001101 2110010010 1?10012221
1222210330 1100?10000 0000010012 1101112100 2000000110
000000?112 12??????00 1211111?011 ?????

Spalacotherium (22%)
?????????? ?????????? ?????????? ?????????? ??????????
?????????? ?????????? ?????????? ?????????? ??????????
?????????? ?????????? ?????????? ?????????? ??????????
?????????? ?????????? ?????????? ?????????? ??????????
?????????? ?????????? ?????????? ?????????? ??????????
?????????? ?????????? ?????????? ?????????? ????1?21?1
2202???111 111?0???11 32?000110? 3????????? ?????12201
1022102?0 ??00110010 0??1010012 1101110100 2000000110
0112111?112 12??????00 122111?0?? ?????

Heishanlestes (17%)
?????????? ?????????? ?????????? ?????????? ??????????
?????????? ?????????? ?????????? ?????????? ??????????
?????????? ?????????? ?????????? ?????????? ??????????
?????????? ?????????? ?????????? ?????????? ??????????
?????????? ?????????? ?????????? ?????????? ??????????
?????????? ?????????? ?????????? ?????????? ????112121
2202???111 12320???11 322000110? 3????????? ?????1?20?
1??2210?0 ?????0001? 21110????? ??0??????? ????000110
0112111?122 12??????00 122111?0?? ?????

Dryolestes (31%)
?????????? ?????????? ?????????? ?????????? ??????????
?????????? ?????????? ?????????? ????0????? 1?????????
???0?????? ?????????? ?????????? ?????????? ??????????
?????????? ?????????? ?????????? ?100?1???? ??????????
?????????? ?????????? ?????????? ?????????? ??????????
?????????? ?????????? ?????????? ?????????? ????102120
2202???110 1122201011 2210001101 3000000001 0101012200
1022101?0 1000110011 0001011012 100?112100 2000000010
00000?0122 23??????01 122111?012 10000

Henkelotherium (52%)
11???????? ?????????? ?????????? ??1???00?0 ?0?0?11112
??1??????? 111122323? 1101212?? ?1?111?112 100?000011
?1?1?????? ??????1211 1111000011 ?111112111 1111020112
1100110??? ????????11? ???1?1???? 1????110?? ????????1??
??1??????? ?????????? ????200200 221122???? ??????????
????????1? 12??1????? ?????????? ?????????? ????102120
2202???110 1122201011 2210000110? 3????????01 0?0??12200
1022210110 1000110011 0001011012 100?112100 200000001?
00000?0122 23??????01 122111?0?? 1000?

Peramus (23%)
?????????? ?????????? ?????????? ?????????? ??????????
?????????? ?????????? ?????????? ?????????? ??????????
?????????? ?????????? ?????????? ?????????? ??????????
?????????? ?????????? ?????????? ?????????? ??????????
?????????? ?????????? ?????????? ?????????? ??????????
?????????? ?????????? ?????????? ?????????? ????10????
?202???110 11??????11 ?2??0011?? 3?1??0???? ?????12221
1022210000 1000110000 0000201012 111?110000 2000000111
20000?0112 2400000121 122111?0?? ?????

Amphitherium (19%)
?????????? ?????????? ?????????? ?????????? ??????????
?????????? ?????????? ?????????? ?????????? ??????????
?????????? ?????????? ?????????? ?????????? ??????????
?????????? ?????????? ?????????? ?????????? ??????????
?????????? ?????????? ?????????? ?????????? ??????????
?????????? ?????????? ?????????? ?????????? ????102120
2202???1?0 1122201011 2210000110? 3?0??0???? ?????12200
1??2210?0? ????10011 00010????? ?????????? ????000110
00000?0112 23????????1 122111???2 ?????

Vincelestes (89%)
11101?1111 1211210010 111??11100 0011110001 ?000?11112
11111???00 111122323? 12?12?2?12 1111111102 1001000011
1100000?? ????111211 1111000111 01?1112101 1021020112
1100100100 0100111101 2????01100 1100010011 0011111100
0101111000 2010121110 1012200200 22??202011 1111011121
1101110111 1200111211 111??????? ?01?021011 01??102120
2202???110 1122201011 2210001101 2120010001 0101012251
1022210330 0000?00011 0000200?2 001??02010 2000000110
00000?0112 1410001?1 122111?1?? 10000

Kielantherium (16%)

?????????? ?????????? ?????????? ?????????? ??????????
?????????? ?????????? ?????????? ?????????? ??????????
?????????? ?????????? ?????????? ?????????? ??????????
?????????? ?????????? ?????????? ?????????? ??????????
?????????? ?????????? ?????????? ?????????? ??????????
?????????? ?????????? ?????????? ?????????? ????10????
?202???1?0 ?222????1? ?2??0011?? 3????????? ????????2B?
1??2210?0 ?????????? ????1????? ?????????? ????000211
21000?0122 ?400000121 1221110B?? ?????

Aegialodon (9%)
?????????? ?????????? ?????????? ?????????? ??????????
?????????? ?????????? ?????????? ?????????? ??????????
?????????? ?????????? ?????????? ?????????? ??????????
?????????? ?????????? ?????????? ?????????? ??????????
?????????? ?????????? ?????????? ?????????? ??????????
?????????? ?????????? ?????????? ?????????? ??????????
?????????? ?????????? ???????1?? 3????????? ??????22??
1??221???? ?????????? ?????????? ?????????? ????000211
21000?0122 ?400?00121 1221110B?? ?????

Prokennalestes (35%)
?????????? ?????????? ?????????? ?????????? ??????????
?????????? ?????????? ?????????? ?????????? ??????????
?????????? ?????????? ?????????? ?????????? ??????????
?????????? ?????????? ?????????? ?????????? ??????????
?????????? ?????????? ???2?????0 231120??11 23???0?121
1?0?0??112 121?111211 1????????? ???????1?? ????102120
2202???110 1122201011 021000110? 3????????? ??01012221
1022211?00 ??11110001 0000202022 112?112000 2001000011
21000?0122 2400100221 122111102?? 10000

Eomaia (55%)
???1????1? ?????????? ?????????? ??11?100?? 0000?111?2
??110????1 111122323? 12012?2112 ?11?111?22 210??10??1
?1?1000012 0211111211 ?11?010111 1?11112101 11?2021?12
1?00101??? 1200212111 200120?21? ??0111???? ?????????0
?????11??? 2????????? ???2??12?? ???1202??? ??????????
?????????? ?????????? ?????????? ?????2???? 0???1?2120
2202???110 1132201011 021000110? 3000000000 0100012221
102221?000 10??110001 ?00020???? ?????1?000 ???1000111
210?0?0122 240010???1 122111?2?? ?????

Ukhaatherium (53%)
??????1?11 ?2????????? ??1????11 0011110001 0000?11112
111??????? 1111122323? 12012?21?2 1111111122 2101010011
1111?????? ????111211 1111000?11 ?111112101 1112021?12

1100???210 1211212?01 200??????0 ??0??????? ??????????
?????????? ?????????? ?????????2? ??2??????? ??????4???
????????1?2 ?2????????? ?????????? ?????????? ????1?????
????????1?? ?????????2? 0????011?? 3000000100 0100012231
1022211110 1011110000 0000202022 112?112000 2001000011
21000?0122 2400?00??1 122111102? ?????

Montanalestes (21%)
?????????? ?????????? ?????????? ?????????? ??????????
?????????? ?????????? ?????????? ?????????? ??????????
?????????? ?????????? ?????????? ?????????? ??????????
?????????? ?????????? ??????1??? ?????????? ??????????
?????????? ?????????? ?????????? ?????????1 ??????????
?????????? ?????????? ?????????? ?????????? ????112120
2202???110 1232201021 0210001102 3????????? ?????1?22?
1??2110?0 10????0000 00012????? ??2?11???? ????000111
21000?0122 2400100221 122111?2?? ?????

Kennalestes (51%)
???0?????0 ?2????????? ?????????? ?????????? ??????????
?????????? ?????????? ?????????? ?????????? ??????????
?????????? ?????????? ?????????? ?????????? ??????????
?????????? ?????????? ???????1210 1101111?0? ?011121200
0110111?0? 2123?21110 1112201221 232?2020?1 ?311004121
110?010112 1210110??? ?01??????? ??11?2121? 01??102120
2202???110 1132201021 0210001101 3110000?01 0101012231
1022211110 1011110011 0000202022 112?112000 2001000011
21000?0122 2400200221 122111102? ?????

Asioryctes (65%)
1110?11110 1211211110 111??11111 001111?00? ??????????
?????????? ?????????? ?????????? ?????????? ??????????
???10?1011 01???????? ?????????? ?????????? ??????????
????100210 121?212111 200??01210 1101?11?0? ?0111??200
1110111?02 2123221110 1112201221 232?2020?1 ?311004?21
110?010112 1210110211 101??????? ??11?2121? 01??102120
2202???110 1232201021 0210001101 3000000001 0101012231
1022211110 1011110001 0000202022 112?112000 2001000011
21000?0122 2400200221 1221110??2 ?????

Zalambdalestes (85%)
11???????? 1211211110 111??11111 0011111000? ??00?1111?
111??????? 111122323? 12012??2?2 111?111122 2101?102?1
?1?1001012 0111?11211 1111000111 1111112101 11????2?112
11??1?1311 1201212111 2001?01210 1101110?01 0011121200
0110111101 2122?21111 1112201220 232?202011 2311004121
110?010112 1210110211 101??????? ?111?21111 01??102120

2202???111 1132201021 0210001101 3311021001 1110012231
1022210220 1011110100 1000202022 112?112000 2001001011
21000?0122 2400200311 122111022? ?????

Erinaceus (95%)
1111111110 1211211110 1?1??11111 001111000? 0000111112
11110???01 111122323? 12012?2112 1111111122 2101110221
1111????1? ?211111211 11110?0101 1111112111 1112021112
1110010311 1211212111 2001201211 1?111110?1 0?11121210
0010111101 2122221110 1112201211 2321202011 2311003121
110?010112 1210111211 1012111011 0111131111 0111102120
2202212111 1132201021 0210001101 3211010011 0110012251
1022210330 0011?10100 2000202023 002?112011 2001000011
21000?0122 2411011312 1221110212 21211

Deltatheridium (47%)
?????????? ?????????? ?????????? ?????????? ??????????
?????????? ?????????? ?????????? ?????????? ??????????
?????????? ?????????? ?????????? ?????????? ??????????
??????0??? ????11101 ????????210 1001110111 01?11?????
0110?????? ???????1? 1??2211?20 231?202011 03?1103121
1?0?010111 121?1003?1 ?1????????? ???1???1?? ????112120
2202???111 1232211011 1210001101 3?00000000 0100012231
1022210220 0000010011 0000102022 112?112000 2001000211
21000?0122 2400100121 122111022? 10000

Sinodelphys (45%)
?1????????? ?????????? ?????????? ??11?1000? 0000?111??
???1?????1 111122323? 12012?2112 ?11????122 210??10??1
?1?1100?12 1211111211 1???????11 ?????121?1 ??????0??2
1???001??? 121?211111 100?20???? ??0?1????? ??????????0
?????????? 2????????? ?????????? ?????????? ??????????
?????????? ?????????? ?????????? ?????2???? ????112120
2202???1?? 1232201021 1210001110? 3100000000 0100012231
1022210110 1100010101 000?20???? ????????0?? ????0???11
21000??122 2401?????1 122111022? ?????

Asiatherium (67%)
1????????? ?????????? ??1??11?10 0?11111000? ?000?1111?
??1??????? 111122323? 12012?21?2 1111111122 2101010?1
1111?1?1?? 0211111211 111100?111 1?11112101 1112000?12
1110?????? ?????????? ?????????0 110?11???? ???1121?00
?110?11??? 2??2??111? 1012211211 231?2020?1 ?311103???
1?1?0???11 121?1?0??? ??1??????? ??11121?11 01??112120
2202???111 1232211021 1210001101 3???????00 01???12231
1022210220 1000010011 0000102022 112?112011 2011000111
21000?1122 2401211211 122111022? ?????

Pucadelphys (87%)
1110?11110 1211211110 111??11110 0011110001 ?000?11112
11110???01 111122323? 12012?2112 1111011122 2101010111
111??????? ??????1211 1111000111 1111112101 1112010112
1110110110 1211211111 100??01210 1111110111 0011121110
0110111101 2020221117 1012211210 231???2011 2311?04121
110?010111 1211100??1 ?11??????? ?111121111 01??112120
2202???111 1232211021 1210001101 3000000000 010?012231
1022210220 1000010011 0000102022 112?112011 2111001011
21000?1122 2401211311 1221110213 ?????

Didelphis (96%)
1111111110 1211211110 101??11110 0011110007 0000111112
11110???01 111122323? 12012?2112 1111111122 2101010111
1111011112 2211111211 1111000111 1111112101 1112010112
1110111210 1211211111 1001201210 11111?1111 0111121200
0?00111101 2023221111 1012211210 2311202011 2311103121
111?010111 1210100??1 ?112111011 0111021111 0111112120
2202212111 1232211021 1210001101 3000000000 0100012231
1022210220 1100010011 0000102022 112?112011 2111001011
21000?1122 2401211311 1221110213 21211

Percentages following taxon names indicate completeness of coding for each taxon.
A = 0,1; B = 1,2; C = 1,3; D = 2,3; E = 0,1,2; F = 1,2,3; G = 2,3,4
Data source is indicated in the Mesquite database file.

Appendix III

CLADOGRAM AND APOMORPHY LISTS

1. Cladogram

The cladogram is identical to that in figure 4-1 and with all internodes (58 to 104) numbered.

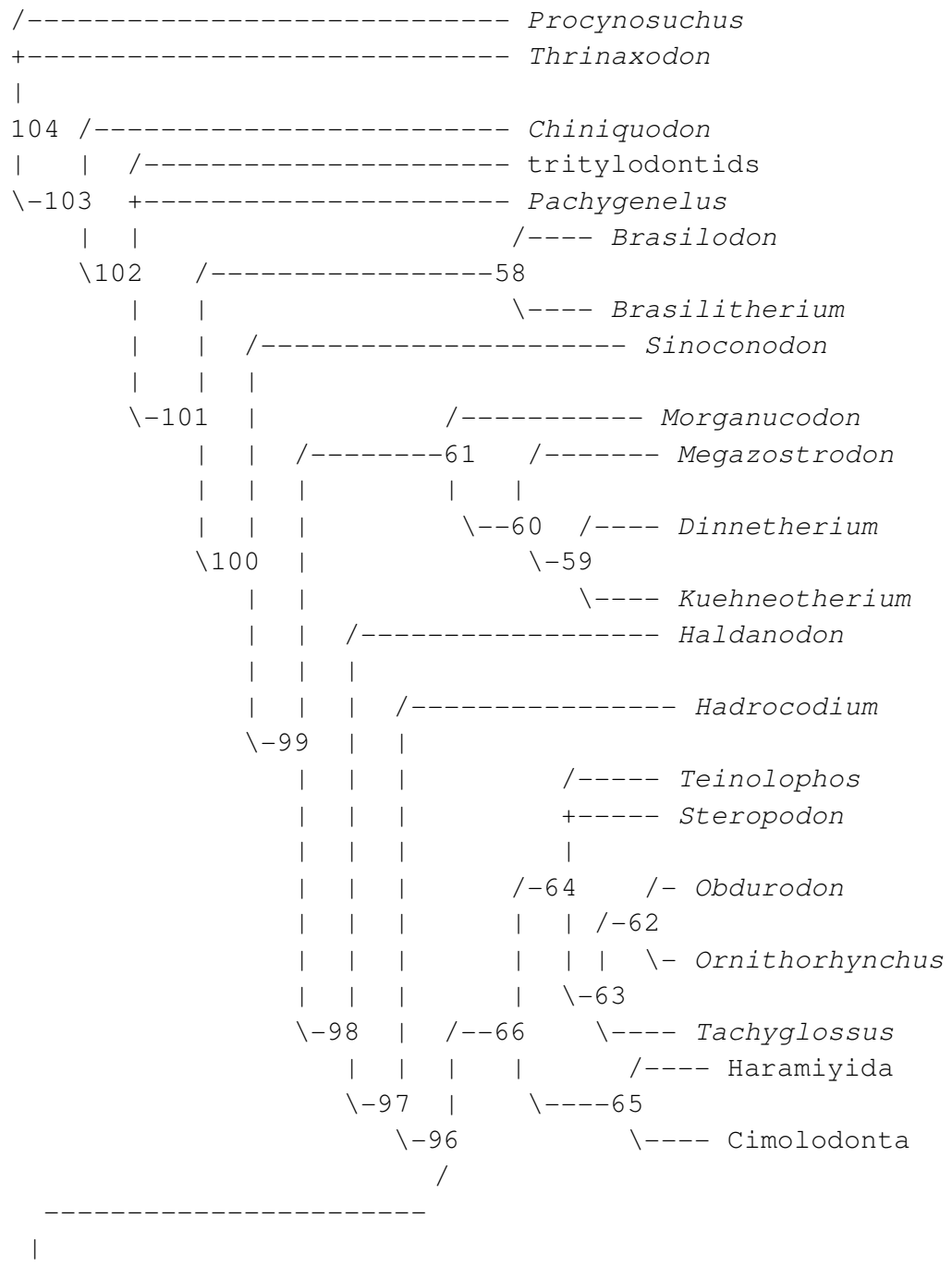

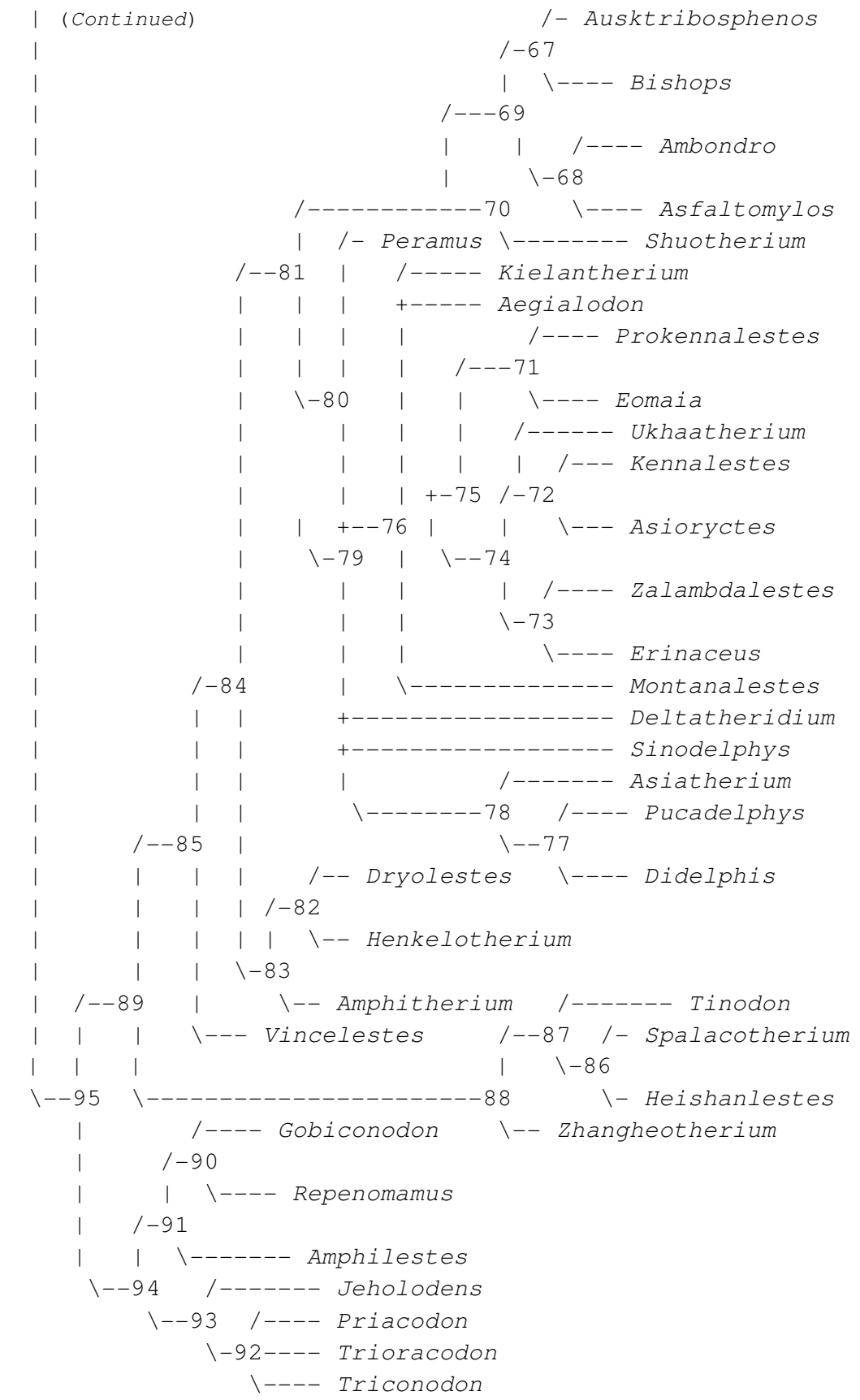
(Continued)
Ausktribosphenos
67
Bishops
69
Ambondro
68
70
Asfaltomylos
Peramus
Shuotherium
81
Kielantherium
Aegialodon
Prokennalestes
71
80
Eomaia
Ukhaatherium
Kennalestes
75
72
76
Asioryctes
79
74
Zalambdalestes
73
Erinaceus
84
Montanalestes
Deltatheridium
Sinodelphys
Asiatherium
78
Pucadelphys
85
77
Dryolestes
Didelphis
82
Henkelotherium
83
89
Amphitherium
Tinodon
Vincelestes
87
Spalacotherium
86
95
88
Heishanlestes
Gobiconodon
Zhangheotherium
90
Repenomamus
91
Amphilestes
94
Jeholodens
93
Priacodon
92
Trioracodon
Triconodon

2. Apomorphy lists:

The lists apply to the above cladogram. Characters changed on each internode (Node X --> Node Y) are list in the following format: character number, consistency index of the character and change of the character state from the node X to Y. The double arrow (==>) indicates an unequivocal transformation that occurs in both ACCTRAN and DELTRAN reconstructions. The single arrow (-->) represents an equivocal transformation that occurs either in ACCTRAN or DELTRAN reconstruction, but not in both; here only those in ACCTRAN are lised.

Node 104 --> *Procynosuchus*:

Ch 02, 1.000 1 ==> 0;
Ch 12, 1.000 1 ==> 0;
Ch 33, 1.000 1 ==> 0;
Ch 35, 1.000 1 ==> 0;
Ch 40, 0.333 1 ==> 0;
Ch 46, 1.000 1 ==> 0;
Ch 49, 1.000 1 ==> 0;
Ch 50, 0.400 0 ==> 1;
Ch 62, 1.000 1 ==> 0;
Ch 75, 0.667 1 ==> 0;
Ch 77, 0.667 1 ==> 0;
Ch 123, 1.000 1 ==> 0;
Ch 143, 0.333 1 ==> 0;
Ch 182, 0.333 2 ==> 0;
Ch 190, 1.000 1 ==> 0;
Ch 193, 1.000 1 ==> 0;
Ch 194, 1.000 1 ==> 0;
Ch 195, 1.000 1 ==> 0;
Ch 218, 0.333 1 ==> 0;
Ch 289, 1.000 1 ==> 0;
Ch 292, 1.000 1 ==> 0;
Ch 311, 0.667 1 ==> 0;
Ch 322, 1.000 1 ==> 0;
Ch 332, 0.267 1 ==> 0;
Ch 333, 0.308 1 ==> 0;
Ch 349, 0.273 3 ==> 0;
Ch 353, 0.667 1 ==> 0;
Ch 355, 0.500 1 ==> 0;
Ch 380, 0.333 1 ==> 0;
Ch 421, 1.000 1 ==> 0

Node 104 --> *Thrinaxodon*:

Ch 15, 1.000 0 --> 1;
Ch 20, 1.000 0 ==> 1;
Ch 32, 0.500 0 ==> 1;
Ch 48, 1.000 1 ==> 0;
Ch 118, 1.000 0 --> 1;
Ch 301, 0.400 0 --> 1;
Ch 342, 0.333 0 --> 1;
Ch 352, 0.286 0 ==> 1;
Ch 354, 0.667 0 ==> 1;
Ch 356, 0.250 0 --> 1;
Ch 387, 0.250 0 --> 1;
Ch 395, 0.250 0 --> 1;
Ch 399, 0.333 0 ==> 1;
Ch 412, 0.500 0 --> 1

Node 104 --> node 103:

Ch 03, 1.000 0 --> 1;
Ch 07, 1.000 0 --> 1;
Ch 10, 0.250 0 --> 1;
Ch 11, 1.000 0 --> 1;
Ch 14, 1.000 0 --> 1;
Ch 15, 1.000 0 --> 2;
Ch 16, 1.000 0 --> 1;
Ch 19, 1.000 0 --> 1;
Ch 24, 1.000 0 --> 1;
Ch 34, 1.000 0 ==> 1;
Ch 36, 1.000 0 --> 1;
Ch 53, 1.000 0 --> 1;
Ch 64, 1.000 0 --> 1;

Ch 65, 0.667 0 ==> 1;
Ch 66, 0.667 0 --> 1;
Ch 70, 1.000 0 ==> 1;
Ch 94, 1.000 0 ==> 1;
Ch 105, 0.333 0 --> 1;
Ch 109, 1.000 0 --> 1;
Ch 112, 0.500 0 --> 2;
Ch 113, 1.000 0 ==> 1;
Ch 114, 1.000 0 ==> 1;
Ch 115, 0.500 0 --> 1;
Ch 116, 0.500 0 --> 1;
Ch 118, 1.000 0 --> 2;
Ch 120, 1.000 0 ==> 1;
Ch 121, 1.000 0 --> 1;
Ch 122, 1.000 0 --> 1;
Ch 124, 1.000 0 --> 1;
Ch 129, 0.500 0 --> 1;
Ch 132, 1.000 0 --> 1;
Ch 134, 0.500 0 --> 1;
Ch 138, 1.000 0 ==> 1;
Ch 148, 0.500 1 ==> 0;
Ch 149, 1.000 0 --> 1;
Ch 150, 1.000 0 --> 1;
Ch 152, 0.500 0 --> 1;
Ch 185, 0.200 0 ==> 1;
Ch 187, 0.125 0 ==> 1;
Ch 188, 0.143 1 --> 0;
Ch 191, 0.500 0 --> 1;
Ch 197, 1.000 0 ==> 1;
Ch 211, 0.667 0 ==> 1;
Ch 217, 1.000 0 --> 1;
Ch 243, 0.500 0 ==> 1;
Ch 250, 1.000 0 ==> 1;
Ch 270, 0.500 0 --> 1;
Ch 273, 0.500 0 ==> 1;
Ch 277, 1.000 0 --> 1;
Ch 279, 1.000 0 ==> 1;
Ch 283, 1.000 0 ==> 1;
Ch 298, 1.000 0 ==> 1;
Ch 301, 0.400 0 --> 2;
Ch 302, 0.286 0 ==> 1;
Ch 303, 0.200 0 ==> 1;
Ch 304, 1.000 0 ==> 1;
Ch 305, 1.000 0 ==> 1;
Ch 306, 1.000 0 ==> 1;
Ch 308, 1.000 0 ==> 1;
Ch 312, 0.167 0 --> 1;
Ch 315, 0.250 0 ==> 2;
Ch 387, 0.250 0 --> 2;
Ch 404, 0.200 2 ==> 0;
Ch 429, 0.333 0 --> 1

Node 103 --> *Chiniquodon*:

Ch 58, 0.500 0 ==> 1;
Ch 210, 0.400 0 ==> 2;
Ch 323, 0.222 0 ==> 1;
Ch 349, 0.273 3 ==> 1;
Ch 395, 0.250 0 --> 1

Node 103 --> node 102:

Ch 1, 1.000 0 ==> 1;
Ch 25, 1.000 0 ==> 1;
Ch 26, 1.000 0 ==> 1;
Ch 27, 1.000 0 ==> 1;
Ch 28, 1.000 0 ==> 1;
Ch 30, 0.333 0 ==> 1;
Ch 59, 0.200 0 --> 1;
Ch 61, 0.333 0 --> 1;
Ch 66, 0.667 1 --> 2;
Ch 67, 0.750 0 ==> 1;
Ch 69, 0.750 0 --> 1;
Ch 78, 1.000 0 ==> 1;
Ch 80, 0.667 0 ==> 1;
Ch 81, 0.333 0 --> 1;
Ch 87, 0.500 0 ==> 1;
Ch 88, 0.500 1 ==> 0;
Ch 99, 0.500 0 ==> 1;
Ch 100, 1.000 0 ==> 1;
Ch 117, 1.000 0 ==> 1;
Ch 119, 1.000 0 ==> 1;
Ch 130, 1.000 0 ==> 1;
Ch 133, 1.000 0 ==> 1;
Ch 136, 1.000 0 ==> 1;
Ch 137, 0.667 0 ==> 1;
Ch 178, 0.500 0 --> 1;
Ch 181, 1.000 0 ==> 1;
Ch 198, 0.500 0 ==> 1;
Ch 199, 0.143 0 ==> 1;

Ch 203, 0.167 0 --> 1;
Ch 205, 0.500 0 --> 1;
Ch 206, 1.000 0 ==> 1;
Ch 207, 1.000 0 ==> 1;
Ch 208, 0.333 0 ==> 1;
Ch 216, 0.667 0 ==> 1;
Ch 224, 0.500 0 --> 1;
Ch 225, 0.500 0 --> 1;
Ch 228, 0.500 0 --> 1;
Ch 230, 0.125 0 --> 1;
Ch 239, 1.000 0 ==> 1;
Ch 249, 0.667 0 --> 1;
Ch 258, 0.333 0 --> 1;
Ch 262, 1.000 0 ==> 1;
Ch 274, 0.667 0 --> 1;
Ch 285, 0.222 0 --> 1;
Ch 297, 0.667 0 --> 1;
Ch 307, 1.000 0 ==> 1;
Ch 329, 0.333 0 --> 1;
Ch 330, 0.667 0 ==> 2;
Ch 331, 0.333 0 ==> 2;
Ch 332, 0.267 1 --> 3;
Ch 334, 0.400 0 --> 1;
Ch 336, 0.200 0 --> 1;
Ch 337, 0.250 0 --> 1;
Ch 341, 0.167 0 --> 1;
Ch 342, 0.333 0 --> 1;
Ch 345, 0.200 0 --> 1;
Ch 347, 0.750 0 ==> 1;
Ch 348, 0.750 0 ==> 1;
Ch 355, 0.500 1 ==> 2;
Ch 356, 0.250 0 --> 1;
Ch 412, 0.500 0 --> 1;
Ch 423, 0.250 0 --> 1;
Ch 424, 0.667 0 ==> 1

Node 102 -> tritylodontids:

Ch 66, 0.667 2 --> 1;
Ch 69, 0.750 1 --> 0;
Ch 178, 0.500 1 --> 0;
Ch 188, 0.143 0 --> 1;
Ch 203, 0.167 1 --> 0;
Ch 204, 0.333 0 ==> 1;
Ch 211, 0.667 1 ==> 2;
Ch 212, 0.333 0 ==> 1;
Ch 225, 0.500 1 --> 0;
Ch 228, 0.500 1 --> 0;
Ch 255, 0.250 0 ==> 1;
Ch 285, 0.222 1 --> 0;
Ch 297, 0.667 1 --> 0;
Ch 312, 0.167 1 ==> 2;
Ch 325, 0.667 0 ==> 1;
Ch 327, 0.333 0 ==> 1;
Ch 328, 0.500 0 ==> 1;
Ch 331, 0.333 2 ==> 1;
Ch 336, 0.200 1 ==> 2;
Ch 338, 0.333 0 ==> 1;
Ch 339, 0.286 0 ==> 2;
Ch 343, 0.286 0 ==> 2;
Ch 347, 0.750 1 ==> 3;
Ch 348, 0.750 1 --> 2;
Ch 351, 0.667 0 ==> 2;
Ch 353, 0.667 1 ==> 0;
Ch 355, 0.500 2 ==> 0;
Ch 356, 0.250 1 --> 0;
Ch 361, 0.286 0 ==> 2;
Ch 366, 0.143 0 ==> 1;
Ch 377, 0.333 0 ==> 1;
Ch 379, 0.600 0 ==> 3;
Ch 380, 0.333 1 ==> 3;
Ch 422, 0.500 0 ==> 3;
Ch 423, 0.250 1 --> 0;
Ch 424, 0.667 1 ==> 2;
Ch 430, 0.667 0 ==> 4;
Ch 431, 0.250 1 ==> 0

Node 102 --> *Pachygenelus*:

Ch 59, 0.200 1 --> 0;
Ch 61, 0.333 1 --> 0;
Ch 79, 0.333 0 ==> 1;
Ch 81, 0.333 1 --> 0;
Ch 143, 0.333 1 ==> 2;
Ch 179, 0.333 0 ==> 1;
Ch 196, 0.400 0 ==> 1;
Ch 201, 0.250 0 ==> 1;
Ch 205, 0.500 1 --> 0;
Ch 218, 0.333 1 ==> 0;
Ch 220, 0.250 0 ==> 1;

Ch 224, 0.500 1 --> 0;
Ch 249, 0.667 1 --> 0;
Ch 258, 0.333 1 --> 0;
Ch 270, 0.500 1 --> 0;
Ch 274, 0.667 1 --> 0;
Ch 302, 0.286 1 ==> 0;
Ch 333, 0.308 1 ==> 2;
Ch 350, 0.250 0 ==> 1;
Ch 352, 0.286 0 ==> 1;
Ch 357, 0.250 0 ==> 1;
Ch 387, 0.250 2 ==> 0;
Ch 395, 0.250 0 --> 1;
Ch 404, 0.200 0 ==> 2;
Ch 435, 0.250 0 --> 1

Node 102 --> node 101:

Ch 5, 1.000 0 --> 1;
Ch 6, 1.000 0 --> 1;
Ch 9, 1.000 0 --> 1;
Ch 12, 1.000 1 --> 2;
Ch 29, 0.333 0 --> 1;
Ch 50, 0.400 0 --> 2;
Ch 51, 1.000 0 --> 1;
Ch 52, 1.000 0 --> 1;
Ch 58, 0.500 0 --> 2;
Ch 63, 1.000 0 --> 1;
Ch 90, 0.750 0 --> 1;
Ch 102, 1.000 0 --> 1;
Ch 144, 0.600 0 --> 1;
Ch 150, 1.000 1 --> 2;
Ch 191, 0.500 1 --> 0;
Ch 192, 0.167 0 --> 1;
Ch 196, 0.400 0 ==> 2;
Ch 214, 0.375 0 --> 1;
Ch 215, 0.667 0 ==> 1;
Ch 223, 1.000 0 ==> 1;
Ch 230, 0.125 1 --> 0;
Ch 231, 0.500 0 --> 1;
Ch 272, 0.667 0 ==> 1;
Ch 295, 1.000 0 ==> 1;
Ch 299, 0.500 0 --> 1;
Ch 312, 0.167 1 --> 0;
Ch 329, 0.333 1 --> 0;
Ch 330, 0.667 2 ==> 1;
Ch 332, 0.267 3 --> 0;
Ch 334, 0.400 1 --> 0;
Ch 337, 0.250 1 --> 0;
Ch 349, 0.273 3 ==> 2;
Ch 351, 0.667 0 ==> 1;
Ch 352, 0.286 0 ==> 2;
Ch 353, 0.667 1 ==> 2;
Ch 354, 0.667 0 ==> 2;
Ch 379, 0.600 0 ==> 1;
Ch 399, 0.333 0 ==> 1;
Ch 403, 0.125 0 --> 1;
Ch 418, 0.500 0 --> 3;
Ch 433, 0.286 0 --> 1

Node 101 --> node 58:

Ch 182, 0.333 2 --> 1;
Ch 201, 0.250 0 --> 1;
Ch 218, 0.333 1 ==> 0;
Ch 243, 0.500 1 ==> 0;
Ch 244, 0.333 0 ==> 1;
Ch 282, 0.500 0 --> 1;
Ch 301, 0.400 2 ==> 1;
Ch 315, 0.250 2 ==> 1;
Ch 323, 0.222 0 ==> 1;
Ch 332, 0.267 0 --> 1;
Ch 380, 0.333 1 ==> 3;
Ch 401, 0.375 0 ==> 1

Node 58 --> *Brasilodon*:

Ch 210, 0.400 0 ==> 2;
Ch 231, 0.500 1 --> 0;
Ch 398, 0.143 0 ==> 1

Node 58 --> *Brasilitherium*:

Ch 214, 0.375 1 --> 0;
Ch 230, 0.125 0 --> 1;
Ch 235, 0.500 0 ==> 1;
Ch 339, 0.286 0 ==> 1;
Ch 341, 0.167 1 --> 0;
Ch 342, 0.333 1 ==> 0;
Ch 343, 0.286 0 ==> 1;
Ch 345, 0.200 1 --> 0;
Ch 354, 0.667 2 ==> 1;
Ch 357, 0.250 0 ==> 1

Node 101 --> node 100:

Ch 185, 0.200 1 ==> 0;
Ch 188, 0.143 0 --> 1;
Ch 202, 0.250 0 ==> 1;
Ch 211, 0.667 1 ==> 2;
Ch 221, 0.667 0 ==> 1;
Ch 235, 0.500 0 ==> 2;
Ch 237, 1.000 0 ==> 1;
Ch 240, 1.000 0 ==> 1;
Ch 241, 0.500 0 ==> 1;
Ch 242, 1.000 0 ==> 1;
Ch 246, 0.500 0 ==> 1;
Ch 247, 0.667 0 ==> 1;
Ch 261, 1.000 0 ==> 1;
Ch 265, 1.000 0 ==> 1;
Ch 268, 0.750 0 ==> 1;
Ch 284, 0.500 0 ==> 1;
Ch 286, 0.500 0 ==> 1;
Ch 328, 0.500 0 ==> 1;
Ch 333, 0.308 1 ==> 0;
Ch 336, 0.200 1 --> 0;
Ch 346, 1.000 0 ==> 1;
Ch 347, 0.750 1 ==> 2;
Ch 348, 0.750 1 --> 2;
Ch 391, 0.500 0 ==> 1;
Ch 430, 0.667 0 --> 1

Node 100 --> *Sinoconodon*:

Ch 135, 0.333 0 ==> 1;
Ch 220, 0.250 0 ==> 1;
Ch 285, 0.222 1 --> 0;
Ch 349, 0.273 2 ==> 4;
Ch 371, 0.250 0 --> 2;
Ch 375, 0.267 0 --> 1;
Ch 403, 0.125 1 --> 0;
Ch 429, 0.333 1 --> 0

Node 100 --> node 99:

Ch 79, 0.333 0 --> 1;
Ch 146, 0.400 0 ==> 1;
Ch 148, 0.500 0 ==> 1;
Ch 187, 0.125 1 --> 0;
Ch 192, 0.167 1 --> 0;
Ch 225, 0.500 1 ==> 2;
Ch 232, 0.750 0 ==> 1;
Ch 249, 0.667 1 ==> 2;
Ch 255, 0.250 0 ==> 1;
Ch 262, 1.000 1 ==> 2;
Ch 287, 1.000 0 ==> 1;
Ch 341, 0.167 1 --> 0;
Ch 345, 0.200 1 --> 0;
Ch 350, 0.250 0 ==> 1;
Ch 404, 0.200 0 --> 2;
Ch 422, 0.500 0 ==> 2;
Ch 430, 0.667 1 --> 2

Node 99 --> node 61:

Ch 32, 0.500 0 ==> 1;
Ch 59, 0.200 1 --> 0;
Ch 85, 0.250 0 ==> 1;
Ch 182, 0.333 2 --> 1;
Ch 282, 0.500 0 --> 1;
Ch 332, 0.267 0 --> 1;
Ch 358, 0.158 3 ==> 0;
Ch 359, 0.250 3 ==> 0;
Ch 387, 0.250 2 ==> 0;
Ch 401, 0.375 0 ==> 1;
Ch 402, 0.286 0 ==> 1

Node 61 --> *Morganucodon*:

Ch 345, 0.200 0 --> 1;
Ch 374, 0.143 0 ==> 1;
Ch 422, 0.500 2 ==> 1

Node 61 --> node 60:

Ch 349, 0.273 2 ==> 0

Node 60 --> *Megazostrodon*:

Ch 224, 0.500 1 ==> 2;
Ch 312, 0.167 0 ==> 1;
Ch 405, 0.500 0 ==> 2;
Ch 433, 0.286 1 ==> 0;
Ch 435, 0.250 0 ==> 1

Node 60 --> node 59:

Ch 327, 0.333 0 ==> 1;

Ch 336, 0.200 0 --> 1;
Ch 358, 0.158 0 --> 1;
Ch 400, 0.200 0 ==> 1;
Ch 401, 0.375 1 ==> 2

Node 59 --> *Dinnetherium*:
Ch 299, 0.500 1 ==> 2;
Ch 349, 0.273 0 ==> 1;
Ch 422, 0.500 2 ==> 1

Node 59 --> *Kuehneotherium*:
Ch 301, 0.400 2 ==> 1;
Ch 315, 0.250 2 ==> 0;
Ch 331, 0.333 2 ==> 1;
Ch 380, 0.333 1 ==> 2;
Ch 381, 0.250 0 ==> 1;
Ch 384, 0.500 0 ==> 1;
Ch 385, 0.500 0 ==> 1;
Ch 386, 0.333 0 ==> 1;
Ch 388, 0.333 0 ==> 1;
Ch 391, 0.500 1 ==> 2;
Ch 398, 0.143 0 ==> 2;
Ch 408, 0.333 0 ==> 1;
Ch 409, 0.286 0 ==> 1;
Ch 410, 0.750 0 ==> 1;
Ch 425, 0.333 0 ==> 1;
Ch 426, 0.500 0 ==> 1;
Ch 431, 0.250 1 ==> 0

Node 99 --> node 98:
Ch 8, 0.333 0 --> 1;
Ch 13, 0.500 0 --> 1;
Ch 17, 0.333 0 --> 1;
Ch 55, 0.667 0 --> 1;
Ch 57, 0.500 0 --> 1;
Ch 69, 0.750 1 --> 3;
Ch 71, 1.000 0 ==> 1;
Ch 84, 0.500 0 --> 1;
Ch 143, 0.333 1 --> 2;
Ch 144, 0.600 1 --> 0;
Ch 158, 0.429 0 --> 1;
Ch 165, 1.000 0 --> 1;
Ch 166, 1.000 0 --> 1;
Ch 175, 0.500 0 --> 1;
Ch 199, 0.143 1 --> 0;
Ch 214, 0.375 1 --> 0;
Ch 219, 0.250 0 --> 1;
Ch 221, 0.667 1 ==> 2;
Ch 224, 0.500 1 ==> 2;
Ch 228, 0.500 1 ==> 2;
Ch 244, 0.333 0 --> 1;
Ch 248, 0.333 0 --> 1;
Ch 254, 0.500 0 --> 1;
Ch 256, 0.500 0 --> 1;
Ch 268, 0.750 1 --> 2;
Ch 271, 0.500 0 --> 1;
Ch 274, 0.667 1 --> 2;
Ch 275, 1.000 0 --> 1;
Ch 276, 1.000 0 --> 1;
Ch 286, 0.500 1 ==> 2;
Ch 290, 0.333 0 --> 1;
Ch 299, 0.500 1 ==> 2;
Ch 307, 1.000 1 ==> 2;
Ch 312, 0.167 0 ==> 1;
Ch 327, 0.333 0 ==> 1;
Ch 331, 0.333 2 ==> 1;
Ch 365, 0.250 1 ==> 0;
Ch 366, 0.143 0 ==> 1;
Ch 370, 0.125 0 --> 1;
Ch 398, 0.143 0 --> 1;
Ch 431, 0.250 1 --> 0

Node 98 --> *Haldanodon*:
Ch 90, 0.750 1 ==> 3;
Ch 97, 0.500 0 ==> 1;
Ch 99, 0.500 1 ==> 0;
Ch 201, 0.250 0 ==> 1;
Ch 203, 0.167 1 ==> 0;
Ch 215, 0.667 1 ==> 0;
Ch 284, 0.500 1 ==> 0;
Ch 323, 0.222 0 ==> 1;
Ch 340, 0.200 0 ==> 1;
Ch 344, 0.143 0 ==> 1;
Ch 352, 0.286 2 ==> 0;
Ch 355, 0.500 2 ==> 0;
Ch 358, 0.158 3 ==> 2;
Ch 359, 0.250 3 ==> 2;
Ch 373, 0.333 0 ==> 1;

Ch 374, 0.143 0 ==> 1;
Ch 377, 0.333 0 ==> 1;
Ch 379, 0.600 1 ==> 2;
Ch 380, 0.333 1 ==> 2;
Ch 402, 0.286 0 ==> 2;
Ch 423, 0.250 1 ==> 0

Node 98 --> node 97:

Ch 65, 0.667 1 --> 2;
Ch 67, 0.750 1 --> 0;
Ch 72, 0.500 0 --> 1;
Ch 74, 1.000 0 --> 1;
Ch 75, 0.667 1 --> 2;
Ch 76, 0.500 0 --> 1;
Ch 101, 0.500 0 --> 1;
Ch 141, 1.000 0 --> 1;
Ch 146, 0.400 1 --> 2;
Ch 177, 1.000 0 --> 1;
Ch 185, 0.200 0 ==> 1;
Ch 187, 0.125 0 --> 1;
Ch 192, 0.167 0 --> 1;
Ch 202, 0.250 1 --> 0;
Ch 214, 0.375 0 --> 3;
Ch 280, 1.000 0 --> 1;
Ch 297, 0.667 1 ==> 2;
Ch 302, 0.286 1 ==> 2;
Ch 303, 0.200 1 ==> 0;
Ch 304, 1.000 1 ==> 2;
Ch 305, 1.000 1 --> 2;
Ch 309, 1.000 0 --> 1;
Ch 310, 0.125 0 --> 1;
Ch 313, 0.250 0 --> 1;
Ch 314, 1.000 0 ==> 2;
Ch 319, 0.200 0 --> 1;
Ch 336, 0.200 0 ==> 1;
Ch 349, 0.273 2 ==> 5;
Ch 375, 0.267 0 --> 3;
Ch 403, 0.125 1 --> 0;
Ch 404, 0.200 2 --> 0

Node 97 --> *Hadrocodium*:

Ch 189, 0.250 0 ==> 1;
Ch 225, 0.500 2 ==> 1;
Ch 231, 0.500 1 ==> 2;
Ch 251, 0.500 0 ==> 1;
Ch 255, 0.250 1 ==> 0;
Ch 256, 0.500 1 --> 0;
Ch 285, 0.222 1 ==> 2;
Ch 286, 0.500 2 ==> 3;
Ch 291, 0.500 0 ==> 1;
Ch 319, 0.200 1 --> 2;
Ch 341, 0.167 0 ==> 1;
Ch 345, 0.200 0 --> 1;
Ch 362, 0.250 0 ==> 1

Node 97 --> node 96:

Ch 188, 0.143 1 --> 0;
Ch 199, 0.143 0 --> 1;
Ch 219, 0.250 1 --> 0;
Ch 252, 1.000 0 --> 1;
Ch 300, 0.600 0 ==> 1;
Ch 315, 0.250 2 --> 0;
Ch 321, 0.600 0 --> 1;
Ch 322, 1.000 1 ==> 2;
Ch 323, 0.222 0 --> 2;
Ch 332, 0.267 0 ==> 3;
Ch 339, 0.286 0 --> 1;
Ch 343, 0.286 0 --> 1;
Ch 370, 0.125 1 --> 0;
Ch 391, 0.500 1 --> 2;
Ch 408, 0.333 0 --> 1;
Ch 412, 0.500 1 --> 4

Node 96 --> node 66:

Ch 22, 0.500 1 ==> 0;
Ch 40, 0.333 1 --> 0;
Ch 58, 0.500 2 --> 0;
Ch 103, 0.500 0 --> 1;
Ch 111, 0.667 0 --> 1;
Ch 115, 0.500 1 --> 0;
Ch 116, 0.500 1 --> 0;
Ch 125, 1.000 0 ==> 1;
Ch 128, 0.333 0 ==> 1;
Ch 147, 0.500 0 ==> 1;
Ch 152, 0.500 1 --> 0;
Ch 155, 0.250 0 ==> 1;
Ch 159, 0.333 0 --> 1;
Ch 162, 1.000 1 ==> 0;

Ch 176, 0.250 0 ==> 1;
Ch 182, 0.333 2 ==> 0;
Ch 200, 0.500 0 ==> 1;
Ch 204, 0.333 0 --> 1;
Ch 208, 0.333 1 --> 0;
Ch 209, 1.000 0 ==> 1;
Ch 210, 0.400 0 ==> 2;
Ch 276, 1.000 1 --> 2;
Ch 278, 1.000 0 ==> 1;
Ch 280, 1.000 1 --> 2;
Ch 281, 1.000 0 ==> 1;
Ch 313, 0.250 1 --> 3;
Ch 316, 0.400 0 --> 1;
Ch 318, 0.500 0 --> 1;
Ch 337, 0.250 0 --> 1;
Ch 338, 0.333 0 --> 1;
Ch 339, 0.286 1 --> 2;
Ch 343, 0.286 1 --> 2;
Ch 352, 0.286 2 --> 0;
Ch 366, 0.143 1 --> 0;
Ch 368, 0.500 0 --> 2;
Ch 380, 0.333 1 ==> 3;
Ch 389, 0.250 0 --> 1;
Ch 390, 0.333 0 --> 1;
Ch 397, 0.200 0 --> 1;
Ch 398, 0.143 1 --> 0;
Ch 407, 0.667 0 --> 2;
Ch 409, 0.286 0 --> 2;
Ch 410, 0.750 0 --> 3;
Ch 411, 0.500 0 --> 2;
Ch 414, 0.200 0 --> 1;
Ch 416, 0.250 0 --> 1;
Ch 417, 0.333 0 --> 2;
Ch 418, 0.500 3 --> 4;
Ch 420, 0.400 0 --> 2;
Ch 423, 0.250 1 ==> 0;
Ch 432, 0.250 0 --> 1

Node 66 --> node 64:

Ch 4, 0.250 0 --> 1;
Ch 10, 0.250 1 --> 0;
Ch 17, 0.333 1 --> 0;
Ch 23, 0.500 0 --> 1;
Ch 31, 1.000 0 --> 1;
Ch 37, 0.500 0 --> 1;
Ch 38, 1.000 0 --> 1;
Ch 39, 1.000 0 --> 1;
Ch 41, 1.000 0 --> 1;
Ch 42, 1.000 0 --> 1;
Ch 43, 1.000 0 --> 1;
Ch 44, 1.000 0 --> 1;
Ch 55, 0.667 1 --> 2;
Ch 57, 0.500 1 --> 0;
Ch 58, 0.500 0 --> 1;
Ch 65, 0.667 2 --> 1;
Ch 69, 0.750 3 --> 2;
Ch 72, 0.500 1 --> 0;
Ch 73, 1.000 0 --> 1;
Ch 74, 1.000 1 --> 2;
Ch 75, 0.667 2 --> 1;
Ch 76, 0.500 1 --> 0;
Ch 77, 0.667 1 --> 0;
Ch 79, 0.333 1 --> 0;
Ch 81, 0.333 1 --> 0;
Ch 84, 0.500 1 --> 0;
Ch 87, 0.500 1 --> 0;
Ch 90, 0.750 1 --> 3;
Ch 93, 1.000 0 --> 1;
Ch 97, 0.500 0 --> 1;
Ch 99, 0.500 1 --> 0;
Ch 101, 0.500 1 --> 0;
Ch 127, 1.000 0 --> 1;
Ch 131, 0.333 0 --> 1;
Ch 132, 1.000 1 --> 2;
Ch 134, 0.500 1 --> 0;
Ch 145, 1.000 0 --> 1;
Ch 154, 1.000 0 --> 1;
Ch 165, 1.000 1 --> 3;
Ch 166, 1.000 1 --> 2;
Ch 172, 1.000 0 --> 1;
Ch 173, 1.000 0 --> 1;
Ch 180, 0.500 0 --> 1;
Ch 183, 0.333 0 --> 1;
Ch 186, 1.000 0 --> 2;
Ch 198, 0.500 1 --> 0;
Ch 199, 0.143 1 --> 0;
Ch 219, 0.250 0 --> 1;
Ch 228, 0.500 2 --> 1;

Ch 232, 0.750 1 --> 2;
Ch 235, 0.500 2 --> 0;
Ch 238, 1.000 0 --> 1;
Ch 257, 1.000 0 --> 1;
Ch 258, 0.333 1 --> 0;
Ch 273, 0.500 1 --> 0;
Ch 286, 0.500 2 --> 3;
Ch 291, 0.500 0 --> 1;
Ch 315, 0.250 0 --> 1;
Ch 324, 0.500 0 --> 1;
Ch 331, 0.333 1 ==> 0;
Ch 332, 0.267 3 --> 5;
Ch 333, 0.308 0 --> 4;
Ch 347, 0.750 2 --> 3;
Ch 361, 0.286 0 --> 1;
Ch 363, 0.500 0 --> 1;
Ch 379, 0.600 1 --> 3;
Ch 387, 0.250 2 --> 0;
Ch 402, 0.286 0 ==> 2;
Ch 404, 0.200 0 ==> 1;
Ch 405, 0.500 0 --> 1;
Ch 419, 0.600 0 ==> 3;
Ch 434, 0.333 0 --> 1

Node 64 --> *Teinolophos*:
Ch 300, 0.600 1 ==> 2;
Ch 302, 0.286 2 ==> 1;
Ch 303, 0.200 0 ==> 1;
Ch 313, 0.250 3 --> 0;
Ch 315, 0.250 1 --> 2;
Ch 316, 0.400 1 --> 2;
Ch 319, 0.200 1 ==> 0;
Ch 405, 0.500 1 --> 0;
Ch 407, 0.667 2 --> 0

Node 64 --> *Steropodon*:
Ch 313, 0.250 3 ==> 2;
Ch 403, 0.125 0 ==> 1

Node 64 --> node 63:
Ch 311, 0.667 1 ==> 2;
Ch 325, 0.667 0 ==> 2;
Ch 326, 1.000 0 ==> 1;
Ch 348, 0.750 2 --> 3;
Ch 397, 0.200 1 --> 0;
Ch 398, 0.143 0 --> 1

Node 63 --> node 62:
Ch 158, 0.429 1 --> 0;
Ch 272, 0.667 1 ==> 2;
Ch 320, 0.250 0 ==> 1

Node 62 --> *Obdurodon*:
Ch 230, 0.125 0 ==> 1;
Ch 313, 0.250 3 ==> 2;
Ch 431, 0.250 0 --> 2;
Ch 433, 0.286 1 ==> 2

Node 62--> *Ornithorhynchus*:
Ch 235, 0.500 0 --> 2

Node 63 --> *Tachyglossus*:
Ch 159, 0.333 1 --> 0;
Ch 164, 0.333 0 ==> 1;
Ch 319, 0.200 1 ==> 2;
Ch 323, 0.222 2 --> 0;
Ch 324, 0.500 1 --> 0;
Ch 349, 0.273 5 ==> 6;
Ch 375, 0.267 3 ==> 4

Node 66 --> node 65:
Ch 8, 0.333 1 --> 0;
Ch 47, 0.500 0 --> 1;
Ch 50, 0.400 2 --> 1;
Ch 61, 0.333 1 --> 0;
Ch 67, 0.750 0 --> 2;
Ch 68, 1.000 0 --> 1;
Ch 80, 0.667 1 --> 2;
Ch 86, 0.500 0 --> 1;
Ch 104, 0.333 0 --> 1;
Ch 135, 0.333 0 --> 1;
Ch 137, 0.667 1 --> 2;
Ch 139, 0.250 0 --> 1;
Ch 140, 0.500 0 --> 1;
Ch 142, 0.333 0 --> 1;
Ch 143, 0.333 2 --> 0;
Ch 144, 0.600 0 --> 3;
Ch 151, 1.000 0 --> 2;

Ch 153, 0.250 0 --> 1;
Ch 156, 0.250 0 --> 1;
Ch 158, 0.429 1 --> 2;
Ch 168, 0.500 0 --> 1;
Ch 169, 0.250 0 --> 1;
Ch 170, 1.000 0 --> 2;
Ch 171, 0.500 0 --> 1;
Ch 175, 0.500 1 --> 2;
Ch 178, 0.500 1 --> 2;
Ch 179, 0.333 0 --> 1;
Ch 184, 0.250 0 --> 1;
Ch 185, 0.200 1 --> 0;
Ch 188, 0.143 0 --> 1;
Ch 196, 0.400 2 --> 0;
Ch 216, 0.667 1 --> 2;
Ch 233, 0.667 0 --> 1;
Ch 241, 0.500 1 --> 2;
Ch 242, 1.000 1 --> 2;
Ch 248, 0.333 1 --> 0;
Ch 260, 0.667 0 --> 1;
Ch 282, 0.500 0 --> 2;
Ch 285, 0.222 1 --> 2;
Ch 290, 0.333 1 --> 0;
Ch 300, 0.600 1 --> 3;
Ch 311, 0.667 1 --> 0;
Ch 323, 0.222 2 --> 0;
Ch 329, 0.333 0 ==> 1;
Ch 330, 0.667 1 --> 2;
Ch 350, 0.250 1 ==> 0;
Ch 351, 0.667 1 ==> 2;
Ch 356, 0.250 1 ==> 0;
Ch 359, 0.250 3 --> 1;
Ch 364, 1.000 0 ==> 2;
Ch 377, 0.333 0 ==> 1;
Ch 399, 0.333 1 ==> 0;
Ch 412, 0.500 4 --> 0;
Ch 422, 0.500 2 ==> 3;
Ch 424, 0.667 1 ==> 2;
Ch 433, 0.286 1 --> 0

Node 65 --> Haramiyida:

Ch 302, 0.286 2 ==> 1;
Ch 349, 0.273 5 ==> 3;
Ch 358, 0.158 3 ==> 1;
Ch 375, 0.267 3 ==> 2;
Ch 432, 0.250 1 --> 0

Node 65 --> Cimolodonta:

Ch 320, 0.250 0 ==> 1;
Ch 325, 0.667 0 ==> 1;
Ch 333, 0.308 0 ==> 3;
Ch 334, 0.400 0 ==> 1;
Ch 335, 1.000 0 ==> 1;
Ch 336, 0.200 1 ==> 2;
Ch 431, 0.250 0 --> 1

Node 96 --> node 95:

Ch 21, 1.000 0 ==> 1;
Ch 29, 0.333 1 --> 0;
Ch 30, 0.333 1 ==> 0;
Ch 45, 1.000 0 --> 1;
Ch 56, 1.000 0 ==> 1;
Ch 67, 0.750 0 --> 3;
Ch 68, 1.000 0 ==> 2;
Ch 77, 0.667 1 ==> 2;
Ch 91, 1.000 0 ==> 1;
Ch 105, 0.333 1 --> 0;
Ch 107, 0.250 0 --> 1;
Ch 143, 0.333 2 --> 1;
Ch 144, 0.600 0 --> 1;
Ch 221, 0.667 2 ==> 1;
Ch 293, 1.000 0 --> 1;
Ch 317, 1.000 0 --> 1;
Ch 320, 0.250 0 ==> 1;
Ch 321, 0.600 1 --> 2;
Ch 331, 0.333 1 ==> 2;
Ch 333, 0.308 0 --> 2;
Ch 365, 0.250 0 ==> 1;
Ch 375, 0.267 3 --> 0;
Ch 425, 0.333 0 --> 1;
Ch 430, 0.667 2 --> 1;
Ch 431, 0.250 0 --> 1

Node 95 --> node 89:

Ch 47, 0.500 0 ==> 1;
Ch 80, 0.667 1 ==> 2;
Ch 82, 1.000 0 ==> 1;
Ch 83, 1.000 0 ==> 1;

Ch 86, 0.500 0 ==> 1;
Ch 88, 0.500 0 ==> 1;
Ch 89, 0.500 0 --> 1;
Ch 90, 0.750 1 ==> 2;
Ch 110, 0.667 0 --> 1;
Ch 131, 0.333 0 --> 1;
Ch 135, 0.333 0 ==> 1;
Ch 137, 0.667 1 ==> 2;
Ch 140, 0.500 0 ==> 1;
Ch 142, 0.333 0 --> 1;
Ch 151, 1.000 0 ==> 1;
Ch 167, 1.000 0 ==> 1;
Ch 168, 0.500 0 ==> 1;
Ch 170, 1.000 0 ==> 1;
Ch 171, 0.500 0 ==> 2;
Ch 175, 0.500 1 --> 2;
Ch 196, 0.400 2 --> 1;
Ch 213, 1.000 0 --> 1;
Ch 216, 0.667 1 --> 2;
Ch 233, 0.667 0 ==> 1;
Ch 234, 1.000 0 --> 1;
Ch 237, 1.000 1 --> 2;
Ch 251, 0.500 0 ==> 1;
Ch 259, 1.000 0 ==> 1;
Ch 260, 0.667 0 ==> 1;
Ch 294, 1.000 0 --> 1;
Ch 310, 0.125 1 --> 0;
Ch 332, 0.267 3 ==> 1;
Ch 344, 0.143 0 --> 1;
Ch 361, 0.286 0 --> 1;
Ch 380, 0.333 1 ==> 2;
Ch 381, 0.250 0 --> 1;
Ch 384, 0.500 0 --> 1;
Ch 385, 0.500 0 ==> 1;
Ch 386, 0.333 0 --> 1;
Ch 409, 0.286 0 ==> 1;
Ch 410, 0.750 0 ==> 2;
Ch 411, 0.500 0 ==> 1;
Ch 426, 0.500 0 ==> 1;
Ch 433, 0.286 1 --> 0

Node 89 --> node 85:
Ch 23, 0.500 0 ==> 1;
Ch 54, 1.000 0 ==> 1;
Ch 59, 0.200 1 --> 0;
Ch 72, 0.500 1 --> 2;
Ch 85, 0.250 0 ==> 1;
Ch 107, 0.250 1 --> 0;
Ch 110, 0.667 1 --> 2;
Ch 128, 0.333 0 --> 1;
Ch 155, 0.250 0 ==> 1;
Ch 182, 0.333 2 ==> 1;
Ch 186, 1.000 0 ==> 1;
Ch 189, 0.250 0 ==> 1;
Ch 192, 0.167 1 --> 0;
Ch 199, 0.143 1 --> 0;
Ch 202, 0.250 0 ==> 1;
Ch 219, 0.250 0 --> 1;
Ch 231, 0.500 1 ==> 2;
Ch 232, 0.750 1 ==> 2;
Ch 269, 1.000 0 ==> 1;
Ch 300, 0.600 1 ==> 0;
Ch 313, 0.250 1 ==> 2;
Ch 315, 0.250 0 --> 2;
Ch 323, 0.222 2 ==> 1;
Ch 339, 0.286 1 --> 0;
Ch 340, 0.200 0 --> 1;
Ch 343, 0.286 1 --> 0;
Ch 352, 0.286 2 ==> 0;
Ch 369, 0.125 0 --> 1;
Ch 370, 0.125 0 --> 1;
Ch 375, 0.267 0 --> 2;
Ch 420, 0.400 0 ==> 1;
Ch 423, 0.250 1 ==> 2;
Ch 430, 0.667 1 --> 2

Node 85 --> node 84:
Ch 4, 0.250 0 --> 1;
Ch 10, 0.250 1 --> 0;
Ch 18, 1.000 0 --> 1;
Ch 29, 0.333 0 --> 1;
Ch 55, 0.667 1 --> 0;
Ch 60, 1.000 0 --> 1;
Ch 103, 0.500 0 --> 1;
Ch 104, 0.333 0 --> 1;
Ch 158, 0.429 1 --> 2;
Ch 159, 0.333 0 --> 1;
Ch 161, 1.000 0 --> 1;

Ch 162, 1.000 1 --> 2;
Ch 163, 0.333 0 --> 1;
Ch 164, 0.333 0 --> 1;
Ch 165, 1.000 1 --> 2;
Ch 169, 0.250 0 ==> 1;
Ch 171, 0.500 2 --> 1;
Ch 178, 0.500 1 --> 2;
Ch 179, 0.333 0 --> 1;
Ch 196, 0.400 1 --> 2;
Ch 210, 0.400 0 --> 1;
Ch 213, 1.000 1 --> 2;
Ch 215, 0.667 1 --> 2;
Ch 241, 0.500 1 --> 2;
Ch 242, 1.000 1 --> 3;
Ch 245, 0.500 0 --> 1;
Ch 246, 0.500 1 --> 0;
Ch 247, 0.667 1 --> 3;
Ch 255, 0.250 1 --> 0;
Ch 263, 1.000 0 --> 1;
Ch 282, 0.500 0 --> 1;
Ch 288, 1.000 0 --> 1;
Ch 331, 0.333 2 --> 3;
Ch 332, 0.267 1 ==> 0;
Ch 333, 0.308 2 --> 0;
Ch 336, 0.200 1 ==> 0;
Ch 349, 0.273 5 ==> 0;
Ch 358, 0.158 3 ==> 0;
Ch 359, 0.250 3 ==> 1;
Ch 374, 0.143 0 --> 1;
Ch 377, 0.333 0 ==> 1;
Ch 411, 0.500 1 ==> 2;
Ch 413, 0.333 1 --> 0

Node 84 --> node 81:
Ch 89, 0.500 1 --> 2;
Ch 91, 1.000 1 --> 2;
Ch 92, 1.000 0 --> 1;
Ch 96, 0.333 0 --> 1;
Ch 144, 0.600 1 --> 2;
Ch 184, 0.250 0 --> 1;
Ch 188, 0.143 0 --> 1;
Ch 198, 0.500 1 --> 2;
Ch 226, 0.500 0 --> 1;
Ch 227, 1.000 0 --> 1;
Ch 229, 0.667 0 --> 1;
Ch 232, 0.750 2 --> 3;
Ch 321, 0.600 2 ==> 1;
Ch 340, 0.200 1 --> 0;
Ch 344, 0.143 1 --> 0;
Ch 369, 0.125 1 --> 0;
Ch 370, 0.125 1 --> 0;
Ch 382, 0.333 0 ==> 1;
Ch 383, 0.667 0 ==> 2

Node 81 --> node 70:
Ch 299, 0.500 2 --> 1;
Ch 302, 0.286 2 ==> 1;
Ch 303, 0.200 0 --> 1;
Ch 316, 0.400 0 --> 2;
Ch 319, 0.200 1 ==> 0;
Ch 320, 0.250 1 ==> 0;
Ch 323, 0.222 1 --> 0;
Ch 331, 0.333 3 --> 2;
Ch 402, 0.286 0 ==> 2;
Ch 403, 0.125 0 --> 1;
Ch 404, 0.200 0 --> 1;
Ch 423, 0.250 2 --> 1

Node 70 --> node 69:
Ch 300, 0.600 0 ==> 2;
Ch 368, 0.500 0 ==> 1;
Ch 398, 0.143 1 --> 0;
Ch 419, 0.600 0 ==> 1

Node 69 --> node 67:
Ch 303, 0.200 1 --> 0;
Ch 318, 0.500 0 ==> 1;
Ch 371, 0.250 0 ==> 2;
Ch 372, 0.500 0 ==> 1;
Ch 409, 0.286 1 ==> 2;
Ch 413, 0.333 0 --> 1;
Ch 414, 0.200 0 ==> 1;
Ch 415, 0.286 0 ==> 2;
Ch 416, 0.250 0 ==> 1;
Ch 417, 0.333 0 --> 2;
Ch 420, 0.400 1 ==> 2;
Ch 423, 0.250 1 --> 2

Node 67-> *Ausktribosphenos*:
Ch 313, 0.250 2 ==> 1;
Ch 373, 0.333 0 ==> 1

Node 67 --> *Bishops*:
Ch 302, 0.286 1 ==> 2;
Ch 310, 0.125 0 ==> 1;
Ch 319, 0.200 0 ==> 2;
Ch 323, 0.222 0 --> 1;
Ch 403, 0.125 1 --> 0

Node 69 --> node 68:
Ch 402, 0.286 2 ==> 1;
Ch 411, 0.500 2 ==> 1

Node 68 --> Ambondro:
Ch 400, 0.200 0 ==> 1;
Ch 401, 0.375 0 ==> 2;
Ch 415, 0.286 0 ==> 1;
Ch 417, 0.333 0 --> 1;
Ch 418, 0.500 3 ==> 1

Node 68 --> *Asfaltomylos*:
Ch 403, 0.125 1 --> 0

Node 70 --> *Shuotherium*:
Ch 313, 0.250 2 ==> 0;
Ch 315, 0.250 2 ==> 0;
Ch 375, 0.267 2 --> 1;
Ch 404, 0.200 1 --> 2;
Ch 412, 0.500 4 ==> 1;
Ch 420, 0.400 1 ==> 0

Node 81 --> node 80:
Ch 313, 0.250 2 --> 3;
Ch 349, 0.273 0 --> 2;
Ch 374, 0.143 1 --> 0;
Ch 400, 0.200 0 ==> 1;
Ch 401, 0.375 0 ==> 2;
Ch 418, 0.500 3 ==> 1;
Ch 419, 0.600 0 ==> 2;
Ch 427, 1.000 1 --> 0

Node 80 --> *Peramus*:
Ch 333, 0.308 0 ==> 1;
Ch 359, 0.250 1 ==> 0;
Ch 383, 0.667 2 ==> 1;
Ch 387, 0.250 2 ==> 0

Node 80 --> node 79:
Ch 296, 0.200 0 --> 1;
Ch 312, 0.167 1 ==> 2;
Ch 319, 0.200 1 --> 2;
Ch 349, 0.273 2 --> 3;
Ch 358, 0.158 0 --> 1;
Ch 365, 0.250 1 ==> 0;
Ch 370, 0.125 0 --> 1;
Ch 375, 0.267 2 --> 1;
Ch 377, 0.333 1 ==> 2;
Ch 379, 0.600 1 ==> 2;
Ch 394, 1.000 0 ==> 1;
Ch 398, 0.143 1 --> 2;
Ch 402, 0.286 0 ==> 1;
Ch 409, 0.286 1 ==> 2;
Ch 415, 0.286 0 --> 1;
Ch 428, 1.000 0 ==> 2

Node 79 --> *Kielantherium*:
Ch 296, 0.200 1 --> 0;
Ch 313, 0.250 3 ==> 2;
Ch 319, 0.200 2 --> 1;
Ch 349, 0.273 3 -->;
Ch {12};
Ch 415, 0.286 1 --> 0

Node 79 --> node 76:
Ch 30, 0.333 0 --> 1;
Ch 147, 0.500 0 ==> 1;
Ch 167, 1.000 1 ==> 2;
Ch 171, 0.500 1 --> 2;
Ch 188, 0.143 1 --> 0;
Ch 189, 0.250 1 --> 0;
Ch 212, 0.333 0 --> 1;
Ch 222, 1.000 0 --> 1;
Ch 226, 0.500 1 --> 0;
Ch 229, 0.667 1 --> 2;
Ch 245, 0.500 1 --> 0;

Ch 247, 0.667 3 --> 4;
Ch 260, 0.667 1 ==> 2;
Ch 266, 0.500 0 ==> 1;
Ch 272, 0.667 1 --> 0;
Ch 296, 0.200 1 --> 0;
Ch 312, 0.167 2 --> 1;
Ch 321, 0.600 1 ==> 0;
Ch 349, 0.273 3 --> 2;
Ch 357, 0.250 0 ==> 1;
Ch 358, 0.158 1 --> 0;
Ch 363, 0.500 0 ==> 1;
Ch 364, 1.000 0 ==> 1;
Ch 365, 0.250 0 ==> 1;
Ch 370, 0.125 1 --> 0;
Ch 375, 0.267 1 --> 2;
Ch 398, 0.143 2 --> 0;
Ch 418, 0.500 1 ==> 2

Node 76 --> node 71:
Ch 126, 1.000 0 --> 1;
Ch 157, 0.250 0 --> 1;
Ch 163, 0.333 1 --> 0;
Ch 164, 0.333 1 --> 0;
Ch 267, 0.333 0 --> 1;
Ch 319, 0.200 2 --> 1;
Ch 359, 0.250 1 ==> 0;
Ch 370, 0.125 0 --> 1

Node 71 --> *Prokennalestes*:
Ch 313, 0.250 3 ==> 2;
Ch 344, 0.143 0 ==> 1

Node 71 --> *Eomaia*:
Ch 398, 0.143 0 --> 1

Node 76 --> node 75:
Ch 107, 0.250 0 --> 1;
Ch 112, 0.500 2 --> 1;
Ch 230, 0.125 0 --> 1;
Ch 233, 0.667 1 ==> 2;
Ch 349, 0.273 2 --> 3;
Ch 358, 0.158 0 --> 1;
Ch 415, 0.286 1 --> 2;
Ch 431, 0.250 1 --> 2;
Ch 432, 0.250 0 --> 1;
Ch 433, 0.286 0 --> 2;
Ch 434, 0.333 0 --> 1;
Ch 435, 0.250 0 --> 1

Node 75 --> *Ukhaatherium*:
Ch 10, 0.250 0 --> 1;
Ch 169, 0.250 1 ==> 0;
Ch 338, 0.333 0 ==> 1

Node 75 --> node 74:
Ch 95, 1.000 0 --> 1;
Ch 98, 0.667 0 --> 2;
Ch 99, 0.500 1 --> 2;
Ch 153, 0.250 0 --> 1;
Ch 333, 0.308 0 --> 1;
Ch 340, 0.200 0 ==> 1

Node 74 --> node 72:
Ch 4, 0.250 1 --> 0;
Ch 110, 0.667 2 --> 1;
Ch 210, 0.400 1 --> 2;
Ch 288, 1.000 1 ==> 2;
Ch 344, 0.143 0 ==> 1;
Ch 370, 0.125 0 --> 1

Node 72 --> *Kennalestes*:
Ch 332, 0.267 0 ==> 1;
Ch 369, 0.125 0 ==> 1

Node 72 --> *Asioryctes*:
Ch 201, 0.250 0 ==> 1;
Ch 312, 0.167 1 --> 2;
Ch 333, 0.308 1 --> 0

Node 74 --> node 73:
Ch 156, 0.250 0 --> 1;
Ch 158, 0.429 2 ==> 3;
Ch 160, 1.000 0 ==> 1;
Ch 214, 0.375 3 --> 2;
Ch 310, 0.125 0 ==> 1;
Ch 332, 0.267 0 --> 2;
Ch 334, 0.400 0 ==> 1;
Ch 336, 0.200 0 --> 1;

Ch 343, 0.286 0 ==> 1;
Ch 357, 0.250 1 ==> 0;
Ch 358, 0.158 1 --> 2;
Ch 359, 0.250 1 --> 2;
Ch 368, 0.500 0 ==> 1;
Ch 371, 0.250 0 --> 1;
Ch 418, 0.500 2 ==> 3;
Ch 419, 0.600 2 ==> 1

Node 73 --> *Zalambdalestes*:
Ch 157, 0.250 0 ==> 1;
Ch 163, 0.333 1 ==> 0;
Ch 187, 0.125 1 ==> 0;
Ch 220, 0.250 0 ==> 1;
Ch 230, 0.125 1 --> 0;
Ch 332, 0.267 2 --> 3;
Ch 336, 0.200 1 --> 2;
Ch 337, 0.250 0 ==> 1;
Ch 341, 0.167 0 ==> 1;
Ch 397, 0.200 0 ==> 1

Node 73 --> *Erinaceus*:
Ch 112, 0.500 1 --> 2;
Ch 129, 0.500 1 ==> 0;
Ch 139, 0.250 0 ==> 1;
Ch 155, 0.250 1 ==> 0;
Ch 180, 0.500 0 ==> 1;
Ch 183, 0.333 0 ==> 1;
Ch 199, 0.143 0 ==> 1;
Ch 202, 0.250 1 ==> 0;
Ch 229, 0.667 2 ==> 1;
Ch 247, 0.667 4 ==> 3;
Ch 267, 0.333 0 ==> 1;
Ch 286, 0.500 2 ==> 3;
Ch 339, 0.286 0 ==> 1;
Ch 349, 0.273 3 ==> 5;
Ch 358, 0.158 2 --> 3;
Ch 359, 0.250 2 --> 3;
Ch 361, 0.286 1 ==> 0;
Ch 371, 0.250 1 --> 2;
Ch 380, 0.333 2 ==> 3;
Ch 381, 0.250 1 ==> 0;
Ch 382, 0.333 1 ==> 0;
Ch 389, 0.250 0 ==> 1;
Ch 390, 0.333 0 ==> 1;
Ch 413, 0.333 0 ==> 1;
Ch 414, 0.200 0 ==> 1;
Ch 415, 0.286 2 ==> 0;
Ch 416, 0.250 0 ==> 1;
Ch 417, 0.333 0 ==> 1;
Ch 420, 0.400 1 ==> 2

Node 76 --> *Montanalestes*:
Ch 296, 0.200 0 --> 1;
Ch 312, 0.167 1 --> 2;
Ch 374, 0.143 0 ==> 1;
Ch 398, 0.143 0 --> 1

Node 79 --> *Deltatheridium*:
Ch 169, 0.250 1 ==> 0;
Ch 182, 0.333 1 ==> 0;
Ch 187, 0.125 1 ==> 0;
Ch 192, 0.167 0 --> 1;
Ch 241, 0.500 2 ==> 0;
Ch 268, 0.750 2 ==> 3;
Ch 310, 0.125 0 ==> 1;
Ch 316, 0.400 0 ==> 1;
Ch 319, 0.200 2 --> 1;
Ch 358, 0.158 1 --> 2;
Ch 359, 0.250 1 ==> 2;
Ch 361, 0.286 1 ==> 0;
Ch 369, 0.125 0 ==> 1

Node 79 --> *Sinodelphys*:
Ch 105, 0.333 0 ==> 1;
Ch 111, 0.667 0 ==> 1;
Ch 155, 0.250 1 ==> 0;
Ch 157, 0.250 0 ==> 1;
Ch 332, 0.267 0 ==> 1;
Ch 362, 0.250 0 ==> 1;
Ch 368, 0.500 0 ==> 1;
Ch 375, 0.267 1 --> 2;
Ch 414, 0.200 0 ==> 1

Node 79 --> node 78:
Ch 98, 0.667 0 ==> 1;
Ch 106, 1.000 0 ==> 1;
Ch 107, 0.250 0 --> 1;

Ch 108, 1.000 0 ==> 1;
Ch 146, 0.400 2 --> 0;
Ch 153, 0.250 0 ==> 1;
Ch 156, 0.250 0 --> 1;
Ch 220, 0.250 0 --> 1;
Ch 253, 0.500 0 --> 1;
Ch 310, 0.125 0 ==> 1;
Ch 316, 0.400 0 ==> 1;
Ch 358, 0.158 1 --> 2;
Ch 359, 0.250 1 ==> 2;
Ch 369, 0.125 0 ==> 1;
Ch 389, 0.250 0 ==> 1;
Ch 390, 0.333 0 ==> 1;
Ch 393, 1.000 0 ==> 1;
Ch 398, 0.143 2 --> 0;
Ch 407, 0.667 0 ==> 1;
Ch 414, 0.200 0 ==> 1;
Ch 415, 0.286 1 ==> 2;
Ch 416, 0.250 0 ==> 1;
Ch 417, 0.333 0 ==> 1;
Ch 418, 0.500 1 --> 2;
Ch 419, 0.600 2 ==> 1;
Ch 430, 0.667 2 --> 3;
Ch 431, 0.250 1 --> 2;
Ch 432, 0.250 0 --> 1;
Ch 433, 0.286 0 --> 2;
Ch 434, 0.333 0 --> 1;
Ch 435, 0.250 0 --> 1

Node 78 --> *Asiatherium*:
Ch 230, 0.125 0 ==> 1;
Ch 398, 0.143 0 --> 1

Node 78 --> node 77:
Ch 111, 0.667 0 --> 2;
Ch 146, 0.400 0 --> 1;
Ch 183, 0.333 0 ==> 1;
Ch 392, 1.000 0 ==> 1;
Ch 397, 0.200 0 ==> 1;
Ch 418, 0.500 2 --> 3

Node 77 --> *Pucadelphys*:
Ch 4, 0.250 1 --> 0;
Ch 85, 0.250 1 ==> 0;
Ch 158, 0.429 2 --> 1;
Ch 187, 0.125 1 ==> 0;
Ch 198, 0.500 2 --> 1;
Ch 199, 0.143 0 ==> 1;
Ch 214, 0.375 3 --> 0;
Ch 247, 0.667 3 ==> 4;
Ch 253, 0.500 1 --> 0;
Ch 264, 1.000 0 ==> 1

Node 77 --> *Didelphis*:
Ch 22, 0.500 1 ==> 0;
Ch 157, 0.250 0 ==> 1;
Ch 192, 0.167 0 --> 1;
Ch 203, 0.167 1 ==> 0;
Ch 285, 0.222 1 ==> 0;
Ch 362, 0.250 0 ==> 1

Node 84 --> node 83:
Ch 40, 0.333 1 --> 0;
Ch 72, 0.500 2 --> 1;
Ch 128, 0.333 1 --> 0;
Ch 139, 0.250 0 --> 1;
Ch 156, 0.250 0 --> 1;
Ch 176, 0.250 0 --> 1;
Ch 350, 0.250 1 ==> 0;
Ch 375, 0.267 2 --> 0;
Ch 376, 0.333 0 --> 1;
Ch 388, 0.333 0 --> 1;
Ch 412, 0.500 4 ==> 3

Node 83 --> node 82:
Ch 358, 0.158 0 ==> 1;
Ch 398, 0.143 1 ==> 0;
Ch 409, 0.286 1 ==> 2

Node 82 --> *Dryolestes*:
Ch 85, 0.250 1 ==> 0;
Ch 104, 0.333 1 --> 0

Node 85 --> *Vincelestes*:
Ch 17, 0.333 1 ==> 0;
Ch 89, 0.500 1 --> 0;
Ch 131, 0.333 1 --> 0;
Ch 142, 0.333 1 --> 0;

Ch 143, 0.333 1 ==> 2;
Ch 185, 0.200 1 ==> 0;
Ch 187, 0.125 1 ==> 0;
Ch 203, 0.167 1 ==> 0;
Ch 204, 0.333 0 ==> 1;
Ch 208, 0.333 1 ==> 0;
Ch 214, 0.375 3 --> 0;
Ch 266, 0.500 0 ==> 1;
Ch 267, 0.333 0 ==> 1;
Ch 285, 0.222 1 ==> 0;
Ch 361, 0.286 1 --> 0;
Ch 366, 0.143 1 ==> 0;
Ch 381, 0.250 1 --> 0;
Ch 383, 0.667 0 ==> 1;
Ch 386, 0.333 1 --> 0;
Ch 389, 0.250 0 ==> 1;
Ch 417, 0.333 0 --> 1;
Ch 428, 1.000 0 ==> 1

Node 89 --> node 88:

Ch 50, 0.400 2 --> 1;
Ch 96, 0.333 0 --> 1;
Ch 98, 0.667 0 --> 2;
Ch 112, 0.500 2 --> 1;
Ch 139, 0.250 0 --> 1;
Ch 158, 0.429 1 --> 0;
Ch 176, 0.250 0 --> 1;
Ch 285, 0.222 1 --> 2;
Ch 312, 0.167 1 --> 0;
Ch 333, 0.308 2 --> 1;
Ch 341, 0.167 0 --> 1;
Ch 349, 0.273 5 ==> 2;
Ch 362, 0.250 0 --> 1;
Ch 376, 0.333 0 ==> 1;
Ch 382, 0.333 0 ==> 1;
Ch 388, 0.333 0 ==> 1;
Ch 412, 0.500 4 --> 2

Node 88 --> node 87:

Ch 296, 0.200 0 --> 1;
Ch 312, 0.167 0 --> 2;
Ch 358, 0.158 3 ==> 2;
Ch 371, 0.250 0 --> 2;
Ch 374, 0.143 0 ==> 1;
Ch 387, 0.250 2 ==> 0;
Ch 404, 0.200 0 ==> 2

Node 87 --> *Tinodon*:

Ch 375, 0.267 0 ==> 1;
Ch 398, 0.143 1 ==> 2;
Ch 400, 0.200 0 ==> 1;
Ch 401, 0.375 0 ==> 2;
Ch 410, 0.750 2 ==> 1

Node 87 --> node 86:

Ch 310, 0.125 0 ==> 1;
Ch 321, 0.600 2 ==> 3;
Ch 331, 0.333 2 ==> 3;
Ch 349, 0.273 2 ==> 0;
Ch 352, 0.286 2 --> 0;
Ch 369, 0.125 0 ==> 1;
Ch 372, 0.500 0 --> 1;
Ch 373, 0.333 0 --> 1;
Ch 402, 0.286 0 ==> 1;
Ch 403, 0.125 0 ==> 1;
Ch 405, 0.500 0 ==> 1;
Ch 406, 1.000 0 ==> 1;
Ch 423, 0.250 1 ==> 2

Node 86 --> *Spalacotherium*:

Ch 312, 0.167 2 --> 1;
Ch 371, 0.250 2 --> 0

Node 86 --> *Heishanlestes*:

Ch 313, 0.250 1 ==> 3;
Ch 358, 0.158 2 ==> 1;
Ch 366, 0.143 1 ==> 0;
Ch 409, 0.286 1 ==> 2

Node 88 -> *Zhangheotherium*:

Ch 344, 0.143 1 --> 0

Node 95 --> node 94:

Ch 37, 0.500 0 ==> 1;
Ch 146, 0.400 2 --> 1;
Ch 153, 0.250 0 ==> 1;
Ch 184, 0.250 0 --> 1;
Ch 214, 0.375 3 --> 1;

Ch 244, 0.333 1 --> 0;
Ch 247, 0.667 1 --> 2;
Ch 248, 0.333 1 --> 0;
Ch 254, 0.500 1 --> 0;
Ch 268, 0.750 2 ==> 1;
Ch 271, 0.500 1 --> 0;
Ch 290, 0.333 1 --> 0;
Ch 301, 0.400 2 ==> 0;
Ch 314, 1.000 2 --> 1;
Ch 349, 0.273 5 ==> 3;
Ch 358, 0.158 3 --> 2;
Ch 371, 0.250 0 ==> 2;
Ch 378, 1.000 0 ==> 1;
Ch 387, 0.250 2 ==> 1;
Ch 391, 0.500 2 --> 1;
Ch 395, 0.250 0 ==> 1;
Ch 401, 0.375 0 --> 2;
Ch 408, 0.333 1 --> 0;
Ch 412, 0.500 4 --> 1

Node 94 --> node 91:
Ch 50, 0.400 2 --> 1;
Ch 203, 0.167 1 --> 0;
Ch 285, 0.222 1 --> 0;
Ch 286, 0.500 2 --> 1;
Ch 334, 0.400 0 --> 2;
Ch 359, 0.250 3 --> 2;
Ch 377, 0.333 0 --> 1;
Ch 400, 0.200 0 ==> 1;
Ch 429, 0.333 1 --> 0

Node 91 --> node 90:
Ch 360, 1.000 0 ==> 1;
Ch 366, 0.143 1 ==> 0;
Ch 367, 1.000 0 ==> 1;
Ch 369, 0.125 0 ==> 1;
Ch 380, 0.333 1 ==> 3

Node 90 --> *Gobiconodon*:
Ch 176, 0.250 0 ==> 1;
Ch 212, 0.333 0 ==> 1;
Ch 310, 0.125 1 ==> 0;
Ch 333, 0.308 2 --> 3;
Ch 358, 0.158 2 ==> 1;
Ch 376, 0.333 0 ==> 1

Node 90 --> *Repenomamus*:
Ch 89, 0.500 0 ==> 1;
Ch 187, 0.125 1 ==> 0;
Ch 332, 0.267 3 ==> 2;
Ch 375, 0.267 0 ==> 1

Node 91 --> *Amphilestes*:
Ch 349, 0.273 3 ==> 2;
Ch 404, 0.200 0 ==> 2

Node 94 --> node 93:
Ch 8, 0.333 1 --> 0;
Ch 13, 0.500 1 --> 0;
Ch 59, 0.200 1 --> 0;
Ch 96, 0.333 0 ==> 1;
Ch 175, 0.500 1 --> 0;
Ch 200, 0.500 0 --> 1;
Ch 336, 0.200 1 ==> 0;
Ch 375, 0.267 0 ==> 1;
Ch 401, 0.375 2 --> 3;
Ch 422, 0.500 2 ==> 1;
Ch 425, 0.333 1 --> 0

Node 93 --> *Jeholodens*:
Ch 332, 0.267 3 ==> 1;
Ch 333, 0.308 2 --> 0;
Ch 349, 0.273 3 ==> 4;
Ch 358, 0.158 2 --> 3;
Ch 366, 0.143 1 ==> 0

Node 93 --> node 92:
Ch 184, 0.250 1 --> 0;
Ch 189, 0.250 0 --> 1;
Ch 230, 0.125 0 --> 1;
Ch 339, 0.286 1 --> 0;
Ch 343, 0.286 1 --> 0;
Ch 359, 0.250 3 ==> 1;
Ch 361, 0.286 0 ==> 1;
Ch 374, 0.143 0 ==> 1;
Ch 396, 1.000 0 ==> 1;
Ch 397, 0.200 0 ==> 1;
Ch 404, 0.200 0 ==> 2

Ch 375, 0.267 1 ==> 2

Node 92 --> *Priacodon*:
Ch 369, 0.125 0 ==> 1

Node 92 --> *Trioracodon*:
Ch 340, 0.200 0 ==> 1;
Ch 371, 0.250 2 ==> 0;

Node 92 --> *Triconodon*:
Ch 344, 0.143 0 ==> 1;
Ch 349, 0.273 3 ==> 2;
Ch 358, 0.158 2 ==> 1

BIBLIOGRAPHY

Alexander, R. McN., Jayes, A. S., Maloiy, G. M. O., and Wathuta, E. M. (1979). Allometry of limb bones of mammals from shrews (*Sorex*) to elephant (*Loxodonta*). *Journal of Zoology, London*, 189: 305-314.

Averianov, A. O. (2002). Early Cretaceous "symmetrodont" mammal *Gobiotheriodon* from Mongolia and the classification of "Symmetrodonta". *Acta Palaeontologica Polonica*, 47: 705-716.

Averianov, A. O., and Archibald, J. D. (2005). Mammals from the mid-Cretaceous Khodzhakul Formation, Kyzylkum Desert, Uzbekistan. *Cretaceous Research*, 26: 593-608.

Averianov, A. O., Lopatin, A.V., Skutschas, P. P., Martynovich, N. V., Leshchinskiy, S. V., Rezvyi, A. S., Krasnolutskii, S. A., and Fayngertz, A. V. (2005). Discovery of Middle Jurassic mammals from Siberia *Acta Palaeontologica Polonica*, 50: 789-797.

Averianov, A., Starkov, A., and Skutschas, P. P. (2003). Dinosaurs from the Early Cretaceous Murtoi Formation in Buryatia, eastern Russia. *Journal of Vertebrate Paleontology*, 23: 586-594.

Bakker, R. T. (1971). Dinosaur physiology and the origin of mammals. *Evolution,* 25: 636-658.

Bernor, R. L., Tobien, H., Hayek, L.-A., and Mittmann, H.-W. (1997). *Hippotherium primigenium* (Equidae, Mammalia) from the late Miocene of Höwenegg, (Hegau, Germany). *Andrias*, 10: 1-250.

Bonaparte, J. F. (1986). A New and unusual Kate Cretaceous mammal from Patagonia. *Journal of Vertebrate Paleontology*, 6: 264-270.

Bonaparte, J. F. (1992). Una nueva especie de Triconodonta (Mammalia), de la Formación Los Alamitos, Provincia de Rio Negro y comentarios sobre su fauna de mamiferos. *Ameghiniana,* 29: 99-110.

Bonaparte, J. F., Martinelli, A. G., Schultz, C. L., and Rubert, R. (2003). The sister group of mammals: small cynodonts from the Late Triassic of Southern Brazil. *Revista Brasileira de Paleontologia,* 5: 5-27.

Bown, T. M., and Kraus, M. J. (1979). Origin of the tribosphenic molar. In Lillegraven, J. A., Kielan-Jaworowska, Z., and Clemens, W. A. (Eds.), *Mesozoic Mammals: The First Two-thirds of Mammalian History* (pp. (172-181). Berkeley: University of California Press.

Brinkman, D. B., Eberth D. A., Ryan, M. J., and Chen, P.-J. (2001). The occurrence of *Psittacosaurus xinjiangensis* Sereno and Chow, 1988 in the Urho area, Junggar Basin, Xinjiang, People's Republic of China. *Canadian Journal of Earth Sciences*, 38: 1781-1786.

Broderip, W. J. (1828). Observations on the jaw of a fossil mammiferous animal from in the Stonesfield Slate. *Zoological Journal (London)*, 3: 408-412.

Broili, F. (1908). Ein Dicynodontierrest aus Karooformation. *Neues Jahrbuch für Mineralogie, Geologie und Paläontologie*, 1: 1-15.

Brower, A. V. Z. (2000). Evolution is not a necessary assumption of cladistics. *Cladistics*, 16: 143-154.

Butler, P. M., and Hooker, J. J. (2005). New teeth of allotherian mammals from the English Bathonian, including the earliest multituberculates. *Acta Palaeontologica Polonic*a, 50: 185-207.

Carbone C., Mace, G. M., Roberts, S. C., and Macdonald, D. W. (1999). Energetic constraints on the diet of terrestrial carnivores. *Nature*, 402: 286-288.

Cave, A. J. E. (1970). Observation on the monotreme interclavicle. *Journal of Zoology, London*, 160: 297-312.

Chow, M.-z., and Rich, T. H. (1984). Anew triconodontan (Mammalia) from the Jurassic of China. *Journal of Vertebrate Paleontology,* 3: 226-231.

Cifelli, R. L. (2002). *Comodon* Kretzoi and Kretzoi, 2000 replaces *Phascolodon* Simpson 1925 (Mammalia), not *Phascolodon* Stein, 1859. *Acta Palaeontologica Polonica*, 47: 184.

Cifelli, R. L., and Dykes, T. D. (2001). *Phascolotheridium*, a new name for the genus *Phascolodon* Simpson, 1925 (Vertebrata, Mammalia) preoccupied by *Phascolodon* Stein, 1859 (Ciliophora, Phyllopharyngea). *Acta Palaeontologica Polonica*, 46: 392.

Cifelli, R. L., Lipka, T. R., Schaff, C. R., and Rowe, T. B. (1999). First Early Cretaceous mammal from the eastern seaboard of the United States. *Journal of Vertebrate Paleontology,* 19: 199-203.

Cifelli, R. L., and Madsen, S. K. (1998). Triconodont mammals from the medial Cretaceous of Utah. *Journal of Vertebrate Paleontology,* 18: 403-411.

Cifelli, R. L., and Madsen, S. K. (1999). Spalacotheriid symmetrodonts (Mammalia) from the medial Cretaceous (upper Albian or lower Cenomanian) Mussentuchit local fauna, Cedar Mountain Formation, Utah, USA. *Geodiversitas,* 21: 167-214.

Cifelli, R. L., Wible, J. R., and Jenkins, F. A., Jr. (1998). Triconodont mammals from the Cloverly Formation (Lower Cretaceous), Montana and Wyoming. *Journal of Vertebrate Paleontology,* 18: 237-241.

Clemens, W. A. (1979). A problem in morganucodontid taxonomy. *Zoological Journal of the Linnean Society,* 66: 1-14.

Clemens, W. A. (1980). Rhaeto-Liassic mammals from Switzerland and West Germany. *Zitteliana, Abhandlungen der Bayerischen Staatssammlung für Paläontologie und Historische Geologie,* 5: 51-92.

Coombs, W. P. Jr. (1982). Juvenile specimens of the ornithischian dinosaur *Psittacosaurus*. *Palaeontology,* 25: 89-107.

Crompton, A. W. (1964). On the skull of *Oligokyphus*. *Bulletin of the British Museum (Natural History), Geology,* 9: 70-82.

Crompton, A. W. (1971). The origin of the tribosphenic molar. In Kermack, D. M., and Kermack, K. A. (Eds.), *Early Mammals*. *Zoological Journal of the Linnean Society,* 50 (Supplement 1): 65-87.

Crompton, A. W. (1974). The dentition and relationships of the southern African Triassic mammals, *Erythrotherium parringtoni* and *Megazostrodon rudnerae*. *Bulletin of the British Museum (Natural History), Geology,* 24: 397-437.

Crompton, A. W. (1980).Biology of the earliest mammals. In Schmidt-Nielsen, K., Bolis, L., and Taylor, C. R. (Eds.) *Comparative physiology: Primitive mammals* (pp. 1-12) Cambridge: Cambridge University Press.

Crompton, A. W., and Jenkins, F. A. Jr. (1968). Molar occlusion in Late Triassic mammals. *Biological Reviews,* 43: 427-458.

Crompton, A. W., and Jenkins, F. A. Jr. (1979). Origin of mammals. In Lillegraven, J. A., Kielan-Jaworowska, Z., and Clemens, W. A. (Eds.), *Mesozoic Mammals: The First Two-thirds of Mammalian History.* (pp. 59-73). Berkeley: University of California Press.

Crompton, A. W., and Luo, Z.-x. (1993). Relationships of the Liassic mammals, *Sinoconodon*, *Morganucodon oehleri*, and *Dinnetherium*. In Szalay F. S., Novacek, M. J., and McKenna M. C. (Eds.), *Mammal Phylogeny, Volume 1* (pp. 30-44). New York: Springer Verlag.

Crompton, A. W., and Sun, A.-l. (1985). Cranial Structure and relationships of the Liassic mammal *Sinoconodon*. *Zoological Journal of the Linnean Society,* 85: 99-119.

Cuenca-Bescos, G., and Canudo, J. I. (2003). A new gobiconodontid mammal from the Early Cretaceous of Spain and its palaeogeographic implications. *Acta Paleontologica Polonica*, 48: 575-582.

Damuth, J., and MacFadden, B. J. (Eds.). (1990). *Body size in mammalian paleobiology: Estimation and biological implication.* Cambridge: Cambridge University Press.

Datta, P. M. (2005). Earliest mammal with transversely expanded upper molar from the Late Triassic (Carnian) Tiki Formation, South Rewa Gondwana Basin, India. *Journal of Vertebrate Paleontolog*y, 25: 200-207.

Datta, P. M., and Das, D. P. (2001). *Indozostrodon simpsoni* , gen. et sp. nov., an Early Jurassic megozostrodontid mammal from India. *Journal of Vertebrate Paleontology,* 21: 528-534.

Eisenberg, J. F. (1981). *The Mammalian Radiation.* Chicago: The University of Chicago Press.

Eisenberg, J. F. (1990). The behavioural/ecological significance of body size in the Mammalia. In Damuth, J., and MacFadden, B. J. (Eds.), *Body size in mammalian paleobiology: Estimation and biological implication* (pp. 25-38). Cambridge: Cambridge University Press.

Engelmann, G. F., and Callison, G. (1998). Mammalian faunas of the Morrison Formation. *Modern Geology,* 23: 343-379.

Ensom, P. C., and Sigogneau-Russell, D. (1998). New dryolestoid mammals from the basal Cretaceous Purbeck Limestone group of southern England. *Palaeontology*, 41: 35-55.

Evans, F. G. (1939). The morphology and function evolution of the atlas-axis complex from fish to mammals. *Annals of New York Academy of Sciences*, 39: 29-104.

Evans, H. E. (1993). *Miller's anatomy of the dog* (3rd Ed.) Philadelphia: W. B. Saunders Company.

Falkowski, P. G., Katz, M. E., Milligan, A. J., Fennel, K., Cramer, B. S., Aubry, M. P., Berner,R. A., Novacek, M. J., and Zapol, W. M. (2005). The Rise of Oxygen over the past 205 million years and the evolution of large placental mammals. *Science*, 309: 2202-2204.

Farris, J. S., Kluge, A. G., and de Laet, J. E. (2001). Taxic revisions. *Cladistics*, 17: 79-103.

Flower, W. H. (1870). *An introduction to the osteology of Mammalia*. London: Globe.

Fourie, S. (1962). Notes on a new tritylodontid from the Cave Sandstone of South Africa. *Navorsinge van die Nasionale Museum Bloemfontein*, 2: 2-19.

Fox, R. C. (1969). Studies of Late Cretaceous vertebrates. III. A triconodont mammal from Alberta. *Canadian Journal of Zoology,* 47: 1253-1256.

Freeman, E. F. (1979). A Middle Jurassic mammal's bed from Oxfordshire. *Palaeontology,* 22: 135-166.

Gambaryan, P. P., and Averianov, A. O. (2001). Femur of a morganucodontid mammal from the Middle Jurassic of central Russia. *Acta Palaeontologica Polonica,* 46: 99-112.

Gambaryan, P. P., and Kielan-Jaworowska, Z. (1997). Sprawling versus parasagittal stance in multituberculate mammals. *Acta Palaeontologica Polonica*, 42: 13-44.

Gardezi T., Silva J. (1999). Diversity in Relation to Body Size in Mammals: A Comparative Study. *American Naturalist*, 153: 110-123.

Gingerich PD. (1990). Prediction of body mass in mammalian species from long bone lengths and diameters. *Contributions from the Museum of Paleontology, University of Michigan,* 28: 79-92.

Godefroit, P., and Guo, D.-y. (1999). A new amphilestid mammal from the Early Cretaceous of China. *Bulletin de l'Institut royal des Sciences naturelles de Belgique,* 69 (Supplement B): 7-16.

Goodrich, E. S. (1930). *Studies on the structures and development of vertebrates*. London: The MacMillan and Company.

Gow, C. E. (1985). Apomorphies of the Mammalia. *South African Journal of Science,* 81: 558-560.

Gow, C. E. (1986). A new skull of *Megazostrodon* (Mammalia: Triconodonta) from the Elliot Formation (Lower Jurassic) of southern Africa. *Palaeontologia Africana,* 26: 13-23.

Gow, C.E. (2001). A partial skeleton of the tritheledontid *Pachygenelus* (Therapsida: Cynodontia). *Palaeontologia Africana*, 37: 93-97.

Granger, W., and Simpson, G. G. (1929). A revision of the Tertiary Multituberculata. *Bulletin of American Museum of Natural History*, 56: 601-676.

Grossmann M., Sánchez-Villagra, M. R., and Maier, W. (2002). On the development of the shoulder girdle in *Crocidura russula* (Soricidae) and other placental mammals: evolutionary and functional aspects. *Journal of Anatomy*, 201: 371-381.

Hahn, G., Sigogneau-Russell, D., and Godefroit, P. (1991). New data on *Brachyzostrodon* (Mammalia; Upper Triassic). *Geologica et Paleontologica,* 25: 237-249.

Harrison, D. F. N. (1995). *The Anatomy and Physiology of the Mammalian Larynx.* Cambridge: Cambridge University Press.

Hawkins, J. A. (2000). A survey of primary homology assessment: different botanists perceive and define characters in different ways. In Scotland, R., and Pennington, R. T. (Eds.), *Homology and Systematics: coding characters for phylogenetic analysis* (Systematics Association special volume, No. 58) (pp. 22-53). Philadelphia: Taylor and Francis.

Heinrich, W. D. (1998). Late Jurassic mammals from Tendaguru, Tanzania, East Africa. *Journal of Mammalian Evolution,* 5: 269-290.

Hillenius, W. J. (1992). The evolution of nasal turbinates and mammalian endothermy. *Paleobiology*, 18: 17-29.

Hillenius, W. J. (1994). Turbinates in therapsids: evidence for Late Permian origins of mammalian endothermy. *Evolution*, 48: 207-229.

Hillenius, W. J., and Ruben, J. A. (2004). The evolution of endothermy in terrestrial vertebrates: Who? When? Why? *Physiological and Biochemical Zoology*, 77: 1019-1042.

Hopson, J. A. and Crompton, A.W. (1969). Origin of mammals. In T. Dobzhansky, T., Hecht, M. K., and Steere W. C. (Eds.), *Evolutionary Biology, Vol. 3* (pp. 15-72). New York: Appleton-Century-Crofts.

Hopson, J. A. (1973). Endothermy, small size and the origin of mammalian reproduction. *The American Naturalist,* 107: 446-452.

Hopson, J. A. (1994). Synapsid evolution and the radiation of non-eutherian mammals. In Spencer, R. S. (Ed.), *Major Features of VertebrateEvolution* (pp. 190-219). Knoxville: The Paleontological Society.

Hopson, J. A. (1995). Patterns of evolution in the manus and pes of non-mammalian therapsids. *Journal of Vertebrate Paleontology*, 15: 615-639.

Hopson, J. A., and Kitching J. W. (2001). A probainognathian cynodont from South Africa and the phylogeny of nonmammalian cynodonts. *Bulletin of the Museum of Comparative Zoology*, 156: 3-35.

Horovitz, I. (2000). The tarsus of *Ukhaatherium nessovi* (Eutheria, Mammalia) from the Late Cretaceous of Mongolia: an appraisal of the evolution of the ankle in basal therians. *Journal of Vertebrate Paleontology,* 20: 547-56.

Horovitz, I. (2003). Postcranial skeleton of *Ukhaatherium nessovi* (Eutheria, Mammalia) from the Late Cretaceous of Mongolia. *Journal of Vertebrate Paleontology,* 23: 857-868.

Horovitz, I., and Sánchez-Villagra, M. R. (2003). A morphological analysis of marsupial mammal higher-level phylogenetic relationships. *Cladistics*, 19: 181-212.

Howell, A. B. (1937). Morphogenesis of the shoulder architecture, Part V. Monotremata. *Quarterly Review of Biology*, 12: 195-205.

Hu, Y.-m., Wang, Y.-q., Luo, Z.-x., and Li. C.-k. (1997). A new symmetrodont mammal from China and its implications for mammalian evolution. *Nature,* 390:137-142.

Hu, Y.-m., Wang, Y.-q., Li. C.-k., and Luo, Z.-x. (1998). Morphology of dentition and forelimb of *Zhangheotherium*. *Vertebrata PalAsiatica,* 38: 102-125.

Hu, Y.-m., and Wang, Y.-q. (2002). *Sinobaatar* gen. nov.: First multituberculate from the Jehol Biota of Liaoning, Northeast China. *Chinese Science Bulletin,* 47: 933-938.

Hu, Y.-m., Fox, R. C., Wang Y.-q., and and Li C.-k. (2005a). A new spalacotheriid symmetrodont from the Early Cretaceous of northeastern China. *American Museum Novitates,* 3475: 1-20.

Hu, Y.-m., Meng, J., Wang, Y.-q., and Li., C.-k. (2005b). Large Mesozoic mammals fed on young dinosaurs. *Nature*, 433: 149-152.

Hunter, J. P., and Jernvall, J. (1995). The hypocone as a key innovation in mammalian evolution. *Proceedings of the National Academy of Sciences USA,* 92: 10718-10722.

Jenkins, F. A., Jr. (1971). The postcranial skeleton of African cynodonts. *Peabody Museum of Natural History Bulletin,* 36: 1-216.

Jenkins, F. A., Jr. (1973). The functional anatomy and evolution of the mammalian humero–ulnar joint. *American Journal of Anatomy,* 137: 281-296.

Jenkins, F. A. Jr., and Crompton, A. W. (1979). Triconodonta. In Lillegraven, J. A., Kielan-Jaworowska, Z., and Clemens, W. A. (Eds.), *Mesozoic Mammals: The First Two-thirds of Mammalian History* (pp. 74-90). Berkeley: University of California Press.

Jenkins, F. A. Jr., Crompton, A. W., and Downs, W. (1983). Mesozoic mammals from Arizona: New evidence of mammalian evolution. *Science,* 222: 1233-1235.

Jenkins, F. A. Jr., and Krause, D. W. (1983). Adaptation for climbing in North American multituberculates (Mammalia). *Science*, 220: 712-715.

Jenkins, F. A. Jr., and Parrington, F. R. (1976). The postcranial skeletons of the Triassic mammals *Eozostrodon*, *Megazostrodon* and *Erythrotherium*. *Philosophical Transactions of the Royal Society of London,* 273: 387-431.

Jenkins, F. A. Jr., and Schaff, C. R. (1988). The Early Cretaceous mammal *Gobiconodon* (Mammalian, Triconodonta) from the Cloverly Formation in Montana. *Journal of Vertebrate Paleontology,* 6:1-24.

Jerison, H. J. (1973). *Evolution of the brain and intelligence*. New York: Academic Press.

Ji, Q., Luo, Z.-x., and Ji, S.-a. (1999). A Chinese triconodont mammal and mosaic evolution of mammalian skeleton. *Nature,* 398:326-330.

Ji, Q., Luo, Z.-x. Yuan C.-x., Wible, J. R., Zhang, J.-p., and Georgi J. A. (2002). The earliest known eutherian mammals. *Nature,* 416: 816-822.

Jouffroy, F. K., and M. F. Medina. (2002). Radio-ulnar deviation of the primate carpus: An X-ray study. Zeitschrift für Morphologie und Anthropologie, 83: 275-289.

Kemp, T. S. (1980). The primitive cynodont *Procynosuchus*: Structure, function and evolution of the postcranial skeleton. *Philosophical Transactions of the Royal Society of London (Series B), Biological Sciences*, 288: 217-258.

Kemp, T. S. (1983). The relationships of mammals. *Zoological Journal of the Linnean Society*, 77: 353-384.

Kemp, T. S. (2005). *The origin and evolution of mammals*. Oxford: Oxford University Press.

Kermack, K. A. (1963). The cranial structure of the triconodontids. *Philosophical Transactions of the Royal Society of London* 246(B): 83-103.

Kermack, K. A. (1967). The interrelations of early mammals. *Journal of the Linnean Society (Zoology),* 47: 241-249.

Kermack, K. A., and Kielan-Jaworowska, Z. (1971). Therian and nontherian mammals. In Kermack, D. M., and Kermack, K.A. (Eds.), *Early Mammals*. *Zoological Journal of the Linnean Society,* 50 (Supplement 1): 103-115.

Kermack, K. A., Mussett F., and Rigney, H. W. (1973). The lower jaw of *Morganucodon*. *Zoological Journal of the Linnean Society,* 53: 87-175.

Kermack, K. A., Mussett, F., and Rigney, H. W. (1981). The skull of *Morganucodon*. *Zoological Journal of the Linnean Society,* 71: 1-158.

Kielan-Jaworowska, Z. (1977). Evolution of the therian mammals in the Late Cretaceous of Asia. Part II. Postcranial skeleton in *Kennalestes* and *Asioryctes*.. In Kielan-Jaworowska, Z. (Ed.), *Results of the Polish-Mongolian Palaeontological Expeditions, Part VII. Palaeontologia Polonica 37* (pp. 65-83).

Kielan-Jaworowska, Z. (1978). Evolution of the therian mammals in the Late Cretaceous of Asia. Part III. Postcranial skeleton in Zalambdalestidae. In Kielan-Jaworowska,

Z. (Ed.), *Results of the Polish-Mongolian Palaeontological Expeditions, Part VIII. Palaeontologia Polonica 38* (pp. 5-41).

Kielan-Jaworowska, Z. (1979). Pelvic structure and nature of reproduction in muituberculata. *Nature*, 277: 402-403.

Kielan-Jaworowska, Z. (1989). Postcranial skeleton of a Cretaceous multituberculate mammal. *Acta Palaeontologica Polonica*, 34: 15-18.

Kielan-Jaworowska, Z., and Dashzeveg, D. (1998). New Early Cretaceous amphilestid ('triconodont') mammals from Mongolia. *Acta Palaeontologica Polonica,* 43: 413-438.

Kielan-Jaworowska, Z., and Gambaryan, P. P. (1994). Postcranial anatomy and habits of Asian multituberculate mammals. *Fossils and Strata,* 36: 1-92.

Kielan-Jaworowska, Z., Hurum, J., Currie, P. J., and Barsbold, R. (2002). New data on anatomy of the Late Cretaceous multituberculate mammal *Catopsbaatar. Acta Palaeontologica Polonica,* 47: 557-560.

Klima, M. (1973). Die Frühentwicklung des Schültergürtels und des Brustbeins bei den Monotremen (Mammalia: Prototheria). *Advances in Anatomy, Embryology and Cell Biology,* 47: 1-80.

Klima, M. (1987). Early development of the shoulder girdle and sternum in marsupials (Mammalia: Metatheria). *Advances in Anatomy, Embryology and Cell Biology,* 109: 1-91.

Kluge, A. G. (2001). Parsimony with and without scientific justification. *Cladistics*, 17: 199-210.

Komarek, V. (1985). Vertebrae inflexae. *Folia veterinary*, 29: 103-125.

Krause, D. W., and Jenkins, F. A. Jr. (1983). The postcranial skeleton of North American multituberculates. *Bulletin of the Museum of Comparative Zoology,* 150: 199-246.

Krebs, B. (1991). Das Skelett von *Henkelotherium* guimarotae gen. et sp. nov. (Eupantotheria, Mammalia) aus dem Oberen Jura von Portugal. *Berliner Geowissenschaftliche Abhandlungen(A),* 133: 1-110.

Krusat, G. 1980. Contribuição para o conhecimento da fauna do Kimeridgiano da mina de lignito Guimarota (Leiria, Portugal). IV Parte. *Haldanodon exspectatus* Kühne and Krusat 1972 (Mammalia, Docodonta). *Memórias dos Serviços Geológicos de Portugal*, 27: 1-79.

Krusat, G. (1991). Functional morphology of *Haldanodon expectatus* (Mammalia, Docodonta) from the Upper Jurassic of Portugal. In Kiela-Jaworowska, Z., Heintz, N., and Nakrem, H. A. (Eds.). *Fifth Symposium on Mesozoic Terrestrial Ecosystem and Biota, Extended Abstract* (Contribution from the Paleontological Museum, University of Oslo, 364) (pp. 37-38).

Kühne, W, G. (1949). On a triconodont tooth of a new pattern from a fissure filling in South Glamorgan. *Proceedings of the Zoological Society of London*, 119: 345-350.

Kühne, W, G. (1956). The Liassic therapsid *Oligokyphus*. London: British Museum (Natural History).

Li C.-k., Wang Y.-q., Hu Y.-m., and Meng J. (2003). A new species of *Gobiconodon* from the Jehoh Biota and its implication to the age of the fauna. *Chinese Science Bulletin:* 48: 177-182 (in Chinese).

Li, C.-k., Setoguchi, T., Wang, Y.-q., Hu, Y.-m., and Chang Z.-l. (2005). The first record of "eupantotherian" (Theria, Mammalia) from the late early Cretaceous of western Liaoning, China. *Vertebrata PalAsiatica,* 43: 3-11.

Li, G., and Luo, Z.-x. (2006). A Cretaceous symmetrodont therian with some monotreme-like postcranial features. *Nature*, 439: 195-200.

Li, J.-l., Wang, Y., Wang, Y.-q., and Li, C-k. (2000). A new family of primitive mammal from the Mesozoic of western Lioaning. *Chinese Science Bulletin*, 45: 2545-2549.

Lillegraven, J. A. (1979). Introduction. In Lillegraven, J. A., Kielan-Jaworowska, Z., and Clemens, W. A. (Eds.), *Mesozoic Mammals: The First Two-thirds of Mammalian History* (pp. 1-6). Berkeley: University of California Press.

Lopatin, A. V., Maschenko, E. N., Averianov, A. O., Rezvyi, A. S., Skutschas, P. P., and Leshchinskiy, S. V. (2005). Early Cretaceous mammals from Western Siberia: 1. Tinodontidae. *Paleontological Journal*, 35: 523-534.

Lucas, S. G., and Hunt, A. P. (1990). The oldest mammal. *New Mexico Journal of Science*, 30: 41-49.

Luo, Z.-x. (1994). Sister taxon relationships of mammals and the transformations of the diagnostic mammalian characters. In, Fraser, N. C., and H.-D. Sues (Eds.), *In the Shadow of Dinosaurs--Early Mesozoic Tetrapods* (pp. 98-128). Cambridge: Cambridge University Press.

Luo Z.-x., Cifelli, R. L., and Kielan-Jaworowska, Z. (2001a). Dural origin of tribosphenic mammals. *Nature,* 409: 53-57.

Luo, Z.-x., and Crompton, A. W. (1994). Transformations of the quadrate (incus) through the transition from non-mammalian cynodonts to mammals. *Journal of Vertebrate Paleontology,* 14: 341-374.

Luo, Z.-x., Crompton, A. W., and Lucas, S. G. (1995). Evolutionary origins of the mammalian promontorium and cochlea. *Journal of Vertebrate Paleontology,* 15: 113-121.

Luo Z.-x., Crompton A. W., and Sun A.-l. (2001b). A new Mammaliaform from Early Jurassic and evolution of mammalian characteristics. *Science,* 292: 1535-1540.

Luo, Z.-x., and Ji, Q. (2005). New study on dental and skeletal features of the Cretaceous mammal *Zhangheotherium*. *Journal of Mammalian Evolution,* 12: 337-357.

Luo, Z.-x., Ji, Q., Wible, J. R., and Yuan, C.-x. (2003).An Early Cretaceous tribosphenic mammal and metatherian evolution. *Science* 302: 1934-1940.

Luo, Z.-x., Kielan-Jaworowska, Z., and Cifelli, R. L. (2002). In quest for a phylogeny of Mesozoic mammals. *Acta Palaeontologica Polonica,* 47: 1-78.

Luo Z.-x., and Wible J. R. (2005). A Late Jurassic digging mammal and early mammalian diversification. *Science*, 308: 103-107.

Maddison, W. P., and Maddison, D. R. (2005a). Mesquite: a modular system for evolutionary analysis. Version 1.06 (http://mesquiteproject.org).

Maddison, W. P., and Maddison, D. R. (2005b). *MacClade: analysis of phylogeny and character evolution*. Version 4.08. Sunderland, MA: Sinauer Associates.

Maisch, M. W.,·Matzke, A. T., Grossmann, F., Stöhr·H., Pfretzschner, H.-U., and Sun G. (2005). The first haramiyoid mammal from Asia. *Naturwissenschaften*, 92: 40-44.

Marsh, O. C. (1880). Notice of Jurassic mammals representing two new orders. *American Journal of Science,* 30: 235-239.

Marsh, O. C. (1887). American Jurassic mammals. *American Journal of Science,* 33: 326-348.

Marshall, L. G., and Sigogneau-Russell, D. (1995). Part III: Postcranial skeleton. In de Muizon, C. (Ed.), *Pucadelphys andinus (Marsupialia, Mammalia) from the early Paleocene of Bolivia. Mémoires du Muséum national d'Histoire naturelle,* 165: 91-164.

Martin, T. (2005). Postcranial anatomy of *Haldanodon exspectatus* (Mammalia, Docodonta) from the Late Jurassic (Kimmeridgian) of Portugal and its bearing for mammalian evolution. *Zoological Journal of the Linnean Society*, 145: 219-248.

Martin, T., and Nowotny, M. (2000). The docodont *Haldanodon* from the Guimarota mine. In Martin, T., and Krebs, B. (Eds.), *Guimarota-a Jurassic Ecosystems* (pp 91-96). München: Verlag Dr. Friedrich Pfeil.

Martin, T., and Rauhut, O. W. M. (2005). Mandible and dentition of *Asfaltomylos patagonicus* (Australosphenida, Mammalia) and the evolution of tribosphenic teeth. *Journal of Vertebrate Paleontology*, 25: 414-425.

Matsuoka H. (2000). *Fossils of the Kuwajima 'Kaseki-Kabe' (Fossil-Bluff) - scientific report on a Neocomian (Early Cretaceous) fossil assemblage from the Kuwajima formation, Terori group, Shiramine, Ishikawa, Japan*. Ishikawa, Japan: Shiramine Village Board of Education.

McKenna, M. C. (1961). On the shoulder girdle of the mammalian subclass Allotheria. *American Museum Novitates*, 2066: 1-27.

McKenna, M. C. (1975). Toward a phylogenetic classification of the Mammalia. In Luckett, W. P., and Szalay, F. S. (Eds.), *Phylogeny of the Primates* (pp. 21-46). New York: Plenum Publishing Corporation.

McKenna, M. C., and Bell, S. K. (1997). *Classification of mammals above the species level*. New York: Columbia University Press.

Meng J., Hu, Y.-m., Wang, Y.-q., and Li, C.-k. (2003).The ossified Meckel's cartilage and internal groove in Mesozoic mammaliaforms: implications to origin of the definitive mammalian middle ear. *Zoological Journal of the Linnean Society*, 138: 431-448.

Meng, J., Hu, Y.-m., Li, C.-k., and Wang, Y.-q. The mammal fauna in the early Cretaceous Jehol Biota: Implications to diversity and biology of Mesozoic mammals. *Journal of Geology* (in press).

Meng, J., Hu,Y.-m., Wang, Y.-q., and Li, C.-k. (2005). A New triconodont (Mammalia) from the Early Cretaceous Yixian Formation of Liaoning, China. *Vertebrata PalAsiatica*, 43: 1-10.

Meng, J., and Wyss, A. R. (1995). Monotreme affinities and low-frequency hearing suggested by multituberculate ear. *Nature,* 377: 141-144.

Miao, D.-s. (1991). On the origin of mammals. InSchultze, H.-P., and Trueb, L. (Eds.), *Origins of major groups of tetrapods: Controversies and consensus* (pp579-597). Ithaca: Cornell University Press.

Mills, J. R. E. (1971). The dentition of *Morganucodon*. In*:* Kermack, D. M., and Kermack , K. A. (Eds.), Early Mammals. *Zoological Journal of the Linnean Society* 50 (Supplement 1): 29-63.

Mitter, C., Farrell, B., and Wiegmann, B. (1988). The phylogenetic study of adaptive zones: has phytophagy promoted insect diversification? *American Naturalist*, 132: 107-128.

Mortola, J. P. (1984). Breathing pattern in newborns. *Journal of Application Physiology*, 56: 1533-1540.

Muizon, C. de. 1998. *Mayulestes ferox,* a borhyaenoid (Metatheria, Mammalia) from the early Paleocene of Bolivia. Phylogenetic and palaeobiologic implications. *Geodiversitas*, 20: 19-142.

Negus, V. (1929). *The Mechanism of the larynx.* London: Heinemann.

Nelson, G. (1994). Homology and systematics. In Hall, B. K. (Ed.) *Homology: the hierarchical basis of comparative biology* (pp.101-149). San Diego: Academic Press.

Nelson, G. J., and Platnick, N. J. (1991). TTS: a more precise use of parsimony? *Cladistics*, 7: 351-366.

Novacek, M. J., Rougier, G. W., Wible, J. R., McKenna, M. C., Dashzeveg, D., and Horovitz, I. (1997). Epipubic bones in eutherian mammals from the Late Cretaceous of Mongolia. *Nature,* 389: 483-486.

Nowak R. M. (1999). *Walker's mammals of the world, 6th edition*. Baltimore: The Johns Hopkins University Press.

Olson, E. C. (1959). The evolution of mammalian characters. *Evolution,* 13: 344-353.

Osborn, H. F. (1888). On the structure and classification of the Mesozoic Mammalia. *Journal of the National Academy of Sciences, Philadelphia,* 9: 186-265.

Osborn, H. F. (1907). *Evolution of Mammalian Molar Teeth*. New York: The MacMillan Company.

Owen, R. (1838). On the jaws of the *Thylacotherium prevostii* (Valenciennes) from Stonesfield. *Proceedings of the Geological Society of London*, 3: 5-9.

Owen, R. (1859). Paleontology. *Encyclopedia Britannia* (8th ed.), 17: 156-161.

Owen, R. (1871). Monograph of the fossil Mammalia of Mesozoic formations. *Palaeontographic Society Monograph*, 24: 1-115

Owen, R. (1884). On the skull and dentition of a Triassic mammal (*Tritylodon longaevus*) from South Africa. *Quarterly Journal of the Geological Society of London,* 40: 146-152.

Parker, W. K. (1868). *A monograph on the structure and development of the shoulder-girdle and sternum on the Vertebrata* (Royal Society Series, No. 42). London: R. Hardwicke.

Parrington, F. R. (1941). On two mammalian teeth from the Lower Rhaetic of Somerset. *Annual Magazine of Natural History, London*, 11: 140-144.

Parrington, F. R. (1947). On a collection of Rhaetic mammalian teeth. *Proceedings of the Zoological Society*, 116: 707-728.

Parrington, F. R. (1971). On the Upper Triassic mammals. *Philosophical Transactions of the Royal Society (B),* 261: 231-272.

Parrington, F. R. (1978). A further account of the Triassic mammals. *Philosophical Transactions of the Royal Society of London (B),* 282: 177-204.

Patterson, B. (1951). Early Cretaceous mammals from northern Texas. *American Journal of Science,* 249: 31-46.

Patterson, B., and Olson, E. C. (1961). A triconodontid mammal from the Triassic of Yunnan. In Vandebroek, G. (Ed.) *International Colloquium in the evolution of lower and non-specialized mammals* (pp. 129-191). Brussels: Koninklijke Vlaamse Academiie voor Wetenschapen, Letteren en Schone Kunsten van Belgie.

Patterson, C. (1982). Morphological characters and homology. In Jeysey, K. A., and Friday, A. E. (Eds.) *Problems of Phylogenetic Reconstruction* (pp. 21-74). London: Academic Press.

Pfretzschner H.-U., Martin T., Maisch M. W., Matzke A. T., and Sun G. (2005), A new docodont mammal from the Late Jurassic of the Junggar Basin in northwest China. *Acta Palaeontologica Polonica*, 50: 799-808.

Platnick, N. I. (1979). Philosophy and transformation of cladistics. *Systematic Zoology*, 28: 537-546.

Pough, F. H., Janis C. M., and Heiser, J. B. (1999). *Vertebrate Life* (5th ed.). New Jersey: Prentice Hall.

Prasad, G. V. R., and Manhas, B. K. (1997).Anew symmetrodont mammal from the Lower Jurassic Kota Formation, Pranhita-Godavari Valley, India. *Géobios,* 30: 563-572.

Prasad, G. V. R., and Manhas, B. K. (2002). Triconodont mammals from the Jurassic Kota Formation of India. *Geodiversitas*, 24: 445-464.

Pridmore, P. A., Rich, T. H., Vickers-Rich, P., and Gambaryan, P. P. (2005). A tachyglossid-like humerus from the Early Cretaceous of South-Eastern Australia, *Journal of Mammalian Evolution*, 12: 359-378.

Prothero, D. (1981). New Jurassic mammals from Como Bluff, Wyoming, and the interrelationships of non-tribosphenic Theria. *Bulletin of the American Museum of Natural History*, 167: 281-325.

Rasmussen, T. E., and Callison, G. (1981). Anew species of triconodont mammal from the Upper Jurassic of Colorado. *Journal of Paleontology,* 55: 628-634.

Rauhut, O. W. M., Martin, T., Ortiz-Jaureguizar, E., and Puerta, P. 2002. A Jurassic mammal from South America. *Nature*, 416:165-168.

Reilly S. M., and White, T. D. (2003). Hypaxial Motor Patterns and the Function of Epipubic Bones in Primitive Mammals. *Science*, 299: 400-402.

Reilly, S. M., McBrayer, L. D., and White, T. D. (2001). Prey processing in amniotes: biomechanical and behavioral patterns of food reduction. *Comparative. Biochemistry and Physiology, Part A,* 128: 397-415.

Rich, T. H., Flannery, T. F., Trusler, P., Kool, L., van Klaveren, N. A., and Vickers-Rich, P. (2001). A second tribosphenic mammal from the Mesozoic of Australia. *Records of the Queen Victoria Museum*, 110: 1-9.

Rich, T. H., Flannery, T. F., Trusler, P., Kool, L., van Klaveren, N. A., and Vickers-Rich, P. (2002). Evidence that monotremes and austribisphenids are not sistergroups. *Journal of Vertebrate Paleontology*, 22: 466-469.

Rich, T. H., Hopson, J. A., Musser, A. M., Flannery, T. F., Vickers-Rich, P. (2005). Independent origins of middle ear bones in monotremes and therians. *Science*, 307: 910-914.

Rich, T. H., Vickers-Rich, P., Constantine, A., Flannery, T. F., Kool, L., and van Klaveren, N. A. (1997). A tribosphenic mammal from the Mesozoic of Australia. *Science*, 278: 1438-1442.

Rigney, H. W. (1963). A specimen of *Morganucodon* from Yunnan. *Nature*, 197: 1122.

Romer, A. S. (1922). The locomotor apparatus of certain primitive and mammal-like reptiles. *Bulletin of American Museum of Natural History*, 46: 517-606.

Romer, A. S. (1956). *Osteology of the reptiles*. The University of Chicago Press, Chicago.

Romer, A. S., and Lewis, A. D. (1973). The Chañares (Argentina) Triassic reptile fauna. XIX. Postcranial materials of the cynodonts *Probelesodon* and *Probainognathus*. *Breviora*, 407: 1-26.

Rougier, G. W. (1993). *Vincelestes neuquenianus* Bonaparte *(*Mammalia, Theria), un primitivo mammifero del Cretaccico Inferior de la Cuenca Neuqina. Ph.D. Thesis,

Universidad Nacional de Buenos Aires. Facultad de Ciencias Exactas y Naturales. Buenos Aires.

Rougier, G. W., Ji, Q., and Novacek, M. J. (2003). A new symmetrodont mammal with fur impressions from the Mesozoic of China. *Acta Geologica Sinica*, 77: 7-14.

Rougier G. W, Novacek M. J, McKenna M. C, and Wible, J. R. (2001). Gobiconodonts from the Early Cretaceous of Oshih (Ashile), Mongolia. *American Museum Novitates*, 3348: 1-30.

Rougier, G. W., Wible, J. R., and Hopson, J. A. (1996a). Basicranial anatomy of *Priacodon fruitaensis* (Triconodontidae, Mammalia) from the Late Jurassic of Colorado, and a reappraisal of mammaliaform interrelationships. *American Museum Novitates,* 3183: 1-28.

Rougier, G. W., Wible, J. R., and Novacek, M. J. (1996b). Middle–ear ossicles of *Kryptobataar dashzevegi* (Mammalia, Multituberculata): implications for mammaliamorph relationships and evolution of the auditory apparatus. *American Museum Novitates,* 3187: 1-43.

Rowe, T. B. (1986). *Osteological Diagnosis of Mammalia, Linnaeus, 1758 and its Relationship to Extinct Synapsida*. Unpublished Ph.D. dissertation. University of California, Berkeley.

Rowe, T. B. (1988). Definition, diagnosis, and origin of Mammalia. *Journal of Vertebrate Paleontology,* 8: 241-264.

Ruben, J. A., Jones, T. T., and Geist, N. R. (2003). Respiratory and reproductive paleophysiology of dinosaurs and early birds. *Physiological and Biochemical Zoology,* 76: 141-164.

Sánchez-Villagra, M. R., and Maier, W. (2002). Ontogenetic data and the evolutionary origin of the mammalian scapula. *Naturwissenschaften*, 89: 459-461.

Sánchez-Villagra, M. R., and Maier, W. (2003). Ontogenesis of the scapula in marsupial mammals, with special emphasis on perinatal stages of didelphids and remarks on the origin of the therian scapula. *Journal of Morphology*, 258: 115-129.

Schaeffer, B. (1941). The morphology and functional evolution of the tarsus in amphibians and reptiles. *Bulletin of the American Museum of Natural History*, 78: 395-472.

Schneider, R . (1964). Der Larynx der Säugetiere. *Handbuch der Zoologie, Band* 8 (5): 1-128.

Schuh, R. T. (2000). Biological systematics: Principles and Applications. Ithaca and London: Cornell University Press.

Scotland, R. (2000). Homology, coding and three-taxon statement analysis. In Scotland, R., and Pennington, R. T. (Eds.), *Homology and Systematics: coding characters for phylogenetic analysis* (Systematics Association special volume, No. 58) (pp.145-182). Philadelphia: Taylor and Francis.

Sereno, P. C., and McKenna, M. C. (1995). Cretaceous multituberculate skeleton and the early evolution of the mammalian shoulder girdle. *Nature,* 377: 144-147.

Sidor, C. A., and Hopson, J. A. (1998). Ghost lineages and "mammalness": assessing the temporal pattern of character acquisition in the Synapsida. *Paleobiology,* 24: 254-273.

Sigogneau-Russell, D. (1983).Anew therian mammal from the Rhaetic locality of Saint-Nicolas-de-Port (France). *Zoological Journal of the Linnean Society,* 78: 175-186.

Sigogneau-Russell, D. (1995). Two possibly aquatic triconodont mammals from the Early Cretaceous of Morocco. *Acta Palaeontologica Polonica*, 40: 149-162.

Silva, M., and Downing, J. A. (1995). *CRC handbook of mammalian body mass.* Boca Raton: CRC Press.

Simpson, G. G. (1925). Mesozoic Mammalia. I. American triconodonts (Parts 1 and 2). II. Tinodon and its allies. III. Preliminary comparison of Jurassic mammals, except multituberculates. *American Journal of Science*, (5) x: I. 145-165, 332-358; II. 451-470; III. 559-569.

Simpson, G. G. (1928). *A Catalogue of the Mesozoic Mammalia in the Geological Department of the British Museum.* London: Oxford University Press.

Simpson, G. G. (1929). American Mesozoic Mammals. *Memoirs of Peabody Museum of Yale University,* 3: 1-171.

Simpson, G. G. (1945). The principles of classification and a classification of mammals. *Bulletin of the American Museum of Natural History,* 85: 1-350.

Simpson, G. G. (1959). Mesozoic mammals and the polyphyletic origin of mammals. *Evolution,* 13: 405-414.

Simpson, G. G. (1960). Diagnosis of the classes Reptilia and Mammalia. *Evolution*, 14: 388-392.

Simpson, G. G. (1971). Concluding remarks: Mesozoic mammals revisited. In Kermack, D. M., and Kermack, K. A. (Eds.), Early Mammals. *Zoological Journal of the Linnean Society*, 50 (Supplement 1): 181-198.

Slaughter, B. H. (1969). *Astroconodon*, the Cretaceous triconodont. *Journal of Mammalogy*, 50: 102-107.

Sliper, E. J. (1946). Comparative biologic-anatomical investigations on the vertebral column and spinal musculature of mammals. *Verhandelingen der Koninklijke Nederlandse Akademie van Wetenschappen. Apfling Natuurkunde*, 42: 1-128.

Slowinski, J. B., Guyer, C. (1993). Testing whether certain traits have caused amplified diversification: an improved method based on a model of random speciation and extinction. *American Naturalist,* 142: 1019-1024.

Stucky, R. K., and McKenna, M. C. (1993). Mammalia. In Benton, M. J. (Ed.), *The Fossil Record, 2* (pp. 739-771). London: Chapman and Hall.

Sues, H.-D. (1985). The relationships of the Tritylodontidae (Synapsida). *Zoological Journal of the Linnean Society*, 85: 205-217.

Sun, A.-l., and Li, Y.-h. (1985). The postcranial skeleton of Jurassic tritylodonts from Sichuan Province. *Vertebrata PalAsiatica,* 23: 135-151.

Swofford, D. L. (2002). *PAUP*. Phylogenetic Analysis Using Parsimony (*and Other Methods). Version 4.* Sinauer Associates, Sunderland, Massachusetts.

Symington, J. (1899). The marsupial larynx. *Journal of Anatomy and Physiology,* 33: 31-49.

Symington, J. (1900). The monotreme larynx. *Journal of Anatomy and Physiology,* 34: 90-100.

Szalay, F. S. (1993). Pedal evolution of mammals in the Mesozoic: Tests for taxic relationships. In Szalay, F. S., Novacek, M. J., and McKenna, M. C. (Eds.), *Mammal Phylogeny, Volume 1* (pp. 108-128). New York: Springer Verlag.

Szalay, F. S. (1994). *Evolutionary history of the marsupials and an analysis of osteological characters.* Cambridge: Cambridge University Press.

Szalay, F. S., and Trofimov, B. A. (1996). The Mongolian Late Cretaceous *Asiatherium*, and the early phylogeny and paleobiogeography of Metatheria. *Journal of Vertebrate Paleontology,* 16: 474-509.

Tang F., Luo Z.-x., Zhou Z.-h. (2001). Biostratigraphy and palaeoenvironment of the dinosaur-bearing sediments in Lower Cretaceous of Mazongshan area, Gansu Province, China. *Cretaceous Research*, 22: 115-129

Trofimov, B. A. (1978). The first triconodonts (Mammalia, Triconodonta) from Mongolia. *Doklady Akademii Nauk SSSR*, 243: 213-216 (In Russian).

Turnbull, W. D., and Cifelli, R. L. (1999). Triconodont mammals of the Aptian-Albian Trinity Group, Texas and Oklahoma. In Mayhall, J. T., and Heikkin, T. (Eds.), *Dental Morpholy'98* (pp. 252-272). Oulu: University of Oulu Press.

Van Valkenburgh B., Jenkins I. (2002). Evolutionary patterns in the history of Permo-Triassic and Cenozoic synapsid predators. *Paleontological Society Papers*, 8: 267-288.

Van Valkenburgh B. (1990). Skeleton and dental predictors of body mass in carnivores. In Damuth J., MacFadden, B. J. (Eds.), *Body size in mammalian paleobiology: Estimation and biological implication* (pp.181-205). Cambridge:bCambridge University Press.

Van Valkenburgh, B., Sacco, T., and Wang, X.-m. (2004). Pack hunting in Miocene Borophagine dogs: Evidence from craniodental morphology and body size. *Bulletin of American Museum of Natural History*, 279: 147-162.

Vaughn, P. P. (1956). The phylogenetic migrations of the ambiens muscles. *Journal of the Elisha Mitchell Scientific Society*, 72: 243-262.

Vrba E. S. (1987). Ecology in relation to speciation rates: some case histories of Miocene-Recent mammal clades. *Evolutionary Ecology*, 1: 283-300.

Walker, W. F. Jr., and Liem K. F. (1994). Functional anatomy of the vertebrates: an evolutionary perspective (2nd ed.). Fort Worth: Sauders College Publishing.

Wang S.-s., Wang, Y.-q., Hu, H.-g., and Li, H.-m. (2001). The existing time of Sihetun vertebrate in western Liaoning, China-Evidence from U-Pb dating of zircon. *Chinese Science Bulletin,* 46: 779-782.

Wang, X.-l., and Zhou, Z.-h. (2003). Mesozoic Pompeii. In M.-m. Chang, P.-j. Chen, Y.-q. Wang, and Y. Wang (Eds.), *The Jehol Biota* (pp. 19-36). Shanghai: Shanghai Scientific and Technological Publishers.

Wang, Y.-q., Hu, Y.-m., and Li, C.-k. Review of recent advances on study of Mesozoic mammals in China. Veretbrata PaleoAsiatica (in press).

Wang, Y.-q., Hu, Y.-m., Meng, J., and Li, C.-k. (2001). An ossified Meckel's cartilage in two Cretaceous mammals and origin of the mammalian middle ear. *Science*, 294: 357-361.

Watson, A. G. (1981). The phylogeny and development of the atlas-axis complex in the dog. Thesis, Cornell University, Ithaca, New York.

Wible, J. R. (1991). Origin of Mammalia: the craniodental evidence reexamined. *Journal of Vertebrate Paleontology,* 11: 1-28.

Wible, J. R., and Hopson, J. A. (1993). Basicranial evidence for early mammal phylogeny. In Szalay, F. S., Novacek, M. J., and McKenna, M. C. (Eds.), *Mammal Phylogeny, Volume 1* (pp. 45-62). New York: Springer Verlag.

Wible, J. R., Rougier, G. W., Novacek, M. J., McKenna, M. C., and Dashzeveg, D. (1995). A mammalian petrosal from the Early Cretaceous of Mongolia: implications for the evolution of the ear region and mammaliamorph relationships. *American Museum Novitates,* 3149: 1-19.

Wible, J. R., Rougier,G. W., Novacek, M. J., and McKenna, M. C. 2001. Earliest eutherian ear region: a petrosal referred to *Prokennalestes* from the Early Cretaceous of Mongolia. *American Museum Novitates,* 3322: 1-44.

Wilkinson, M. (1995). A comparison of two methods of character construction. *Cladistics*, 11: 297-308.

Williams D. M., and Sieber, D. J. (2000). Characters, homology and three-item analysis. In Scotland, R., and Pennington, R. T. (Eds.), *Homology and Systematics: coding characters for phylogenetic analysis* (Systemaics Association special volume, No. 58). Philadelphia: Taylor and Francis, 183-208.

Woodburne, M. O. (2003). Monotremes as pretribosphenic mammals. *Journal of Mammalian Evolution,* 10: 195-248.

Woodburne, M. O., Rich, T. H., Springer, M. S. (2003). The evolution of tribospheny and the antiquity of mammalian clades. *Molecular Phylogenetics and Evolution,* 28: 360-385.

Xu, X., Makovicky P. J., Wang, X.-l., and Norell, M. A. (2002). A ceratopsian dinosaur from China and the early evolution of Ceratopsia. *Nature*, 416: 314-317.

Xu, X., and Norell M. A. (2004). A new troodontid dinosaur from China with avian-like sleeping posture. *Nature*, 431: 838-841.

Xu, X., Norell, M. A., Kuang, X.-w., Wang, X.-l., Zhao, Q., and Jia, C.-k. (2004). Basal tyrannosauroids from China and evidence for protofeathers in tyrannosauroids. *Nature*, 431: 680-684.

Xu, X., and Wang, X.-l. (2004). A new dromaeosaur (Dinosauria: Theropoda) from the Early Cretaceous Yixian Formation of western Liaoning. *Vertebrata PalAsiatica.* **42**: 111-119

Yadagiri, P. (1984). New symmetrodonts from Kota Formation (Early Jurassic), India. *Journal of the Geological Society of India*, 25: 514-621.

Yalden, D. W. (1970). The functional morphology of the carpal bones in carnivores. *Acta Anatomica*, 77: 481-500.

Young, C.-c. (1947). Mammal-like reptiles from Lufeng, Yunnan, China. *Proceedings of the Zoological Society of London,* 117: 537-597.

Young, C.-c. (1978). New materials of *Eozostrodon. Vertebrata PalAsiatica,* 16: 1-3.

Young, C.-c. (1982). *Selected Works of Yang Zhongjian (Young Chung-Chien).* (Edited by Editorial Committee for Selected Works of Yang Zhongjian). Beijing: Science Press.

Zhang, F.-k. (1984). The fossil record of Mesozoic mammals of China. *Vertebrata PalAsiatica,* 22: 29-38.

Zhang, F.-k., and Cui, G.-h. (1983). New material and new understanding of *Sinoconodon*. *Vertebrata PalAsiatica,* 21: 32-41.

Zhang, F.-k., Crompton, A. W., Luo, Z.-x., and Schaff, C. R. (1998). Pattern of dental replacement of *Sinoconodon* and its implications for evolution of mammals. *Vertebrata PalAsiatica,* 36: 197-217.

Zhou, M.-z., Cheng, Z.-w., and Wang, Y.-q. (1991). A note on a Jurassic mammalian lower jaw bone from the west of Liaoning Province. *Vertebrata PalAsiatica*, 29: 165-175.

Zhou, Z.-h.,. Barrett, P. M., and Hilton, J. (2003). An exceptionally preserved Lower Cretaceous ecosystem. *Nature*, 421: 807-814.

Zittel, K. A. von. (1893). *Handbuch der Palaeontologie. Abteilung I. Palaeozoologie. Band IV, Vertebrata (Mammalia)*. Munich: R. Oldenbourg.